AFFDL-TR-71-127

ANNEALED FOIL FATIGUE SENSOR DEVELOPMENT

ROBERT S. HORNE AND OSCAR L. FREYRE

LOCKHEED-GEORGIA COMPANY

TECHNICAL REPORT AFFDL-TR-71-127

MARCH 1972

AIR FORCE FLIGHT DYNAMICS LABORATORY
AIR FORCE SYSTEMS COMMAND
WRIGHT-PATTERSON AIR FORCE BASE, OHIO

NOTICE

When Government drawings, specifications, or other data are used for any purpose other than in connection with a definitely related Government procurement operation, the United States Government thereby incurs no responsibility nor any obligation whatsoever; and the fact that the government may have formulated, furnished, or in any way supplied the said drawings, specifications, or other data, is not to be regarded by implication or otherwise as in any manner licensing the holder or any other person or corporation, or conveying any rights or permission to manufacture, use, or sell any patented invention that may in any way be related thereto.

Copies of this report should not be returned unless return is required by security considerations, contractual obligations, or notice on a specific document.

AIR FORCE: 20-4-72/350

ANNEALED FOIL FATIGUE SENSOR DEVELOPMENT

ROBERT S. HORNE AND OSCAR L. FREYRE

LOCKHEED-GEORGIA COMPANY

FOREWORD

This research and development program was conducted by the Lockheed-Georgia Company of Marietta, Georgia under Air Force Contract No. F33(615)-68-C-1221. The contract was initiated under Project No. 3170, "Flight Dynamics Laboratory Instrumentation," and Task No. 317007, "Development of Structural Test Instrumentation."

The work was supervised and directed by Robert S. Horne, Project Engineer. The report was prepared by he and Oscar L. Freyre, Structural Research Scientist. This project was initiated by the Air Force Flight Dynamics Laboratory, Wright-Patterson Air Force Base, Ohio and was administered under the technical coordination of Robert A. Crouch (AFFDL/FBT), Project Engineer. The authors also wish to acknowledge the assistance and guidance of Ken E. Brown, Lockheed-Georgia Company, Stress Analyst.

Some of the items evaluated in this report were modified from commercial items that were not developed or manufactured to meet government specifications; to withstand the tests to which they were subjected or to operate as applied during this study. Any failure to meet the objectives of this investigation is no reflection on any of the commercial items discussed herein or on any manufacturer.

This report covers work conducted from December 1967 until May 1971 and constitutes the final report under Contract No. F33(615)-68-C-1221. It was submitted by the authors in August, 1971. The contractor's report number is ER 11411.

Publication of this report does not constitute Air Force approval of the report's findings or conclusions. It is published only for the exchange and stimulation of ideas.

Robert L. Cavanagh

ROBERT L. CAVANAGH
Chief, Experimental Branch
Structures Division
Air Force Flight Dynamics Laboratory

ABSTRACT

The development testing of the C-5A full-scale fatigue specimens presented a timely opportunity to continue the development of a system of fatigue sensing devices. The fatigue sensor selected for use was previously evaluated during an Air Force funded feasibility study and has been adapted to meet the application requirements on full-scale C-5A structure. This document constitutes the final report regarding this effort and applies specifically to an evaluation of the sensor on the C-5A laboratory fatigue test specimens. The techniques of sensor installation, location, data acquisition methods, and analysis of sensor response are herein evaluated in view of potential utilization on fleet aircraft. A review of the test results indicates that a structure's relative exposure to repeated load occurrences can be monitored, and the cumulative strain history can be registered and stored by a simple foil sensor.

TABLE OF CONTENTS

ILLUSTRATIONS

TABLES

TERMINOLOGY AND SYMBOLS

The following constitutes a list of terms and symbols used throughout the report. As far as possible, the terms used are those compatible with recognized standards such as MIL-HDBK-5, Handbook of Experimental Stress Analysis and ASTM Standards. It is believed these definitions will reduce ambiguity and permit a common basis for later communications.

TERMINOLOGY

Anneal, Full	A heating and quenching procedure for metals which leads to their maximum softness, ductility and formability
Cold Working	The plastic deformation of metal at a temperature lower than recrystallization temperature
Constantan	A group of copper-nickel alloys containing 45 to 65% copper. The most favored composition is 43% nickel and 57% copper
Deformation, Plastic	The deformation that remains after removal of the load which caused it
Discontinuity; Stress Concentrator	An abrupt change in load path associated with holes, notches, rivets or reentrant corners
Die Cut	A process for obtaining a particular sensor grid configuration by the use of precision dies rather than by use of chemicals
*Fatigue Damage	Any level of material or structural physical damage resulting from the application of cyclic loads, up to and including stable fatigue crack growth, providing the damage does not interfere with the safe operation of the airplane
*Fatigue Failure	A structural failure resulting from stable or unstable fatigue crack growth which requires replacement, repair, and/or redesign of the component in order to permit the safe operation of the airplane for a specific period of time or equivalent load history
Faying Surface	The contact area formed by the overlap in a splice or joint
Hardened, Fully	The maximum hardness obtainable, by strain hardening, cold rolling, drawing, or heat treatment
Kapton	A polyimide film (H-film) manufactured by E. I. PuPont Co.
Multiplying Factor	The ratio of the artificial strain produced at the sensor to the true strain in the structural specimen accomplished by a particular mechanical configuration of the sensing device.

Pass	A sequence of cyclic load conditions which constitute a fixed number of simulated flight hours, or landings
Sensor Grid	That portion of the sensor which is most sensitive to mechanical forces and produces an electrical resistance change
Sensitivity	The unit electrical resistance change of a sensor in response to a unit mechanical input
Spectrum	A predetermined grouping of fatigue loading conditions to be applied in sequence
Shim	A thin strip of metal used in this program as a mounting surface for the sensor
Strain Survey	A procedure for determining the distribution of internal loads and stress levels produced in a structure for a particular loading condition
Supersensitivity	The progressive fatigue failure of the foil grid of a sensor. The failure consists of microscopic cracks in the strained portion of the foil which will intermittantly open and close under dynamic conditions
Threshold of Sensitivity	The cyclic strain level at which the sensor foil begins to yield, resulting in a permanent electrical resistance change
Work Hardening	A process which results in an induced change in the hardness of a ductile metal as a result of plastic deformation of the material
Zero Shift	An increase in electrical resistance of the foil due to cyclic strain induced work hardening

*These terms are defined solely for the purpose of interpreting the results of the "Annealed Foil Fatigue Sensor Development" program and are not proposed as general definitions.

SYMBOLS

B.L.	buttock line
BBS	box beam station
C.G.	center of gravity
CW	center wing
F.S.	fuselage station
F	fuselage
G-A-G	ground-air-ground cycles
G.F.	gage factor
H	height of stringer
HS	horizontal stabilizer
H.S.S	horizontal stabilizer station
IW	inner wing
K_t	theoretical stress concentration factor
KSI	thousand pounds per square inch
L.H.	left hand side
L	length
ΔL	change in length
M.F.	multiplying factor
MLG	main landing gear
N	number of cycles to fatigue failure
OW	outer wing
PB	pressure bulkhead
ΔR	permanent zero shift resistance change in the fatigue sensor (ohms, $\mu\epsilon$) due to cyclic strain induced work hardening
Ri	initial sensor resistance

S/N	ship number
TCR	temperature coefficient of resistance
TSK	thickness of skin
TW	thickness of web
V.S.B.R	vertical stabilizer box rib station
V.S.S	vertical stabilizer station
W_f	width of flange
W.L.	water line
X996	main landing gear specimen
X997	aft fuselage-empennage specimen
X998	fuselage-wing specimen
ϵ	strain $\left(\frac{\Delta L}{L}\right)$
f	stress
f_m	mean stress (the stress level about which the variable stress is cycled)
f_v	varying stress (the stress due to the varying load)
n	number of cycles the specimen has endured at any stage of its useful life.
μ	microunits or 10^{-6}
Δ	incremental change
$\sim$	cycles
Ω	resistance in ohms
Σ	summation
"	inches
$\pm$	plus or minus
-	(minus) compression sense
+	(plus) tension sense
f	function of
$\overrightarrow{+}$	vectorial summation

SECTION I

INTRODUCTION

Airframe structural fatigue problems have plagued the Air Force since the early fifties. These problems became epidemic in proportion in 1958 when the Strategic Air Command discovered serious fatigue damage on their B-47's and predicted additional problems on the B-52's. The first priority effort was to measure the load environment experienced by these aircraft and to qualify their structural integrity with full-scale cyclic load tests. Even at this time, however, there was an interest in developing a sensor (Ref. 1) which could monitor fatigue life more directly by sensing pertinent information from the critical airframe component itself.

Since these early days, the Air Force has created an effective program to control the detrimental effects of aircraft structural fatigue. This program, (Refs. 2 and 3) referred to as the Aircraft Structural Integrity Program (ASIP) has always been based upon full-scale structural fatigue testing and load occurrence measurement. Refinements in the tests, loads data gathering, and analysis have been made over the years (Ref. 4) as the result of practical operating experience. Today the Air Force recommends a program wherein the structural integrity of the fleet is established based upon a fatigue analysis of the airframe, a full-scale fatigue test of a typical airframe, a body of load data derived from multichannel recorders on at least 20% of the fleet, and crew log or other mission experience data from 100% of the fleet. This program, though expensive, had been shown to be absolutely essential to the long time structure integrity of Air Force systems. Still persisting, however, is the idea that a sensor which can be installed on a critical structural component would be a useful adjunct to the ASIP. If it was inexpensive, it could be installed on 100% of the fleet and thus become a valuable addition to the crew log data for an improved parametric analysis of individual fleet aircraft. Periodic inspections would be made more meaningful since damage discovered on particular components could be related to load experience on that same component more accurately.

The problem of fatigue and structural reliability has continually grown in importance as demands for extended aircraft service life and severity of operating conditions have increased. Fruedenthal (Ref. 5) states that more than 95% of all reported aircraft structural failures are fatigue failures. The continued trend toward development of larger and more structurally complex aircraft points out the need for an information system to monitor the fatigue status of the aircraft structure.

The search for fatigue damage instrumentation has for many years been a continuous effort at the Lockheed-Georgia Company. Of the wide variety of techniques investigated for assessing structural fatigue damage, one type that appears encouraging is a bonded fatigue sensing device investigated under AF 33(615)-2505 (Ref. 6). This R&D contract concerned the validity of using bonded work hardenable foils as a device to indicate a structure's fatigue experience . The results obtained during the feasibility study of a fatigue damage indicator indicated that the sensing device had excellent potential if it were optimized and calibrated to a specific structural system. This method is based upon the permanent resistance change of an

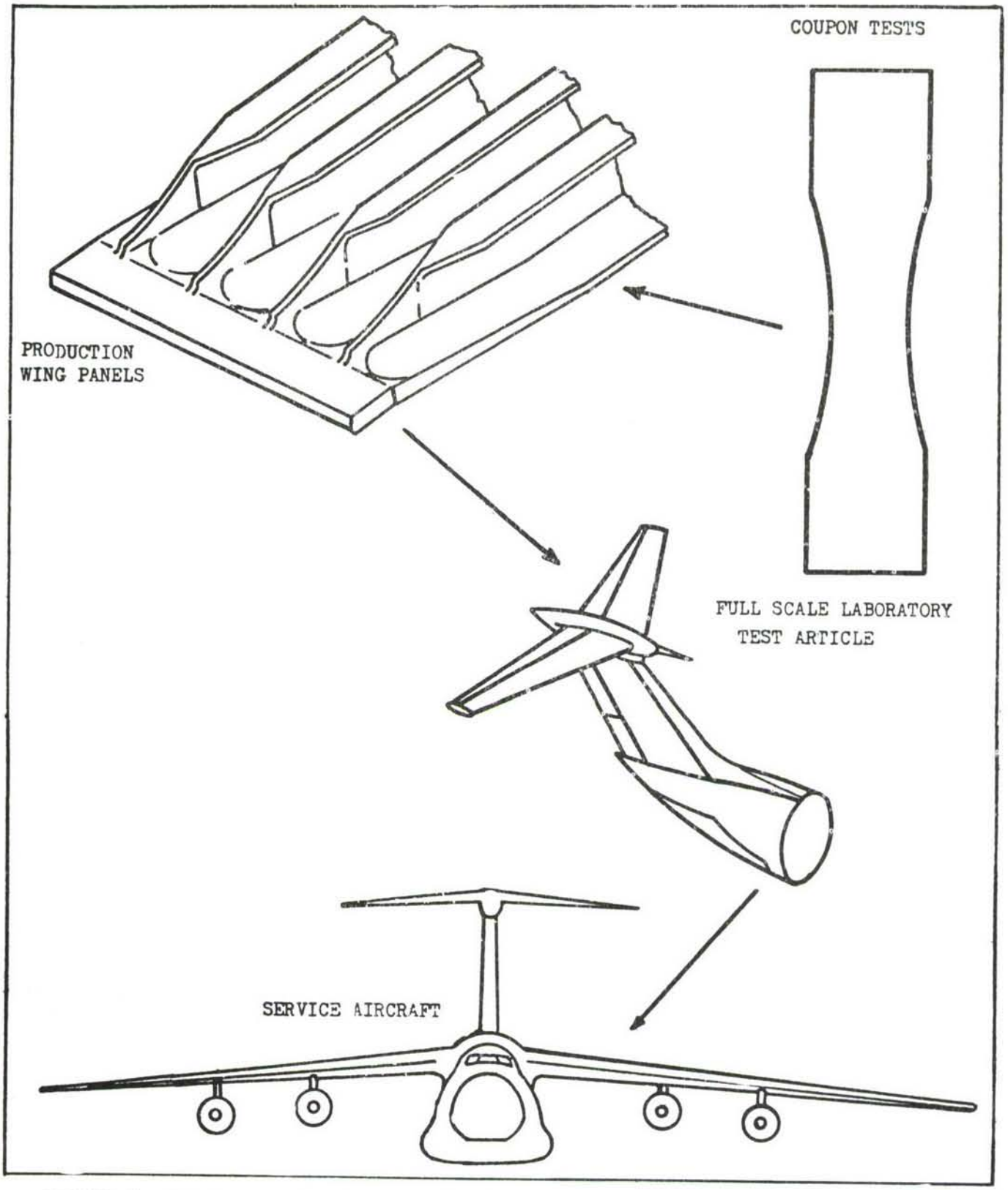

FIGURE 1 THE PROGRESSIVE SEQUENCE OF SENSOR EVALUATION ACTIVITIES TO OBTAIN UTILIZATION ON SERVICE AIRCRAFT

electrical resistive material when subjected to cyclic or fatigue loading. In practice, the material or sensor is bonded to the structure and experiences cyclic strains that are directly related to those experienced by the structure at the point of application. Of course, the sensor does not measure fatigue damage of the structure directly, but experiences a permanent resistance change which at any time is dependent on the cyclic strain history of the structure. Since structural fatigue is a function of this cyclic strain history, the resistance change can be considered as an indication of the structure's fatigue status. This sensor concept has many advantages over others that have been proposed throughout the years. It is inexpensive, light weight, and requires very little space. Since the mechanically induced resistance change is permanent, instrumentation is necessary only when it is desired to measure the resistances. There are many other advantages, however these are considered to be the most important and indicate the unique suitability of the fatigue sensor concept for monitoring the service load experience of operational aircraft. This concept has been evaluated during Air Force sponsored programs oriented toward the eventual practical application of a fatigue sensor system to military fleet aircraft. The feasibility of measuring the resistance change of a bonded work hardenable foil sensor as a function of a structure's exposure to repeated load occurrences was demonstrated as a result of performances on Contract AF33(615)2505 (Ref. 6). This program indicated the potential for a practical sensor application to subsonic aircraft structure, and resulted in Contract No. F33(615)-68-C-1221 to evaluate the performance of fatigue sensors on the C-5A fatigue test airplane.

Figure 1 illustrates the sequence of engineering steps deemed necessary, and the approach now being followed to produce a practical fatigue damage information system for service aircraft. Coupon tests (Ref. 6) were first used to determine the behavior characteristics of the sensor. The attainment of satisfactory sensor performance on simple test coupons resulted in follow-on evaluations of the sensor (Ref. 7) on more complex production wing panels. Knowledge and experience gained during these initial programs indicated the feasibility of implementing the system on service aircraft provided a sensor/aircraft calibration was first obtained for the particular type aircraft to be instrumented.

The results of previous programs had also indicated the necessity for further developments and optimization of the practical aspects of sensor installation, monitoring, and interpretation on full scale structural integrity fatigue test specimens. Continued development of the fatigue sensor at this time was economically attractive since the development of the C-5A airplane presented a timely opportunity to concurrently evaluate the practicality of the sensor system along with other contractually required structural test programs. The C-5A fatigue test specimens represented production aircraft structures that would be strain gage instrumented and evaluated under a controlled fatigue environment. A "piggy back" sensor installation on laboratory fatigue test structure presented a unique opportunity to concurrently obtain sensor calibration data for later correlation with similarly instrumented flight vehicles.

Figure 2 shows the allocation of sensors to the major components of the C-5A airplane. For test purposes the complete C-5A structure was sub-divided into separate basic specimens to simplify the test loading and the evaluation of

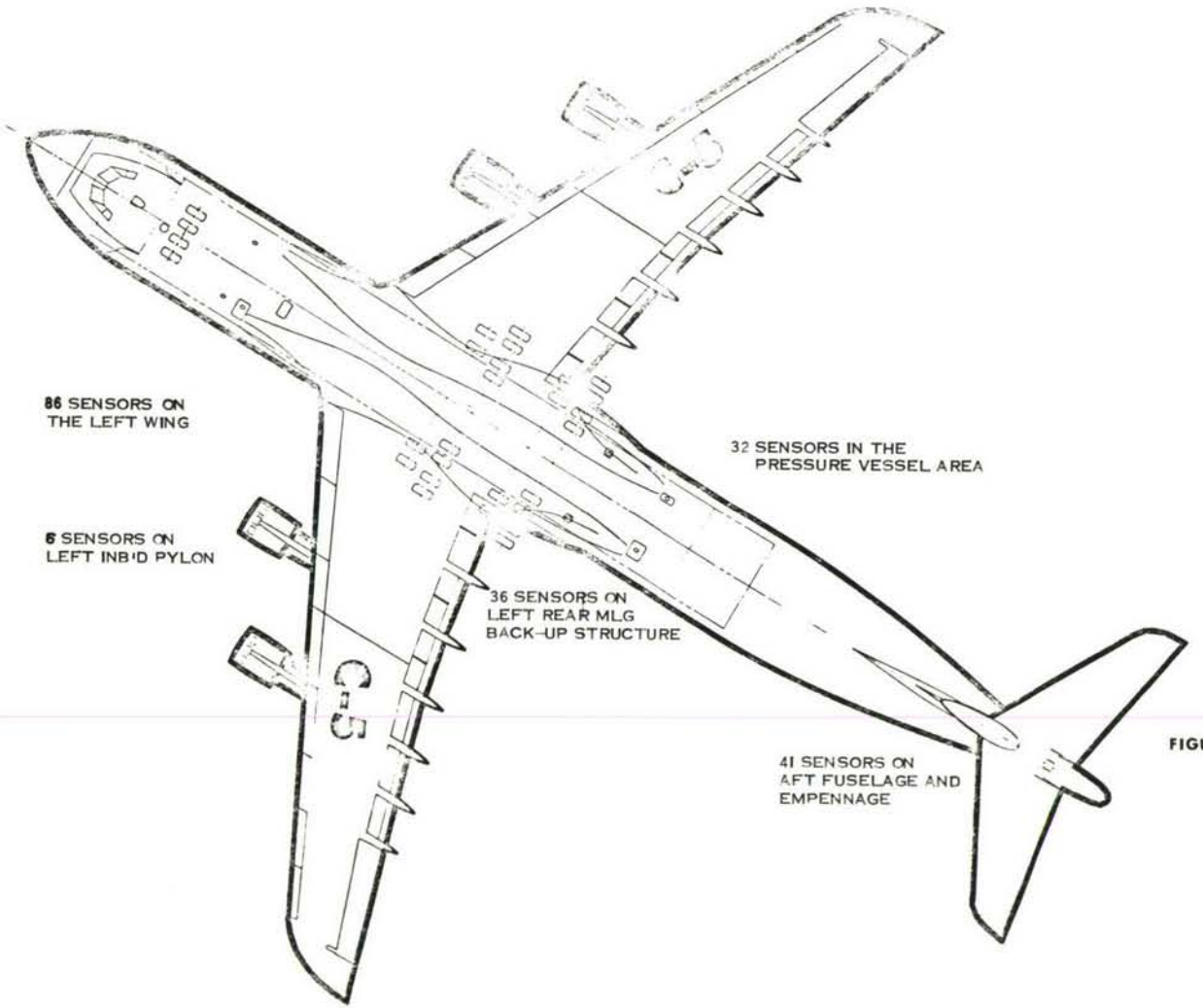

FIGURE 2. ALLOCA ON OF SENS RS ON THE COMPLE F C-5A AIRCRAFT

the results. Fatigue sensors were applied to the three major fatigue test specimens which constituted the equivalent of one complete C-5A airplane structure. These components are specifically identified as the (1) Main Landing Gear Specimen, (2) Empennage-Aft Fuselage Specimen, and (3) Wing-Fuselage Specimen.

A sensor-to-structure calibration was obtained on each specimen by periodically monitoring the sensor output response for a selected period of time. This calibration provides base line data for later correlation and assessment of fatigue damage on a similarly instrumented flight aircraft.

The instrumentation on the test specimen is terminated at a central location and the sensor outputs are sampled at periodic intervals such as the end of each pass or any interval representing a specific number of simulated flight hours. Since the change in the sensor is metallurgical in nature, continuous electrical energization is not required. The electrical resistance change as a function of the metallurgical state is an irreversible process (within temperature limitations) and constitutes a sensor "memory capacity" for repetitive cyclic strain.

One method of predicting fatigue damage is to monitor the cyclic strain history of a structural component in service, and compare it to the strain history of an identical component which had been fatigue tested to failure. Basically this approach for utilizing sensor information encompasses two fundamental methods for assessing fatigue damage. They are as follows:

- o THE STRUCTURAL FATIGUE DAMAGE ALLOWABLES MAY BE EXPRESSED IN TERMS OF SENSOR RESISTANCE CHANGE.

  The technique is to establish the relationship of structural load experience to bracket values of sensor resistance change necessary to produce visible fatigue damage. This method requires that once a sensor calibration is obtained, duplicate sensor locations must be used for follow-on instrumented airframes.

- o REDISTRIBUTION OF INTERNAL LOADS FOR LOCATING AN AREA OF FATIGUE DAMAGE.

  This technique for locating a fatigue crack or area of visible fatigue damage depends upon load redistribution. Additionally, there must be an adequate number of sensors in the area which would be influenced by this redistribution. The sensor outputs when displayed graphically, will show an abnormal rate of change in the plotted values of resistance.

Test data previously obtained (Ref. 6) have indicated the sensors will also show what type of service produced the more severe structural loading and in what area of the structure this loading occurred. Information of this nature becomes valuable when comparing the relative severity of test loading with that of service loading. Regardless of the degree of utilization of sensor capabilities, it has become more and more apparent that the strain history of a flight structure can be registered and stored by a simple foil sensor.

Previous investigations (Refs. 6 and 7) suggested that a sensor calibration could be obtained using a lead-the-force aircraft in lieu of a full-scale fatigue test specimen. The same discussions also indicated the advantages of sensor calibration on a full-scale laboratory specimen which could be repetitively loaded to structural failure. It has been shown (Ref. 6) that the sensor resistance change at structural failure could not be anticipated, but once established, the sensor response becomes a calibration for all subsequent structures. Laboratory and field evaluations (Ref. 7) have indicated that the approach conducive to the greatest service potential requires (1) laboratory calibration on full-scale structure, (2) application to "virgin" structures only, (3) knowledge of structural loads under service conditions, and (4) full utilization of standard airplane development and operational test programs to support interpretation of sensor readings.

The laboratory calibration of fatigue sensors on the C-5A fatigue test specimens, as discussed in this document, represents one more step considered necessary to obtain system utilization on service aircraft.

SECTION II

TECHNICAL DISCUSSION

2.1 BASIC OPERATING PRINCIPLE OF THE SENSING ELEMENT

A detailed discussion of the behavior characteristics of annealed Constantan foil is contained in reports regarding previous investigations (Refs. 6 and 7); however, a brief review of the basic fundamentals will be repeated here.

The strain gage user normally associates a change in gage electrical resistance with a dimensional change in the gage strand. This is further recognized as being related to the following classical formula:

$$R = \rho \frac{L}{A}$$

Where:

- R = Resistance (ohms)
- L = Length (in.)
- A = Cross sectional area (sq. in.)
- ρ = Resistivity constant

Fatigue sensor utilization requires that the user think in terms of electrical resistance change as a function of a metallurgical condition rather than a dimensional change in the sensor. Therefore, if one wanted to produce a resistance change without producing a corresponding dimensional change he could do so by altering the metallurgical condition of the sensing material (Refs. 8 through 10). That is, if one starts with a material in the soft state he can produce a resistance change by hardening the material e.g., by heat treatment, cold working, strain hardening, shot peening, etc.

Metallurgical handbooks (Refs. 11 and 12) indicate that the relationship between electrical resistance change and material hardening is a logarithmic function as shown in Figure 3 and follows the general form of $y = \log X$. It can be observed that up to a value of about five ohms the sensor resistance change with respect to work hardening shows maximum linearity and sensitivity. Further electrical resistance change of the sensor approaches the full hard metallurgical condition asymptotically and with corresponding minute resistance changes.

Since this change is metallurgical in nature it is not necessary that the sensor be electrically energized in order for this phenomenon to occur. The variable used then to produce a resistance change in the bonded sensor during structural application is strain hardening. It should be noted that the same basic mechanisms which produce fatigue damage in an aircraft structure will also produce strain hardening in an annealed foil bonded to that structure. That is, the operational and environmental loads imposed on the aircraft structure produce a movement of metal which results in strain hardening of the sensor and a corresponding electrical resistance change.

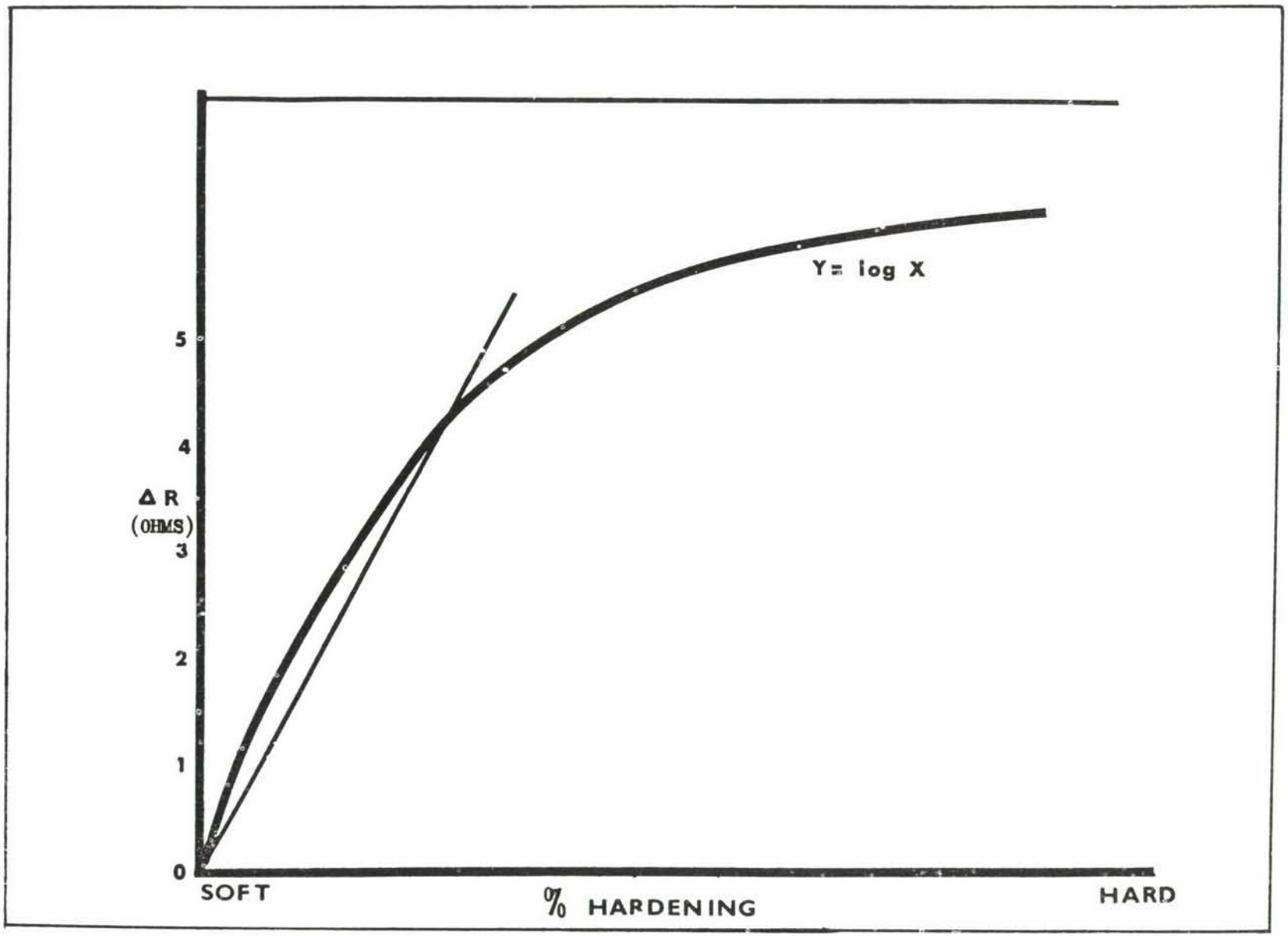

FIGURE 3. RELATIONSHIP OF SENSOR RESISTANCE CHANGE TO STRAIN HARDENING

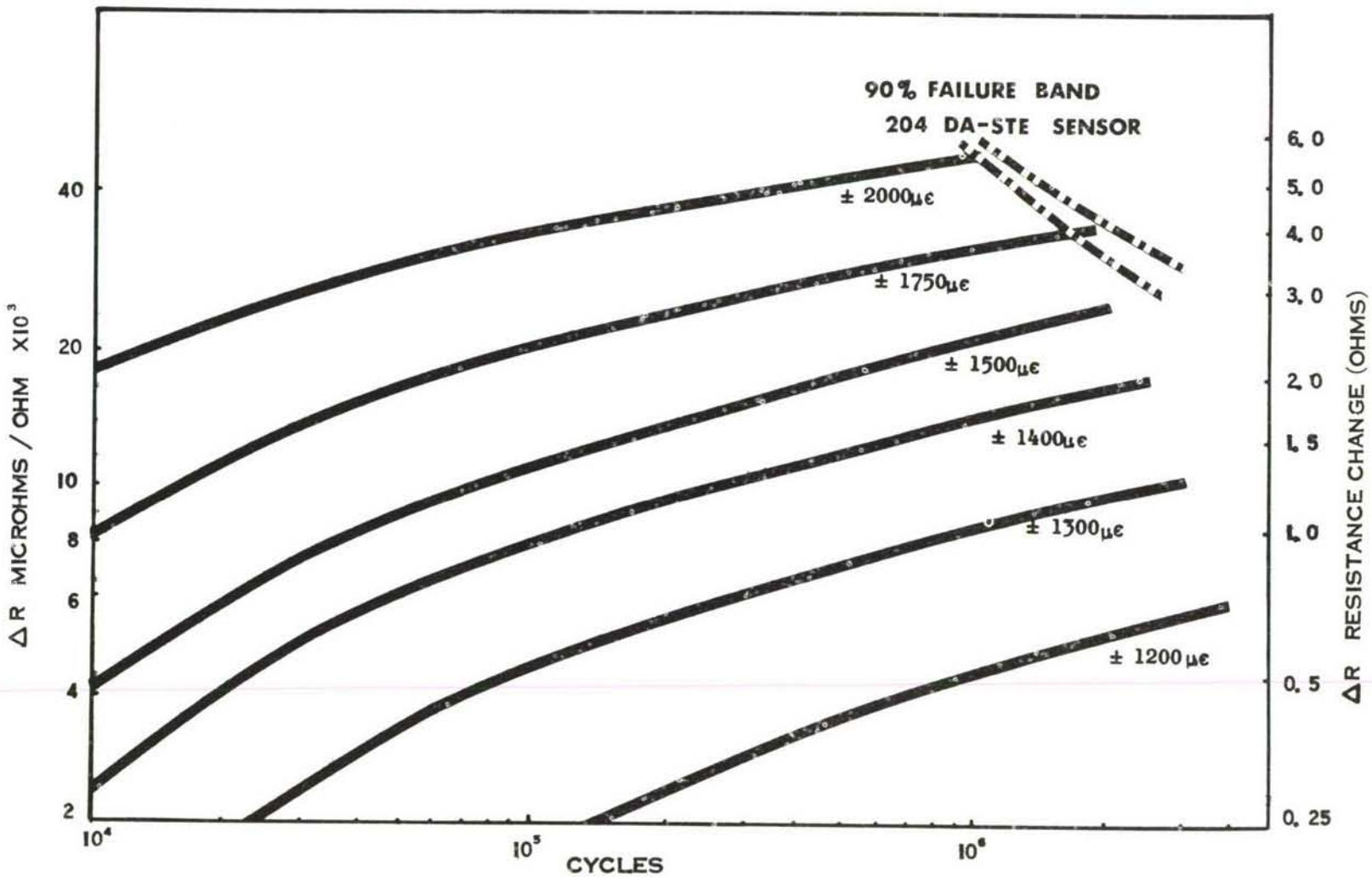

FIGURE 4. RESPONSE OF ANNEALED CONSTANTAN TO REVERSED STRAIN CYCLES (ZERO MEAN)

TABLE I

VARIABLES WHICH AFFECT THE FATIGUE LIFE OF A SUBSONIC AIRCRAFT STRUCTURE

1. AMPLITUDE OF STRAIN CYCLES.
2. NUMBER OF STRAIN CYCLES.
3. MEAN STRAIN LEVEL.
4. SENSE OF STRAIN CYCLES.
5. ORDER OF STRAIN CYCLES.
6. STRESS CORROSION.
7. TEMPERATURE

The behavior characteristics of the sensor when subjected to zero mean, constant amplitude, completely reversed cyclic strain level, is shown in Figure 4. Each curve of the family illustrates the electrical resistance change of annealed Constantan as a function of exposure to cumulative cycles at a particular strain level. Although these curves are not used for the correlation of sensor resistance with structural fatigue status, they do provide information regarding the fatigue life and repeatability of the sensor itself. An S-N curve "dotted in" shows the scatter in fatigue life and resistance change expected at various strain levels for high cycle applications. The S-N curve also indicates that allowing the sensor to exceed five ohms in resistance change approaches a "high-risk" area of operation.

The basic sensing element used is a die-cut high elongation strain gage (annealed Constantan grid) as manufactured by Dentronics Inc. Other types and configurations of annealed Constantan gages have been evaluated (Ref. 6) and all show essentially the same resistance change characteristics. Extensive fatigue tests, however, have indicated that an annealed Constantan grid fabricated by the die-cut method resulted in less scatter and a longer life expectancy for the sensor material.

2.2 VARIABLES WHICH PRODUCE STRUCTURAL FATIGUE DAMAGE

The influence of the variables shown in Table I on fatigue was assessed in terms of the structural engineering experience accumulated throughout the aircraft industry. On the basis of the assessment, the variables are arranged in a decreasing order of severity, that is, the variables listed at the top have the greatest affect on the fatigue life of the structure. It is recognized that exceptions can be cited which would alter the order in which the variables are listed, for example, fatigue can be greatly accelerated in a corrosive environment thus altering the sequence of significant parameters. The list, however, is generally applicable in the majority of the cases for subsonic cargo/transport category aircraft in the Air Force inventory. Only those items which are a function of the operational environment have been considered. The tabulation does not include specific airplane or material variables such as residual stresses, stress concentrations, fabrication and metallurgical defects, etc., all of which influence the fatigue life of a structure but which are not directly sensed by the fatigue sensor.

The mechanical fatigue process is basically load-cycle dependent. It is this feature, in conjunction with the strain hardening characteristics of the sensor material, that is exploited in this program. Previous investigations with annealed Constantan foils (Ref. 6 and 7) have indicated a strong and consistent response to the number of cycles and the amplitude of the applied loads. The response of the sensor is less affected by variations in mean load, a trend which is consistent with experimental fatigue results.

Strain hardening of the sensor material can be accomplished with compressive as well as tensile loads. This being the case, the sensor can be expected to show a similar response to compression-compression and tension-tension fatigue loads of equal magnitude. Since the two loading conditions do not cause the same extent of fatigue damage, this characteristic must be considered in the application of the sensor as a fatigue monitoring device. In the proposed application the effect is of little significance because of the comparative nature of the assessment in terms of a calibrated article. Independent investigations and developments however, have produced a reduction in sensor response for compressive fatigue loadings when the sensor is used in combination with a strain multiplier (see Section 2.3).

Load sequence effects can be significant depending on the relative magnitude of the loads in the spectrum and the degree of simulation with the actual load occurrence experienced by the structure. Test procedures must include sufficient mixing of loads to minimize the influence of sequencing effects on the response of the fatigue sensor. Sensor application discussions (Section 3.7), concerning the use of the strain multiplier elaborates on the need to properly "weight" the influence of occassional large strain excursions upon the resistance change of the basic sensor material.

The sensor installation includes the application of a sealer to insulate the sensor from humid or corrosive environments. Corrosion is therefore not included as a measured function of the fatigue sensor. Similarly, temperature effects on sensor readings are discounted by compensating for thermal expansion or collecting the data within specified temperature limits.

Since it was desired to obtain a more favorable overall response i.e., a resistance change more properly weighted to actual structural damage incurred, some mechanical manipulations seemed appropriate for the Constantan sensor. These requirements led to the application of the mechanical strain multiplier.

2.3 MECHANICAL STRAIN MULTIPLIER TECHNIQUES

Experience with the unamplified annealed Constantan sensor on typical aircraft structure has illustrated very dramatically that the sensor's threshold sensitivity was inadequate for a practical application to subsonic fleet aircraft. This problem first became apparent during the feasibility study (Ref. 6) and resulted in an electrical resistive material which cannot respond to all of the nominal cyclic strains producing fatigue damage in subsonic aircraft structure. Since this material produces no measurable resistance change at strain levels less than $\pm$ 1000 $\mu\varepsilon$ it must either be used in areas of stress

concentration or manipulated so that it senses higher strain than normally experienced in nominal areas of subsonic aircraft structure. Contrary to the approach for application of the S/N gage (Ref. 13) (which advocates installation of the sensing device at the point where structural failure will occur) the configuration and geometry of modern aircraft structure forces the user to locate the sensor in nominal areas.

Previous attempts to mechanically adjust the sensor apparent threshold sensitivity were conducted during the feasibility study (Ref. 6). This effort resulted in the development of techniques for mounting the sensor on a concave curved aluminum shim so that upon bonding the shim to the structure a tensile pre-stress was produced in the sensor. Although these attempts to alter the threshold sensitivity did not produce the results desired, the potential for employing a multiplying shim was evident even at this time. Subsequent efforts by industry resulted in annealed Constantan gages mounted on various configurations of mechanical strain amplifiers. Harting (Ref. 14) discussed a type of mechanical strain multiplier and Thomas (Ref. 15) discussed a strain multiplier technique investigated by Hawker Siddely Aviation of England. Regardless of the configuration of the mechanical strain amplifying device, all of the various techniques have one thing in common and that is; to circumvent the threshold sensitivity limitation of annealed Constantan. This material's lack of sensitivity to low strain levels was recognized by the AFFDL early in 1967 from results of the feasibility study. An independent investigation to correct this deficiency and develop an improved sensor was initiated in April 1969 and reported in AFFDL-TR-70-141 (Ref. 16). Due to the timing, however, these sensor improvements could not be implemented in the practical sensor application effort on the C-5A test specimens.

Although previous experience had indicated that errors and erratic operation are inherent with most mechanical strain multiplying devices, reasonable care in utilizing the type shown in Figure 5 did produce reasonable results. The basic device is composed of an aluminum shim with accordian like grids over which an encapsulated sensor is mounted. The composite is then bonded to the structure so that it has a specific ratio of unbonded length to sensor grid length. The sensing element used through out the program is a high elongation die-cut strain gage as manufactured by Dentronic Inc., and designated as either a 204DA-STE or 202DA-E depending upon its gage length. The sensor-multiplier is assigned the prefix "SAP" with the "SA" meaning strain amplifier and the "P" designating a polymide backing.

The construction and typical installation features of the device can best be explained by reference to the illustrations in Figures 5 and 6. The shim for the 1/4 inch gage length sensor (SAP204DA-STE) contains 8 slots and 7 lands which are equally spaced over the quarter inch gage length producing slots and lands each approximately 0.0166 inches wide. The shim for the 1/8 inch gage length sensor (SAP202DA-E) contains 6 slots and 5 lands equally spaced over the one-eighth gage length producing slots and lands each approximately .0113 inches wide. The fabrication of the slots appeared as the most time consuming and

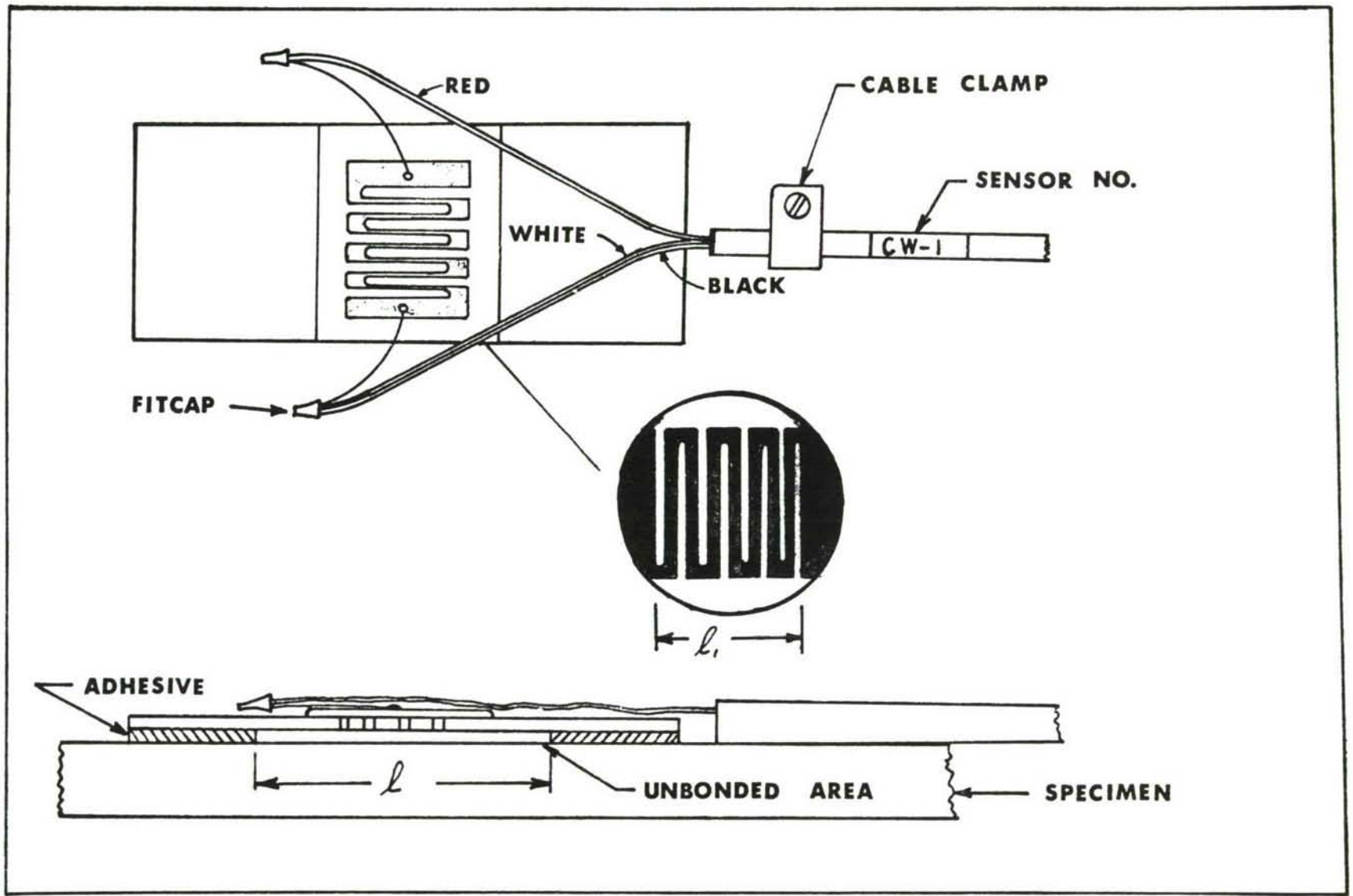

FIGURE 5. TYPICAL SENSOR INSTALLATION (SAP 204DA-STE)

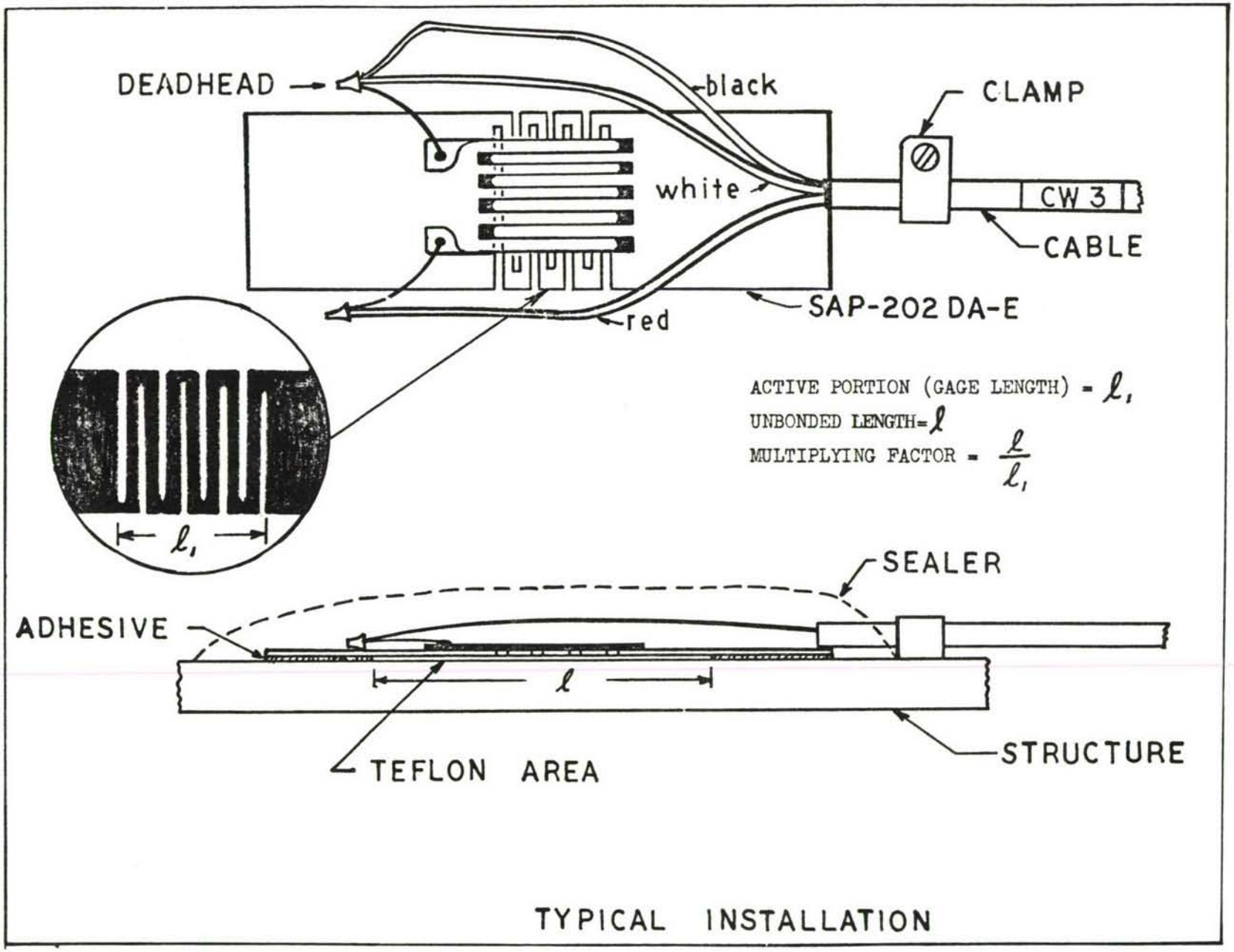

FIGURE 6. TYPICAL SENSOR INSTALLATION (SAP 202DA-E)

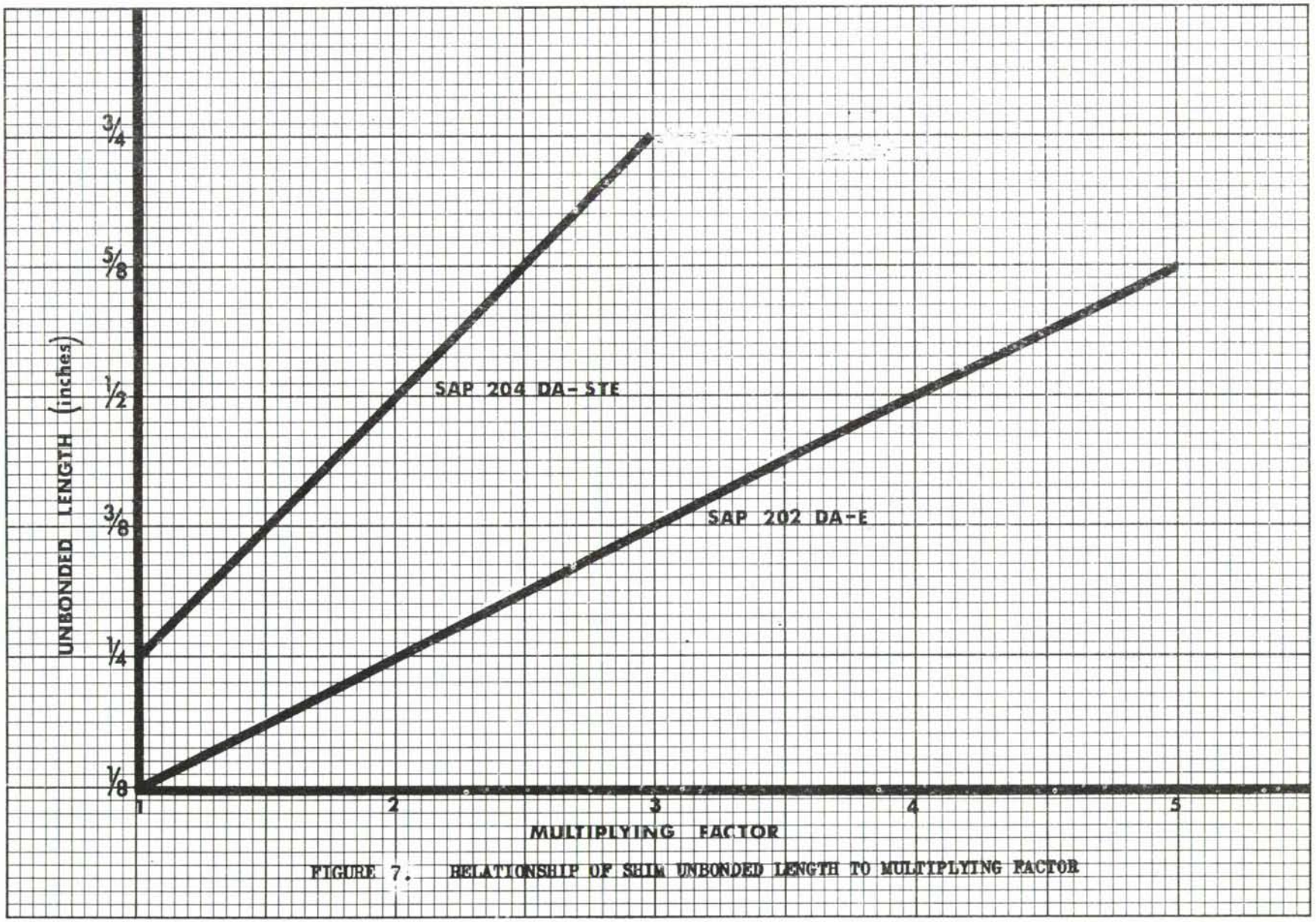

FIGURE 7. RELATIONSHIP OF SHIM UNBONDED LENGTH TO MULTIPLYING FACTOR

essential part of the device's construction. Although slots could be formed by a spark erosion technique using a commercial "ELOX" machine (Model AP100NW) this method proved expensive and time consuming for volume production. A milling technique resulted in the forming of precise slots at a reasonable cost. The slots as shown are filled with viscoelastic material which will allow this section to axially move in "accordian" fashion yet the configuration is stiff enough to prevent bowing when subjected to small compression loads. There is an additional extra layer of Kapton 0.002 inches thick underneath the sensor to prevent the possibility of a stress concentrator developing where the sensor strands cross the slots. The elastic filler also is used to prevent the sensor bonding epoxy from getting into the slots and bridging across.

Emphasis was placed on fabrication methods and configuration techniques which will prevent the field installation from becoming critical. The only critical portion of the installation is the ratio of the bonded area to the unbonded area. To simplify this, two mil thick Teflon tape is centrally placed, sticky side down on the specimen and underneath the shim slotted area to prevent the epoxy from flowing into unwanted areas and upsetting the amplifier ratio. When the shim is bonded the Teflon is left in place beneath the slots leaving this portion of the shim free to "breathe". The theoretical mechanical strain multiplier ratio can be determined by selecting proper values of "ℓ" and "ℓ_1" and as shown in this case, (Fig. 5) the grid length of the 204DA-STE sensor is fixed at 1/4 inch with specific widths of Teflon tape used to fix the unbonded length. The curves of Figure 7 indicate the multiplying factor to be obtained by using a specific tape width.

To evaluate the effect of test structure reinforcement by the shim and the shear strength required for a metal-to-metal bond, additional tests were conducted to determine shim rigidity. A shim sensor combination was mounted in a low range Instron load machine and sensor apparent strain readings versus load were recorded (Fig. 8) for the two types of strain amplifier shims used. These curves show the relative tensile stiffness presented by the slotted area of each size shim. As a case in point, the SAP204DA-STE fatigue sensing device requires a load of only 3.52 pounds to produce a shim elogation of 3000 micro inches per inch. Therefore, even though the shim might be bonded to aircraft thin skins it was concluded that the shim would have negligible restraining effects. It should be noted that the adhesive shear strength required to produce an effective metal-to-metal bond is relatively low since the force required to operate the "accordian like" grids of the shim is insignificant even for elogations of 4000 micro inches per inch. For instance, a calculation of the bonded area on either side of 5/8 inch Teflon tape for the type SAP204DA-STE sensor shows that less than 22 psi shear strength is required to produce an elongation of 6000 micro inches per inch in the device (Appendix II).

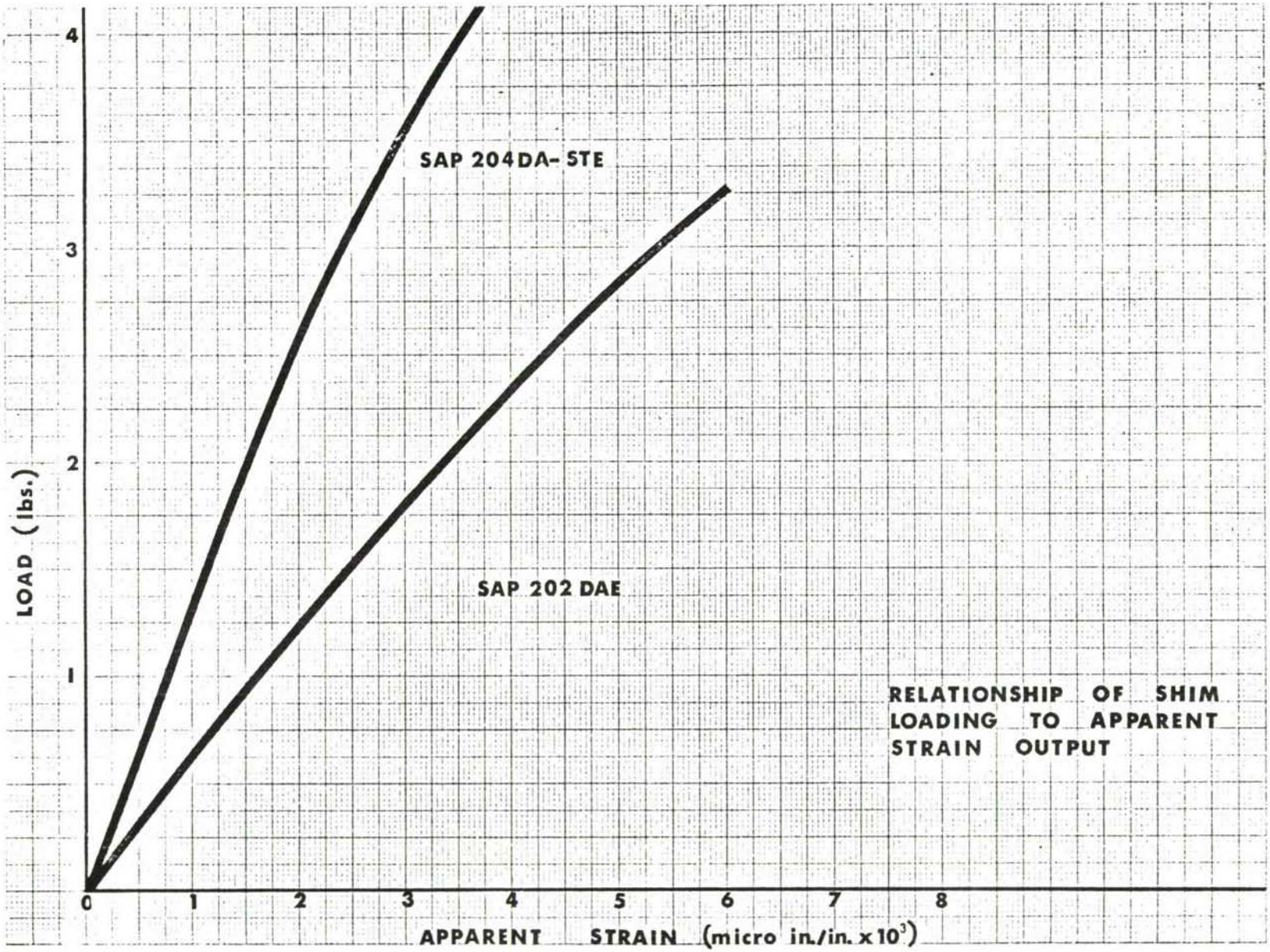

FIGURE 8. RELATIONSHIP OF SENSOR ELONGATION TO SHIM LOAD FOR THE TWO TYPES OF SENSING DEVICES

Another purpose of the viscoelastic filler in the shim slots is to de-emphasize the influence of compressive strains on the resistance change of the sensor. Experimentation with various filler materials resulted in the selection of a filler which offered no restraint to tension strains, however, it attenuated the influence of compressive strains by approximately 30% (Appendix II). That is, the filler allowed the slotted area to freely elongate in tension, yet was so nearly incompressible that the slotted area behaved as almost a solid piece to compressive cycles. This technique tends to bring the sensor resistance change values more in line with fatigue damage occuring during this mode of loading.

The construction of the strain multiplier is such that it appears applicable only for axial strains. The sensing element of the installed transducer is at least 0.020 inches above the structural specimen surface so its application to bending strains is severely limited. This characteristic, however, does not impose any constraints upon its intended usage since the aircraft primary structure will experience axial strains as opposed to bending strains.

The metal-to-metal bonding technique developed for this program appears to be the most practical for application to a flight structure and is the one more tolerant of human error. The bonding techniques used were an outgrowth of the metal-to-metal bonding techniques applied to the pre-stressed shims used during the initial feasibilities studies (Ref. 6). The bonding techniques used have withstood the more severe testing at a cyclic frequency of 30 hertz without a bond failure. The surface preparation and bonding procedures used throughout this program are appended to this report as Appendix I.

Verification testing of the sensor multiplier was initially conducted on simple tension-tension coupons as shown in Figures 9 and 11. Static strain surveys were conducted at selected intervals during fatigue cycling to confirm the stability of the amplification factor after fatigue exposure. No significant changes in multiplying factor occurred, which indicated no deterioration in the metal-to-metal bond. Both sizes of shim mounted sensors were also subjected to completely reversed axial strains in the manner depicted in Figures 10 and 12. The average response and the statistical scatter in data experienced with the type SAP204DA-STE mechanically amplified sensor are shown in the log-log plot of Figure 13. These data represent a limited number (14 samples) of sensor/multiplier evaluations which were conducted subjecting the coupons to a constant amplitude, completely reversed strain level of $\pm$ 500 $\mu\epsilon$. At an actual multiplier of 3.0 the apparant strain level experienced by the sensor is approximately $\pm$ 1500$\mu\epsilon$ and compares favorably with that shown for an unamplified sensor (Fig. 4) at a comparable strain level. Some scatter in sensor ΔR values was expected since errors are inherent with most mechanical strain amplifying devices; however, the repeatability does appear acceptable for the intended application. The bandwidth of $\pm$ 5% of reading on the high cycle

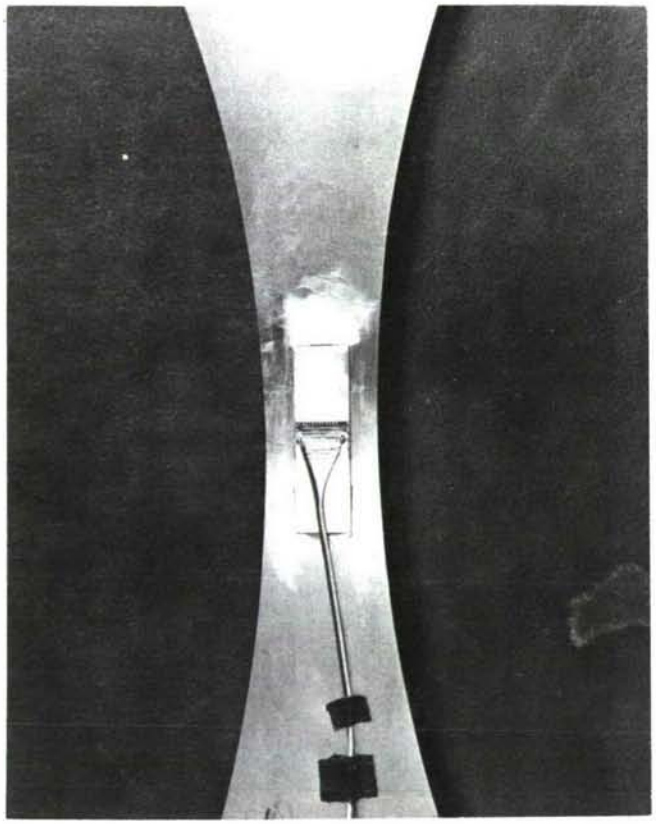

FIGURE 9. VIEW OF SAP204DA-STE SENSOR INSTALLED ON TEST COUPON

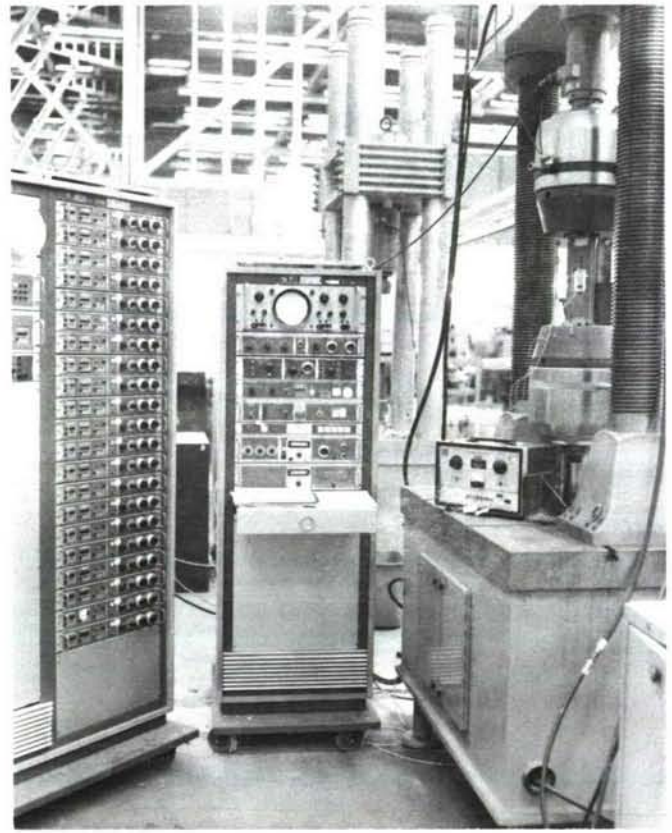

FIGURE 10. TEST SET-UP FOR APPLYING COMPLETELY REVERSED AXIAL LOADS. NOTE LATERAL SUPPORT PLATES TO PREVENT BENDING

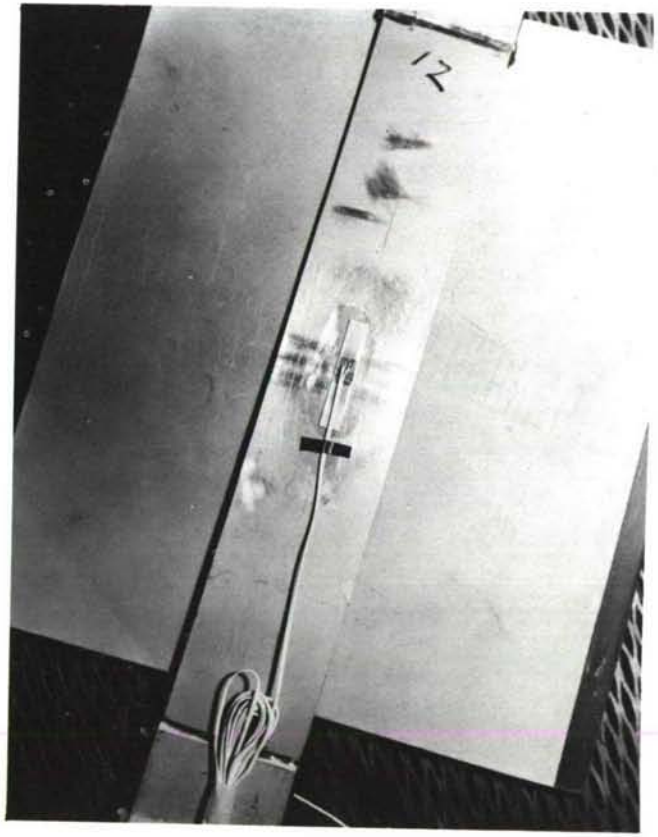

FIGURE 11. VIEW OF THE TYPE SAP202DA-E SENSOR INSTALLED ON AN AXIAL TEST SPECIMEN. A WATERPROOFED SENSOR IS INSTALLED ON THE OPPOSITE SIDE

FIGURE 12. TEST EQUIPMENT USED IN THE PRELIMINARY EVALUATION OF THE STRAIN MULTIPLIER

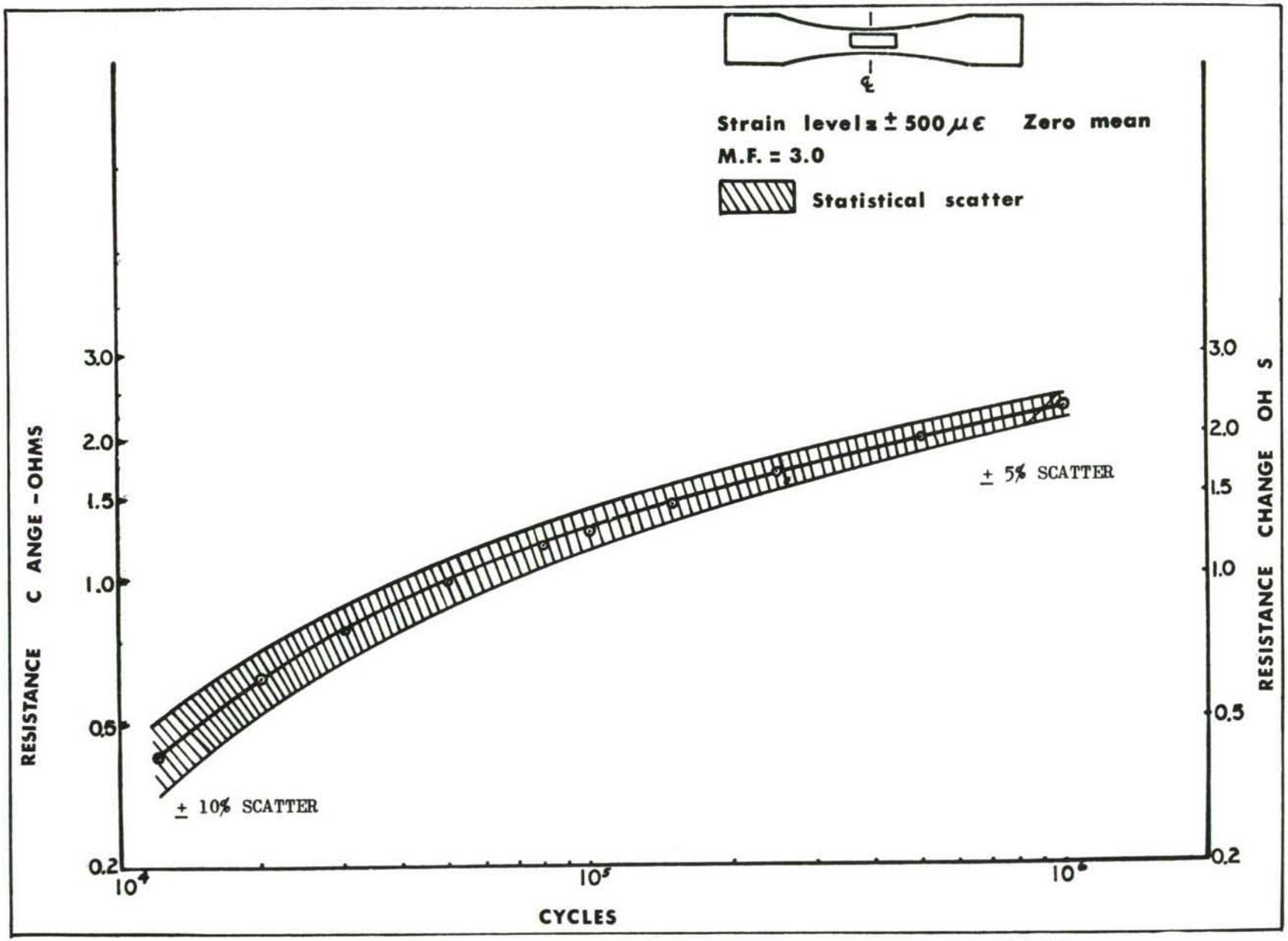

FIGURE 13. RESPONSE OF THE SAP204DA-STE SENSOR TO CONSTANT AMPLITUDE COMPLETELY REVERSED STRAIN

end and ± 10% on the low cycle end appears reasonable. A comparison of the preliminary test data also indicated that the resistance change characteristics of the two types of sensing devices are essentially the same; the primary difference being one of size and configuration. Since bonding and utilization techniques were essentially the same for both, the smaller type SAP202DA-E (Fig. 6) was used in the space limited areas of the C-5A structure.

In some respects the resistance change of the sensor versus accumulated cycles at various strain levels (Fig. 4) is analogous to Miner's theory (Ref. 17). That is, the work hardening of the bonded annealed foil element is a direct function of the net work absorbed by it. The total resistance change of the sensor is related to the total work absorbed by the sensor whether it is composed of a large number of low strain cycles, a small number of high strain cycles, or a random mixture of number and amplitude of strain cycles. Comprehensive testing (Ref. 6) has shown, however, that the total sensor resistance change for a structural failure depends upon the loading mode. Therefore, a comparison technique (calibration) was employed during sensor utilization on the C-5A fatigue test specimens and Miner's theory was not considered.

The intended application of the sensing device required that it be installed in areas of the C-5A aircraft that would either be subjected to hydrostatic pressure or jet fuel. This requirement posed the question of the restraining effects of waterproofing compounds upon the movement of the accordian grids of the multiplier. Baldwin-Lima-Hamilton barrier "E" and Dentronic Inc., Denseal 5 waterproofing compounds were evaluated on laboratory coupon tests. The sensing devices were bonded to the test coupons in a back-to-back arrangement (Fig. 11) so that both were subjected to the same strain level; however, one multiplier was sealed with the waterproofing compound while the opposite one was left uncoated. Statistical data on the two types of strain multipliers and the two types of waterproofing compounds indicated no restraining effects were produced by either of the sealing techniques.

2.4 PROPOSED CORRELATION OF CALIBRATION DATA WITH FLIGHT DATA

Structural fatigue monitoring systems have generally depended on recording the load experience of an airplane and converting the data to stress spectra to evaluate potentially critical fatigue areas. VGH programs provide the information necessary to support this type of fatigue monitoring system. The direct monitoring of strain gage output has also been used to evaluate the fatigue condition of local structure. These approaches require considerable supporting analysis and data reduction which affects cost and the availability of the results on a timely basis. The concept for the utilization of the fatigue sensor is to provide an improved system for monitoring the rate at which the fatigue life of a structure is expended. A practical approach to this problem is to relate the condition of the structure to the level of strain hardening of the sensor measured as a change in resistance. The objective can be progressively accomplished at various stages during the development of new airplane structures.

The full-scale airplane fatigue test program offers the first significant opportunity for calibrating the fatigue performance of the structure in terms of sensor resistance. The quality of the calibration is dependent on the degree to which the test conditions are representative of true operational conditions. In any case, the results must be interpreted considering the limitations of the sensor and the functions that contribute to the scatter observed in the occurrence of fatigue damage.

The fatigue test program serves several important functions in support of the successful application of the fatigue sensor. Verification of the suitability of the sensor location and strain multiplier is achieved to insure efficient sensor performance. Fatigue sensitive areas are also chronologically identified and descriptions of crack growth patterns are obtained. The calibration consists of associating the occurrence of physical structural damage with the change in resistance of appropriate sensors. These data form the basis for later improvements in which sensor readings are adjusted to reflect operational fatigue damage contributions not properly reflected in the test program. Figure 14 illustrates some tentative concepts for sensor data interpretation. The ratio of the sensor resistance of a service airplane, R_{Si}, and the resistance of a test airplane, R_{Ti}, at a given point in time is an indication of the service severity of a particular airplane with respect to the calibration airplane. Initially, the ratio is established to relate the severity of the

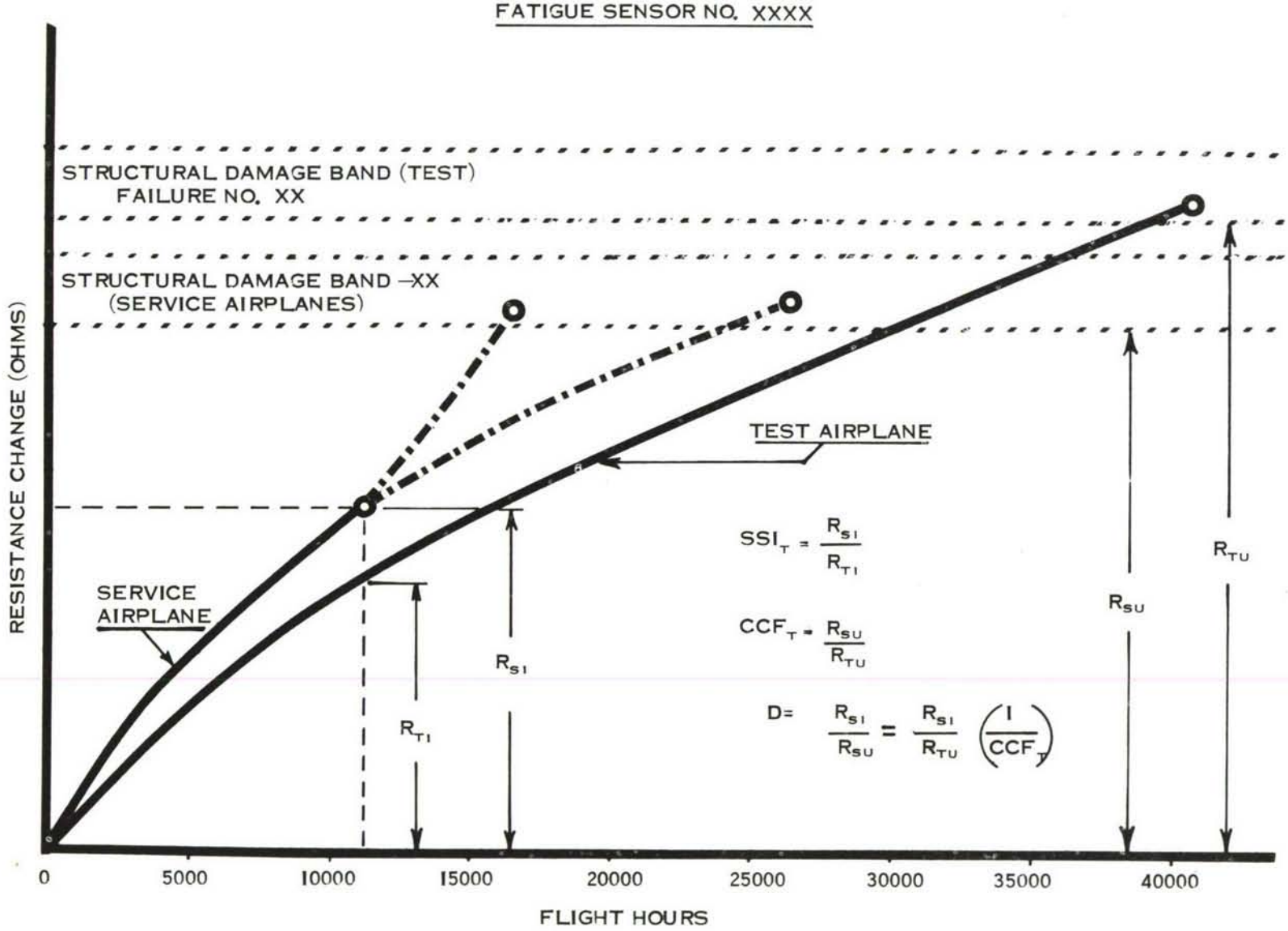

FIGURE 14. PROPOSED CORRELATION OF SENSOR CALIBRATION WITH FLIGHT DATA

load exposure of service airplanes and the fatigue test airplane. Improvements in the monitoring system may be expected by additional use of "Lead the Force" airplanes to establish baseline data. The service severity index may therefore be based on test, SSI_T, or on lead the force data, SSI_{LTF}.

Correlation of results in terms of the development of physical fatigue damage can be established by comparing the sensor resistance of service airplanes and baseline data at the time damage occurs. It is to be expected that the sensor resistance corresponding to fatigue damage in a particular area will be characterized by a series of bandwidths which must be considered in evaluating the condition of the structure. The statistical distribution represented by the bandwidth is a function of sensor performance, airplane usage, variation in environmental loads and structural fatigue scatter. Sensor data corresponding to the occurrence of physical fatigue damage can be used to establish a calibration correction factor, CCF, which is defined as the ratio of sensor resistance of service airplanes, R_{Su}, to baseline data R_{Tu}, for a particular failure. Correlation between service and baseline airplane results is improved by periodically updating the reference data on the basis of developed calibration correction factors. These factors may also be developed employing quantitative assessments of precrack fatigue damage based on nondestructive inspection or metallographic examinations.

The accumulated fatigue damage, D, in a fatigue sensitive area is the ratio of the change in resistance of the applicable sensor, R_{Si}, over the change in resistance corresponding to the failed condition determined from baseline airplane data, R_{Su}. Initial approximations of fatigue damage can be determined from

$$D = \frac{R_{Si}}{R_{Tu}} \qquad \left(\frac{1}{CCF_T} \right)$$

where the calibration correction factor is estimated.

SECTION III

TEST PROGRAM - GENERAL

3.1 PROGRAM OBJECTIVE

The objective of this program is to provide further practical development of annealed foil fatigue sensors by evaluating them on full-scale laboratory fatigue test components. To accomplish this objective, fatigue sensors were installed on C-5A components which were then fatigue tested at the Lockheed-Georgia Company facility.

It was anticipated that the pursuit of this principal objective would also provide information relative to other operating parameters considered pertinent for a practical application to service aircraft. These include the following.

- o Confirm the suitability of a bonded sensing device for long term (10 to 15 years simulation) application to complex aircraft structure.
- o Establish the criteria for selecting sensor locations and adjusting sensor sensitivity to the aircraft mission loading spectrum to obtain an optimum sensor response.
- o Determine sensor resistance change (ΔR) parameters applicable to correlation with structural fatigue damage.
- o Develop a simplified and practical approach for data acquisition.
- o Optimize data handling techniques in order to obtain and display meaningful information.

Accomplishment of these objectives implies a calibration and verification of the sensor system on full-scale aircraft structure subjected to a controlled fatigue environment. Previous investigations (Refs. 6 and 7) suggested a sensor system calibration might be obtained by using a lead-the-force aircraft in lieu of a full-scale laboratory fatigue test specimen. These same discussions noted the advantages of a sensor calibration on a laboratory test article. The advantages obtained by sensor calibration on the C-5A fatigue test article can be enumerated as follows:

- o Failure data can be correlated to sensor measurements without compromising flight safety.

- o Test schedules permitted the simulation of one service lifetime within a reasonable calendar time span (2 years).

- o An abundance of supporting instrumentation was available to assist in the confirmation of sensor behavior.

- o Continuous availability of the test structure for sensor monitoring over controlled loading and environmental conditions.

These advantages were considered very desirable during the initial effort to develop and evaluate the fatigue sensor information system for practical application to fleet aircraft. A return on the invested laboratory effort would be enhanced, however, if test data from the fatigue test specimen were evaluated concurrently with operational data from a lead-the-force aircraft.

3.2 TEST PROCEDURES AND LOAD CONTROL

Fatigue testing of large airplane components is a complex and expensive undertaking. Test procedures are developed to give as representative a test as possible within reasonable limits of time and cost. The block loading method was selected on the basis of these considerations. An average of sequencing effects is achieved by reversing the order of loading on alternate passes of the spectrum. The block loading test procedure used in the C-5A program was particularly suited for an evaluation of the relative severity of the various sources of fatigue damage in terms of sensor resistance change.

The loading spectrum was applied by a servo loading system which is considered state of the art, and although it is beyond the scope of this report to provide a complete discussion of the servo loading system, the basic operation was as follows:

The fatigue load control system used to apply cyclic test loads to the C-5A specimen was a closed-loop continuous-feedback servo control. The feedback was provided by a dual bridge load cell with the additional bridge monitored to provide a separate indication of actual load levels attained as a check on any deterioration of the feedback supplying bridge. The load cells used receive scheduled periodic calibration in accordance with MIL-C-45662A (Ref. 18) assuring traceability to the National Bureau of Standards.

Hybrid techniques were used for digital programming of analog servo-controllers, with test parameters input to the system by punched paper tape or teletype. The system contained all the necessary devices for program verification prior to execution. Selected strain gages, load cells and deflection measuring devices were continuously monitored on strip chart recorders to assure the correct load application. Test article structural weight and test jiggery weight were counter-balanced or otherwise considered when calculating or applying the test loads.

The load control system employed for the wing-fuselage specimen (X998) differed somewhat from that used for either X997 or X996. This system was more sophisticated, in the respect that it contained 150 closed loop servo channels operating as directed by an on-line computer. This type of control served to expedite operation of the larger multi-channel systems. Both types of systems were equally compatible to the sensor monitoring effort.

3.3 APPROACH FOR OPTIMUM SENSOR UTILIZATION

The behavior characteristics of the annealed Constantan sensor have been adequately defined as a result of past experiences. Optimum utilization of the sensor in a practical application requires that its response be adjusted to the cyclic load experience of the test structure in order to obtain meaningful results. The sequence of steps believed necessary to produce meaningful results are enumerated as follows.

- o Obtain preliminary stress analysis and test spectrum data for the specific structure under surveillance.
- o Determine the approximate number of sensing points required to adequately monitor the structures degree of exposure to repeated load occurrences. Select critical structural areas as control points.
- o Calculate the multiplier factor required for the selected structural location to establish proper relationship of cyclic strain experience to sensor resistance change characteristics.
- o Prepare sketches or other written information to define the sensor locations.
- o Install sensors in the selected locations using high quality installation techniques.
- o Verify the sensor multiplying factor by a strain survey and adjust as required or else accept a nominal scatter.
- o Periodically sample sensor resistance change (ΔR) and plot resistance change values as a function of accrued passes or cyclic test hours.
- o Evaluate sensor rate of resistance change, determine "key" sensors and their corresponding ΔR value for a structural failure.
- o Utilize any available supporting instrumentation which will provide an independent means of determining the fatigue status of the test structure.

The above list of guidelines was developed and implemented into the test program as the evaluation progressed. Each individual step is discussed in more detail in the following sections 3.4 through 3.10.

3.4 SENSOR APPLICATION TECHNIQUE

The results of previous programs (Refs. 6 and 7) have shown very conclusively that the sensor does not have the capability of measuring fatigue damage directly. Previous tests, however, have demonstrated that by proper application, the sensor does have the capability of monitoring the effects of repeated load exposure, thereby providing information for the assessment of fatigue damage. Consequently, sensor locations and sensitivities should be selected so that the sensing device would respond to all of the various modes of loading that could possibly contribute to structural fatigue damage. Loading sources which were established from C-5A mission profiles include, taxi, ground-air-ground, gust and maneuver, buffet, pressurization, and landing impact. The loads to be simulated, and an analysis of the damage produced by the applied loads, were developed as a requirement for the basic C-5A fatigue test program. It was believed that optimum sensor utilization during this initial effort required not only a sensor-to-structure calibration, but full usage of available supplementary information. The supplementary information most useful included the preliminary stress analysis, computer developed load occurrence curves, and structural damage analyses. This type of information is available early in a new airplane development program and is believed to be a necessary approach for a successful selection of **locations and sensitivities.**

3.5 SELECTION OF SENSOR LOCATION

The selection of critical sensor location areas was based upon manual screening techniques supplemented by computer data. The manual criteria used as a basis for sensor allocation includes locations

- o where failure would affect flight safety;
- o which were found to be critical on previous tests of component parts;
- o receiving a large number of relatively high varying loads;
- o which have significant area, configuration, or load path direction changes;
- o where weight limitations have created possible fatigue sensitive areas.

The selection of sensor locations were also governed by some physical and mechanical constraints as well as implementation of sensor techniques to obtain optimum operating response. For instance, the test laboratory practice for complete utilization of external structural surfaces for loading pads and test jiggery (Fig. 15) prohibits the practical installation of sensors in these areas. Figure 16 illustrates emphatically the physical difficulties that would be encountered if one attempted to install sensors and associated cabling on external structural surfaces.

In considering the instrumentation of a flight vehicle, it would not be advisable to install sensors on external surfaces since this might alter aircraft aerodynamic characteristics. These restrictions do not impose serious barriers to sensor usage under the present applied concepts, since it has been demonstrated (Ref. 7) that suitable information can be obtained using internal surfaces.

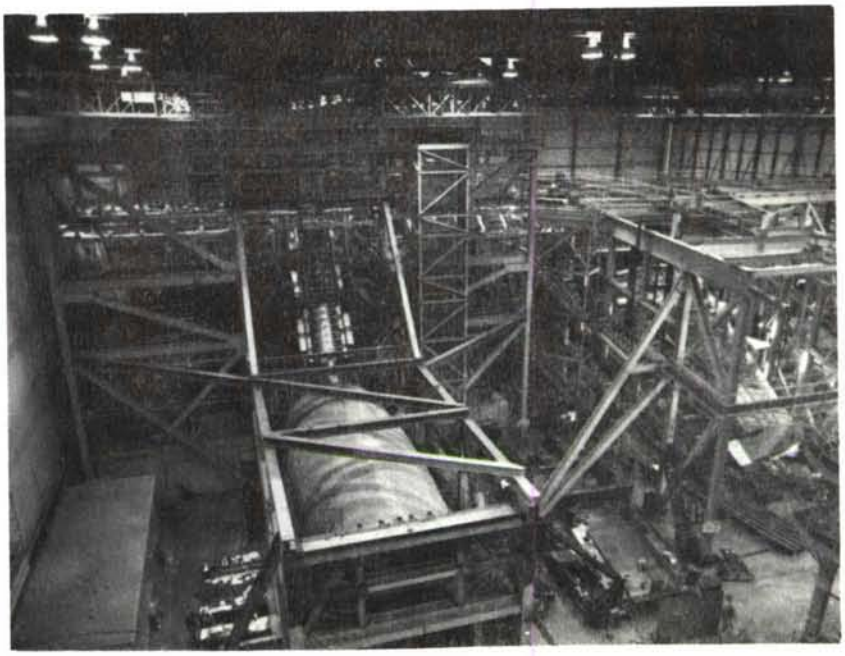

FIGURE 15. VIEW OF EMPENNAGE SPECIMEN AFTER ADDITION OF JACKS AND LINKAGE

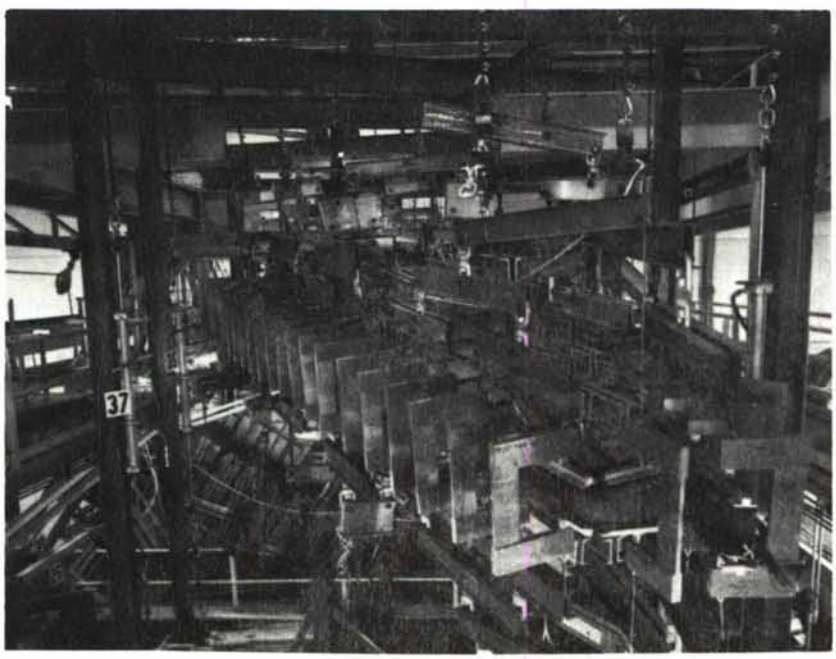

FIGURE 16. LEFT HAND HORIZONTAL STABILIZER AND SURROUNDING TEST FIXTURES. ALL SENSORS INSTALLED ON INTERNAL SURFACES

One school of thought (Ref. 13) states that the sensor must be located at the point where the structure will fail, or else the effort is "doomed" to failure. Although structural fatigue cracks are usually initiated at fastener holes or other areas of stress concentration, access to these areas are often restricted by fastener heads, splice plates or some other covering. These areas normally constitute a faying surface which will not permit a practical installation of the sensor at the point of highest strain. This consideration, coupled with the fact that the number of sensor installations required to monitor all of the myriad of fasteners or other concentrations in a modern aircraft structure, would be economically prohibitive. Futhermore, if anyone could forecast where this failure would occur the designer would simply redesign the part rather than allow the aircraft to be placed in service knowing that it would fail. Consequently, when all of the technical and practical physical factors are considered objectively, it follows that the sensors should be installed on internal, nominally strained areas of the structure. This is especially true if the purpose of the sensor is to monitor repeated load exposure.

For reasons of economy and early design information, preliminary fatigue tests (Ref. 7) are usually run on production components prior to the fatigue evaluation of full-scale structural assemblies. These tests of production components present a timely opportunity to obtain information regarding the practical and optimum location of sensors in similar locations on complete aircraft structure. The use of full-scale production structure in the sensor evaluation, avoids the "scaling down" or "modeling effect" so pronounced in scale models; therefore, the extrapolation hazards associated with modeling can be avoided. Areas which were found to be critical on previous tests (Ref. 7) of production component parts, were selected for sensor instrumentation on the complete C-5A full-scale test assemblies.

Once the monitoring sites (sensor locations) have been determined and documented, the multiplying factor of the sensor shim combination should be "sized" for an optimum response. Since much of the structural analysis of the C-5A aircraft has been automated by computer equipment, computer developed data were used to adapt sensor sensitivities to the selected fatigue control points. Computer "data runs" indicating cyclic and mean stress levels present at all control points, for all load conditions are too voluminous to be presented here; however, this information can be consolidated into occurrence curves to simplify its usage. A typical curve is shown in Figure 17 .

3.6 DOCUMENTATION OF SENSOR LOCATIONS

The structural locations selected for sensor installation are depicted on unscaled drawings which should be considered sketches and not detail drawings. The primary purpose of the sensor sketches as shown throughout this report, was to pictorially indicate to the strain gage technician the structural location for sensor installations. Although the sketches were never intended to conform to drawing standards, they were reasonably accurate for locating sensors on the fatigue test specimens and are of adequate quality for sensor installations in duplicate locations on flight vehicles. Since many of the sensors were located

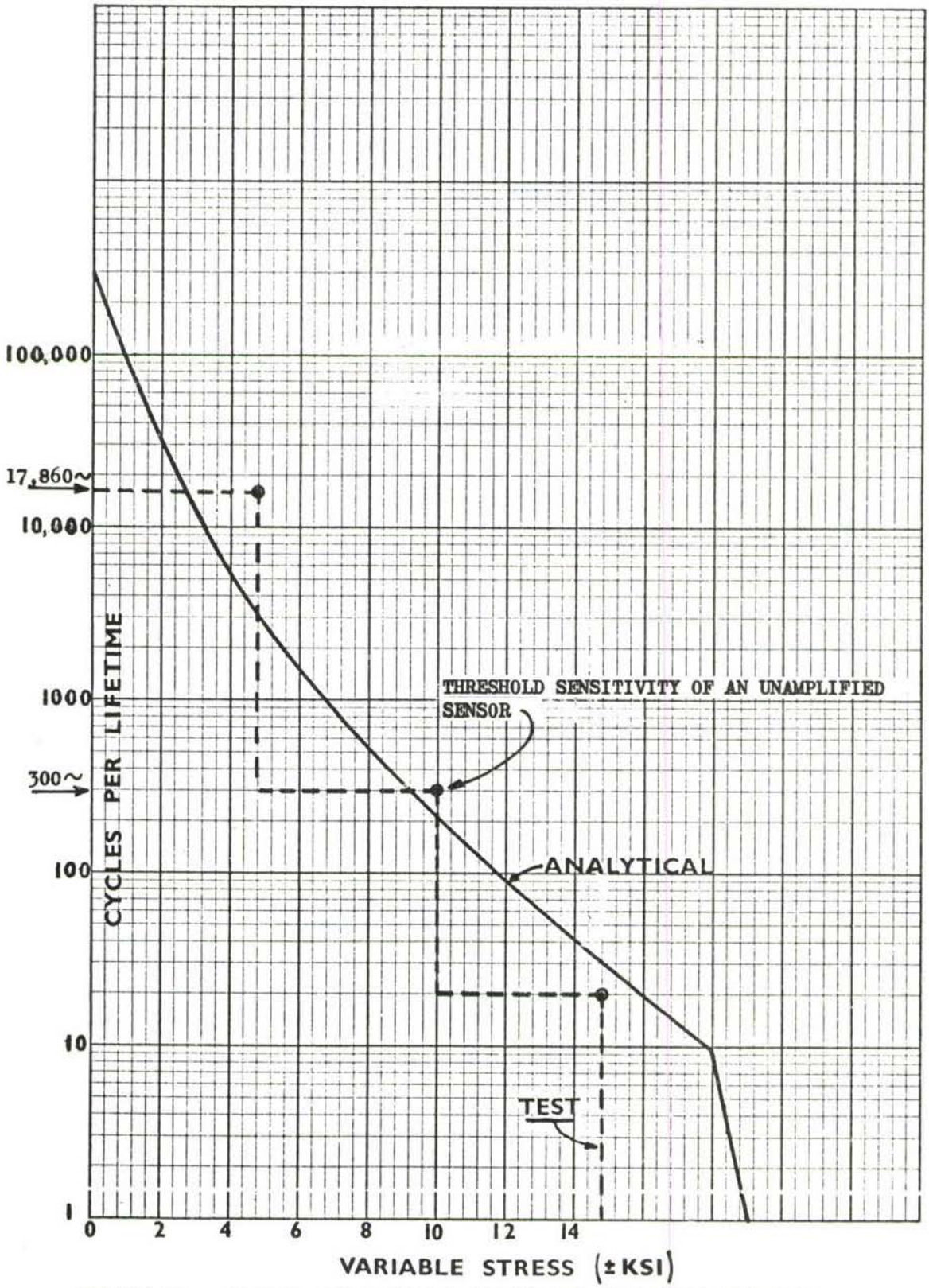

FIGURE 17. TYPICAL OCCURRENCE CURVE SHOWING THE VARIABLE STRESS LEVEL VS ACCUMULATED LOAD CYCLES

in uniformly strained areas of the structure, precise dimensioning was not generally critical; however, the sensors were normally located with an accuracy on the order of 0.1 inch. Typical sensor installations on a test article are shown in Figures 18 and 19 . These photos show the sensor mounted on a mechanical strain amplifier, which in turn is bonded to the test structure.

The sketches also served a secondary purpose by providing sensor location information to assist the stress analyst during the evaluation of sensor data. Where practical, the location of conventional strain gages in relation to the sensor is also shown.

3.7 SIZING OF THE SENSOR MULTIPLIER

A part of the screening techniques used for adjusting the sensor sensitivity to the selected location included an examination of the design occurrence curves to determine the stress levels in the selected structural areas. The occurrence curve typifies aircraft design service loads and mission profiles that have been reduced to a graphical display of accumulated cycles versus stress levels over a specified lifetime. Although many computer developed occurrence curves were required to define the stress levels at all critical points for all load conditions, a typical occurrence curve (Fig. 17) correlated with curves of sensor resistance change characteristics (Fig. 20) can be used to illustrate the technique for sizing the multiplier. The mission design loads are depicted by the solid line identified as "Analytical"; and the laboratory applied loads which simulate the design spectrum in terms of fatigue damage, are marked "Test". The curve marked "Test" was used to establish the appropriate size multiplier for sensor response to all the cyclic loads that could possibly produce fatigue damage in the structure. For instance, as illustrated by Figure 17, an unamplified sensor would respond to only 300 cycles out of a total of approximately 17,860 cycles of the particular loading condition illustrated by the occurrence curve. This occurs because the threshold sensitivity of the unamplified sensor is on the order of $\pm$ 1000 $\mu\varepsilon$ or $\pm$ 10 KSI stress in aluminum. By use of a sensor mounted on a mechanical strain multiplier that produces a multiplying factor of three, the apparent threshold sensitivity now becomes $\pm$ 330 $\mu\varepsilon$ or approximately $\pm$ 3.5 KSI stress in aluminum. Since the lowest cyclic load illustrated by the occurrence curve produces stress levels exceeding $\pm$ 4 KSI, the sensor will now produce a resistance change for all the loads shown. By pursuing the sizing technique further, the occurrence curve also shows that the highest amplitude stress levels exceed $\pm$ 14 KSI but are imposed for only 20 cycles. A family of curves showing the resistance change (ΔR) of annealed Constantan (Fig. 20) as a function of cumulative strain cycles may now be consulted to approximate the sensor resistance change for the total spectrum of applied loads. For instance the dotted line (Fig. 20) shows that 17,560 cycles at an apparent strain level of $\pm$ 1500 $\mu\varepsilon$ would produce a sensor resistance change of approximately 0.50 ohms. At the other end of the spectrum, the high loads occur only 20 times within one lifetime and while they will produce a sensor resistance change, it was ignored for this "rough cut" calculation. Therefore, the cumulative resistance change anticipated for this particular loading condition was 0.81 ohms as illustrated in Figure 20.

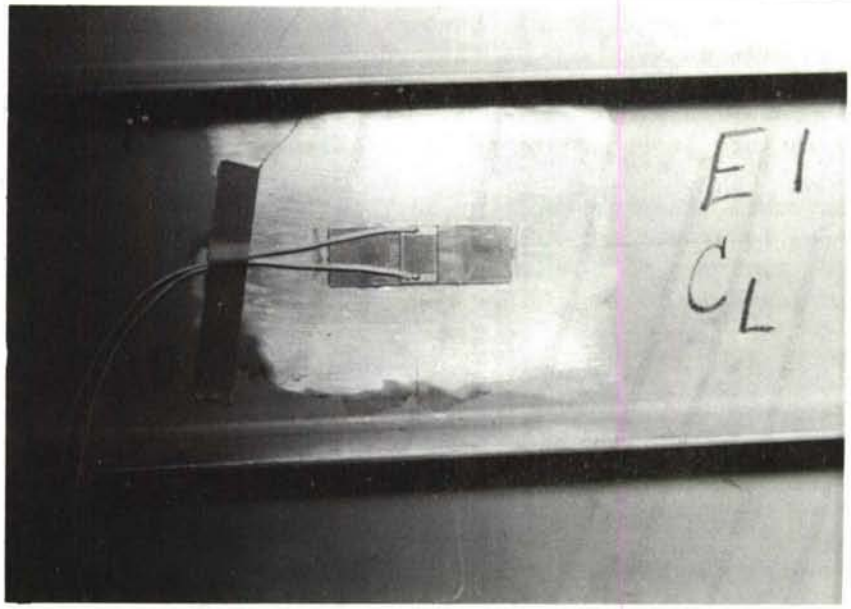

FIGURE 18. TYPICAL SENSOR INSTALLATION AND IDENTIFICATION MARKINGS SHOWN PRIOR TO SEALING

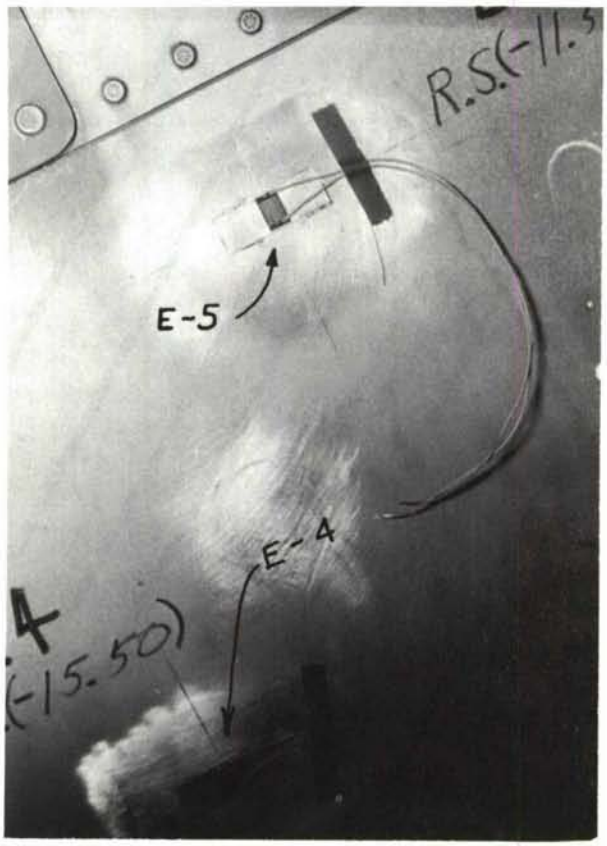

FIGURE 19. TYPICAL SENSOR INSTALLATION ON THE C-5A HORIZONTAL STABILIZER

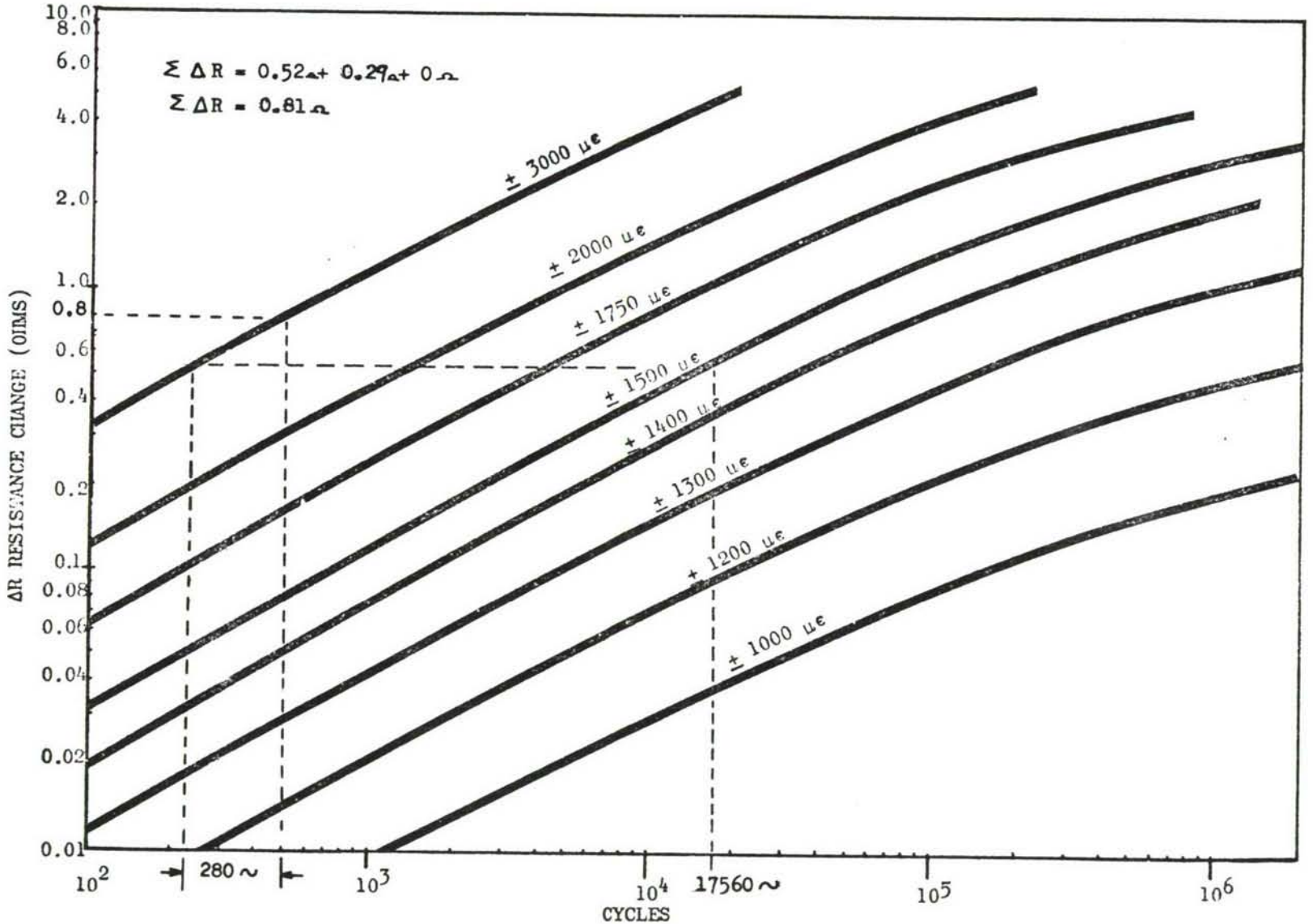

FIGURE 20. RESPONSE OF ANNEALED CONSTANTAN TO REVERSED STRAIN CYCLES (ZERO MEAN)

The technique for sizing the multiplier to a particular location and load spectrum is summarized as follows.

1. Consult the design occurrence curves to determine the number of cycles at each anticipated strain level per lifetime.

2. Refer to a family of curves (Fig. 20) showing the sensor resistance change vs constant amplitude strain levels to estimate the resistance change for the significant loads. Sensor resistance changes outside the envelope of cyclic strain ranges shown in Figure 20 may be extrapolated and those infrequent spectrum loads which produce minute resistance changes may be ignored.

3. Select a sensor multiplication factor that will produce a sensor resistance change for a significant range of cyclic loads and yet not produce excessive resistance change for the higher loads.

4. Approximate the total anticipated sensor resistance change per lifetime by totalizing the calculated resistance change for each load condition.

5. If calculations indicated that the "first cut" at a multiplication factor fell outside of desirable operating boundaries, a different multiplier can be selected and the exercise repeated.

3.8 VERIFICATION OF MULTIPLYING FACTOR

At this stage of fatigue sensor development it was believed that a verification of actual sensor multiplication factor was essential if a reasonable level of confidence in the data were to be obtained. Since the basic concept of fleet utilization is based on a comparison technique of laboratory test airplane data and data from similar fleet aircraft, sensor performance must be repeatable and reliable.

The only known method for verification of actual sensor multiplication factor and the one used during this program was by means of a strain survey. The determination of actual sensor multiplication factor on simple axial test coupons has contributed to improvements in techniques for isolating and correcting the causes of scatter in multiplication factor. While this method proved very reliable on simple coupons, the same approach on complex aircraft structure did not always indicate the same degree of reliability. During normal utilization of the sensor on the three C-5A fatigue test specimens the sensor was located adjacent to a conventional strain gage whenever it was practical to do so. The confirmation of the programmed sensor multiplier for the main landing gear specimen is discussed in Section 4.3 and the percent sensor deviation is shown in Table III. Although the maximum deviation experienced on the first test specimen was 10%, additional care during sensor installations on the remaining specimens did result in a reduction in sensor deviations.

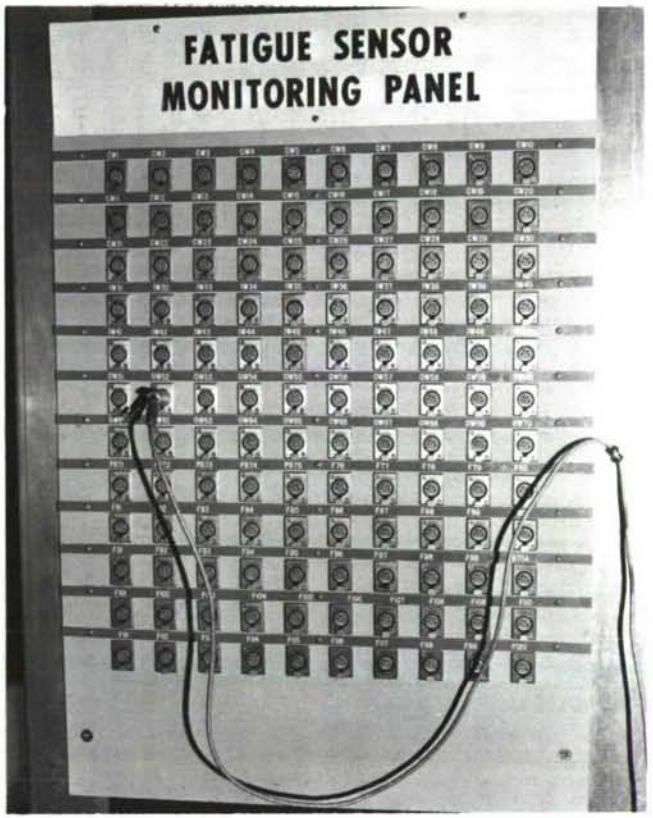

FIGURE 21. A TYPICAL SENSOR TERMINATION PANEL

FIGURE 22. SAMPLING OF SENSOR RESISTANCE CHANGE

A deviation in actual multiplier factor from that programmed is a special concern since the resistance change characteristics of annealed Constantan is a logarithmic function of its metallurgical condition. Therefore, a linear correction is not possible. That is, it would be incorrect to decrease sensor resistance change values by 10% simply because the actual sensor multiplying factor was 10% greater than that programmed. Therefore, one may elect to either "live with" the scatter in multiplying factor or resort to computer corrections in handling the data.

3.9 DATA ACQUISITION TECHNIQUES

The data acquisition procedure was designed to be economical and simple, yet accurate and repeatable. The monitoring instrumentation used in the test laboratory was planned to duplicate the approach anticipated for field usage on fleet aircraft. In this respect, each sensor cable was terminated and identified by number at a monitoring panel located near a convenient sampling point for the particular specimen being monitored. This arrangement permitted each sensor to be sampled by means of a snap-in connection to the monitoring instrument which in this case was an SR-4 strain indicator. A simplified schematic of the arrangement is shown as follows:

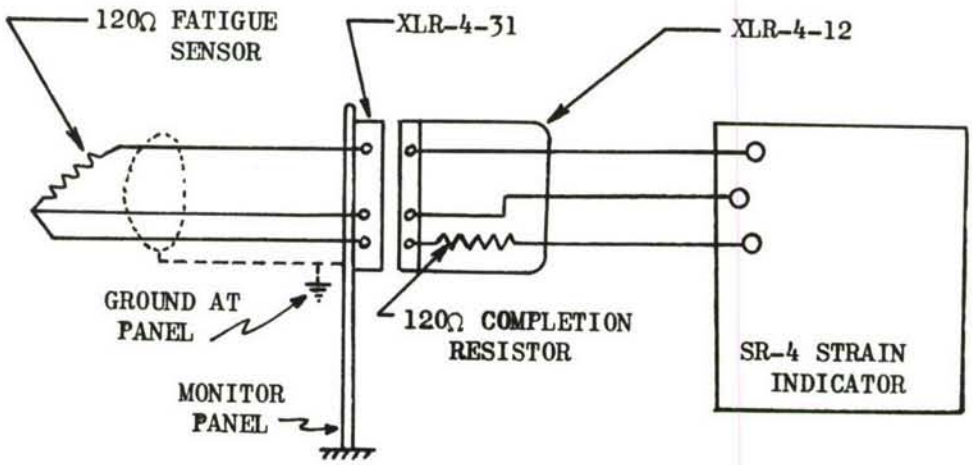

A typical monitoring panel (Fig. 21) shows all sensors for a specific specimen terminating at one central location and with front panel identification for each sensor channel. Figure 22 shows an SR-4 indicator mounted at eye level and arranged for a sequential plug-in connection to each sensor. The mechanics of physically acquiring data consists of periodically connecting a strain indicator to each sensor and manually recording the sensor change in resistance. The operator-recorder need only record channel number, sensor reading, and simulated

flight hours at each sampling period. The frequency of sampling remained flexible; however, a reading was taken an average of once every pass. Readings were taken for all specimen structural failures regardless of programmed sampling intervals. If trends in the plotted data indicated that sensor readings should be taken at more frequent intervals than once per pass, this was done. Quite often the frequency of sensor sampling was dictated by the calendar time required to accumulate an appreciable number of simulated flight hours and also by the specimen availability under a no-load condition. During the first pass, data were recorded after each load condition to ascertain that the sensors were responding to each load condition. It was anticipated that these data would show which test conditions produced the more severe loading of the structure, and if any redistribution of internal loads occurred as testing progressed.

The sensitivity or resistance change range of the sensor for one lifetime of load application on the aft fuselage specimen was designed to range up to two ohms; therefore, almost any resistance sensitive measuring instrument could have been used for data acquisition. That is, a digital voltmeter, a wheatstone bridge, an SR-4 indicator, or most any conventional strain gage indicator would have been adequate. An SR-4 strain indicator, however, was selected because it offered a higher resolution over the desired range and was compatible with the 120 ohm sensor. The parameter which an SR-4 strain indicator measures is resistance change in ohms/ohm and it is capable of resolving micro ohms. The fact that the dial is calibrated in microinches per inch is merely a convenience in which the change in resistance can be related to micro-strain as a result of a particular gage factor setting. For detecting a small resistance change of the fatigue sensor, a strain indicator has an advantage over the conventional four decade wheatstone bridge. For a gage factor (G.F.) of 2.00 the equivalent micro ohm/ohm values may be obtained in the manner shown below:

$$G.F. = \frac{\Delta R/R}{\Delta L/L} = \frac{\Delta R/R}{\varepsilon}$$

$$\Delta R/R = \varepsilon \times G.F.$$

$$\Delta R/R = 1000\ \mu\varepsilon \times 2.00 = 2000\ \mu\ \Omega/\Omega$$

Therefore, a strain indicator reading of 1000 micro in/in. is the equivalent of 2000 micro ohms/ohm.

Assuming an initial sensor resistance (R_i) of 120 ohms and a gage factor (G.F.) of 2.00, the following example illustrates how the resistance change (ΔR) can be expressed in either ohms or micro-strain.

Given a strain indicator reading of: $\frac{\Delta L}{L} = 1000\ \mu\varepsilon$

Then: $\Delta R = \frac{\Delta L}{L} \times R_i \times G.F.$

$$\Delta R = 1000\ \mu\varepsilon \times 120\Omega \times 2.00$$

$$\Delta R = 0.240 \text{ ohms}$$

Consequently the strain indicator reading in microstrain can be expressed in its equivalent ohmic value and vice versa. The strain indicators used receive periodic calibration in accordance with MIL-C-45662A (Ref. 18) assuring traceability to the National Bureau of Standards.

The resolution of the SR-4 strain indicator is within ± 20 micro ohms/ohm which is nearly an order of magnitude greater than will be logically displayed by the graph scales selected. Normal laboratory variations in temperature or zero load conditions at the time of sampling can produce maximum sensor resistance variations of up to 200 micro ohms/ohms. It should be noted that these resistance damages are temporary and not stored in the same manner that resistance changes produced by repeated strain cycles are stored. Therefore, a typical graphical display of ΔR vs number of passes will permit an evaluation of trend data without emphasizing temporary resistance changes due to temperature and/or variations in zero load.

3.10 SUPPORTING INSTRUMENTATION

During this stage of fatigue sensor development the C-5A fatigue test structure was being used to evaluate sensor performance, rather than using the sensor to determine the fatigue status of the C-5A structure. Therefore, utilization was made of existing support instrumentation to define the fatigue status of the structure as well as to evaluate sensor quality.

The supporting instrumentation used in the normal conduct of the fatigue test program included strain gages, deflection measurement devices, crack detection devices, and dual bridge load cells. Approximately 2000 strain gage channels were used to determine the strain in areas of special interest. A strain gage was normally installed adjacent to a fatigue sensor allowing verification of sensor strain multiplying factor. The initial strain survey also provided an opportunity to confirm the selection of sensor locations and to add additional sensors if some unexpected high strain areas were revealed.

The fatigue test program required that a static strain and deflection survey be conducted, prior to the beginning of the test and as required during testing, to verify the programmed loads and load distribution throughout the structure. Strain gage data was statically recorded at programmed increments of load up to a maximum of one hundred percent of mean plus maximum varying load. The fatigue sensor location sketches used in this report also identify those strain gages located adjacent to fatigue sensors.

Since detection of possible damage was an important part of the basic fatigue test program, every effort was made to detect cracks as early as possible. To achieve this objective, daily visual inspections were made in accessible areas during testing periods. These inspections were made during load application whenever feasible. In addition to daily inspections, detail inspections were made every two passes. During these detail inspections the entire structure was closely inspected visually and critical areas inspected by nondestructive techniques as required. These inspection periods were occasionally rescheduled, plus or minus one pass, to fit in with other normal downtimes. Since the sensors were installed on the fatigue test article for the purpose of evaluating sensor capability rather than for determining the fatigue status of the structure, it was necessary to determine specimen structural condition by such independent means as inspections. Therefore, the correlation of sensor reading with structural damage depended upon the completeness of the structural inspections. Where possible, use was made of strain gages, load monitoring equipment, deflection measurements, and other supporting instrumentation to assist in the evaluation of fatigue sensor performance. Additional inspection aids such as penetrant "dye chek" or X-ray of suspect areas were used to assist in locating and defining the extent of the fatigue cracks.

Although it might have been possible to obtain useful sensor information without any supporting data, the concurrent use of the diversified instrumentation required for the basic C-5A fatigue test program did serve to verify sensor data. The object of this approach was to make use of any available instrumentation that would contribute to the confidence level of sensor performance or the fatigue status of the test structure.

SECTION IV

TEST PROGRAM - MAIN LANDING GEAR SPECIMEN (X996)

4.1 TEST SPECIMEN DEFINITION

The Main Landing Gear specimen with associated backup structure is designated X996 and is shown in Figure 23. The total specimen consists of one complete left rear main landing gear strut, a portion of the center fuselage structure from F.S. 1474 to F.S. 1652 including cargo floor, underfloor structure and left hand side panels and frames up to W.L. 314. The pod, gear doors and door operating mechanism as well as wheels, bogie beam, tires and brake installation were omitted from the test specimen. The specimen was installed in a loading fixture accompanied by test jiggery as shown in Figure 24.

4.2 GENERAL TEST REQUIREMENTS

In the past, two schools of thought regarding laboratory simulation of aircraft loads has been found among aircraft structural engineers. One view said that the time-order of stressing is not important. Many other investigators contend that for aircraft structures, the correlation of loads to failure, mode of failure, and failure location on service aircraft with those failures on laboratory fatigue test structure will improve as laboratory simulation becomes more randomized. Although these two views, i.e., one stating order is important and the other that it is not, have been compromised in regard to materials, structural configuration, etc., the preponderance of evidence indicates that order is a contributing factor to aircraft fatigue life. One could therefore reason that if simulation were so real and complete that it amounted to a re-creation of service usage, then field failures would duplicate laboratory failures in all respects.

Since time and economics dictated that laboratory simulation be accomplished by block loading rather than flight-by-flight loading and since all service environmental variables cannot be simulated, emphasis has been placed on mechanically manipulating the sensor to respond to only those variables which produce fatigue damage. At the same time considerable effort was expended in making the block loading type of simulation as representative as possible by reversing the order of loading on successive passes of the spectrum.

The test loads for the C-5A Main Landing Gear were developed to simulate the design spectrum in terms of fatigue damage. Two concepts were utilized in converting the design spectrum into its equivalent test spectrum. First, structural integrity must be demonstrated for all significant types of loads. Secondly, the

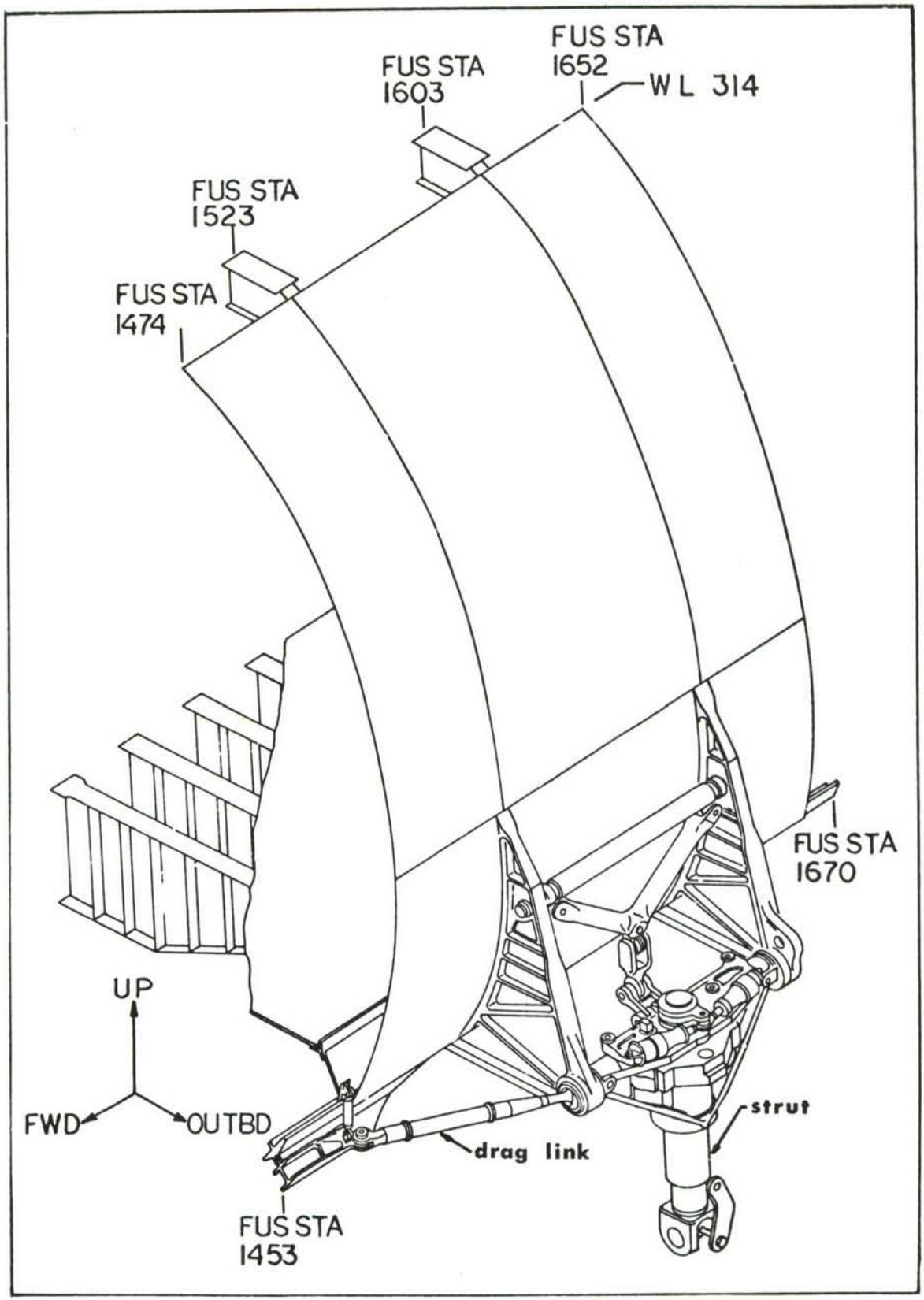

FIGURE 23. C-5A MAIN LANDING GEAR TEST SPECIMEN

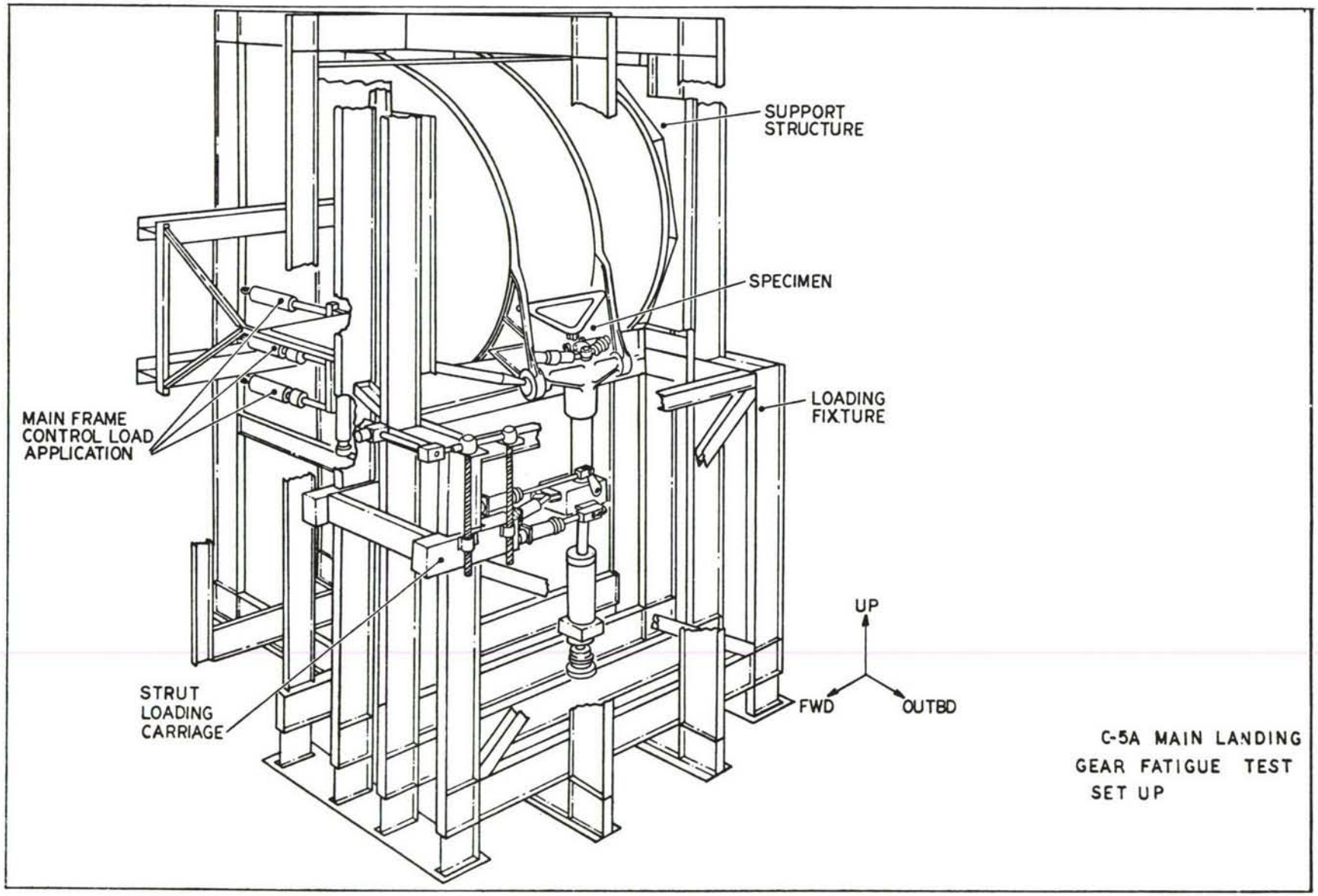

FIGURE 24. C-5A MAIN LANDING GEAR TEST SPECIMEN MOUNTED IN THE LOADING JIG

TABLE II

MLG STRUT FATIGUE LOAD SPECTRUM

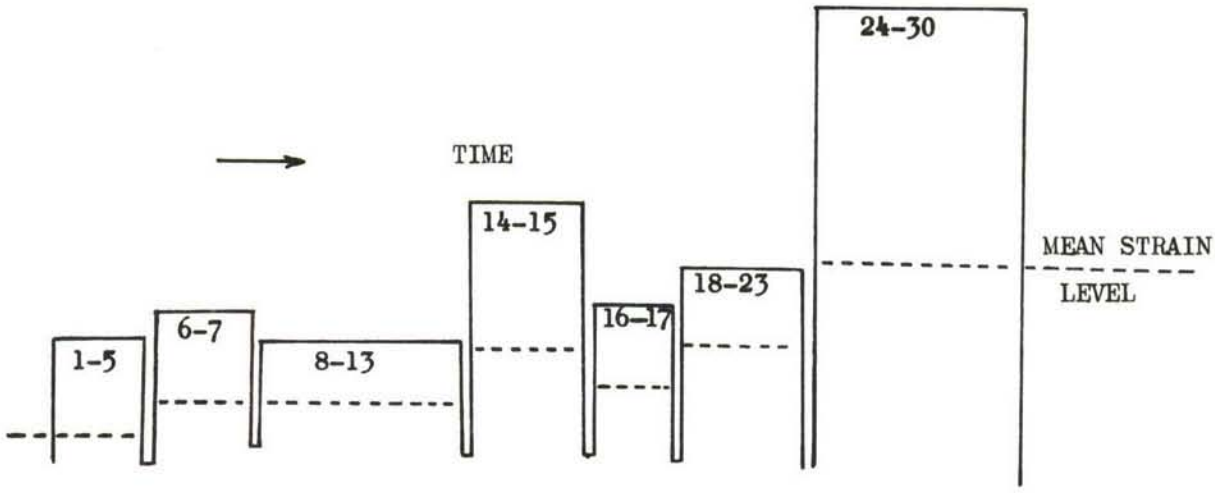

SEQUENCE NUMBER	CYCLES PER PASS	LOAD SOURCE	SEQUENCE NUMBER	CYCLES PER PASS	LOAD SOURCE
1	2.5	Landing Impact	16	228	Braking
2	52.5	↓	17	73	↓
3	395.0		18	19	Minimum
4	25.0		19	19	Radius Turn
5	25.0	↓	20	122	Turning
6	218.0	G.A.G.	21	132	↓
7	282.0	G.A.G.	22	95	
8	1269.0	Taxi	23	122	↓
9	54.0	↓	24	24	Kneeling
10	1.0		25	152.5	↓
11	1269.0		26	122	
12	54.0		27	31	
13	1.0	↓	28	204.5	
14	211.0	Kneeling	29	237	
15	403.0	↓	30	33.5	↓

applied test loads must accurately represent the fatigue damage effects of all load sources. The load sources established from C-5A mission profiles include landing impact, ground-air-ground, taxi, kneeling, braking, and minimum radius turns. Sensor locations were selected so as to obtain a response to all of the various modes of loading that could contribute to fatigue damage. The fatigue test requirements for the C-5A Main Landing Gear strut and backup structure consisted of the application of the equivalent of four design lifetimes of repeated loading. This was further broken down into 20 passes per lifetime, or the simulation of 12,000 landings. Although the overall basic fatigue test program was planned to apply load cycles equivalent to four times those anticipated for one aircraft design life, the fatigue sensor evaluation program was planned to cover only the first lifetime. A pass is composed of a specific sequence of load conditions as shown in Table II. The test loads applied per pass should therefore produce test specimen damage equivalent to that encountered by fleet aircraft operational loads during a service period of 600 landings or 1500 flight hours.

The diagram shown below illustrates the relative anticipated sensor resistance change in response to the basic load sources applied to the C-5A Main Landing Gear fatigue test specimen. The relative severity of each load source must be considered when locating the sensor and selecting its multiplying factor.

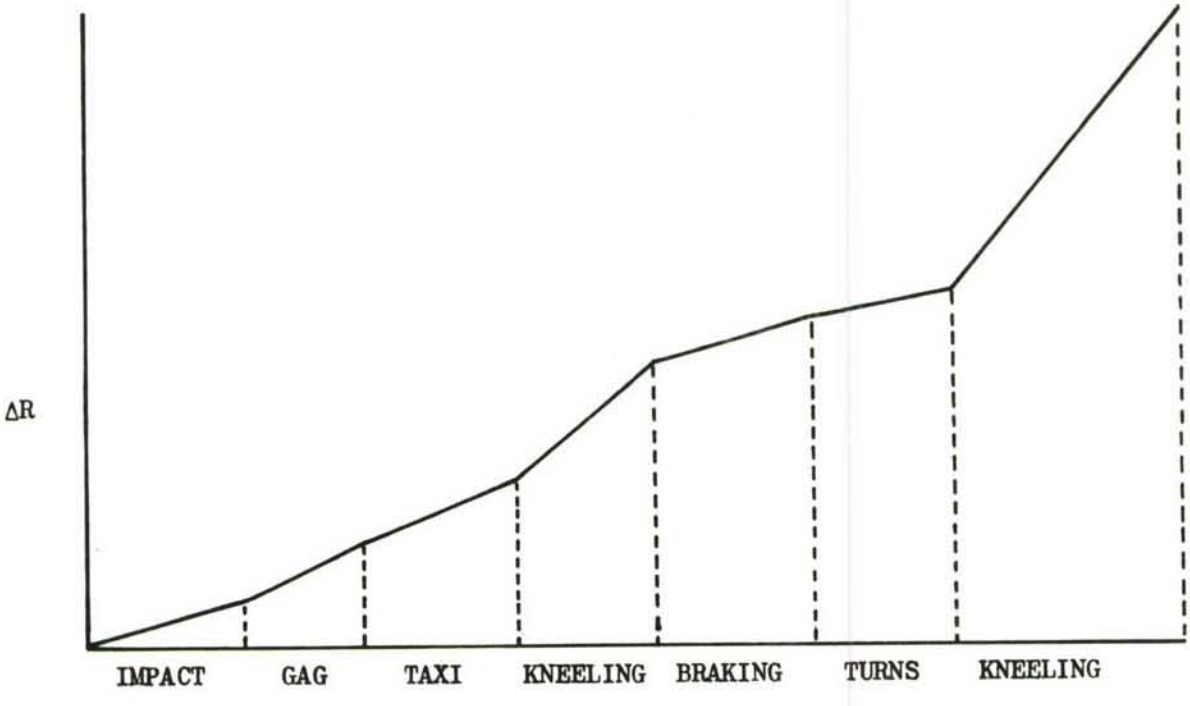

The selection of critical sensor location areas was based on manual screening techniques supplemented by computer data. Computer runs indicating cyclic and mean stress levels present in the backup structure were evaluated in view of shim mounted sensor threshold capabilities. Computer data which specified the most critical points, i.e., those that would sustain the greater fatigue damage, were used for selecting some sensor locations. A review of the varying stresses for these critical areas permitted the selection of a common multiplier so adjusted to the programmed loads that the total sensor resistance change for one lifetime would be within certain boundaries. That is, the multiplier was selected so that the applied loads for one specimen lifetime would produce total sensor resistance changes of 10,000 to 12,000 micro ohms/ohm. This targeted operational range gave adequate resolution, plus the capability of extending sensor utilization to two or more lifetimes if desirable.

It appeared that for nominal area strains a multiplier of approximately three would be optimum if only a single multiplier were used. Several multipliers could have been used to more ideally respond to strain levels at the various locations but this would have complicated the documentation. It was felt that if the same multiplier could be used on all specimens, while not optimum for each individual specimen, a common basis of comparison between specimens would be provided, and the additional documentation inherent with a wide variety of multipliers could be avoided. Therefore, in nearly all cases the SAP 204DA-STE sensors were installed with the 3/4 inch Teflon tape for a theoretical multiplier of three. The exception to this was the five unamplified sensors installed in stress concentration areas. These five locations are identified in Figures 25 and 29.

Thirty-six sensors were installed on the Main Landing Gear (MLG) specimen prior to the static strain survey. These sensors were located as shown in Figures 25 through 29.

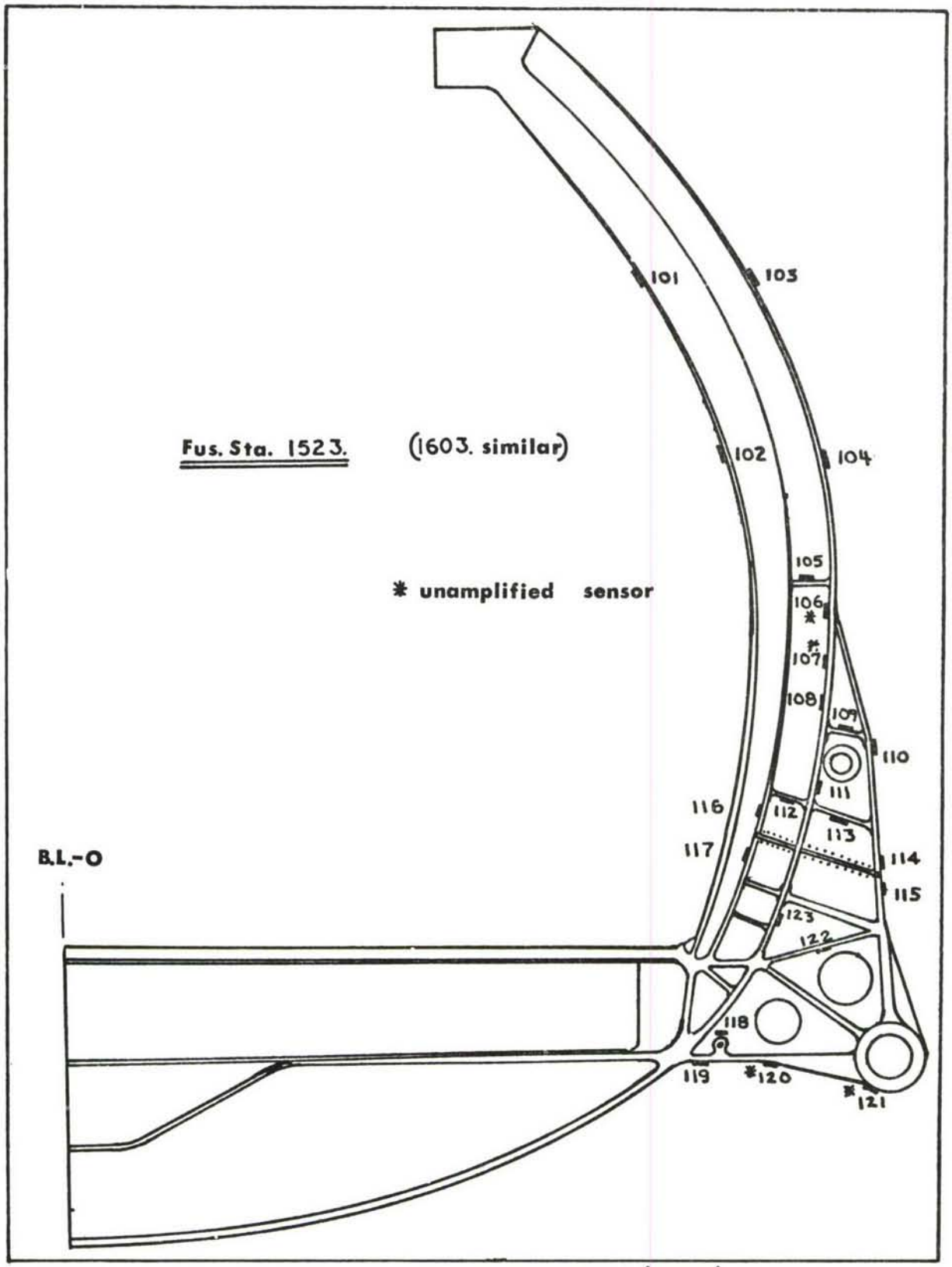

FIGURE 25. GENERAL SENSOR LOCATIONS (M L G)

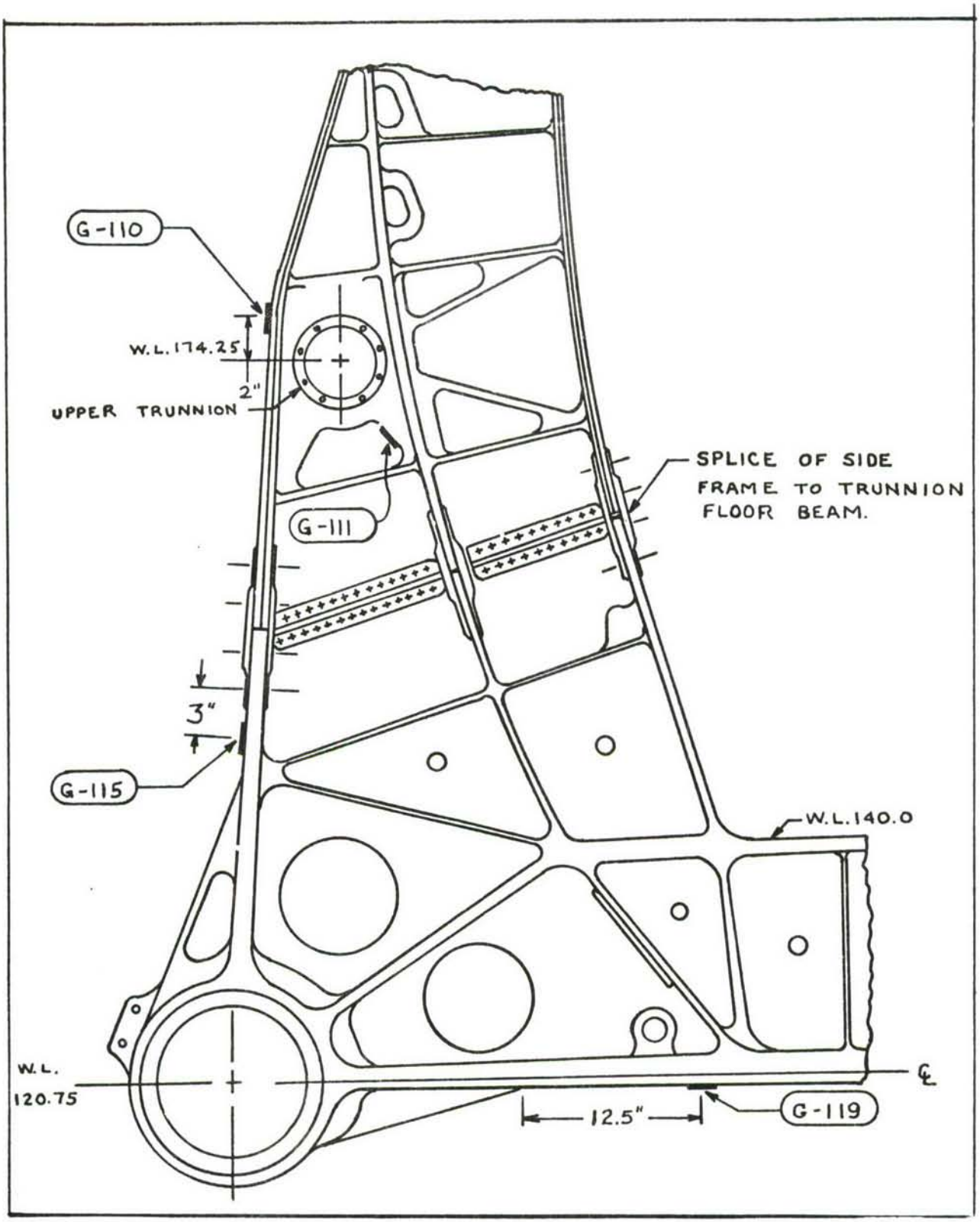

FIGURE 26. LOCATION OF THE MOST ACTIVE SENSORS ON THE F.S. 1523 MAIN FRAME

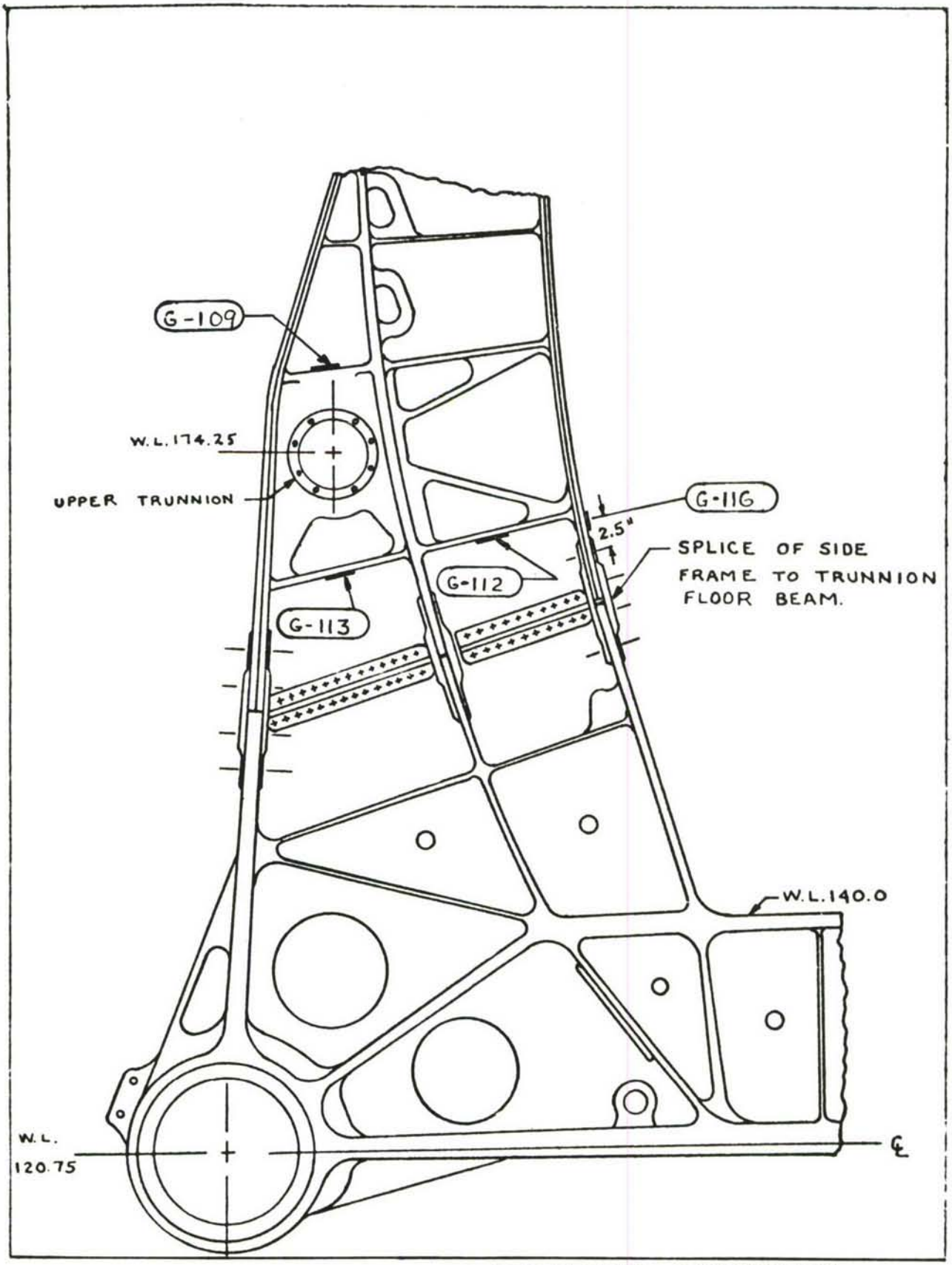

FIGURE 27. LOCATION OF THE LEAST ACTIVE SENSORS ON THE F.S. 1523 MAIN FRAME

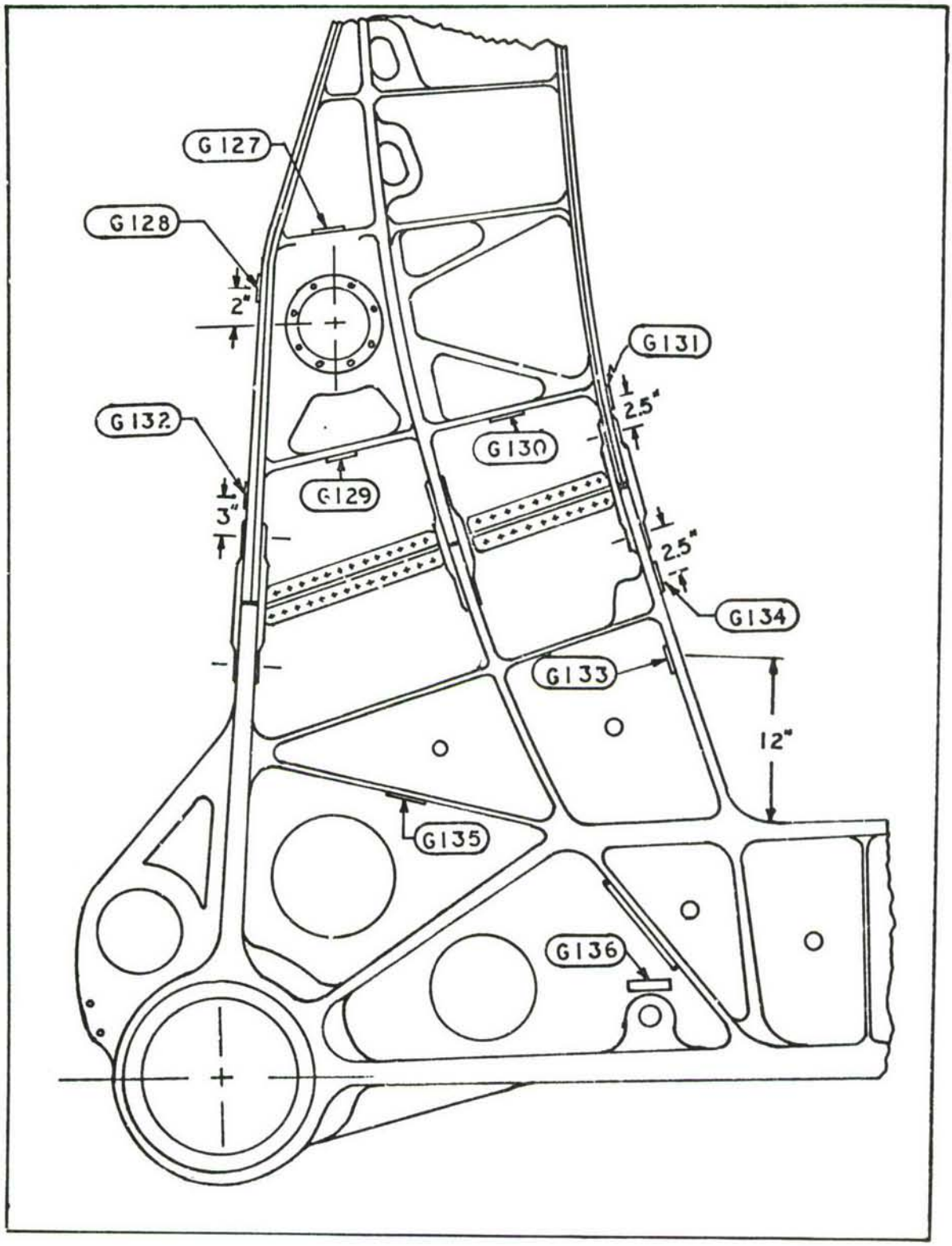

FIGURE 28. PARTIAL MAIN FRAME F.S. 1603

* unamplified sensor

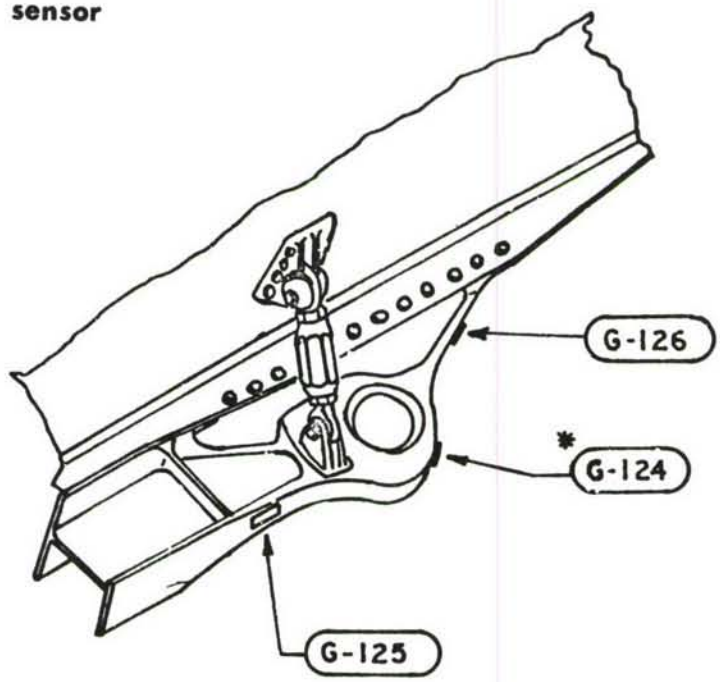

DRAG FITTING

FIGURE 29. SENSOR LOCATIONS M.L.G. DRAG FITTING

In practice the multiplier is adjusted to the loading program such that the sensor will produce a resistance change (ΔR) for the low (taxi) loads yet not produce an excessive resistance change (ΔR) for the higher (kneeling) loads. If an excessive resistance change is permitted for the kneeling load condition the operating range of the sensor will exceed the aircraft's targeted one lifetime value. One of the more critical limitations is the selection of a multiplier factor such that the sensor output does not exceed five ohms for any programmed structural lifetime. If sensor coverage is desired for one lifetime of the aircraft structure, multiplying factors should be made compatible with nominal area strains so that a resistance change will occur for the significant loading conditions that produce structural fatigue damage.

4.3 STRAIN SURVEY

The static strain survey conducted on the MLG specimen prior to fatigue cycling has been found to yield valuable sensor information regarding:

(1) Confirmation of sensor multiplier.

(2) Approximation of initial strain distribution in the test structure.

(3) Criticality of installation techniques to obtain precise multiplier.

(4) Confirmation of sensor bond.

(5) Location of any unusually high strain areas.

The safe conduct of the basic fatigue test program required the use of approximately 284 strain gages located at strategic control points for periodic or continuous monitoring. These strain gages were used to determine the amplitude and distribution of stresses in areas of special interest. A total of thirty-six fatigue sensors were installed on the MLG test specimen, many of them adjacent to strain gages. This arrangement permitted the sampling of sensor outputs under a known static load condition concurrently with the sampling of strain gage information. Although all the sensor outputs were recorded during the strain survey, only those located adjacent to a strain gage are shown in Table III. The strain survey provided an opportunity to confirm the programmed sensor multiplier since the sensor also responds to instantaneous strains. Conventional strain gages installed in the same area as the sensor provided a true strain measurement for comparison with the apparent strain response of the sensor. Table III shows the reading of the sensor in apparent strain versus the output of the associated strain gage in true strain. The ratio of one to the other is then accepted as the actual multiplying factor, however it should be recognized that there may be some strain gradient present; and there may also be some redistribution of strain between load increments. These factors along with others may account for the scatter in multiplying factor between the two load increments.

TABLE III

RELATIONSHIP OF SENSOR OUTPUT TO AN ADJACENT STRAIN GAGE

SENSOR NUMBER & CORRESPONDING GAGE NUMBER	STRAIN OUTPUT 100% MEAN	STRAIN OUTPUT 100% MEAN + MAX CYCLIC	APPARENT SENSOR MULT. FACTOR 100% MEAN	APPARENT SENSOR MULT. FACTOR 100% MEAN + MAX CYCLIC	% DEVIATION*
		F.S. 1523 MAIN FRAME			
G 113	520	835	2.89	2.92	-3.3
SG6624	180	285			
G 119	540	900	3.26	3.32	+10
SG6605	165	270			
G 110	-1380	-2205	3.13	2.87	0
SG6641	-440	-770			
G 116	510	940	2.92	2.69	-6.6
SG6650	175	350			
		F.S. 1603 MAIN FRAME			
G 128	-1390	-1940	2.88	2.96	-2.6
SG6741	-485	-650			
G 129	580	995	3.05	3.07	+2.0
SG6724	100	325			
G 131	540	1025	2.84	2.85	-5.0
SG6750	190	360			
		DRAG FITTING			
G 125	780	1410	3.00	2.94	-1.0
SG6680	260	480			

The static load condition (No. 29) applied for this strain survey simulated an aft kneel condition

*This represents the average percent deviation of the mechanical multiplier from the referenced strain gage indication

When all the variables are considered it is conservatively estimated that the response deviation from the theoretical value was a nominal 10% as shown in Table III. It is anticipated that as installation technicians become more experienced, and as the techniques become more refined, theoretical will be more closely approached. In any event, since a tolerance of 10% has been attained on the sensors specifically checked for accuracy of sensor response, the laws of probability imply that a similar tolerance could be expected on the unverified sensors. The variation in actual multiplying factor from theoretical was considered acceptable and no sensors were replaced on the basis of a sensor deviation.

While the attainment of a precise multiplier is interesting and challenging, it is not as critical to the overall effort as adjusting the sensor sensitivity to the structures operating strain level. Lockheed produced stress analysis reports (regarding the primary airframe) were used in matching sensor sensitivity to predicted strain levels at selected locations. Any deficiencies or changes in predicted operating strain levels of the structure tends to compromise the effectiveness of the sensor installation.

The sensor registers and stores all strains above a particular level (threshold); therefore, the instantaneous strain amplitude recorded during the static strain survey is indicative of the cyclic strain amplitudes to be expected during fatigue cycling. This information permitted an estimation of the sensor resistance change that should be anticipated for a given cyclic load condition. At this stage of evaluation, if the sensor response was unreasonable (either too high or too low) an adjusted sensor replacement could be made without interfering with the conduct of the basic fatigue test program.

Although all sensors were read during the strain survey this was primarily to determine quality of bond and response to strain. Strain survey data points are not shown for all sensors since some were located such that they would be primarily responsive to such conditions as turning or braking and not to kneeling. To attempt a comparison between all sensors for one particular load condition could be rather misleading.

It is not unusual for strain levels which correspond to normal operating conditions to be considerably lower than the strains recorded for the critical design conditions. Very often, the design is based on rare occurrence loading conditions or airplane configurations. This is true in the case of the main landing gear which, to some extent, is the reason why it is not normally critical for fatigue conditions. The local area of the gear back-up structure can also benefit from the diversity in loads between normal operating and design limits. The strain survey conducted

on the C-5A main landing gear specimen shows results that are consistent with these principles.

Earlier investigations in which the operating characteristics of the unamplified fatigue sensor were evaluated indicated a threshold alternating strain level below which the sensor demonstrated minimum response in terms of a change in electrical resistance. A secondary purpose of the strain survey was to substantiate that a proper selection had been made regarding the sizing of the strain multiplier for the particular sensor location. Another point of interest was the projected change in sensor resistance corresponding to one lifetime. The objective of this approach was to optimize the relationship of sensor behavior characteristics and airframe structural response to repeated load exposure.

An evaluation of the results of the strain survey indicated that the sensors were adequately located to perform their intended functions and no sensors were replaced or added as a result of the survey. The strain amplitudes measured by conventional strain gages indicated that the selected sensor sensitivity and locations were reasonably appropriate for monitoring the structure's degree of exposure to repeated load occurrences.

4.4 DATA EVALUATION AND DAMAGE CORRELATION

The fatigue test spectrum as shown in Table II was applied to the test specimen on a per pass basis throughout the duration of the test program. Typically, the magnitude and sense of the strain levels shown in Table II represents a sample of the strain experience which would be felt by sensor number G 119 as located on the trunnion floor beam. For any given load condition some sensors will experience tension strains while others are exposed to compression strains. Regardless of the sense of strain, cyclic strains above a programmed level results in a permanent resistance change (ΔR) of the sensor.

A graphical display of the resistance change (ΔR) of all sensors are shown in Figures 30 and 31. The output of the most active sensors are plotted individually while the less active ones are displayed in a group. The sensor output is displayed over one simulated aircraft lifetime, with the resistance change shown in both ohms and micro-ohms/ohm units.

The desire to evaluate sensors in the area of stress concentrations still persists although the previous value of such techniques (Refs. 6 and 7) has left a lot to be desired. To further explore the practicality of this approach, five unamplified sensors were installed on the specimen as shown in Figures 25 and 29. These sensors are numbered 106, 107, 120, 121 and 124. A review of the plotted data in Figures 30 and 31 indicates results similar to earlier experiences i.e., a very minimum of output. Perhaps a fatigue crack at the instrumented stress concentrator would have produced a more dramatic resistance change in the sensor; however, in the absence of such information it can be concluded that the data from an unamplified sensor is of minimal value.

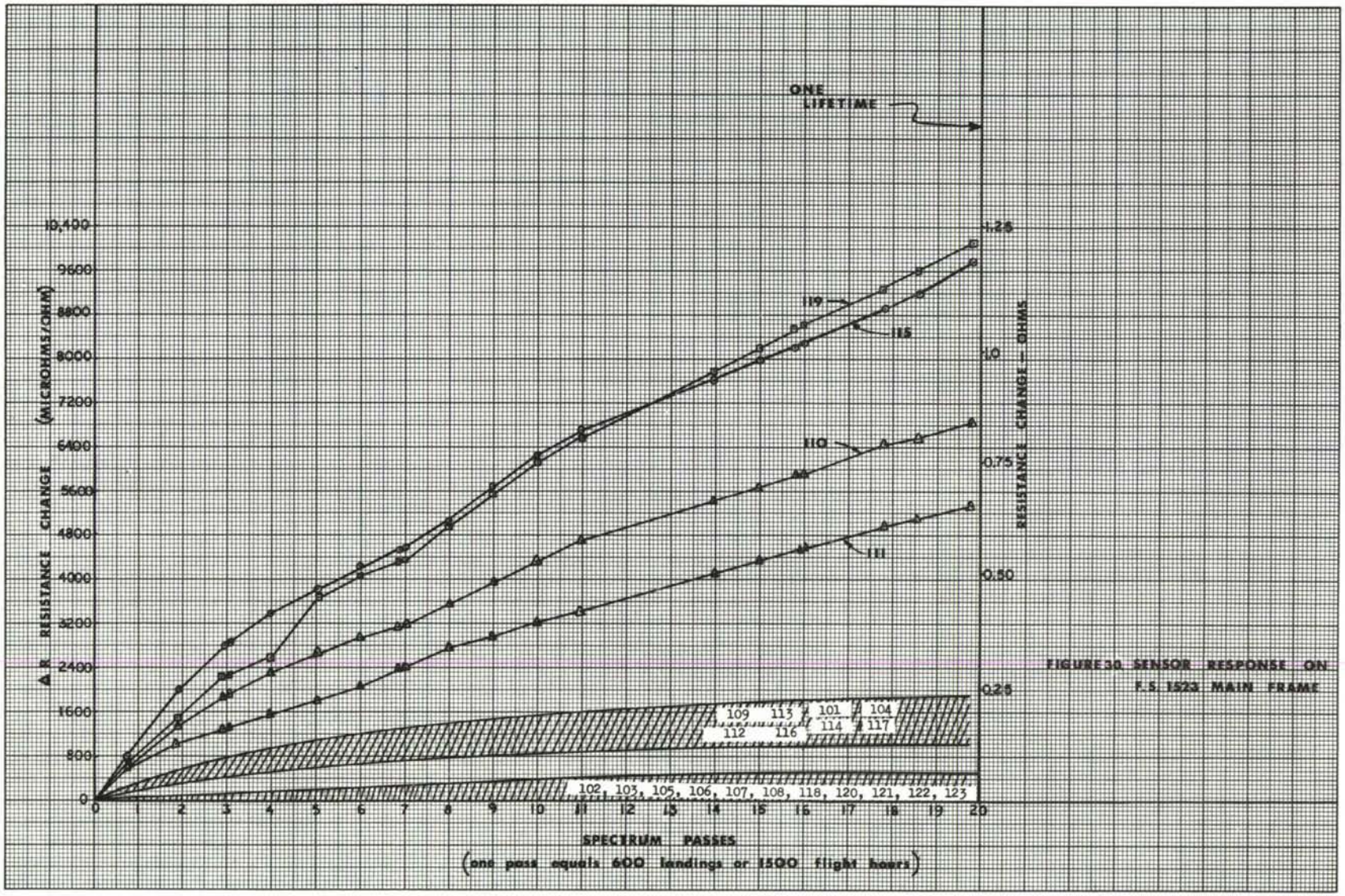

FIGURE 30. SENSOR RESPONSE ON F.S. 1523 MAIN FRAME

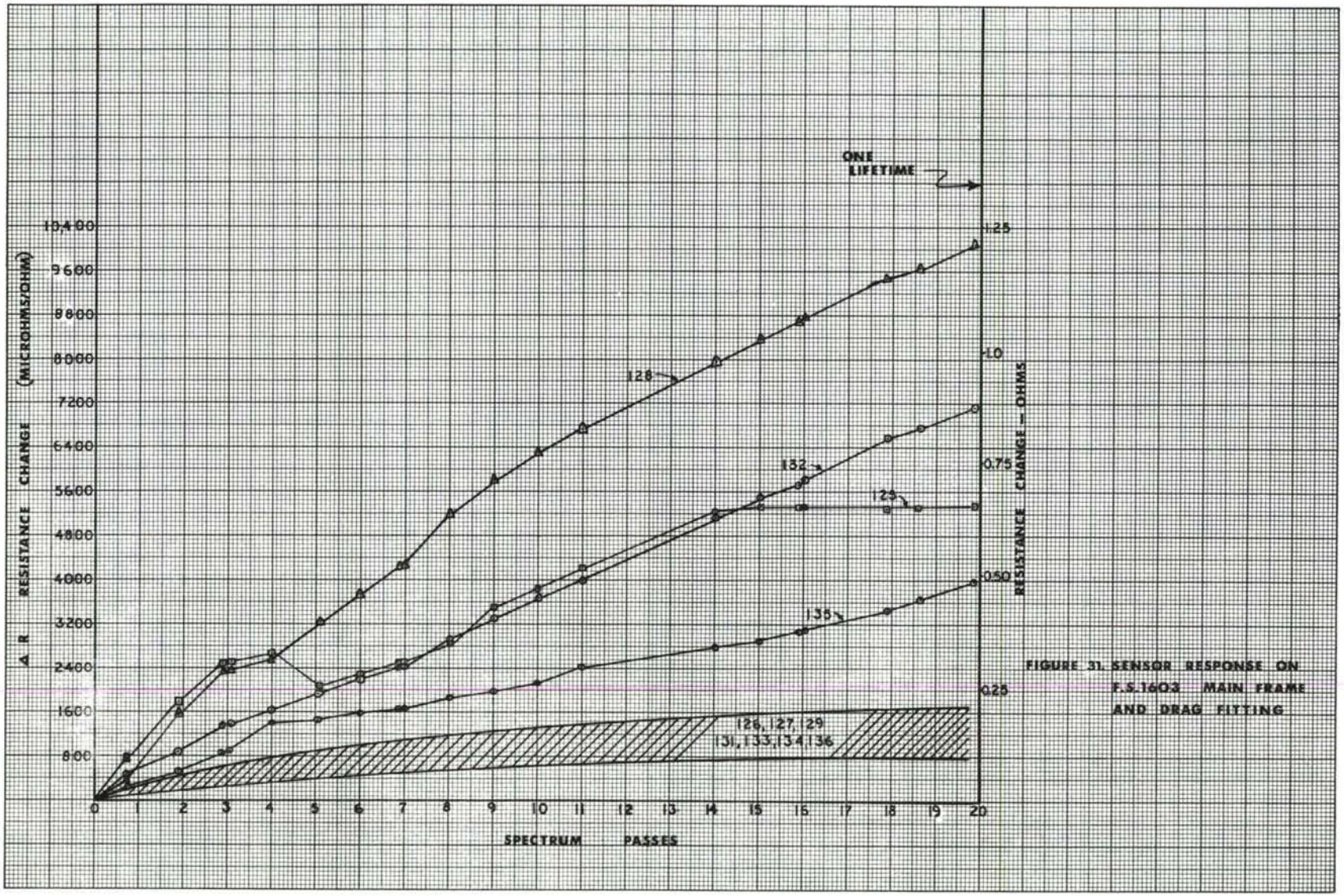

FIGURE 31. SENSOR RESPONSE ON F.S.1603 MAIN FRAME AND DRAG FITTING

The data from the mechanically amplified sensor was much more informative and consistent with previous results. The output of the sensors plotted individually show a uniformity of slope, representative of a uniformity of repeated load exposure. When the sensor behavior was evaluated in view of the conduct of the test program, a satisfactory explanation became available for any variation in slope of the sensor output. As a case in point, sensor 119 indicated a sharp increase in slope during pass five. An investigation showed this was the result of a removal and replacement of the MLG strut. The sensor resistance measured at any time is composed of a temporary resistance change due to static strain as well as permanent resistance change due to cyclic strain; therefore, a change in initial zero load is reflected as an abrupt change in the total sensor resistance.

The majority of the sensors were located for the purpose of monitoring repeated load exposure. In many instances comparable locations were used on each of the F.S. 1523 and F.S. 1603 main frames, i.e., the location of G 110 corresponds to the location of G 128. The behavior characteristics of these two sensors were likewise similar. This could have been anticipated since the static strain output of the two sensors were similar as indicated by the strain survey shown in Table III.

Other sensors installed for the same purpose of monitoring load exposure were located on the inner flange of the main frames. During the assessment of the strain multiplier, it was observed that for the strain survey condition, sensor 116 on the inner flanges developed strains comparable to those measured by sensor 119. However, whereas suitable sensor output was recorded during the fatigue program for sensor 119, little response was obtained from sensor 116 and other sensors located on the inner flange of the frames. In this case, the strain amplification should have been adequate based on stress information from computer developed C-5A stress analyses; however, it appears that the severity of the fatigue conditions was not sufficient to generate a large change in resistance.

A modest level of response prior to the development of local failure is not objectionable. In fact, larger changes in resistance were anticipated for the main landing gear test. However, changes in the load spectrum and insufficient strain data on which to estimate the sensor multiplying factor resulted in values somewhat lower than desired. A more timely updating of the precise strain levels to be expected as a result of the design load could produce a more desirable sizing of sensor sensitivity to location.

After the completion of one lifetime the specimen was subjected to a visual inspection of the main gear and back-up structure. The inspection revealed no fatigue cracks or other fatigue failure. The only visible damage was diagnosed as wear in the strut cylinder, bearings, washers, and other similar operational parts.

Since no failures occurred in the back-up structure during the first lifetime, the resistance change of the sensor can only be related to repeated load exposure, rather than fatigue damage. While it is recognized that some structural damage has been accumulated by the end of one lifetime, the percent damage may be more precisely determined after a structural failure. Knowledge of the total load exposure required to produce a failure (in terms of sensor resistance) would allow a more precise assessment of the fatigue damage existing at the end of one lifetime. The structural integrity program for the C-5A requires fatigue testing of the C-5A main landing gear specimen for a period of four simulated lifetimes. Should a structural fatigue failure occur during this period, the value of each sensor resistance would be of particular interest since it could now be ratioed back to assess accumulated damage at any previous point in time.

4.5 SENSOR RELIABILITY AND PERFORMANCE

As might be expected the sensor installation reliability was a function of quality control during installation and sensor exposure to mechanical damage during the test program. The sensor casualty rates during installation were less than expected and generally were the result of a questionable bond. During installation, if the bond quality was suspect that particular sensor was removed and a new one installed. All of the sensors were moisture proofed with Baldwin-Lima-Hamilton type barrier "E" waterproofing compound, which also provided some modest mechanical protection. Although the sensor installations were subjected to humidity changes of 40% to 100%, as well as hydraulic oil splashes, electrical resistance-to-ground was never a problem. Two sensors (G 120 and G 121) were mechanically damaged during a removal and inspection of the MLG strut at about 50% of the first lifetime. One sensor (G 121) was damaged beyond repair, while the other sensor (G 120) only required the re-soldering of a broken lead to become operable again. Consequently, only one sensor was abandoned at this point. Another sensor (G 125) indicated an erratic output to both static and dynamic strain after approximately 14 passes. A visual inspection of the installation at the end of one lifetime revealed a metal-to-metal bond failure. The output of sensor G 125 as shown in Figure 31 indicates a significant decrease in resistance change (ΔR) during pass five. This behavior is possible since the measured resistance of the sensor at any time includes the effects of a static strain (if present) plus the effects of cumulative strains. It is desired that the structural zero load, and hence, the static strain remain constant for all data samples; however, in practice this does not always occur. Any component, such as the MLG drag link which can be removed and reinstalled, can produce a noticeable zero shift in local sensor readings, which is due to a change in zero load rather than repeated load occurrences.

Sensor performance as opposed to installation reliability can be related to the user's experience with application techniques. The sensor operating deficiencies that were experienced could not be traced to fabrication or manufacturing discrepancies. The deficiencies in sensor output and difficulties with data interpretation were not the result of

sensor performance capabilities, but rather a misadjustment of sensor sensitivity to specimen strain levels. In retrospect, sensor output could have been improved by using a higher multiplier particularly in areas of lower nominal strain levels. The stress levels shown in a Lockheed developed stress analysis report for the MLG was used for sizing the multiplying factor to the selected areas. Subsequent analysis of stresses produced by the design spectrum loads indicated much lower stresses would occur in these areas. Unfortunately, this information did not become available until after the sensors were installed. Sensors numbered 109, 112, 113, 116, and located as shown in Figure 27 were representative of those sensors with a low output. By comparison, sensors 110, 111, 115, and 119 were more ideal since they gave adequate resolution yet had plenty of operational range for an additional lifetime.

A deviation in actual response factor from that programmed is a special concern. Since the resistance change characteristics of annealed Constantan is a logarithmic function of its metallurgical condition, a linear correction is not possible. That is, it would be incorrect to decrease sensor resistance change values by 10% simply because the actual sensor response factor was 10% greater than that programmed. Therefore, one may elect to either "live with" the scatter in response factor or resort to computer corrections in handling the data. To reduce the scatter in sensor data on follow-on specimens, additional care was exercised during the bonding procedures.

SECTION V

TEST PROGRAM - AFT FUSELAGE EMPENNAGE SPECIMEN (X997)

5.1 TEST SPECIMEN DEFINITION

To prove the structural integrity of the C-5A airplane and to demonstrate that it will have a satisfactory service life, fatigue tests were conducted on full-scale major aircraft assemblies. One of the assemblies chosen for use in the sensor evaluation (Aft Fuselage - Empennage Fatigue Test specimen, designated S/N X997) is shown schematically in Figure 32. The specimen consisted of a structurally complete C-5A aft fuselage (aft of F.S. 2100) and empennage mounted to a steel bulkhead at F.S. 1964. That portion of the fuselage between F.S. 1964 and F.S. 2100 was used for a specimen to jig tie-in to insure that the proper stiffness and load distribution exists between the specimen and reaction frame. The aft pressure doors, empennage control surfaces, non-structural fairings, wiring, and hydraulic tubing were omitted.

The test fixture was a steel beam truss structure enclosing the Aft Fuselage - Empennage test specimen. This fixture maintains the spatial relationships and strength required to impart the load conditions to the test specimens by means of servo-controlled hydraulic actuators. The Aft Fuselage - Empennage is suspended from a steel bulkhead at the forward end of the loading support structure at F.S. 1964 as shown in the view of the specimen and test fixture in Figure 33.

5.2 GENERAL TEST PROGRAM REQUIREMENTS

A test spectrum was derived and applied to demonstrate the ability of the test structure to withstand the application of cyclic loads anticipated during the service life of the airplane. The test spectrum development began with a survey of the analytical fatigue damage over broad regions of the structure. Several key locations as indicated in Table IV, were selected for control purposes in establishing test requirements. These analysis stations include potentially critical areas of each major structural section and as discussed in greater detail in Section 3.5, they are also used as sensor control points.

An Air Force approved test plan stipulates that a scatter factor of four is to be applied in the airplane fatigue test. Therefore, the C-5A Aft Fuselage-Empennage specimen was to be subjected to a test spectrum representing four lifetimes, i.e., the load requirements corresponding to one lifetime were repeated four times.

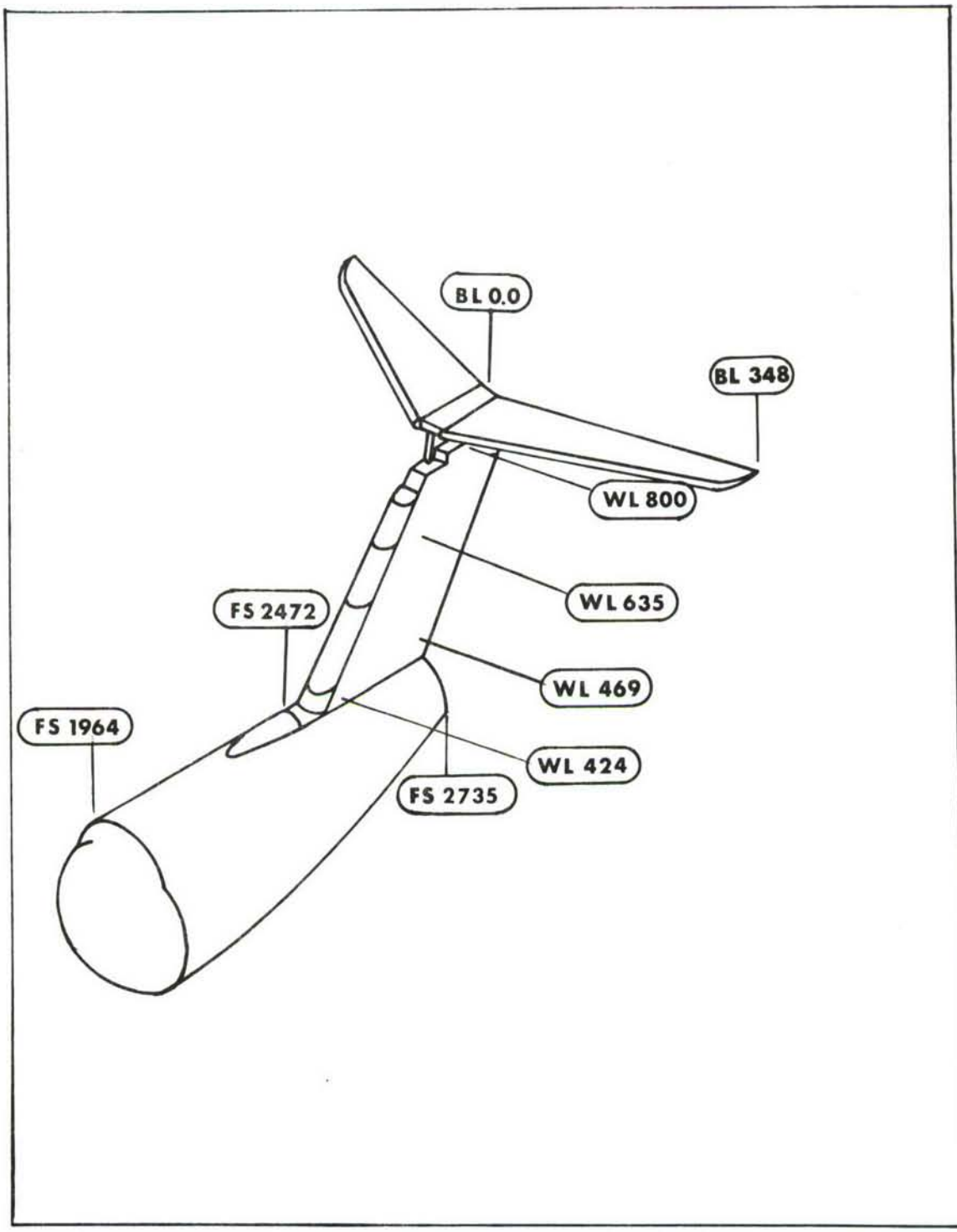

FIGURE 32. C-5A AFT FUSELAGE—EMPENNAGE SPECIMEN

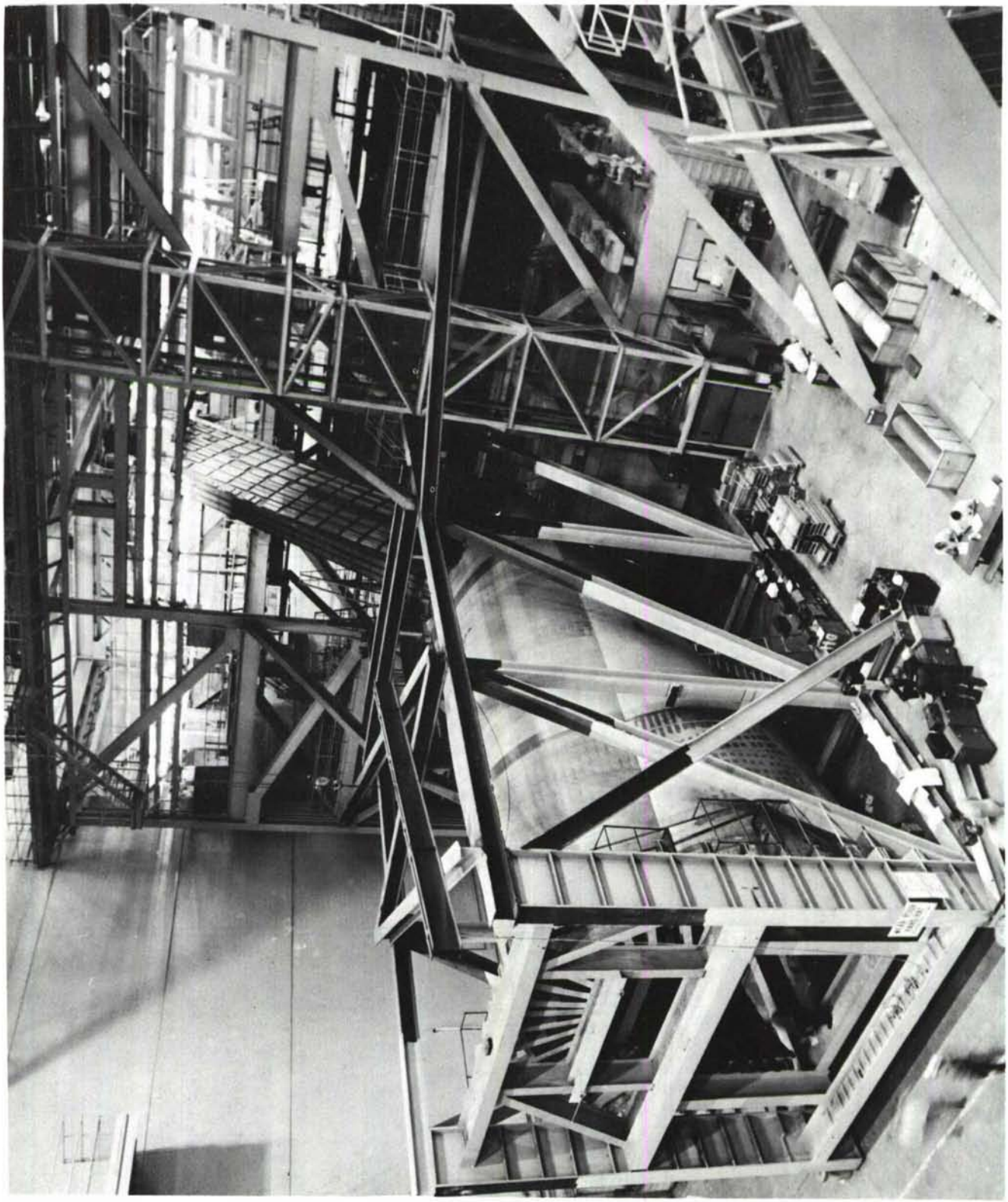

FIGURE 33. C-5A AFT FUSELAGE-EMPENNAGE IN TEST FIXTURE PRIOR TO INSTALLATION OF JACKS AND LINKAGE

TABLE IV
TEST CYCLE ALLOCATIONS FOR THE AFT-FUSELAGE EMPENNAGE SPECIMEN

TEST GROUP	MAXIMUM DAMAGE LOCATIONS	TOTAL TEST CYCLES BY LIFETIME BY GROUP	LOAD CONDITIONS	TEST CYCLES BY LIFETIME BY LOAD CONDITION	TEST CYCLES PER PASS
TAXI	FS 2472	480	T	480	24
GROUND – AIR – GROUND	– – –	12000	G	12000	600
LATERAL GUST AND MANEUVER	VSS469	74640	L–1	40	2
			L–2	260	13
			L–3	2400	120
			L–4	71940	3597
BUFFET	VSS800	17860	B–1	20	1
			B–2	280	14
			B–3	17560	878
VERTICAL GUST, VERTICAL MANEUVER AND LANDING IMPACT	FS 2472	95020	V–1	20	1
			V–2	40	2
			V–3	180	9
			V–4	1160	58
			V–5	8600	430
			V–6	85020	4251
TOTAL / LIFETIME	- - -	200000	15	200000	10000

The fatigue test loads applied to the specimen were based on the fatigue design loads established from the C-5A mission profiles. The test loads consisting of 800,000 cycles (including a scatter factor of four) were distributed in a spectrum equivalent to the fatigue design load spectrum. The test specimen was subjected to repeated passes of the loading spectrum as shown in Table IV. Each spectral pass represented the equivalent of 1500 flight hours (5% of the service life). Therefore, a total of 20 passes were required to simulate 30,000 flight hours or one lifetime. The specimen loading spectra consisted of a group of loads applied in sequence, with their order reversed on alternate passes of the spectrum.

Since the test loads for the C-5A Aft Fuselage - Empennage structure were developed to simulate the design spectrum in terms of fatigue damage, two primary objectives were considered pertinent in converting the design spectrum into its equivalent test spectrum. First, structural integrity must be demonstrated for all significant types of loads. Secondly, the applied test loads must accurately represent the fatigue damage effects of all load sources. The test spectrum was designed to simulate the significant fatigue loads expected to be experienced by the airplane during a lifetime of 30,000 flight hours and 12,000 landings. Test cycle allocations for each basic load source are shown in Table IV. Although the complete fatigue test program was planned to apply load cycles equivalent to four times those anticipated for one aircraft design life, the fatigue sensor evaluation program was planned to cover only the first lifetime.

Figure 34 offers a simplified description of the laboratory simulated loading conditions imposed on the specimen and the selection of sensor locations to respond to these loads. It should be recalled that the fatigue damage information system is based on the concept of monitoring the influence of repeated load occurrences and correlating fatigue damage with sensor readings rather than attempting to measure fatigue damage directly. Therefore, the sensors were located so that they would be responsive to the more significant cyclic fatigue loads. The primary damaging loads in relation to their more critical structural locations are:

- o Landing Impact on Horizontal Stabilizer and Fuselage
- o Buffet on Upper Vertical Stabilizer
- o Lateral Gust on Lower Vertical Stabilizer and Under Fin Frames

The fatigue loads and reactions considered during laboratory simulation are shown in Figure 34 and are listed in the order of significance, that is, gust, maneuver, buffet, and landing impact loads are the most damaging while taxi loads have a negligible effect. The simulated aerodynamic and inertia forces acting on the horizontal stabilizer produce peak cyclic tension strains close to the root and along the crown of the horizontal. Since the sensor response to tensile loads is more informative, all sensors on the horizontal are located on upper surfaces. Sensors numbered E-1 through E-9, occupy positions which should respond to local redistribution of stress on these surfaces, as well as serving to totalize the effects of repeated load exposure imposed on the horizontal stabilizer. The pivot fitting was designed for stiffness rather than strength,

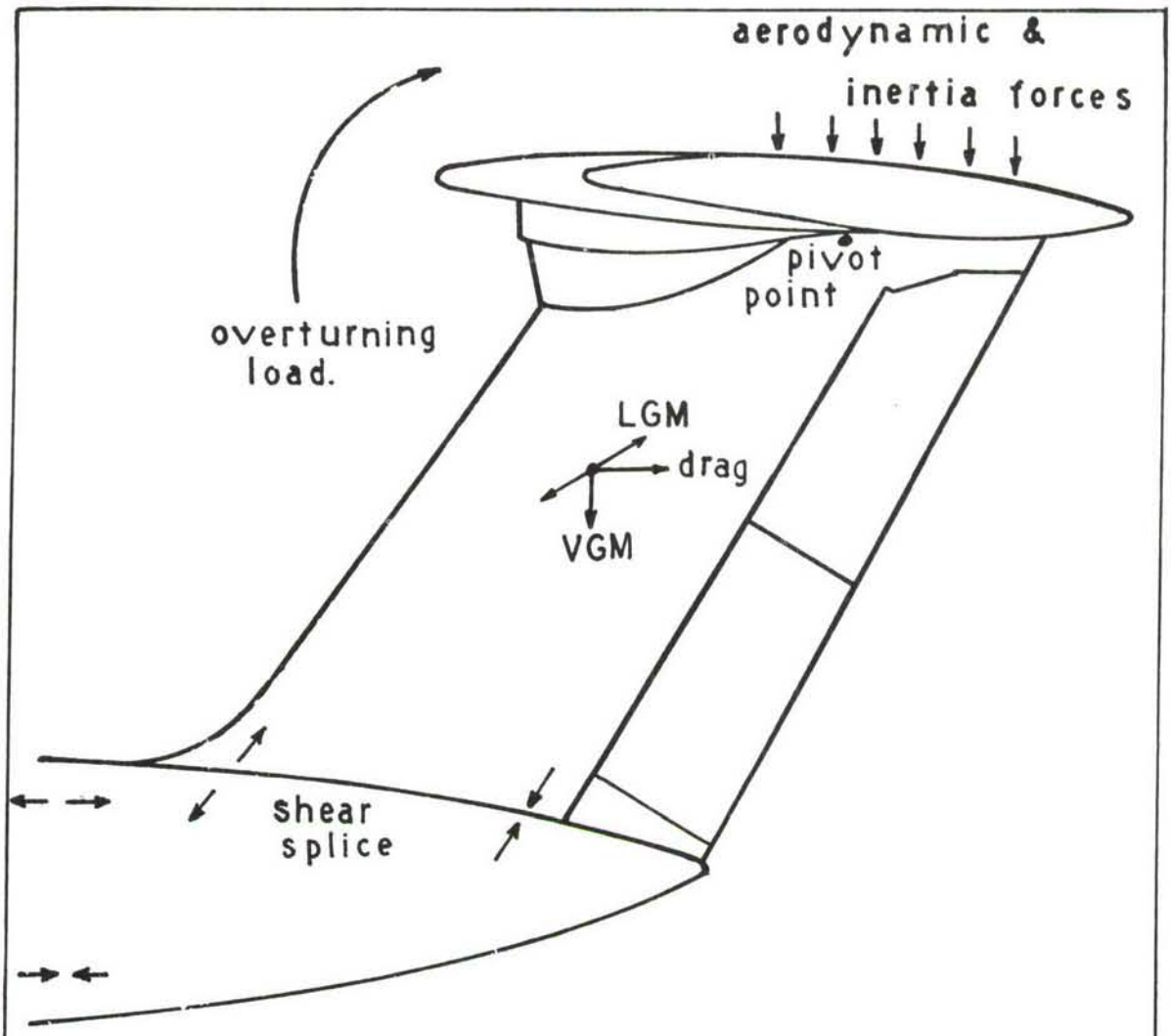

FATIGUE LOAD CONDITIONS TO BE SIMULATED

1. VERTICAL GUST AND MANEUVER
2. LATERAL GUST AND MANEUVER
3. LANDING IMPACT
4. BUFFET
5. GROUND-AIR-GROUND
6. TAXI

FIGURE 34. EFFECTS AND REACTIONS TO APPLIED TEST LOADS

consequently the cyclic strain levels in this area were too low to justify sensor instrumentation. However, since concentrated loads produced at the pivot point of the vertical fin are distributed to the pivot fitting "run-out" area, sensors E-12 and E-13 (Fig. 53) were located to respond to these loads. The aerodynamic and inertia forces imposed on the horizontal stabilizer are distributed through the vertical fin. These loads, in addition to the lateral loads on the fin, are transferred into the aft fuselage by way of attachment fittings and splice plates. Sensors E-14, E-15, E-16, and E-17 (Fig. 52) are located on internal skin surfaces near the root of the vertical fin to respond to these load sources.

In the past, sensor performance on attachment fittings have been somewhat erratic; however, there remains a temptation to instrument attachment fittings primarily because they constitute well defined load paths and sensor readings may be significantly affected by local failure. Sensors AF-3, AF-4, AF-5, AF-6 were symmetrically located on the two dagger fittings which attach the front beam of the vertical to the dorsal longeron and fuselage frame at F.S. 2538. Since the shear splice is inaccessible (outside surface) for sensor installation, sensors AF-9, AF-11, AF-13, AF-15 and AF-22 were located on the underfin frames to respond to the effects of empennage loads. Sensors AF-10, AF-12, AF-14, AF-16, AF-20 and AF-21 located on the frame flanges were not expected to become active (produce a significant resistance change) unless there was a pronounced redistribution of internal load paths. The instrumented areas of the main frames are designed for stiffness, so for this application very low sensor readings or even no resistance change at all can be just as informative as a progressive change in resistance.

The criteria used for physically locating sensors on the Aft Fuselage - Empennage specimen (X997) followed the same approach used previously; i.e., a consideration of stress analysis data, locations proven critical on previous tests of component parts, and an on-site visual inspection of the test structure. After the locations were finalized, sketches were prepared to define the locations for the sensor installation technicians. The location sketches are shown in Figures 36 through 55. Once the monitoring sites (sensor locations) have been determined, the multiplying factor of the sensor shim combination should be "sized" for an optimum response.

To obtain an optimum sensor response to the design spectrum of loads (Table IV) requires a mechanical manipulation during bonding of the sensor shim. A straight forward technique for physically adjusting the mechanical multiplier to a target value was previously explained (Section 2.3); however, methods for satisfactorily calculating the optimum multiplier value for the design spectrum of load is more involved.

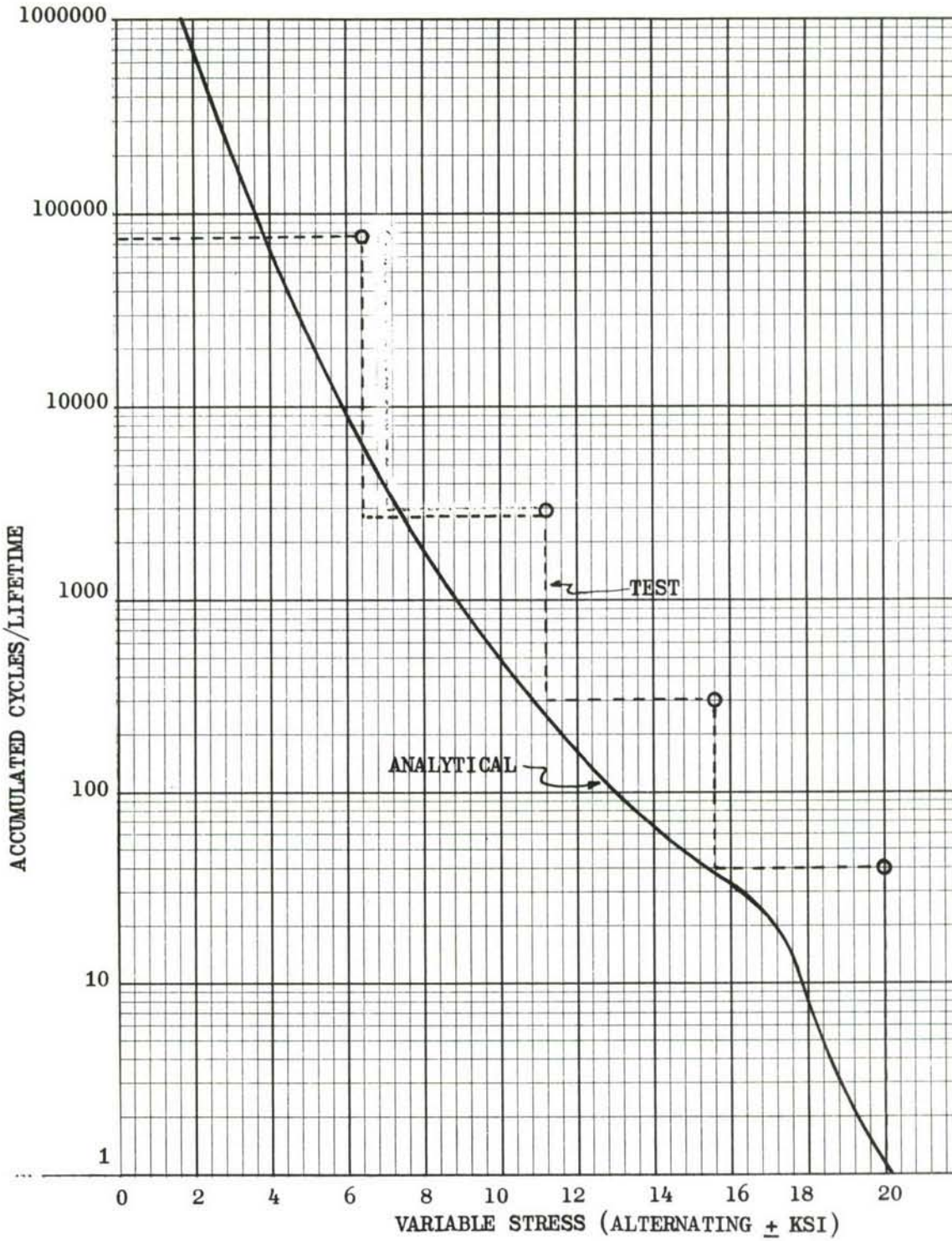

FIGURE 35. TYPICAL OCCURRENCE CURVE SHOWING VARIABLE STRESS AT VSS 424.6 FOR ACCUMULATED CYCLES OF LGM LOADS

The approach utilized for the instrumentation of the Aft Fuselage-Empennage specimen makes use of occurrence curves showing the number of cycles of exposure to specific stress levels at key locations to approximate the size multiplier. As a case in point, the lateral gust manuever (LGM) condition is more severe at VSS 424.6 of the vertical stabilizer; therefore, cyclic loads shown for the LGM condition (Fig. 35) will have a predominent influence on the resistance change of sensors located in these key areas. By correlating information contained in Figure 20, Figure 35, and Table IV, it can be seen that 71,940 cycles of LGM-4 condition should produce a sensor resistance change of approximately two ohms for sensor installations having a multiplier of three.

The diagram below illustrates the projected relationship of sensor resistance change for each basic load condition as approximated by a correlation of sensor behavior characteristics (Fig. 20) with anticipated load exposure (Fig. 35). The diagram as shown with its approximated resistance values is applicable to the sensors (AF-9, AF-11, AF-13, AF-15, AF-22, and AF-23) located in the vicinity of VSS 424.6.

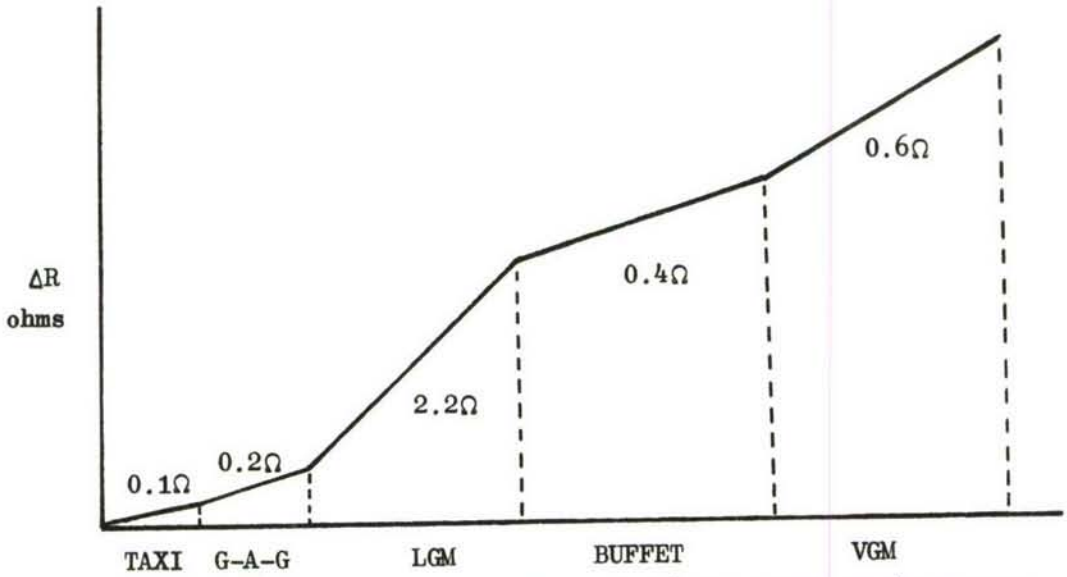

CALCULATED SENSOR RESISTANCE CHANGE/LOAD CONDITION/LIFETIME

According to the previous diagram the total resistance change for typical sensor locations at VSS 424.6 (root of the vertical stabilizer) will approximate 3.5 ohms. In practice the multiplier is adjusted to the loading program such that the sensor will produce a resistance change ($_{\Delta}R$) for the low (taxi) loads yet not produce an excessive resistance change ($_{\Delta}R$) for the higher (LGM) loads. If an excessive resistance change is permitted for the LGM load condition the targeted operating range of the sensor will be exceeded prior to one aircraft lifetime. One of the more critical limitations is the selection of a multiplier factor such that the sensor output does not exceed five ohms for any programmed structural lifetime.

Previous sensor fatigue life tests for high cycle applications (Fig. 4) shows that the type 204DA-STE sensor approaches a "high risk" area of sensor operation if the resistance change exceeds five ohms.

It appeared that for nominal area strains of the Aft Fuselage - Empennage specimen, a multiplier of three would be optimum if a common multiplier factor were used for all locations. While a common multiplier for each specimen would simplify documentation, considerable experimentation with various multipliers was obtained on this specimen in an attempt to produce an optimum resistance change per lifetime. The multipliers used required the use of two different sensor sizes, i.e., the SAP202DA-E and the SAP204DA-STE (Figs. 5 and 6). An examination of the varying stresses in the selected critical areas indicated the possibility that a common multiplier would not be suitable for producing targeted resistance changes of two to three ohms within the programmed one lifetime, therefore, two sizes were used (see Tables V and VI). This targeted resistance change per lifetime would permit adequate resolution, plus the capability of extending sensor utilization to more than one lifetime if desired.

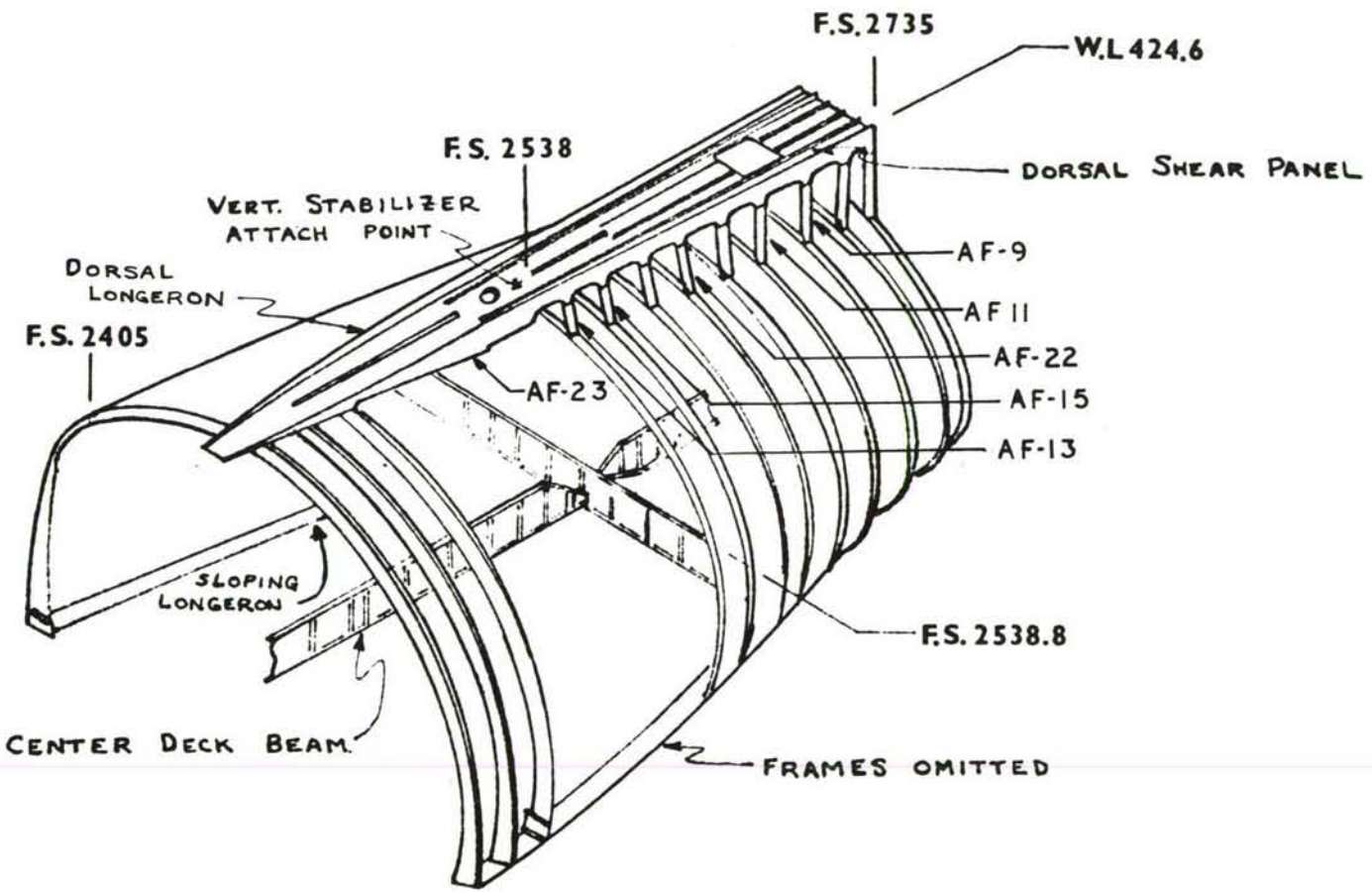

FIGURE 36. AFT FUSELAGE GENERAL SENSOR LOCATIONS

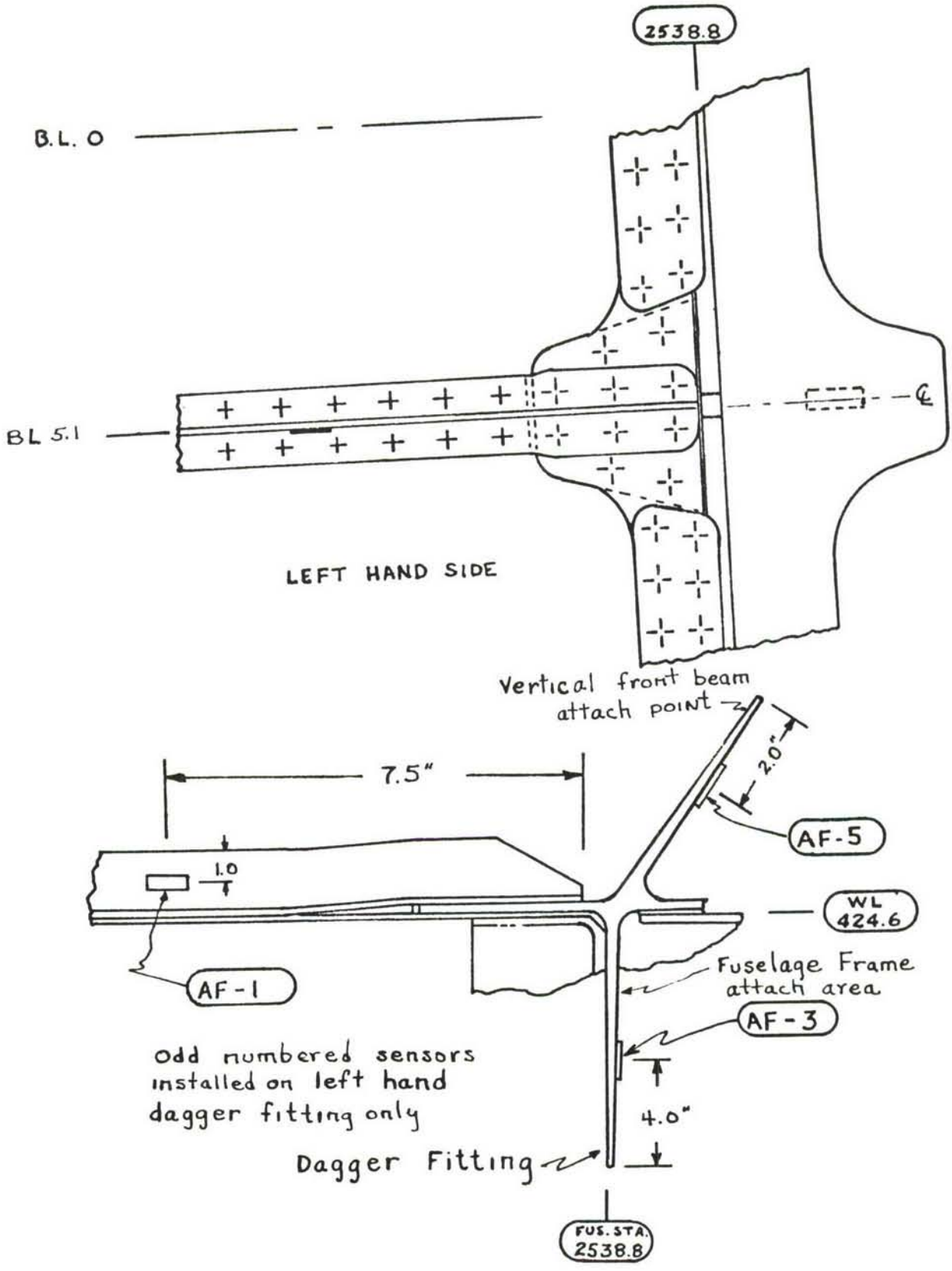

FIGURE 37 DORSAL SHEAR PANEL

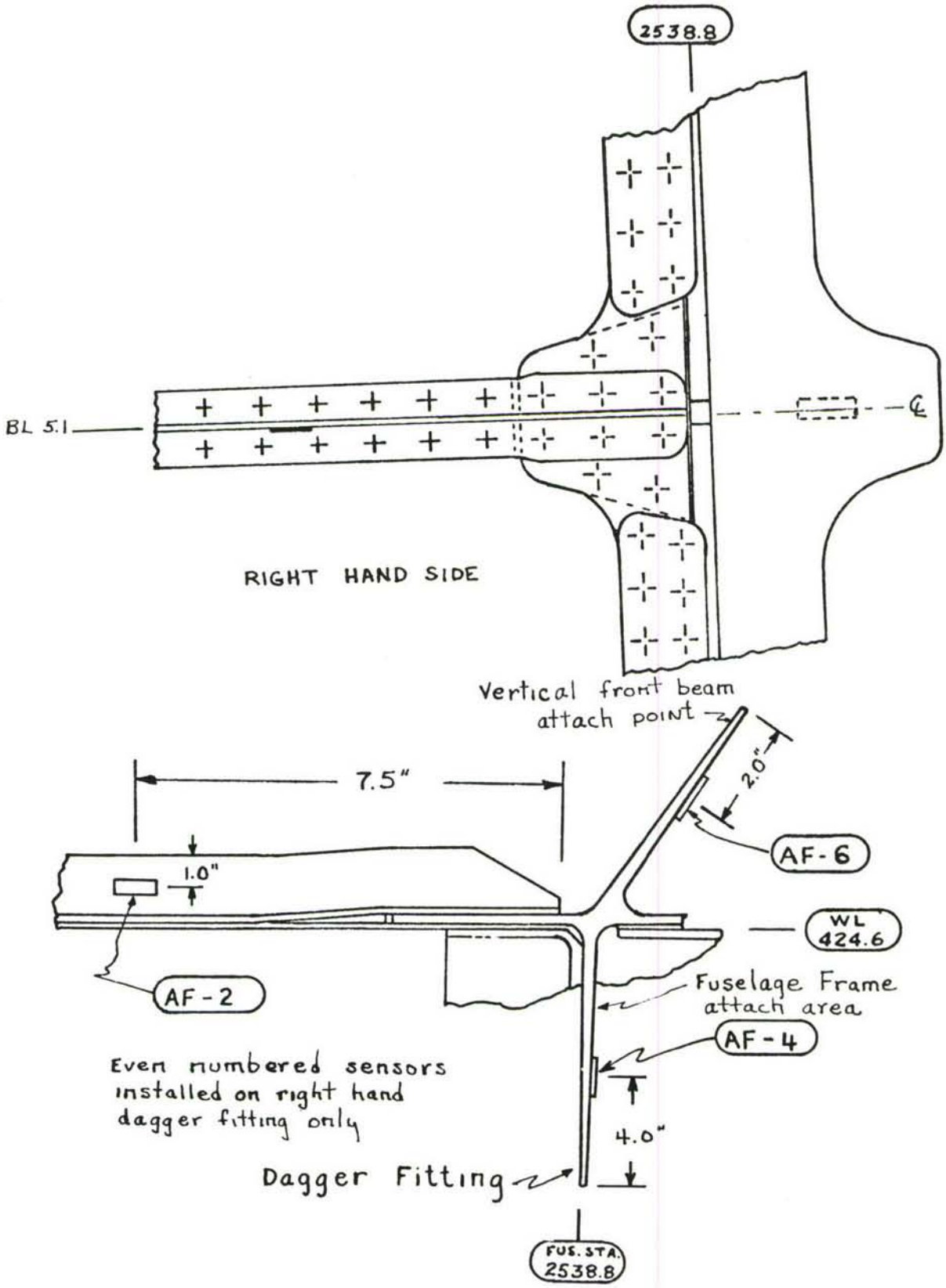

FIGURE 38. DORSAL SHEAR PANEL

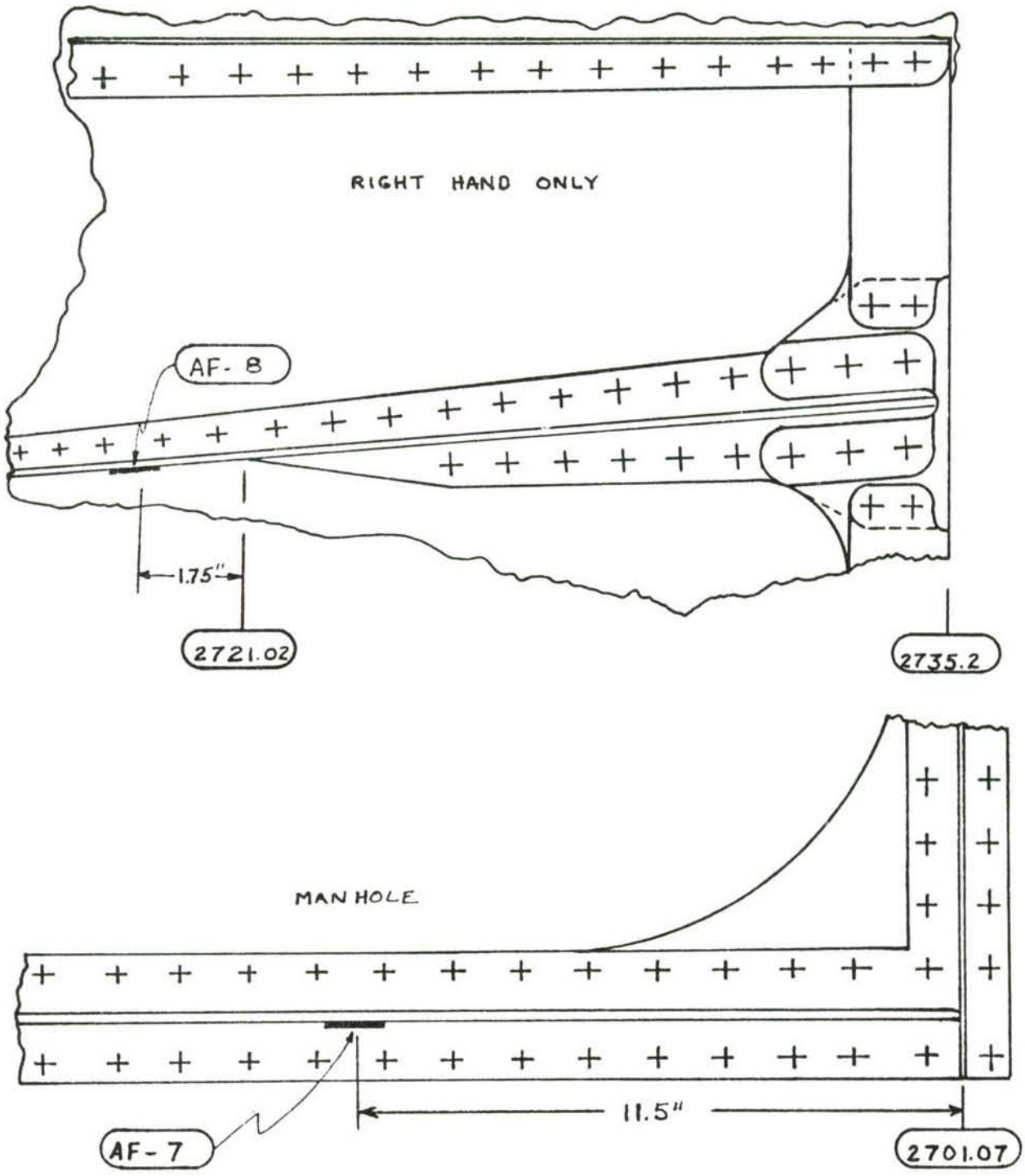

FIGURE 39. DORSAL SHEAR PANEL

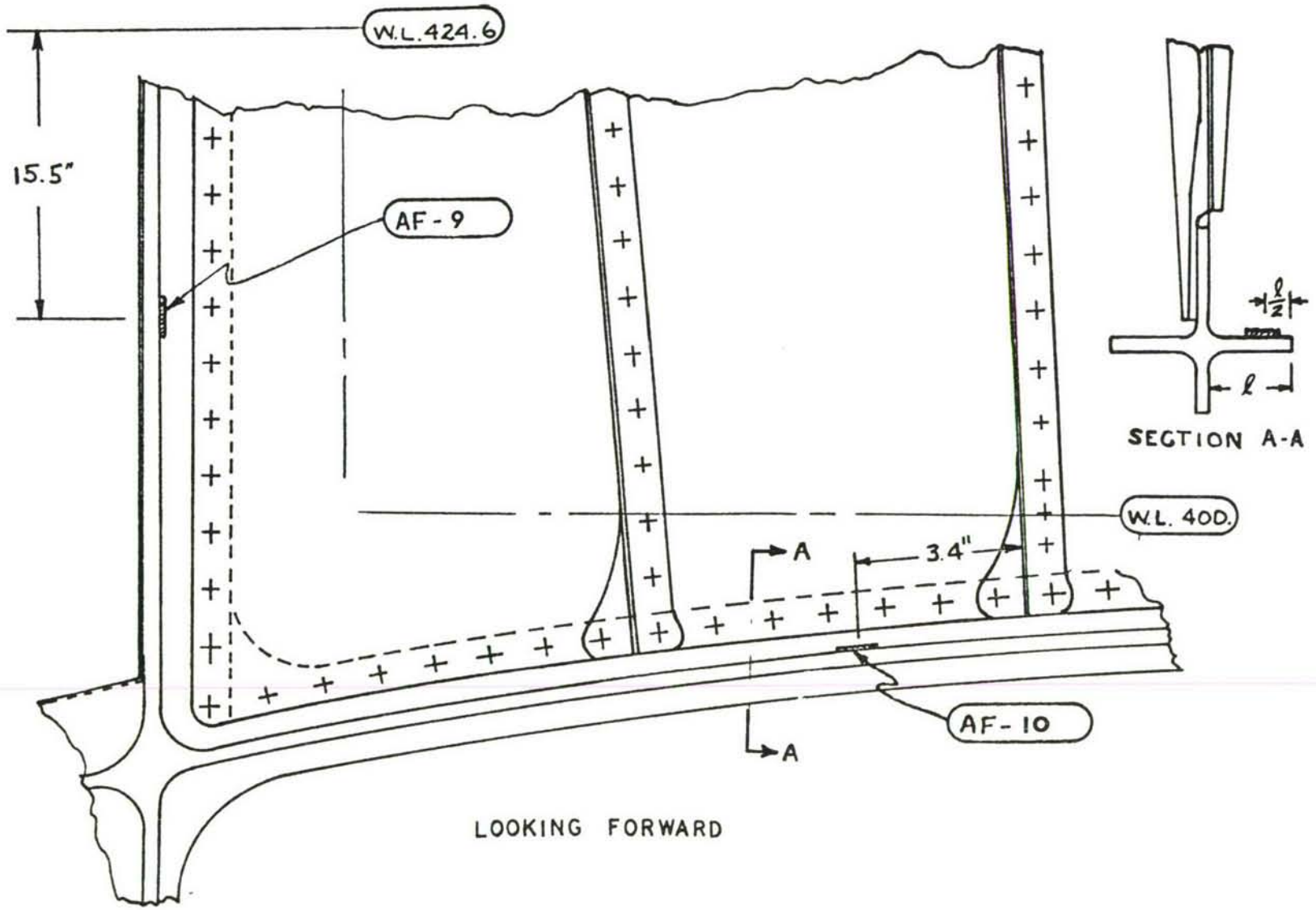

FIGURE 40. UNDER-FIN FRAME F.S. 2701

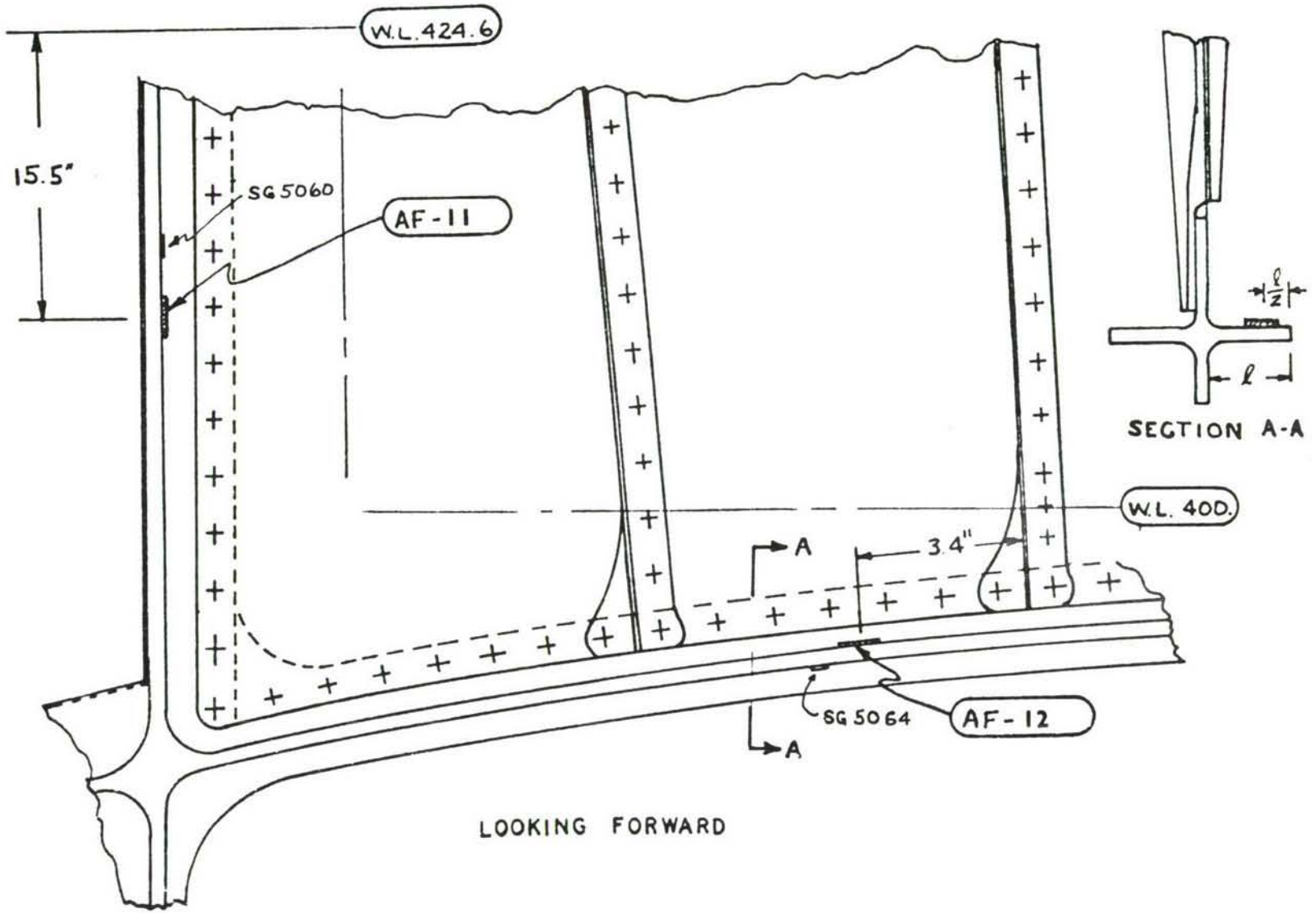

FIGURE 41. UNDER-FIN FRAME F.S. 2657

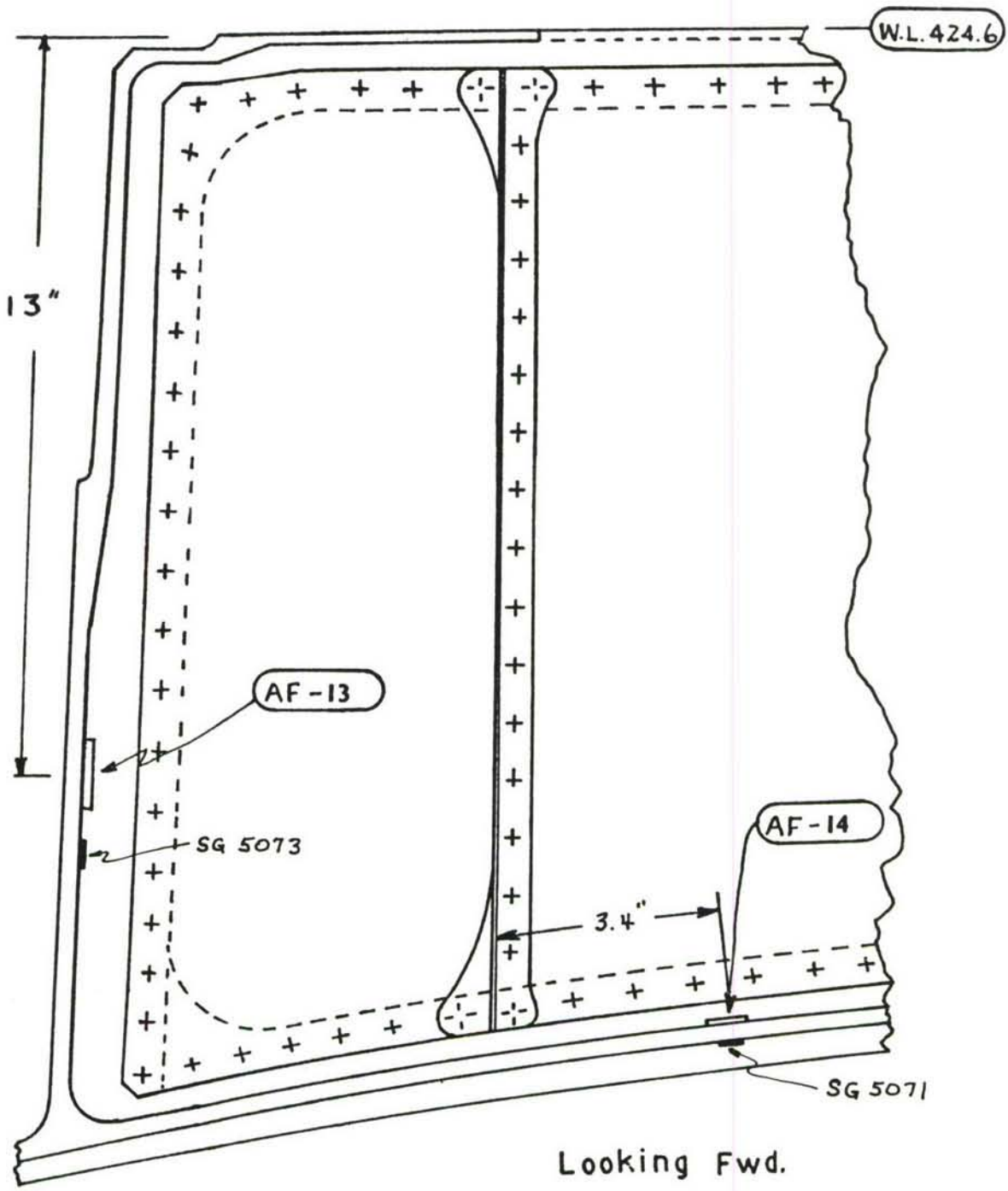

FIGURE 42. UNDER-FIN FRAMES F.S. 2538

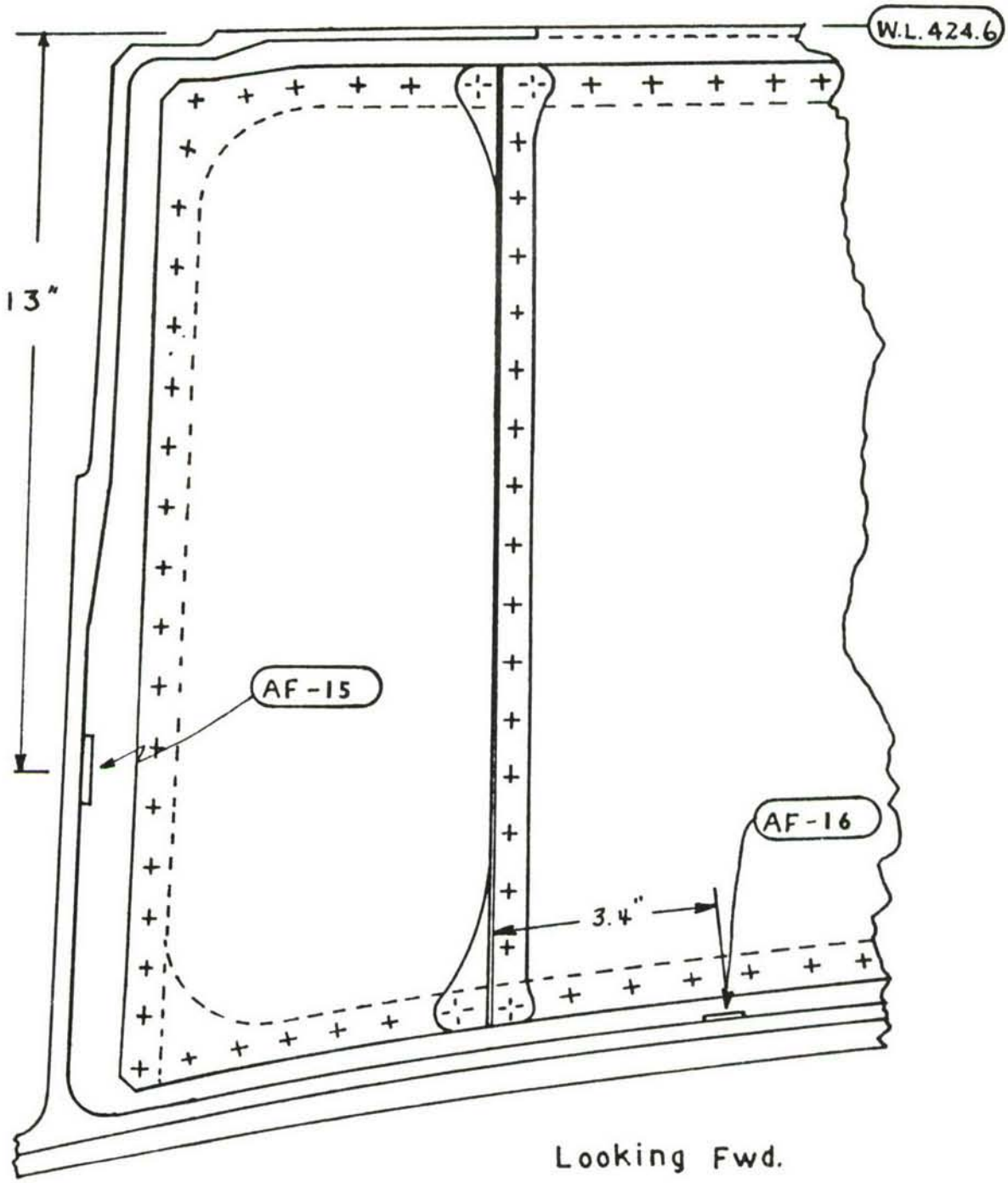

FIGURE 43. UNDER-FIN FRAMES F.S. 2577

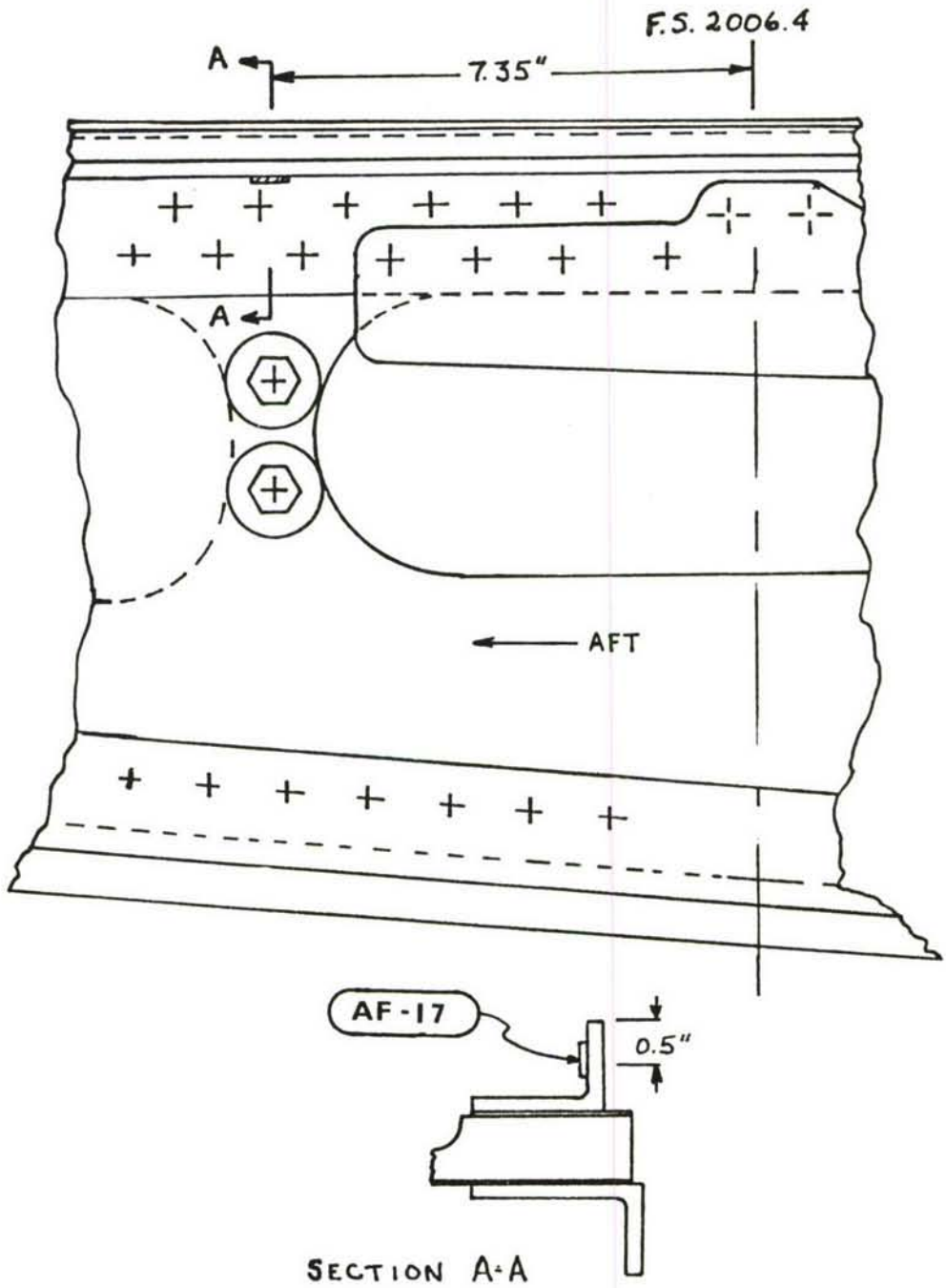

FIGURE 44. SLOPING LONGERON F.S. 2006.4 LH SIDE

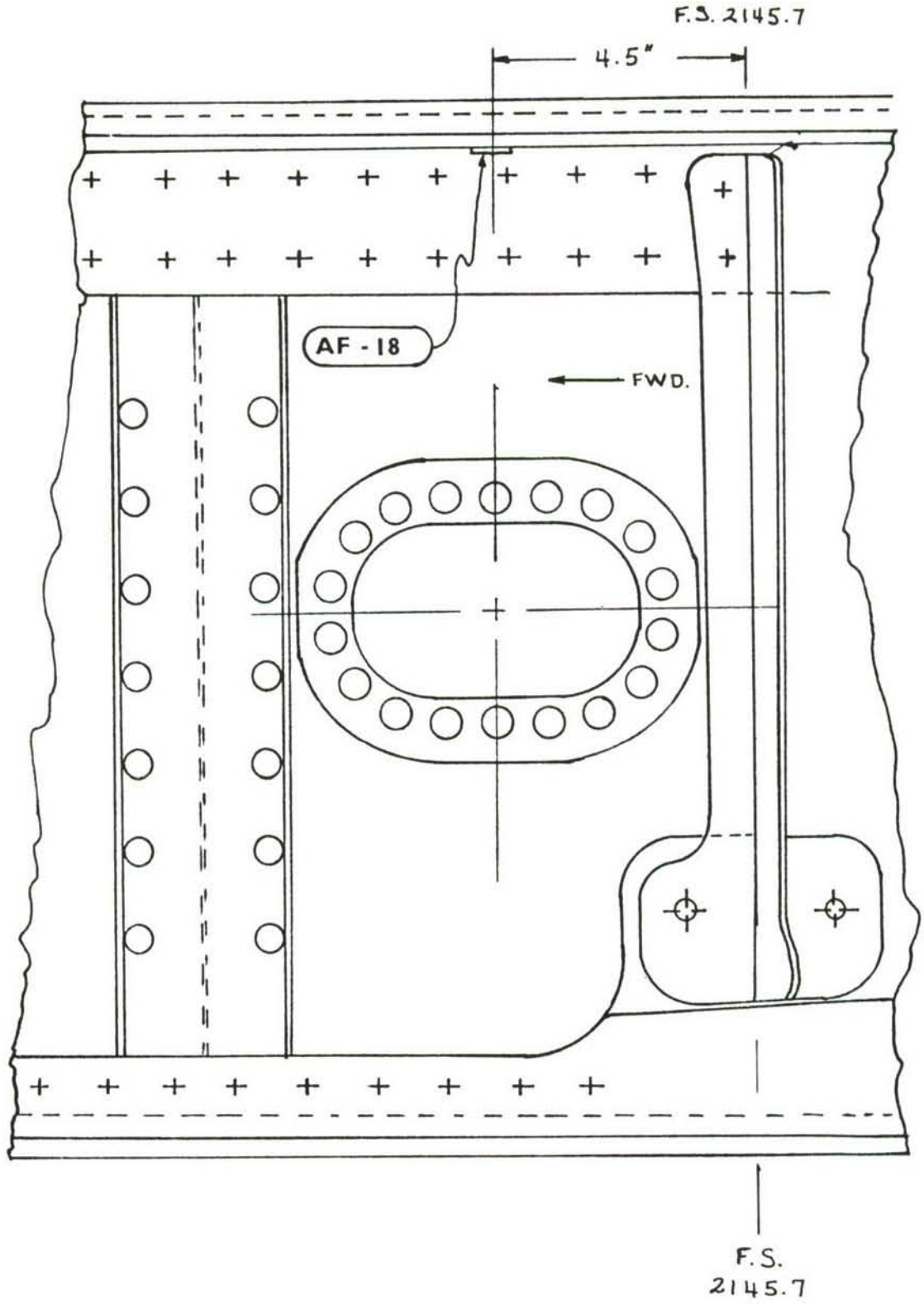

FIGURE 45, SLOPING LONGERON L.H. SIDE

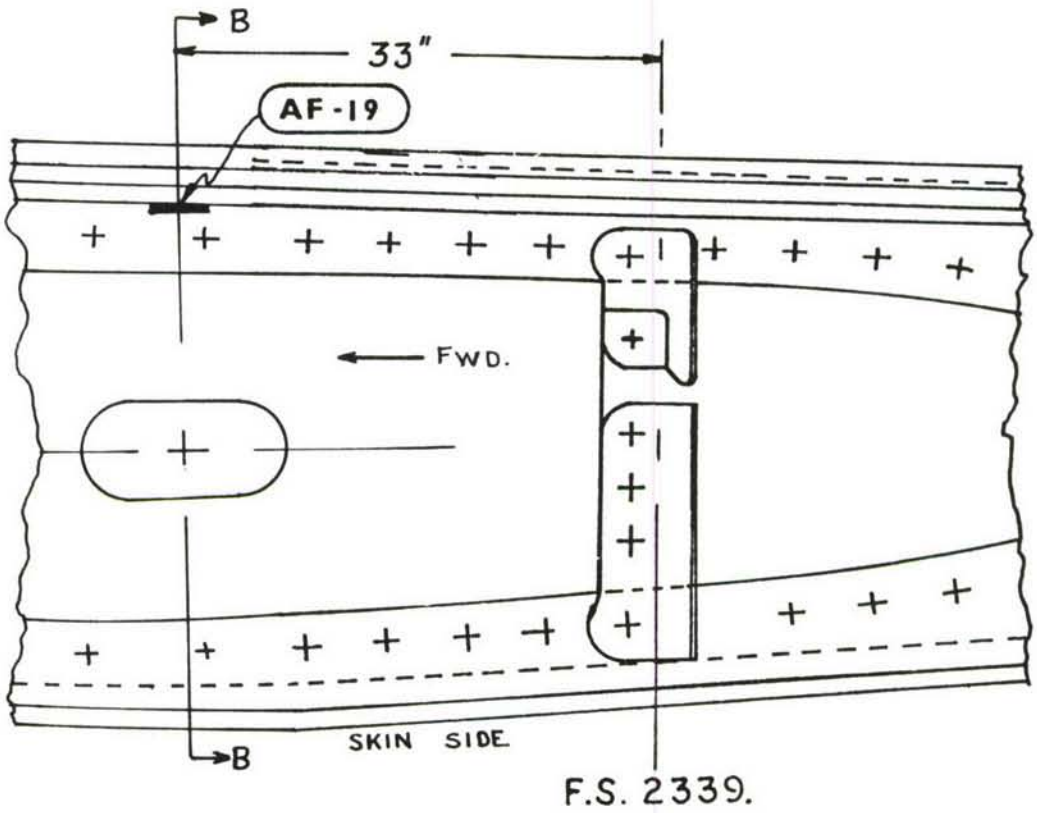

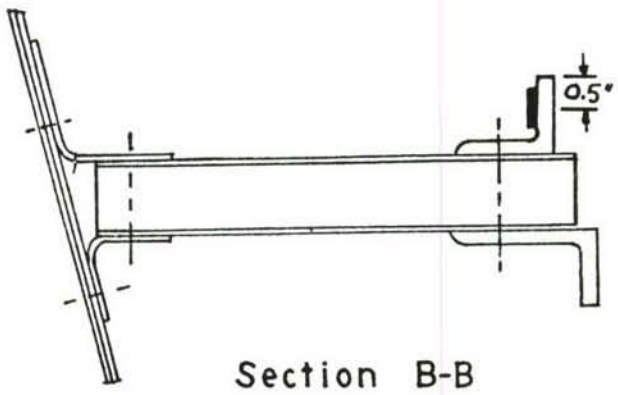

FIGURE 46. SLOPING LONGERON L H SIDE

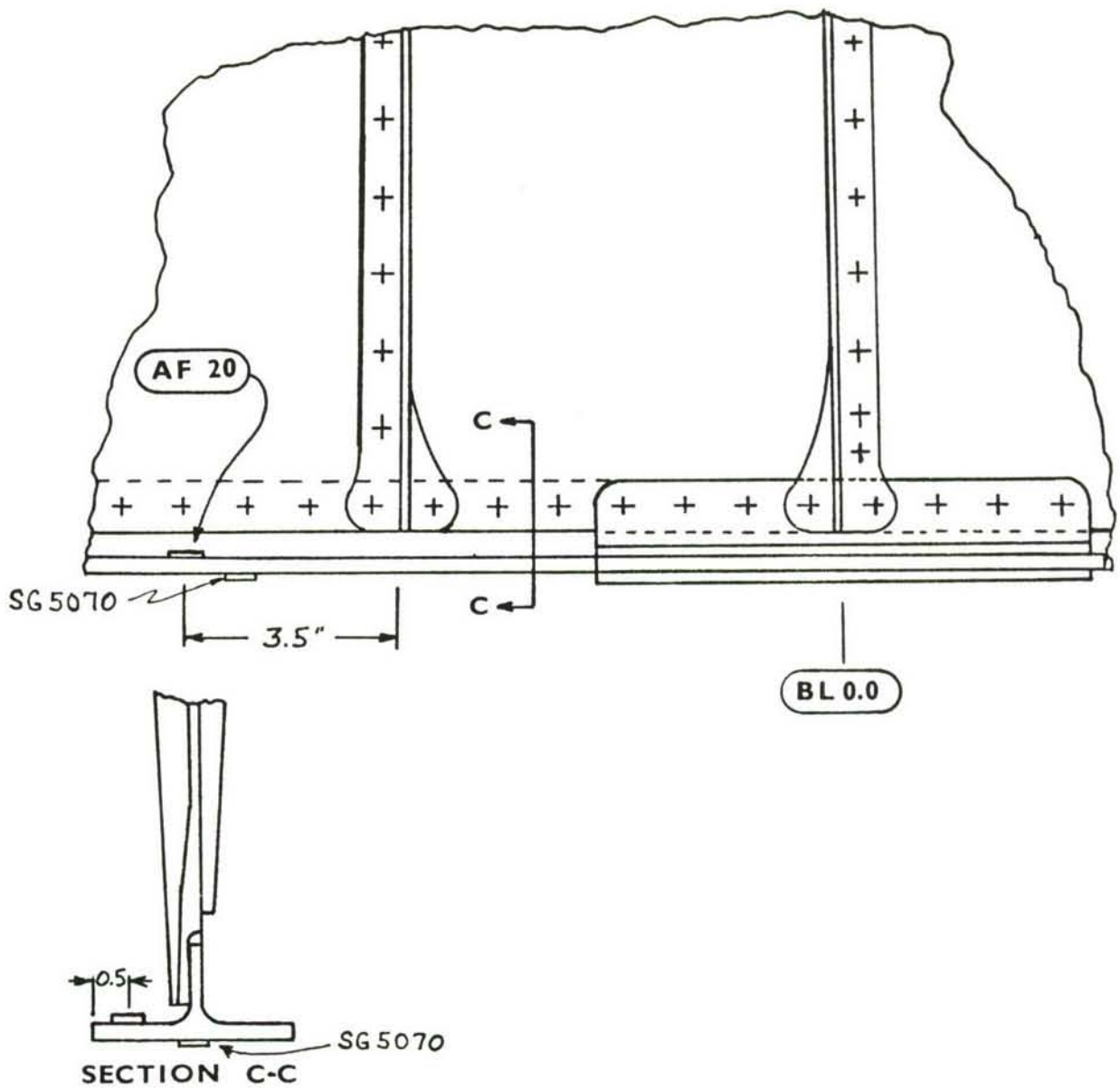

FIGURE 47. AFT FUSELAGE FRAME F.S. 2577

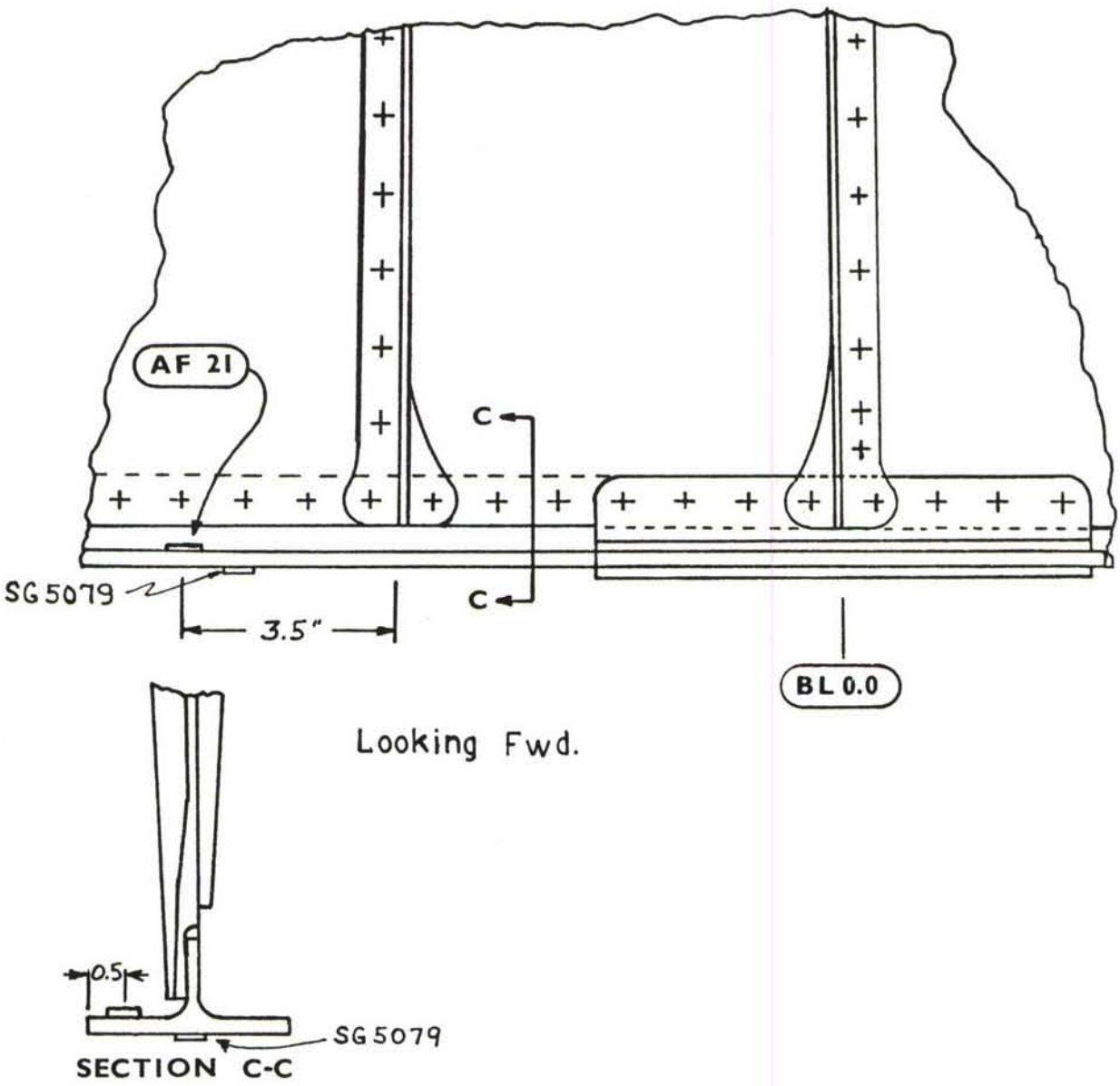

FIGURE 48. AFT FUSELAGE FRAME F.S. 2538

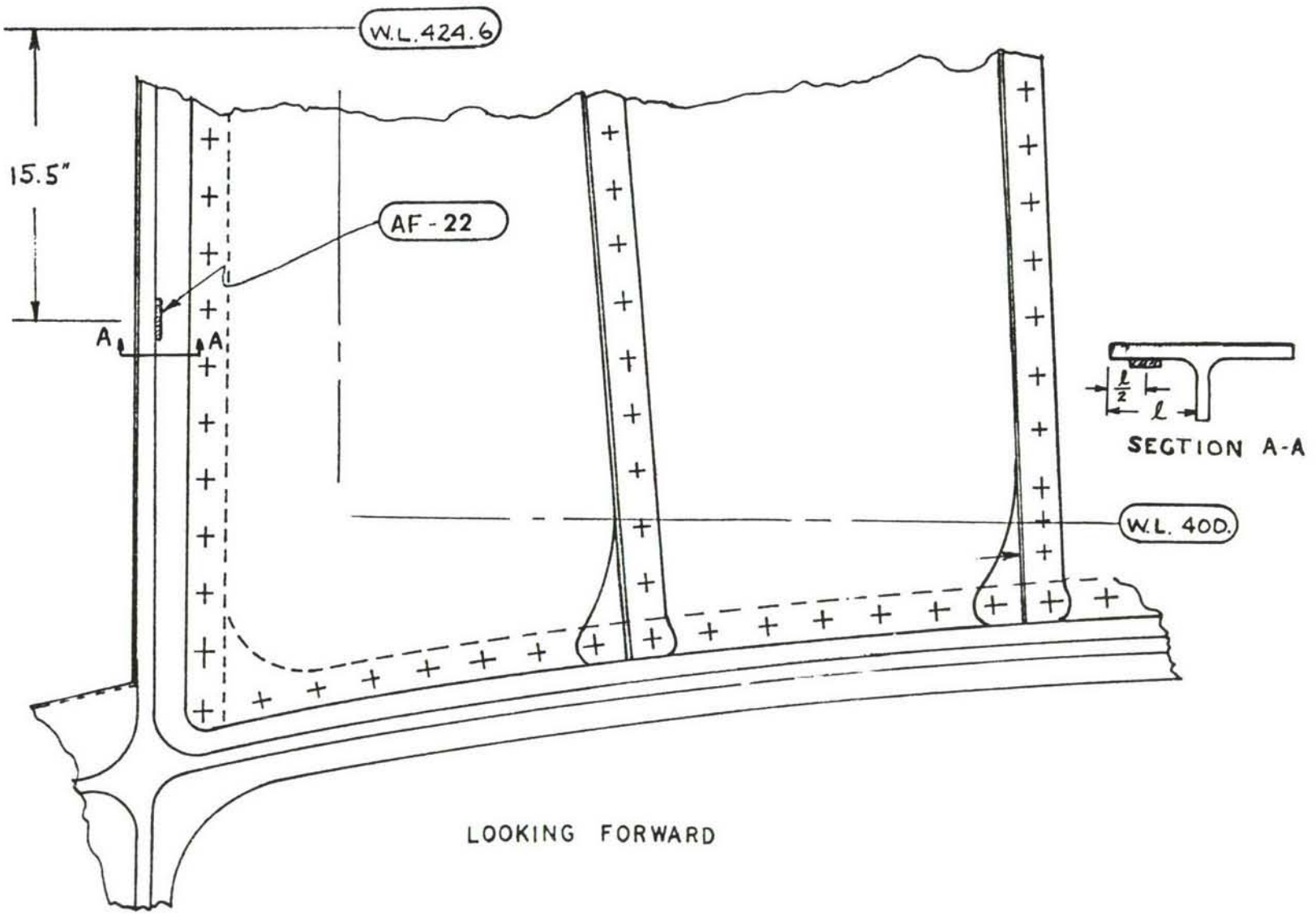

FIGURE 49. UNDER-FIN FRAME F.S. 2617

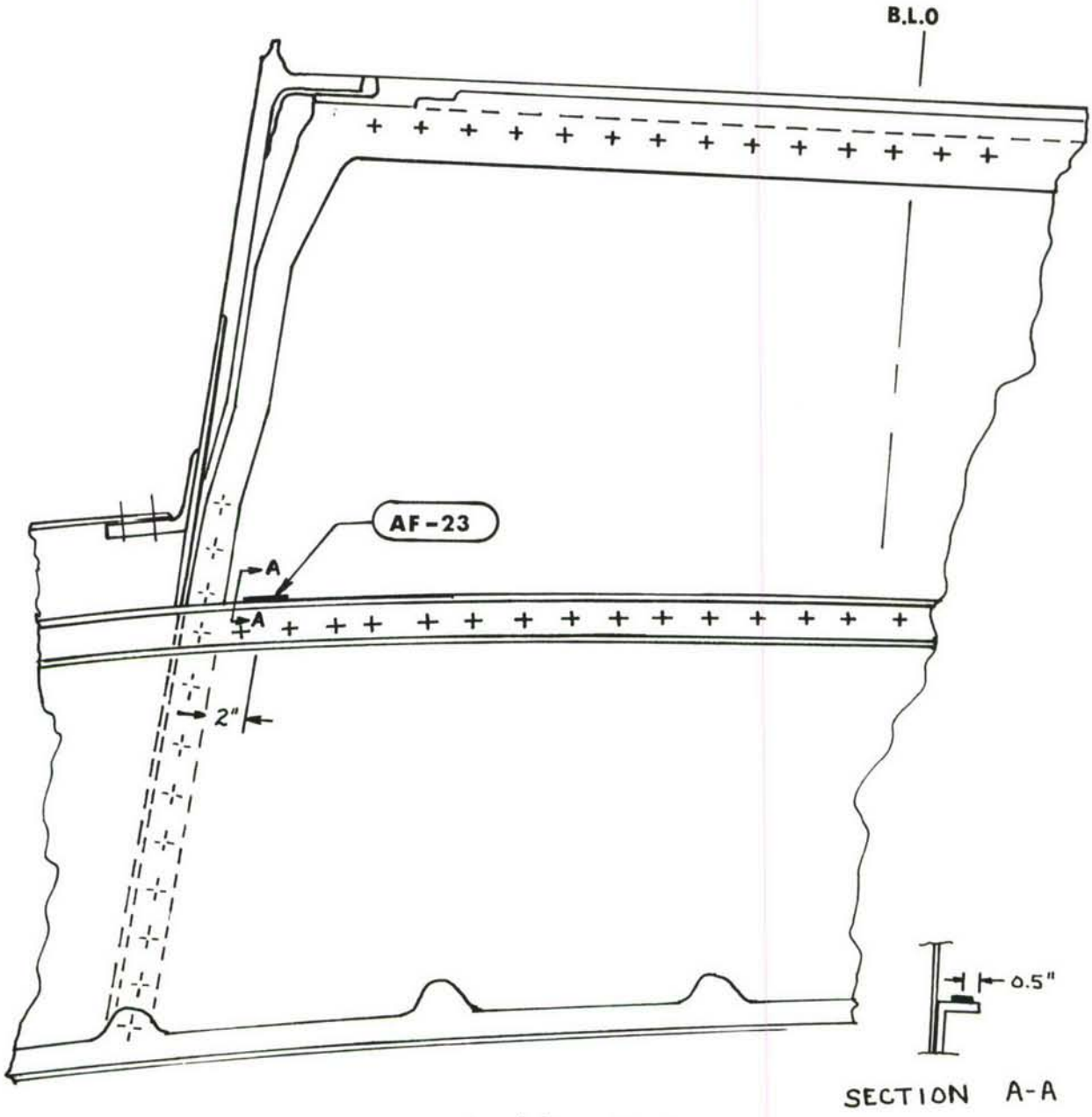

FIGURE 50. UNDERFIN FRAME F.S. 2516

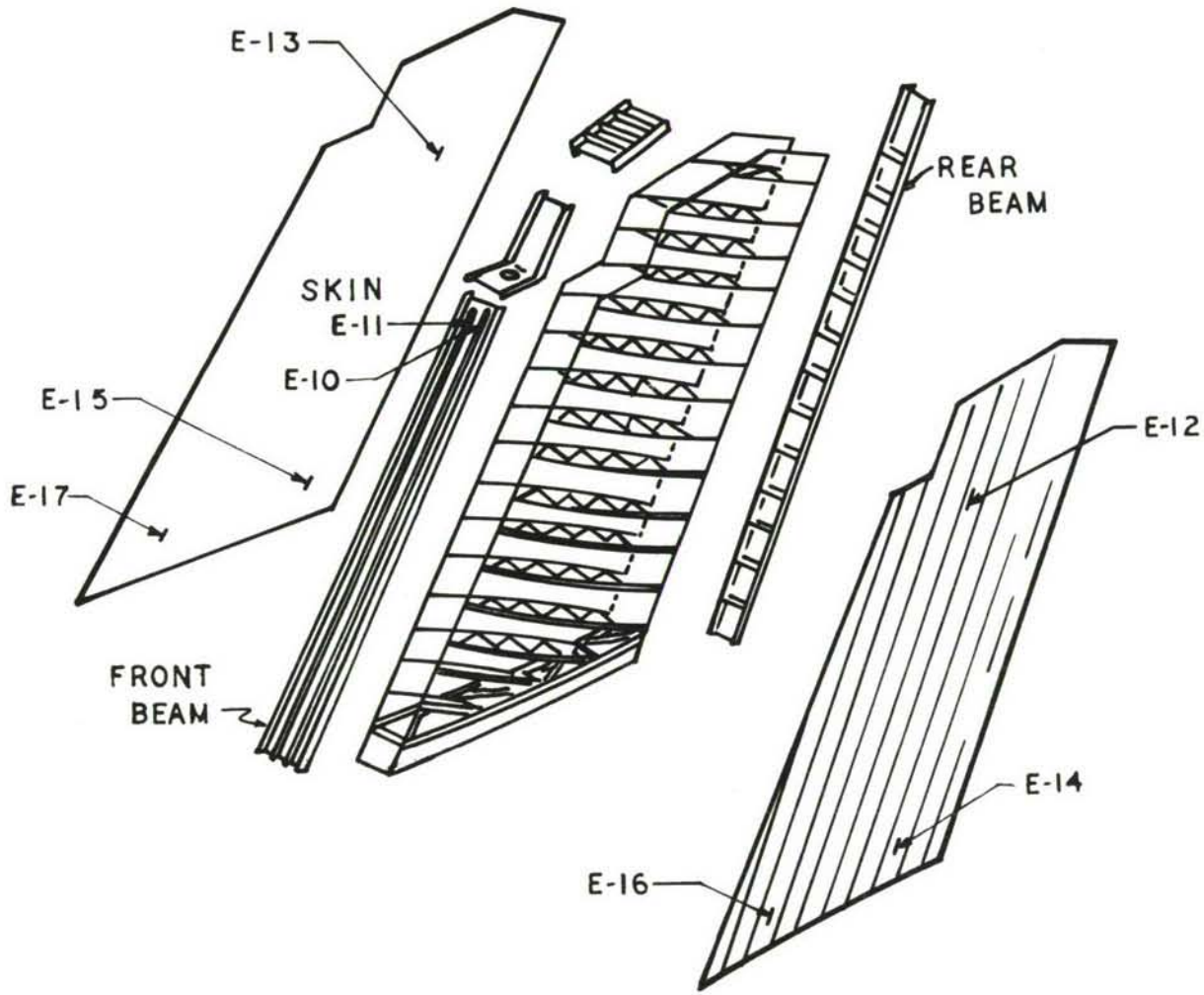

FIGURE 51. VERTICAL STABILIZER

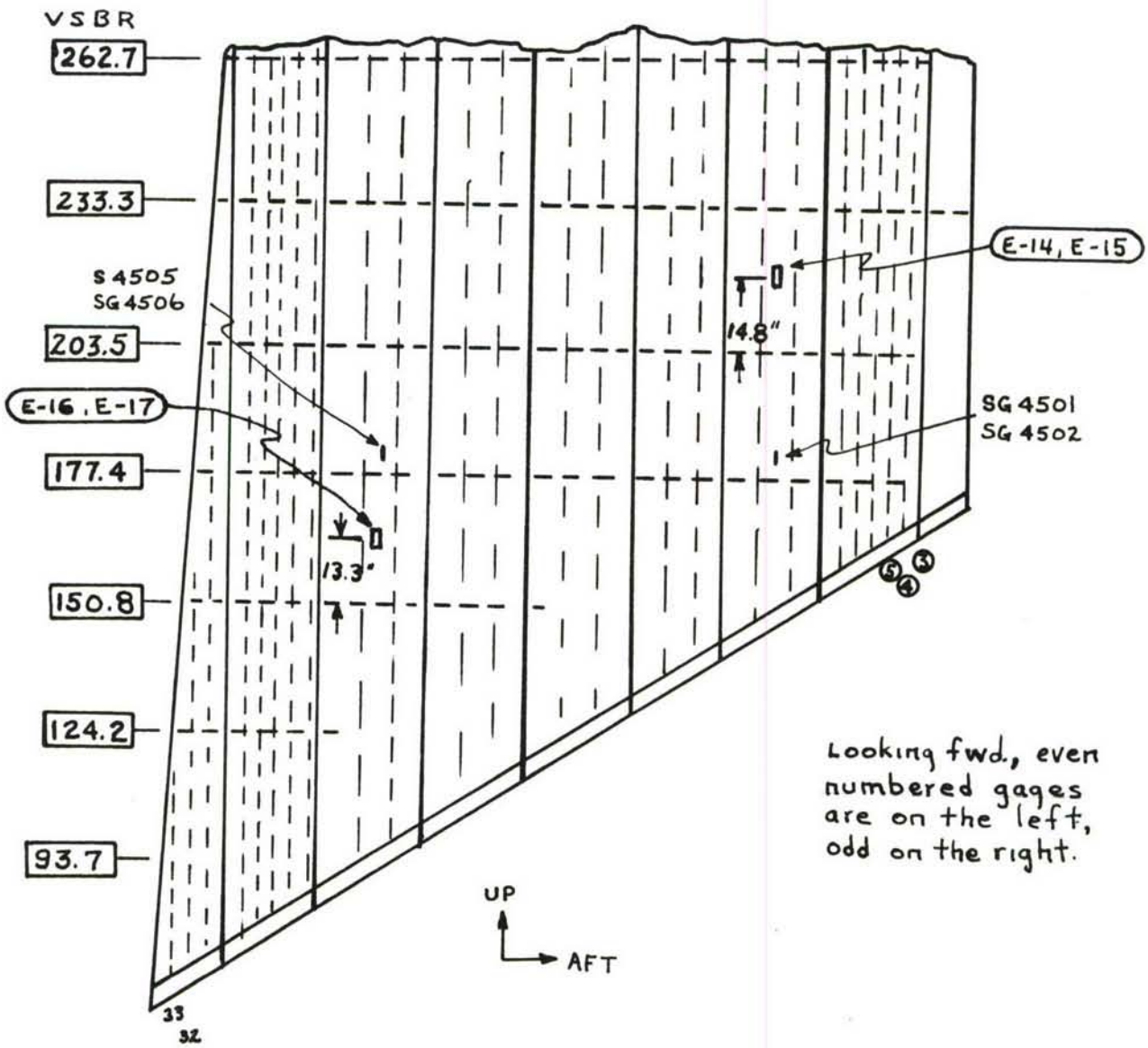

FIGURE 52. VERTICAL STABILIZER - ROOT SECTION

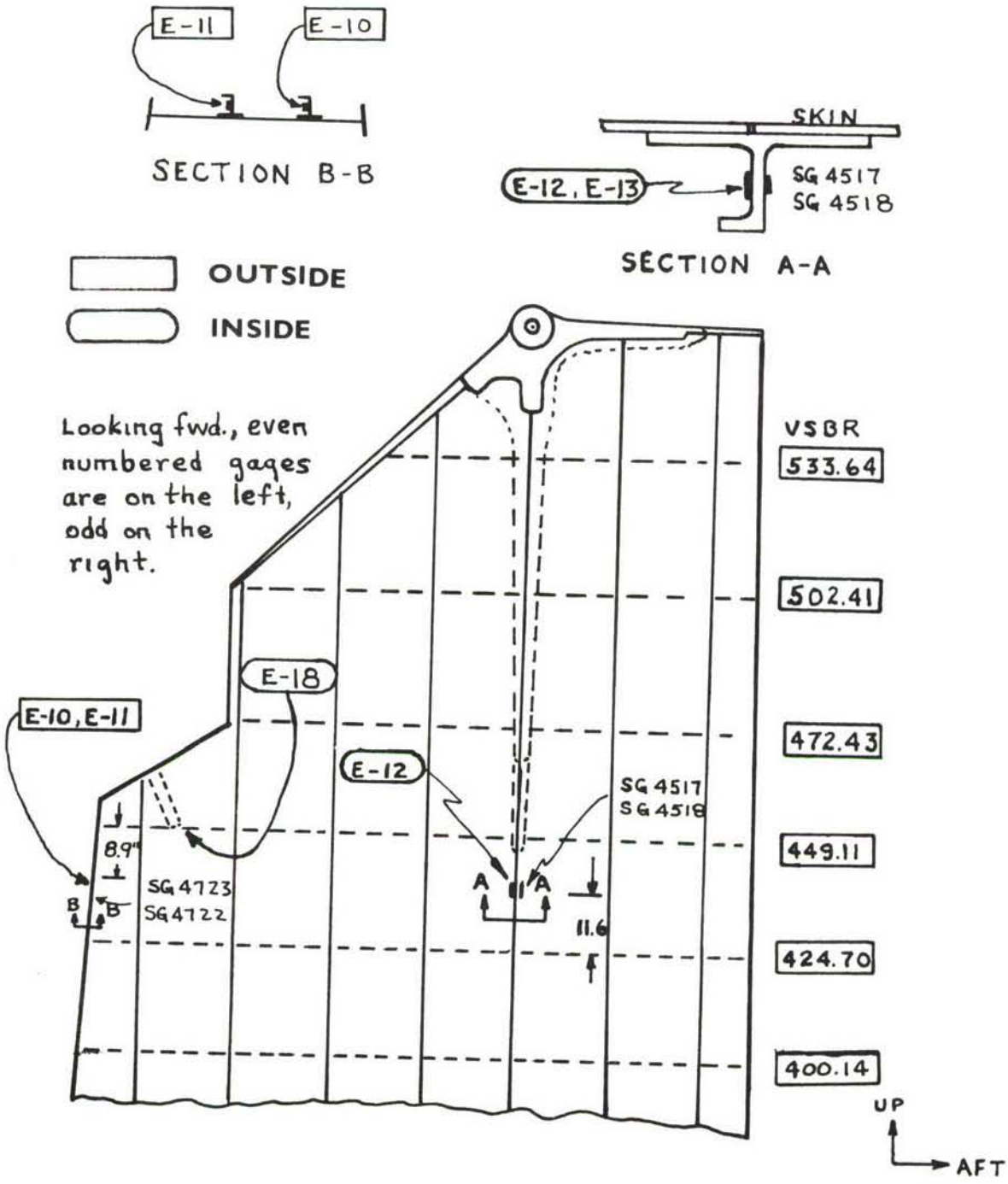

FIGURE 53. VERTICAL STABILIZER - PIVOT AREA

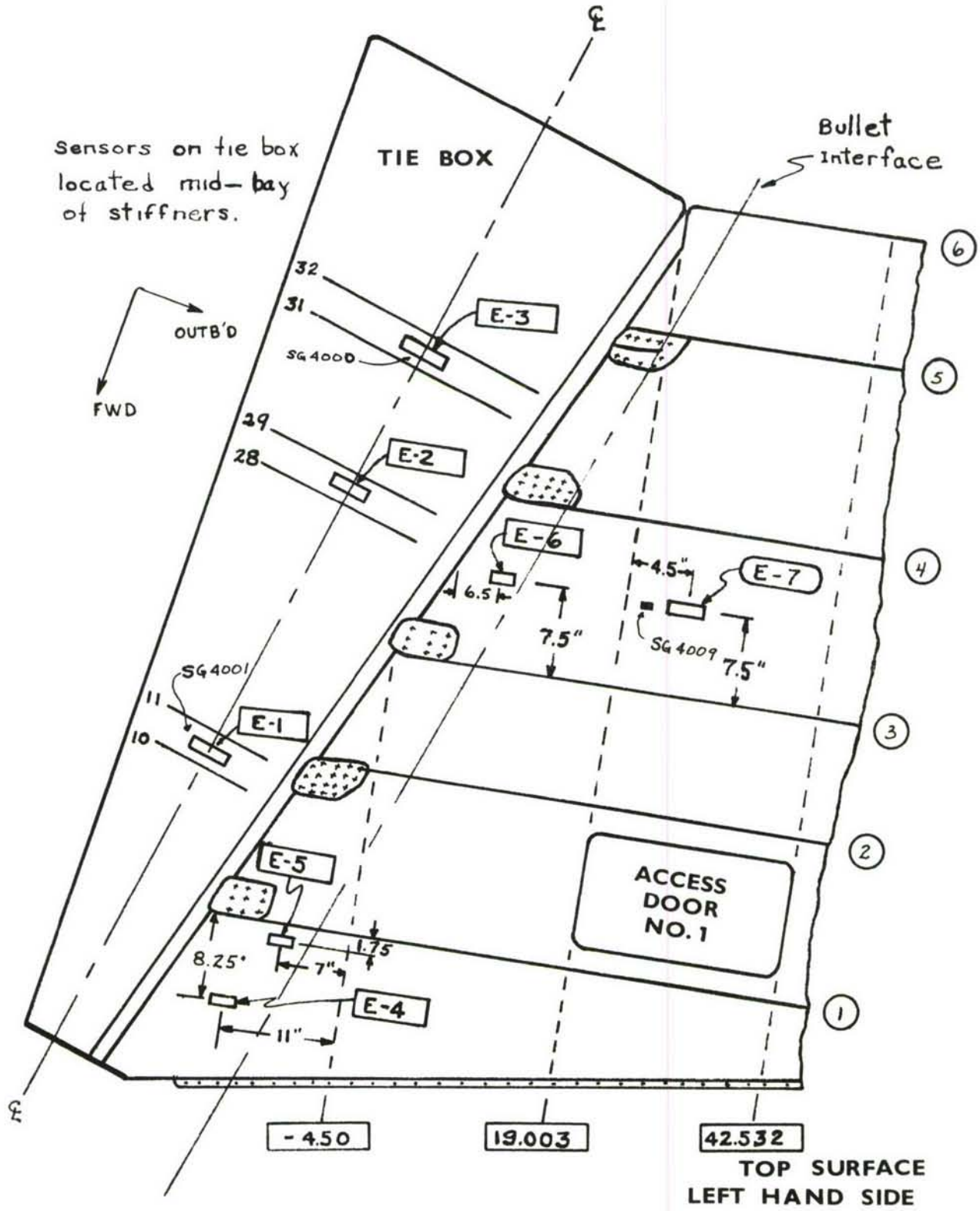

FIGURE 54. HORIZONTAL STABILIZER

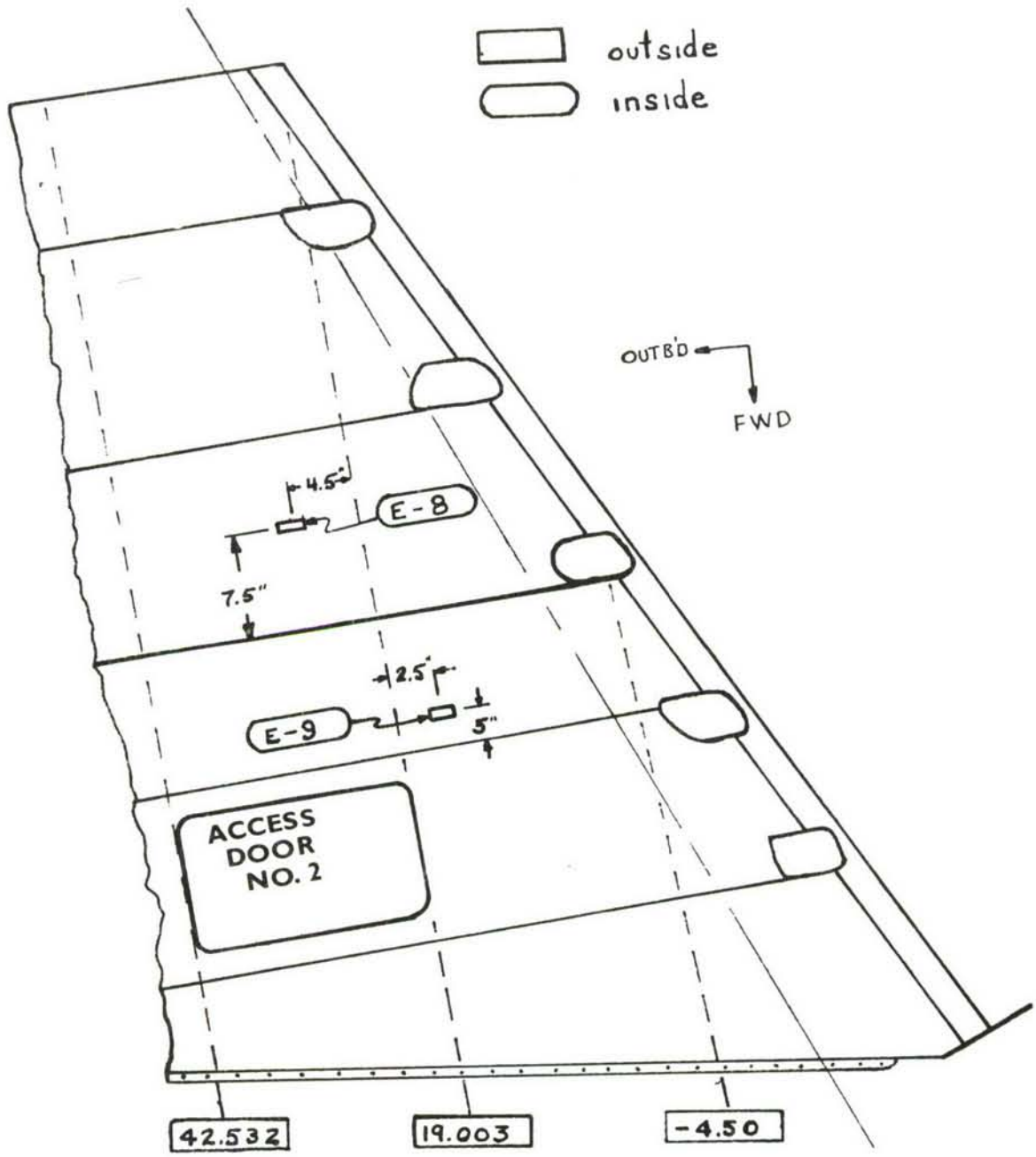

FIGURE 55. HORIZONTAL STABILIZER
TOP SURFACE R.H. SIDE

5.3 STRAIN SURVEY

Prior to the start of specimen cycling some quality control steps may be taken to evaluate the selected sensor sensitivity and location before final acceptance of these values. The static strain survey conducted on the Aft Fuselage - Empennage specimen prior to fatigue cycling was found to yield information valuable to sensor utilization especially in the area of:

(1) Confirmation of sensor multiplier.

(2) Approximation of initial strain distribution in the test structure.

(3) Criticality of installation techniques to obtain a precise multiplier.

(4) Confirmation of sensor bond.

(5) Location of any unusually high strain areas.

Approximately 500 strain gages were installed on the Aft Fuselage - Empennage specimen as a requirement of the basic fatigue test program. These strain gages were used to determine the amplitude and distribution of stresses in areas of special interest. Thirty-nine fatigue sensors were initially installed on the test specimen; many of them adjacent to strain gages. This arrangement permitted the sampling of sensor outputs under a known static load condition concurrently with the sampling of strain gage information.

All sensors were read at various static load increments of both the VGM-1 and LGM-1 load conditions to check for metal-to-metal bond integrity; however, only those sensors adjacent to strain gages could be verified in regard to multiplying factor.

The strain survey provided an opportunity to confirm the programmed sensor multiplier because the sensor also responds to instantaneous strains. Conventional strain gages installed in the same area as the sensor provided a true strain measurement for comparison with the apparent strain response of the sensor. The ratio of one to the other then becomes the actual multiplying factor. It should be recognized, however, that there may be some strain gradient present and there may also be differences in the distribution of strain between load conditions. These factors along with others may account for the scatter in multiplying factor between the two loading conditions. When all the variables are considered it was noted that the multiplier deviation from the theoretical was less than the 10% sensor variation experienced during sensor evaluation on the main landing gear specimen.

With the exception of one sensor (AF-14), which read exceptionally low, all sensors for the two main strain surveys, LGM-1 and VGM-1, indicated a maximum deviation of +8.3%. When one considers the possible errors produced by strain gradients between the sensor and the monitoring strain gage, the variations experienced were not unreasonable. A noteworthy characteristic that has been consistently demonstrated by the strain survey is the tendency for the actual multiplier to read higher than the theoretical values. Since the application technique proposed is one of comparison between the calibration article and the flight article, a statistical mean may be acceptable, thereby reducing the effective multiplier deviation to approximately $\pm$ 4.0%.

A comparison with the deviations experienced on the main landing gear specimen (X996) indicates that as installation technicians become more skilled, and as the techniques become more refined, theoretical values will be more closely approached. In any event, since a tolerance of less than 10% has been attained on the sensors specifically checked for accuracy of multiplying factor, it can be assumed that a similar tolerance would be observed on the unverified sensors. The variation in actual multiplying factor from theoretical values was considered acceptable and no sensors were replaced on the basis of a multiplier deviation.

While the attainment of a precise multiplier is interesting and challenging, it is not as critical to the overall effort as adjusting the sensor sensitivity to the structures operating strain level. Established behavior characteristics of the sensor (Ref. 6) were used in conjunction with information supplied in stress analysis reports to adjust the sensor sensitivity (M.F.) to predicted strain levels at selected locations. Any deficiencies or changes in predicted operating strain levels of the structure tends to compromise the effectiveness of the sensor installation. It may appear that an excess of sensors were used on the calibration article since some sensors on the frame flanges (AF-10, AF-12, AF-14, AF-16, AF-20, and AF-21) indicated low strain levels for nearly all load conditions. The purpose of these sensors, however, was to indicate any redistribution of internal loading in the event of a frame failure. It is believed that in a program of this type an excess of sensors is justified for the calibration article to avoid overlooking potentially critical areas.

An evaluation of the results of the strain survey indicated that the sensors were adequately located to perform their intended function; therefore, no sensors were replaced or added as a result of the survey. The strain amplitudes measured by conventional strain gages indicated that the selected sensor sensitivity and locations were reasonably appropriate for monitoring the structure's degree of exposure to repeated load occurrences.

5.4 DATA EVALUATION

The preliminary stress analysis conducted on selected critical areas of the test structure resulted in locating sensors in designated "key" areas. Some typical maximum damage locations (Table IV) as determined by this analysis resulted in the selection of FS 2538, VSS 424.6 and VSS 469.0 as fatigue control points. Data from sensors located in these special key areas was of particular interest during the sensor data monitoring and evaluation phase. At the start of specimen cycling the sensors were closely monitored to ascertain that each was responding as anticipated. During the first pass, all sensors were sampled at the end of each test grouping as shown in Tables V and VI. Upon the completion of the first pass data sampling periods were normally determined by trends in the plotted data, unless a specimen failure or extensive down-time occurred. In the absence of any unusual events, sensor readings were taken at the end of each pass.

The most informative sensors are those which will indicate a resistance change for all of the load conditions producing structural fatigue damage. This total resistance change is stored as a summation of resistance changes produced by the separate load conditions and may be expressed in the simplified manner illustrated below.

$$\Sigma \Delta R = \Delta R_{taxi} + \Delta R_{G-A-G} + \Delta R_{LGM} + \Delta R_{buffet} + \Delta R_{VGM}$$

During the first pass the sensor resistance change was sampled at the end of each load condition to determine if sensors located at the control points were producing a resistance change for every load condition. A typical sensor installation (AF-6) produced resistance changes for each of the load conditions as shown below.

$$\Sigma \Delta R = \underset{taxi}{40\mu\ \Omega/\Omega} + \underset{G-A-G}{120\mu\ \Omega/\Omega} + \underset{LGM}{780\mu\ \Omega/\Omega} + \underset{buffet}{260\mu\ \Omega/\Omega} + \underset{VGM}{310\mu\ \Omega/\Omega}$$

$$\Sigma \Delta R = 1510\mu\ \Omega/\Omega$$

Based on the resistance change during the first pass, a linear sensor output should have produced a total resistance change for one simulated lifetime of:

$$\Sigma \Delta R/\text{lifetime} = 1510\mu\ \Omega/\Omega \times 120\ \Omega \times 20 \text{ passes}$$

$$\Sigma \Delta R/\text{lifetime} = 3{,}624{,}000\mu\ \Omega \text{ or } 3.624 \text{ ohms}$$

It should be remembered that the sensor registers and stores only those cyclic strains above a selected threshold level and ignores any cyclic strains below that level regardless of loading modes. Once the cumulative resistance changes have been stored in the sensor, the resistance change due to each loading condition cannot be separated; however, separation is not considered necessary for the programmed application. The spectrum of load conditions as summed above, constitutes one pass which is repetitively applied to the specimen. Graphical presentations of the summed resistance changes versus the number of passes were found to approximate a linear display as illustrated in Figures 56 through 62.

TABLE V

AFT FUSELAGE SENSOR RESPONSE TO EACH

TEST GROUP OF THE FIRST PASS

(All Sensors with M.F. 3.0 are Type SAP 204DA-STE)
(All Sensors with M.F. 5.0 or 6.0 are Type SAP 202DA-E)

SENSOR NO.	THEORETICAL MULTIPLIER	ΔR μ Ω/Ω PER TEST GROUP					ΔR μ Ω/Ω **
		TAXI	G-A-G	LGM	BUFFET	VGM	PER PASS
AF-1*	3.0						
AF-2	3.0	10	20	70	140	160	400
AF-3	5.0	0	10	85	115	125	335
AF-4	5.0	20	20	60	155	190	445
AF-5	6.0	40	80	440	80	280	920
AF-6	6.0	40	120	780	260	310	1510
AF-7	6.0	0	0	210	40	240	490
AF-8	6.0	0	0	330	70	210	610
AF-9	3.0	20	20	280	30	150	500
AF-10	3.0	10	40	340	20	170	580
AF-11	3.0	0	60	440	80	110	690
AF-12	3.0	0	10	70	0	100	180
AF-13	6.0	70	280	2740	410	540	4040
AF-14	3.0	0	20	40	10	90	160
AF-15	6.0	40	120	1960	150	560	2830
AF-16	3.0	10	0	60	30	20	120
AF-17	3.0	20	230	30	40	360	680
AF-18	3.0	0	200	70	80	380	730
AF-19	3.0	40	420	60	80	520	1120
AF-20	3.0	20	20	260	90	300	690
AF-21	3.0	10	0	310	40	410	770

* Sensor damaged during the stabilizer fairing installation and was abandoned as inaccessible.

** All sensor readings in micro ohm/ohm units.

TABLE VI

EMPENNAGE SENSOR RESPONSE TO EACH TEST GROUP OF THE FIRST PASS

(All Sensors are Type SAP 204-DA-STE)

SENSOR NO.	THEORETICAL MULTIPLIER	$\Delta R_{\mu}\ \Omega/\Omega$ PER TEST GROUP					$\Delta R_{\mu}\ \Omega/\Omega$ *
		TAXI	G-A-G	LGM	BUFFET	VGM	PER PASS
E-1	3.0	10	30	0	70	100	210
E-2	3.0	20	230	30	230	470	980
E-3	3.0	0	10	10	70	90	180
E-4	3.0	10	20	0	80	110	220
E-5	3.0	0	30	0	110	120	260
E-6	3.0	30	80	20	200	360	690
E-7	3.0	40	100	0	230	410	780
E-8	3.0	40	70	0	180	330	620
E-9	3.0	20	40	0	130	220	410
E-10	3.0	10	10	0	40	110	180
E-11	3.0	0	10	0	60	100	170
E-12	3.0	10	20	310	120	280	740
E-13	3.0	20	30	280	90	260	680
E-14	3.0	0	10	360	40	100	510
E-15	3.0	0	0	180	20	40	240
E-16	3.0	10	40	820	60	170	1090
E-17	3.0	0	0	240	10	130	380
E-18	3.0	0	0	0	30	60	90

* All sensor readings in micro ohm/ohm units.

Continued experience with fatigue sensor application to complex aircraft structure has reinforced the original concept of evaluating sensor response on one section at a time, and especially in those areas where the sensor responds principally to one load condition. The evaluation of sensor data can be simplified if it is grouped according to component assemblies, e.g., horizontal stabilizer, vertical stabilizer, fin attachment area, sloping longerons, etc.

Separation of data according to assemblies has been followed in the graphic displays (Figs. 56 through 62) of sensor response. As a case in point, the sensors located at the front beam vertical fin attach points, i.e., AF-3, AF-4, AF-5, and AF-6 felt basically the gust and manuever loads (VGM and LGM). These sensors, however, indicate an adequate response to taxi, ground-air-ground, and buffet. These particular sensor readings are displayed in Figure 56 and indicate the relationship of the distributed sensor resistance changes at the "dagger" type attachment fittings as well as relative amplitude of cyclic load exposure. The division of sensor cumulative resistance changes in the dagger fitting is partially obscured by the variation in sensor multipliers used. In retrospect, a common multiplier for this fitting would have simplified the analysis; however, the relationship of sensor readings can be vectorially represented as follows:

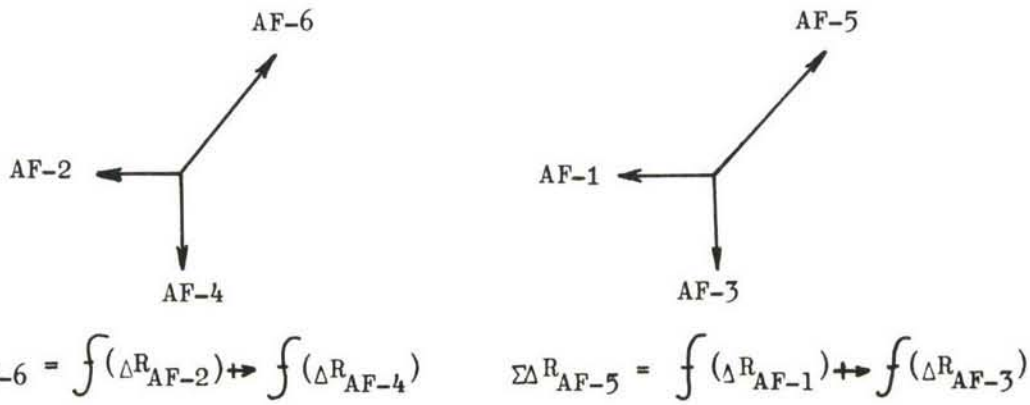

The vector diagram and the plotted sensor readings (Fig. 56) show that the resistance changes produced as a result of empennage cyclic loads were divided into the fuselage frame F.S. 2538 and the dorsal longerons shear panel. Although sensor AF-1 was abandoned as a result of physical damage during a fairing installation, the resistance changes occurring in its companion sensors (AF-3 and AF-5) are still of interest.

A graphical display of sensor readings (Fig. 56) shows the relative cyclic strain history of sensors located on the under fin frames. It was believed that sensors located on the support frames beneath the vertical stabilizer attachment area would permit the continuous monitoring of internal load distribution from the empennage into the aft fuselage. As noted on the graph (Figs. 56 and 57), sensors AF-13 and AF-15 were re-installed during pass five and six with a multiplying factor (M.F.) of three in place of the initial (M.F.) of six. Sensor AF-22 was added near the end of pass eight to assist in a more precise definition of internal load distribution at the root of the vertical. As noted by the slope of some sensor curves (Fig. 56), the sensitivity of some of the sensors on the underfin frames required a downward adjustment to obtain a sensor lifetime for at least 20 passes. The sensors located on the vertical risers of the underfin frames are of special interest since they are located in the key control point area of VSS 424.6. When one contrasts each sensor's cumulative resistance change ($\Sigma \Delta R$) with its position on the structural assembly an informative pattern begins to appear. A plan view of the vertical stabilizer to aft fuselage attachment area, as shown below, indicates the general distribution of sensor resistance change in this area.

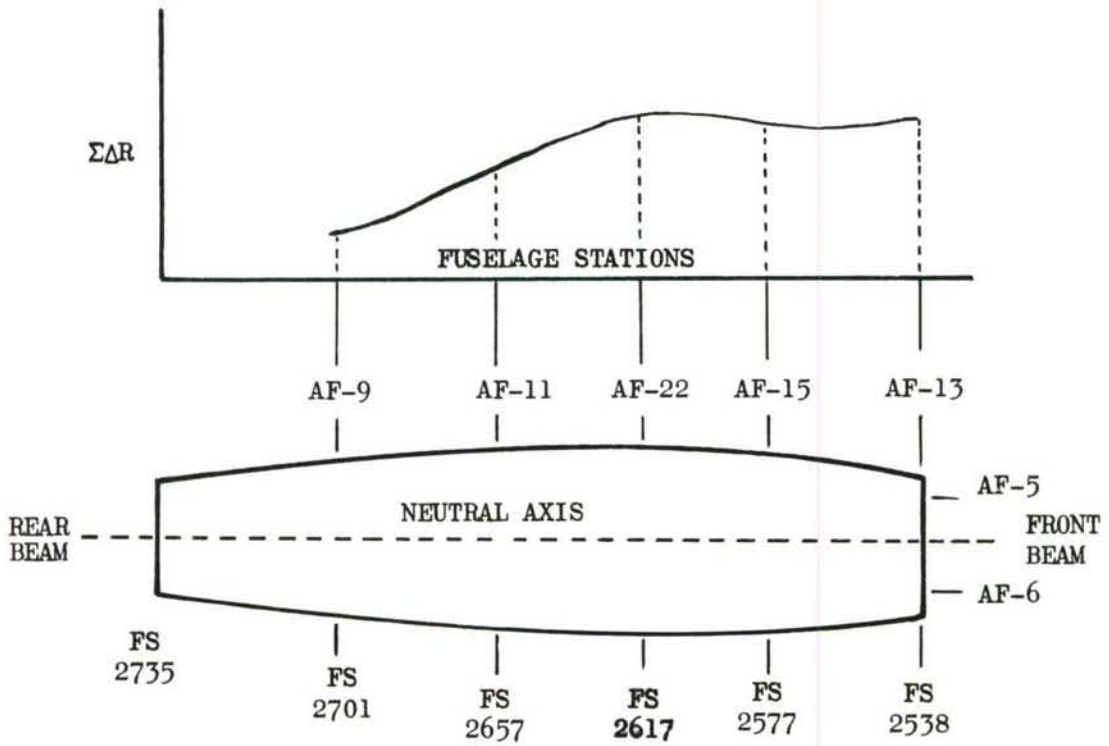

CROSS-SECTIONAL VIEW OF THE VERTICAL STABILIZER

Although sensor locations at AF-13 and AF-15 involved multiplication factors of three and six at different stages in the program, the comparison of resistance change at each fuselage station was made at a M.F. of three.

Sensor AF-22 shows that the accrual of sensor resistance change appears to peak at the crown elements of the fin. No doubt the distance of this structural surface from the neutral axis is a contributing factor - in any event an evaluation of sensor data shows evidence of a definite resistance change profile. An alternate method for evaluating the response of sensor AF-22 is illustrated by the dual plots shown in Figure 56. The initial slope may be used to establish a straight line intercept with zero or it may be more realistically plotted (dashed line display) to follow the response of an adjacent sensor. That is, it is assumed that sensor AF-22 would have been subjected to nearly the same loads experienced by sensor AF-11 if it had been installed at the beginning of pass one.

The magnitude of sensor resistance change per load condition has been judged to be significant in an assessment of the degree of severity of each load source. It is believed that the resistance change occurring can be properly "weighted" to the structural damage sustained, once visible damage has been observed. The following diagram shows the magnitude of resistance change (ohms) for a particular sensor (AF-13); however, the relationship is typical for all sensors located on the under fin frames. The largest resistance change occurs during the lateral-gust maneuver (LGM) load condition with lesser changes occurring as a result of the other conditions.

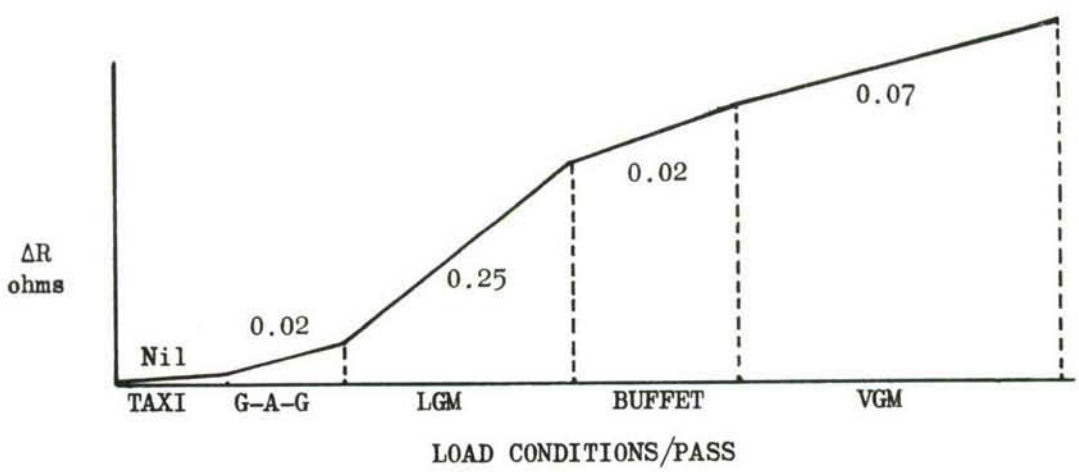

By comparison, typical response curves of sensors located on the horizontal stabilizer would show maximum response to buffet and vertical-gust-maneuver (VGM). The effect of this can be noticed if the outputs of sensors located on the horizontal are plotted at the end of the LGM load condition and then again at the end of the pass. Plotting sensor outputs by load condition will show what type load produces the more severe structural loading and in what areas of the structure it occurs. Figure 56 shows a plot of under-fin frame sensor outputs with some data points taken under zero load condition at points other than the end of a pass. The "hook up" of the curves at 35% of pass six is apparently caused by the effect of the LGM load condition sequence rather than any redistribution. If readings are plotted only at the end of a pass, the rate of resistance change is more uniform. The output of AF-5, 6, 9, 11, as indicated, appears nearly ideal since the sensor response (ΔR) was

adequate for one lifetime and would probably endure two lifetimes. Sensors AF-13 and AF-15 were still operating at the beginning of pass six, however, they had to be replaced since it was obvious they would not have sufficient range to last one lifetime. The multiplier obtained by the 3/4 inch Teflon spacer was obviously too high for the SAP202DA-E type sensors installed in these locations.

Sufficient data and experience has been accumulated during the evaluation of the sensors on the Aft Fuselage - Empennage specimen to formulate some guidelines for selecting the more appropriate sensor location and multiplier for application to a flight vehicle. For instance, the sensors designated E-12 through E-17 on the vertical stabilizer (Fig. 62) appear very suitable for monitoring this assembly's relative exposure to repeated loads. Although the total resistance change for one lifetime is approximately one ohm, the reading resolution was adequate, and sufficient sensor range was available for an additional lifetime.

The vertical gusts and maneuvers as well as lateral gusts and maneuvers will produce bending of the fuselage which will be reacted by the sloping longeron and other longitudinal shell elements. Sensors designated AF-17 through AF-19 were located to monitor these loads. Although the majority of the cyclic loads imposed on the sloping longeron were in the compression direction it was still desirable to document the cyclic strain history in this area. The response of the three sensors located on the longeron (Fig. 60) indicated no unusual behavior and performed as expected.

Sensors numbered AF-2, AF-7, AF-8 installed on the dorsal shear panel were expected to remain relatively dormant unless a significant redistribution of internal loads was experienced. The cumulative resistance change (ΔR) produced by these sensors show (Fig. 58) a consistent rate of accrual with no abrupt changes or redistribution.

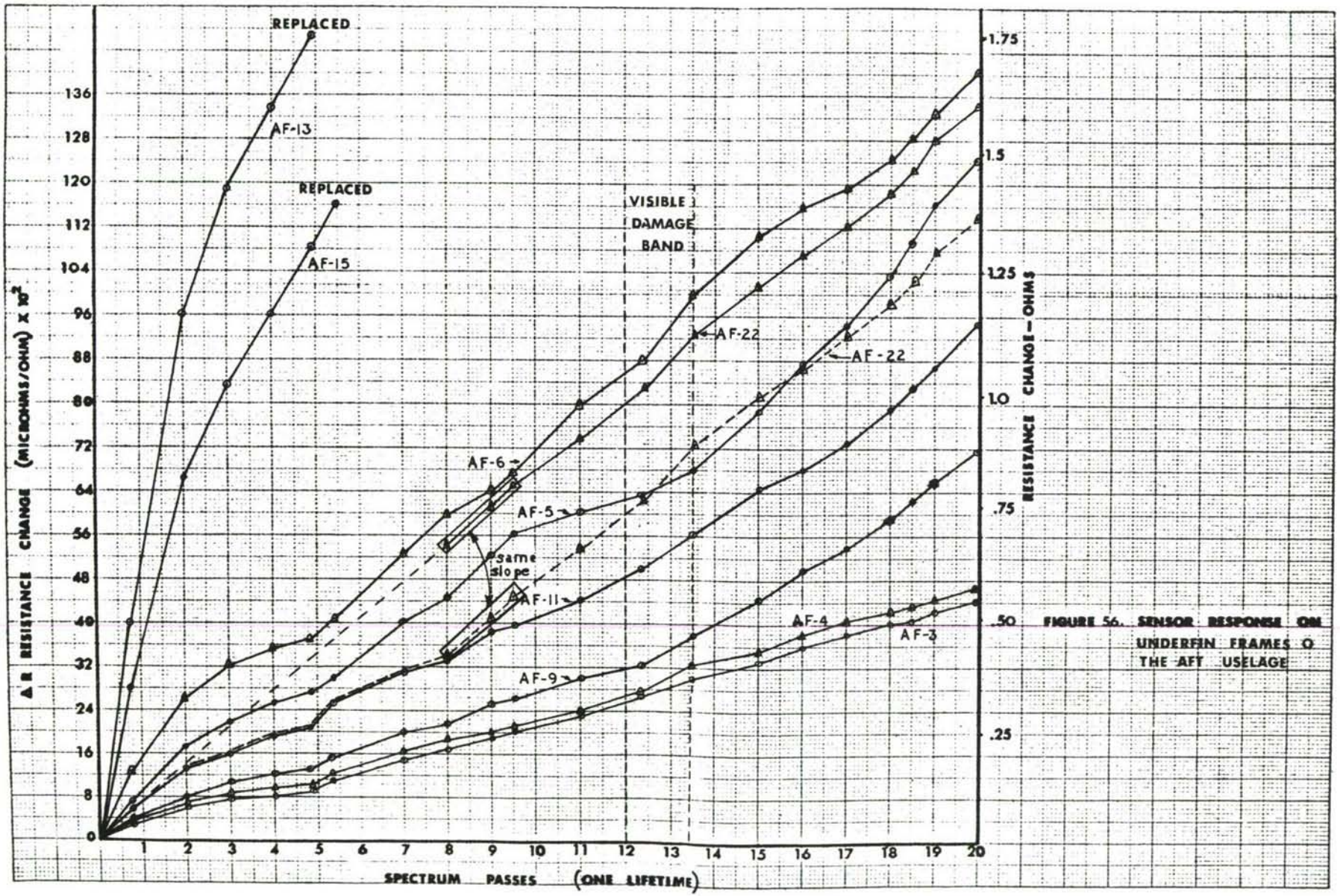

FIGURE 56. SENSOR RESPONSE ON UNDERFIN FRAMES O THE AFT USELAGE

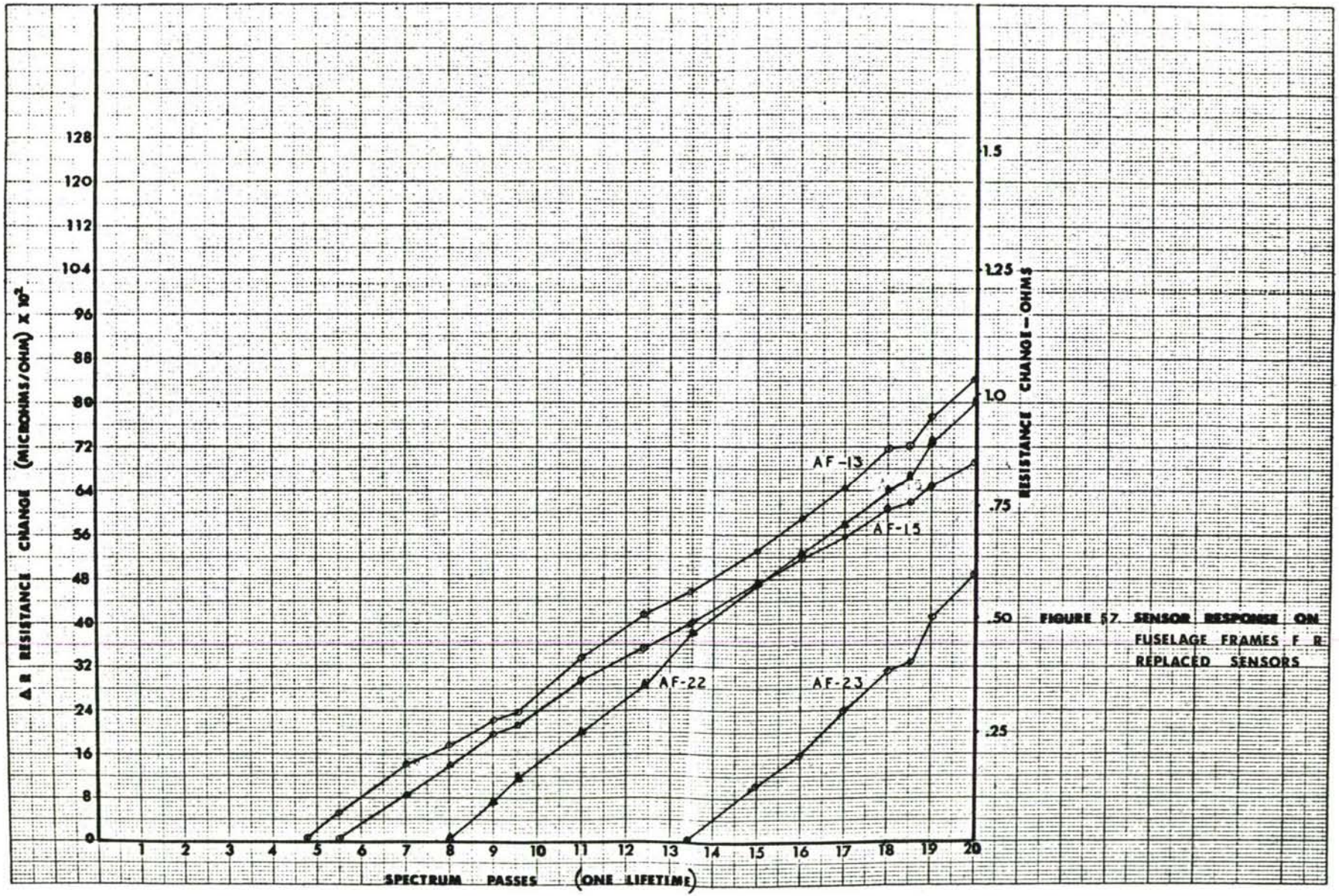

FIGURE 57. SENSOR RESPONSE ON FUSELAGE FRAMES F R REPLACED SENSORS

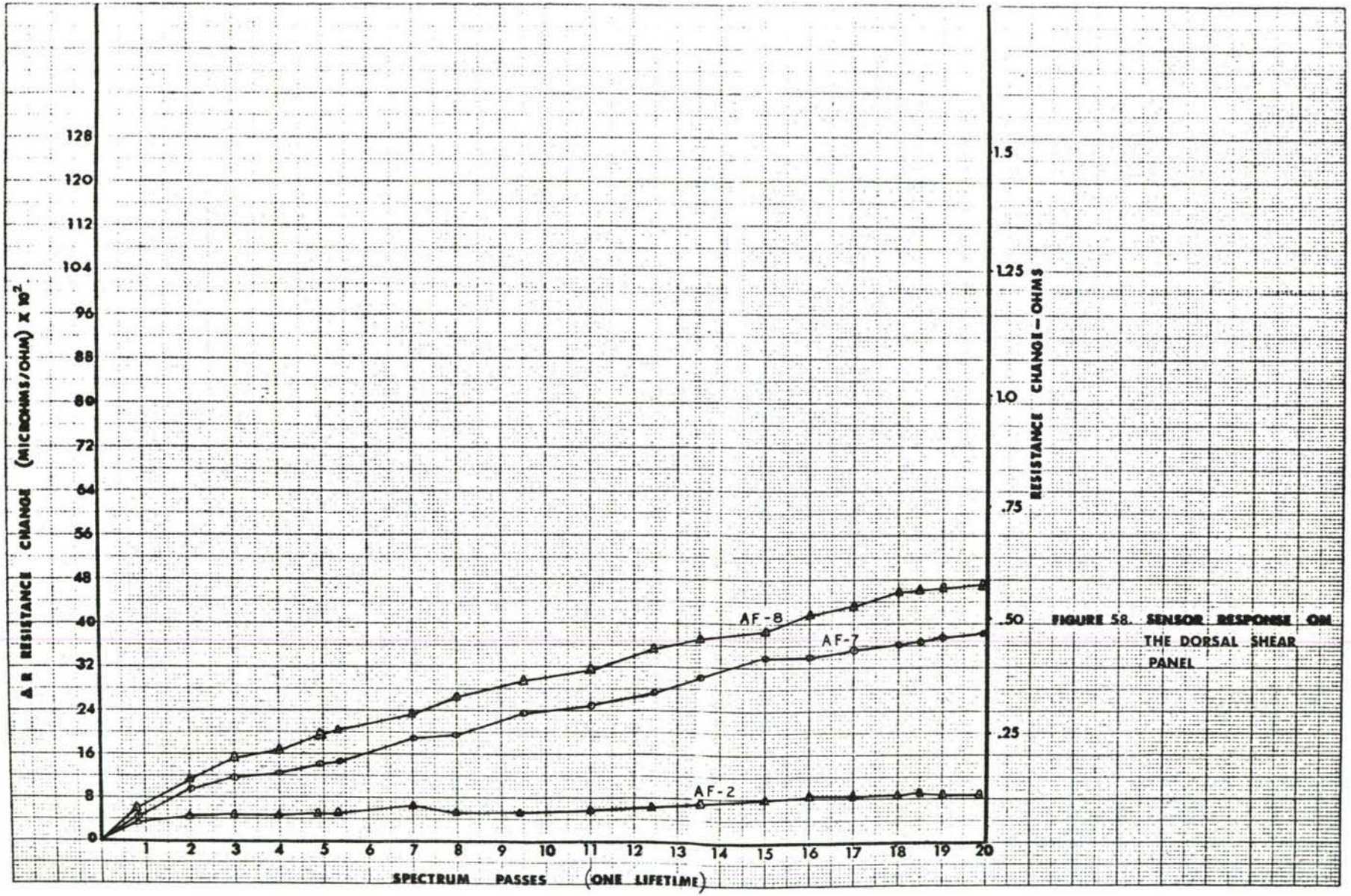

FIGURE 58. SENSOR RESPONSE ON THE DORSAL SHEAR PANEL

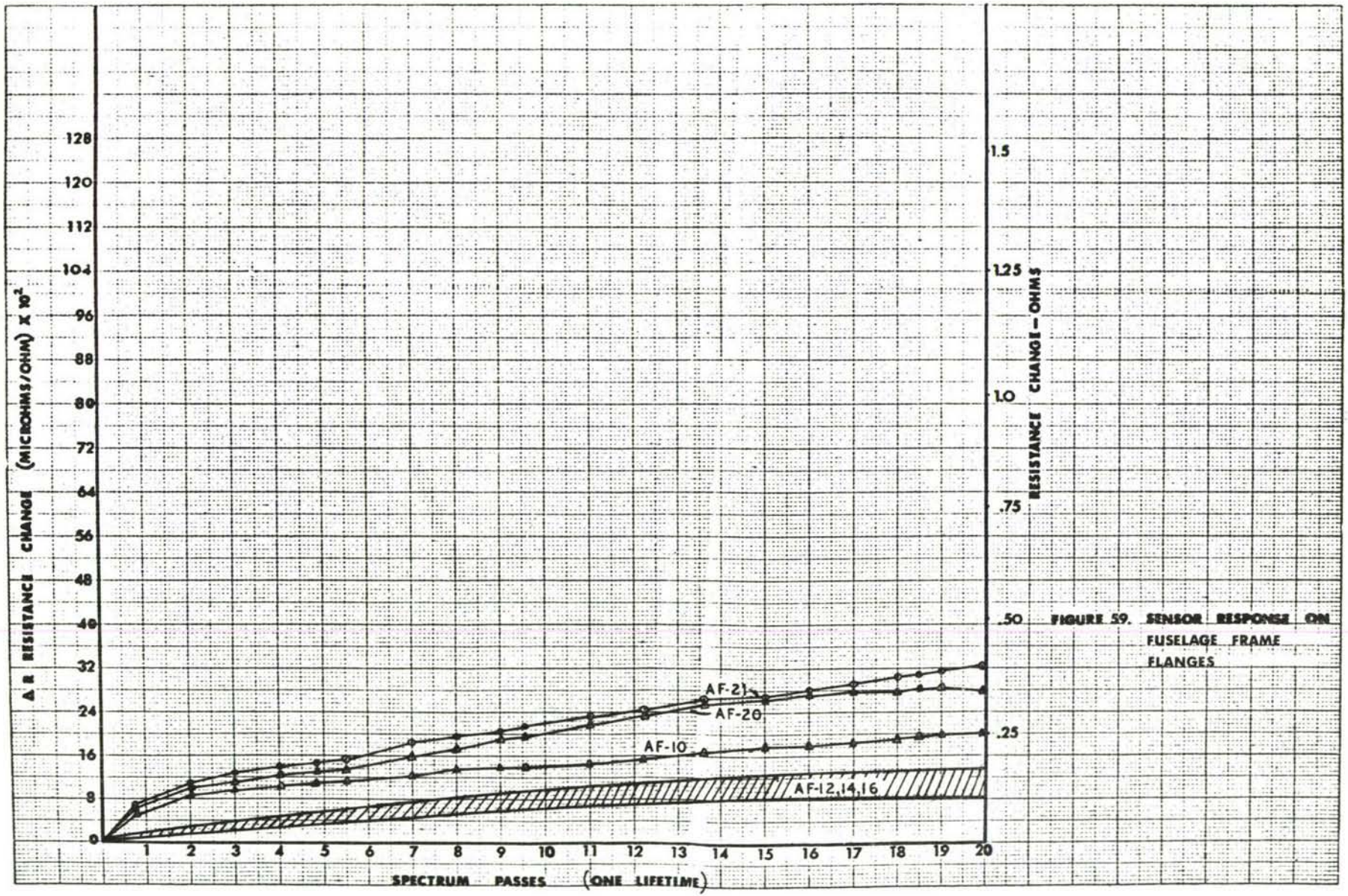

FIGURE 59. SENSOR RESPONSE ON FUSELAGE FRAME FLANGES

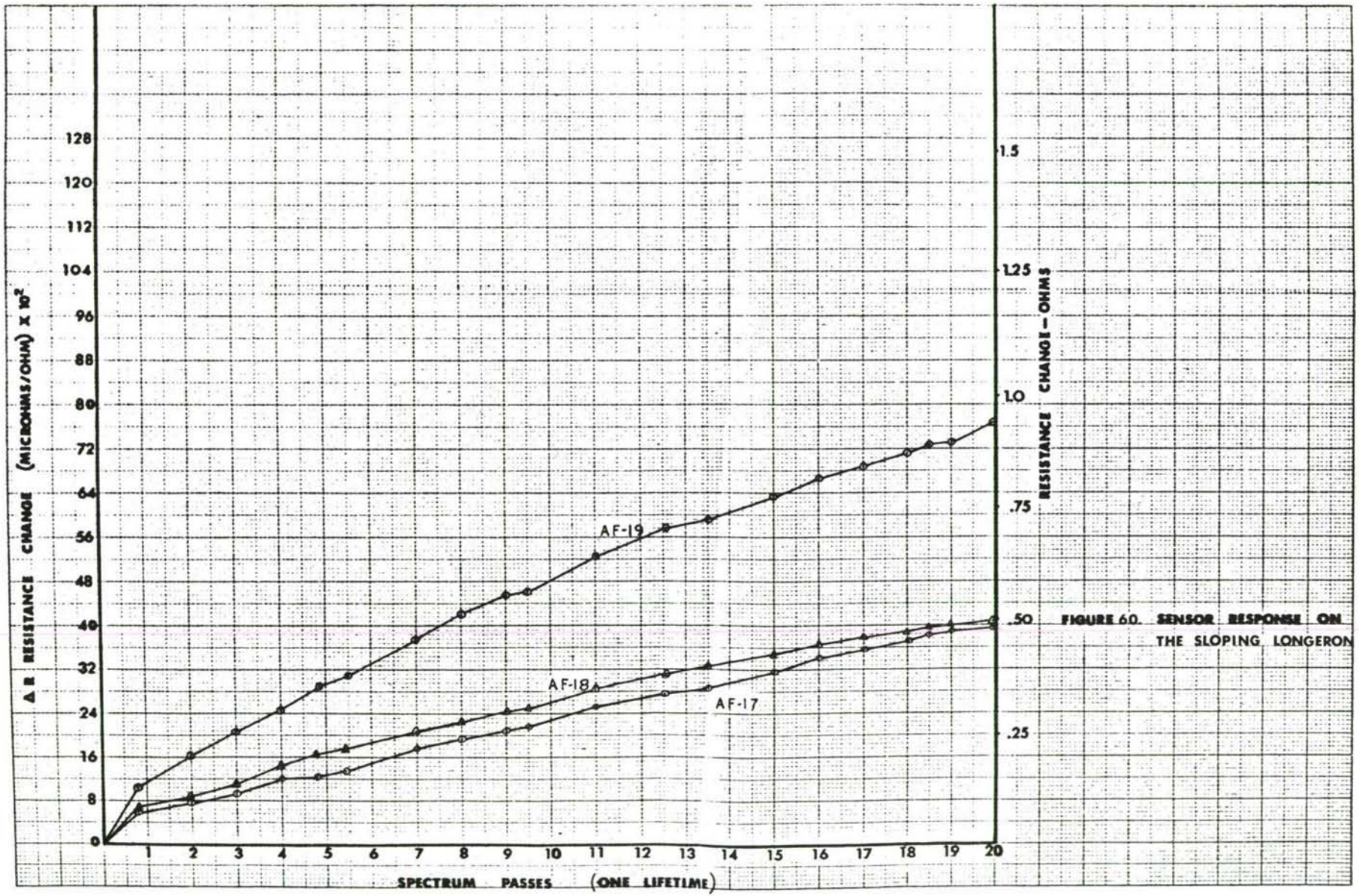

FIGURE 60. SENSOR RESPONSE ON THE SLOPING LONGERON

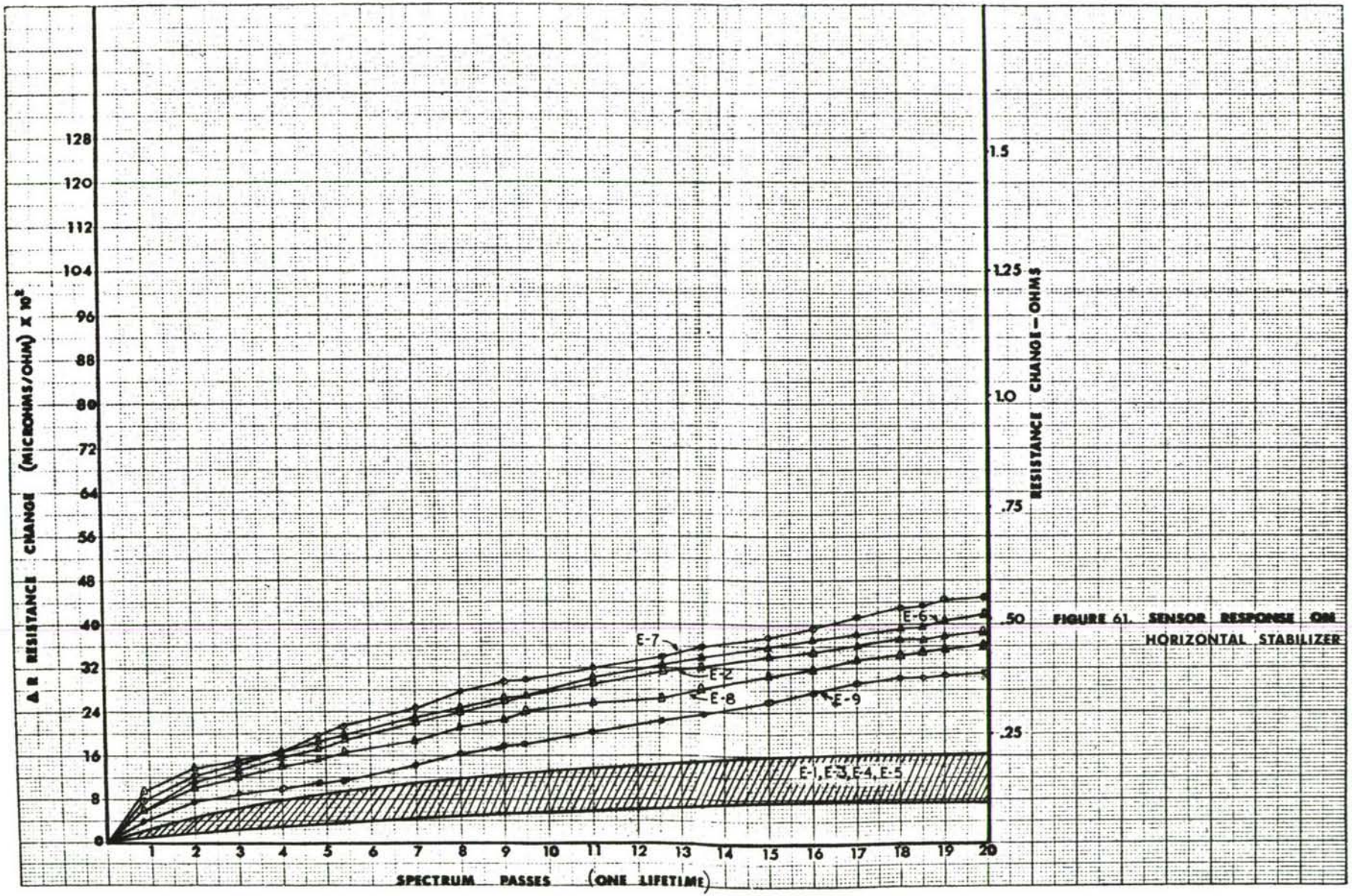

FIGURE 61. SENSOR RESPONSE ON HORIZONTAL STABILIZER

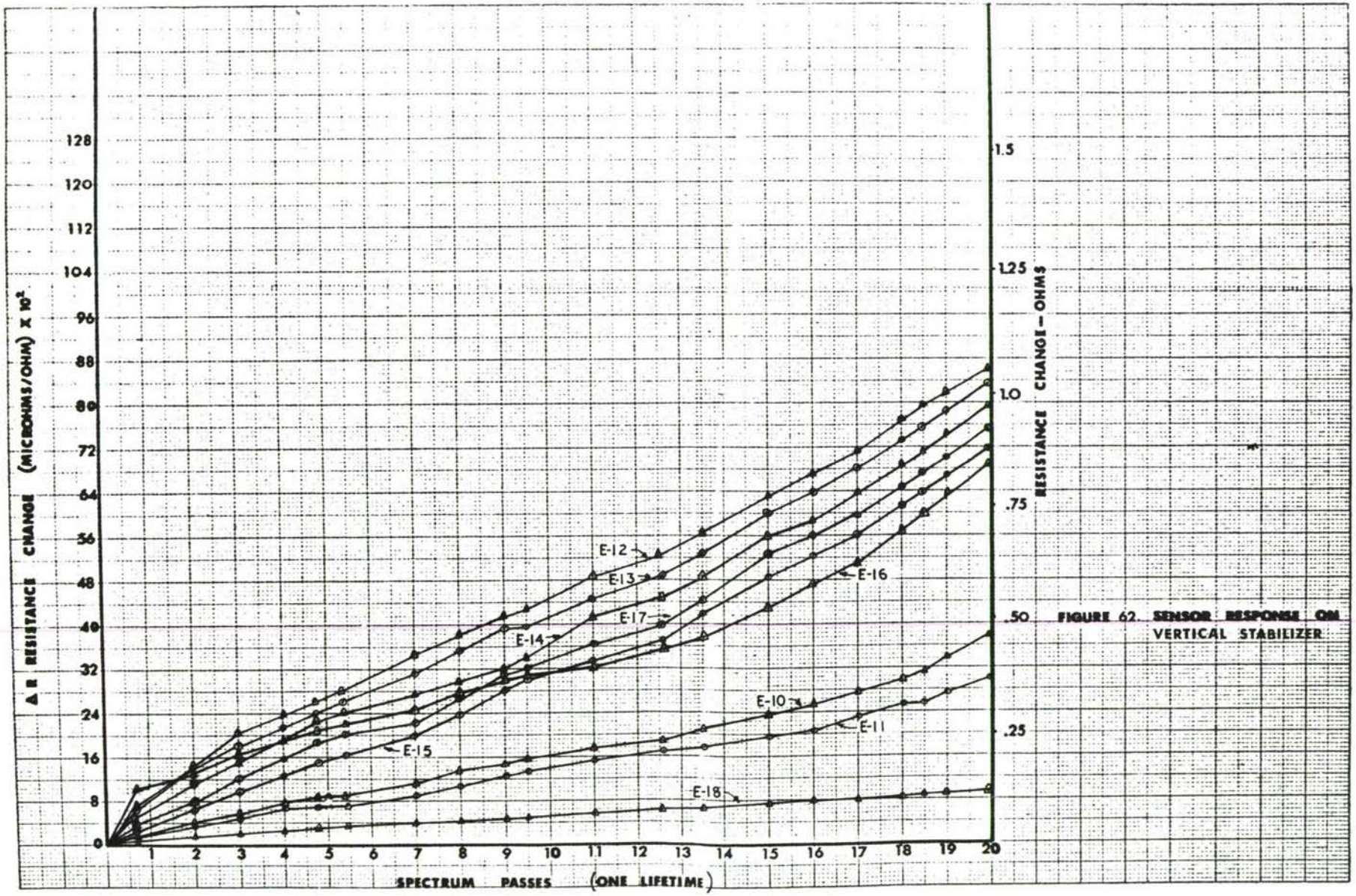

FIGURE 62. SENSOR RESPONSE ON VERTICAL STABILIZER

5.5 DAMAGE CORRELATION

The data provided by the sensors on the Aft-Fuselage Empennage specimen have been separated and displayed (Figs. 56 through 62) according to their structural location, i.e., sloping longeron, vertical stabilizer, horizontal stabilizer, under fin frames, etc. This information was further analyzed and consolidated to reflect the areas of higher cyclic loads since each sensor basically responds to repetitive strain. The shaded area shown in Figure 63 depicts the area of higher sensor resistance change as determined by an analysis of the plotted data illustrated in Figures 56 through 62. This is possible because the effects of the number and amplitude of strain cycles are registered and totalized by the fatigue sensor as a cumulative resistance ($_{\Delta}R$) change. While the resistance change for any one load condition may not be excessive in the illustrated shaded area, the cumulative sensor resistance changes produced by all load sources are highest in the noted area. In other words, the shaded area does not necessarily represent an area of peak stress, but is the area that was worked more severely through all the spectrum. Therefore, if the K_t in the shaded area was higher or equal to the K_t in other areas, then initial cracking should occur in the shaded area. In practice, fatigue damage did occur on the left side of fuselage frames F.S. 2516, F.S. 2494, F.S. 2472 and F.S. 2450 directly beneath the dorsal longeron, which is located in the shaded portion of the specimen.

Visible fatigue damage was observed at approximately 46% of pass 14, in the four fuselage frames immediately forward of F.S. 2538. The fatigue damage at two of the frame stations F.S. 2494 and F.S. 2472 (Figs. 64 through 67) are typical in orientation and severity with the visible damage at F.S. 2516 and F.S. 2450. The sensors located in the general area of the damage were AF-3, AF-4, AF-5, AF-6 and AF-13. The resistance change of these "key" sensors upon discovery of the damage is of special interest since these values are characteristic of the load experience necessary to produce visible structural damage. Information provided by these pertinent sensors was analyzed in view of the totalized resistance change and the associated fatigue damage. An approach to define the critical ΔR value of each "key" sensor is typified in the following diagram.

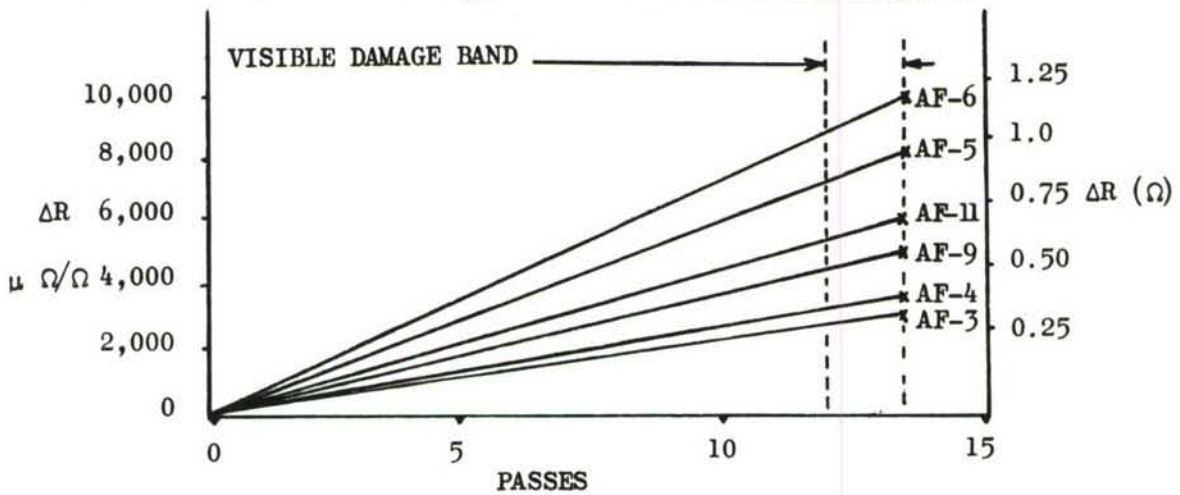

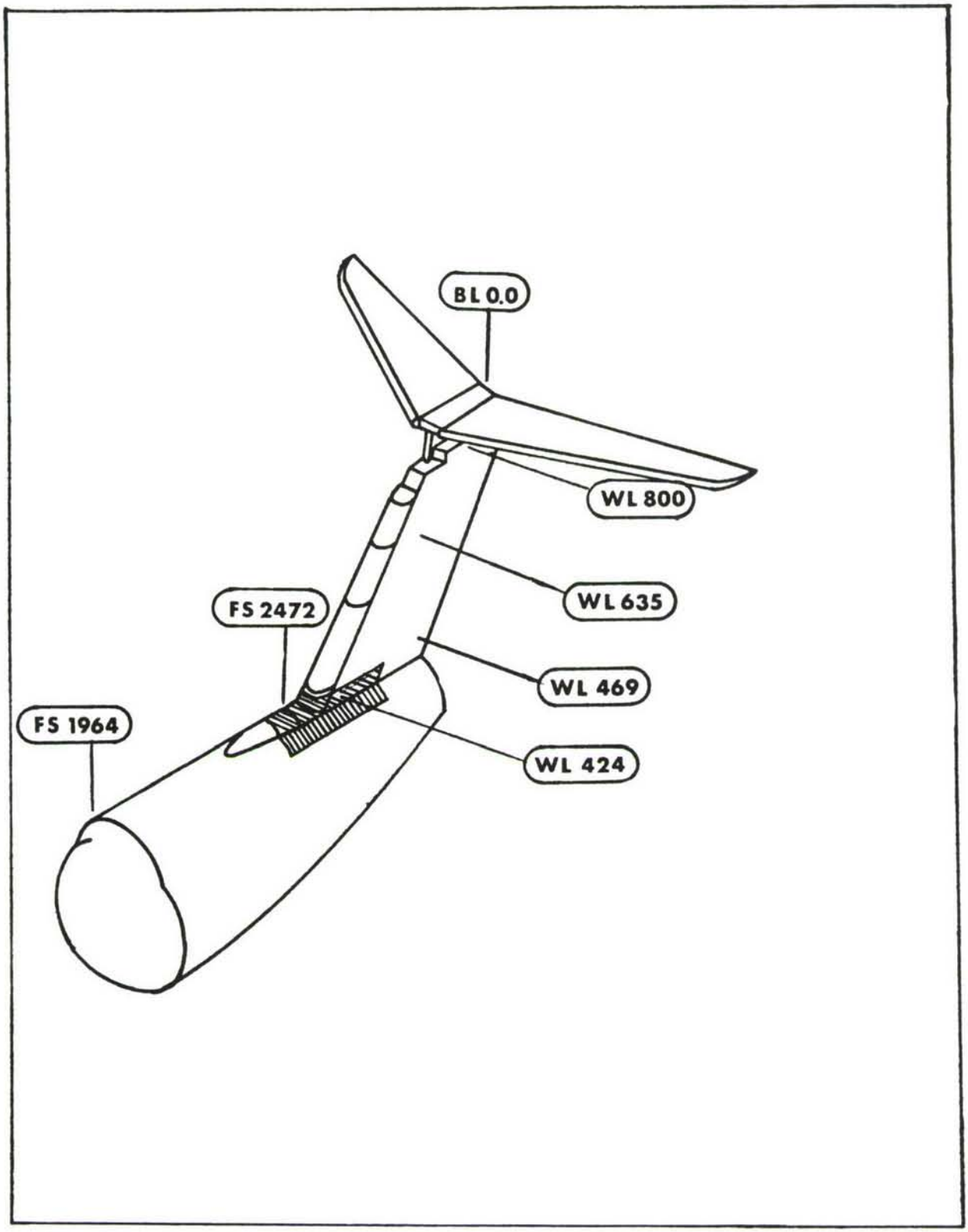

FIGURE 63. C-5A AFT FUSELAGE— EMPENNAGE SHOWING AREA OF HIGHER SENSOR RESISTANCE CHANGE

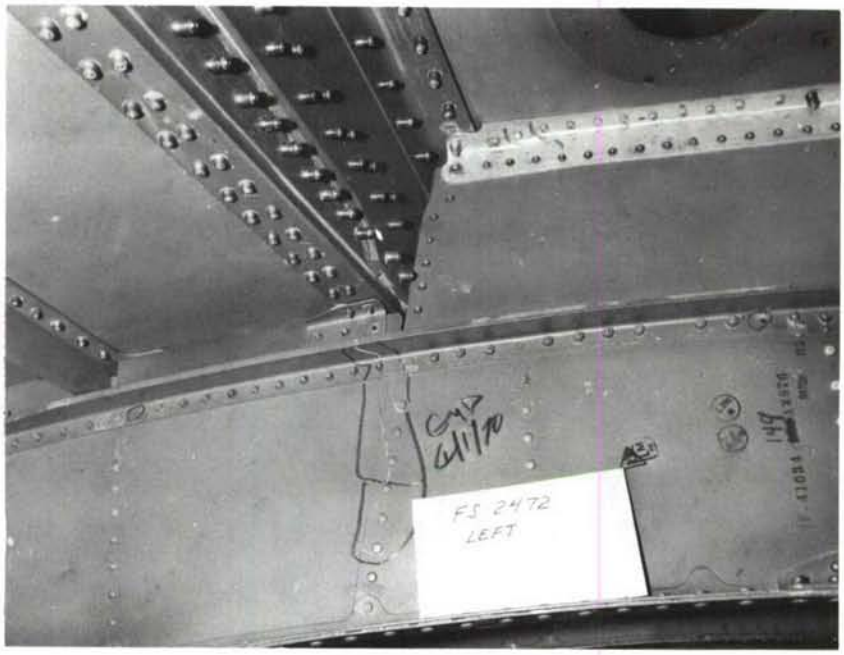

FIGURE 64. FATIGUE CRACK IN FUSELAGE FRAME WHICH OCCURRED DURING PASS 14 (LOOKING FORWARD)

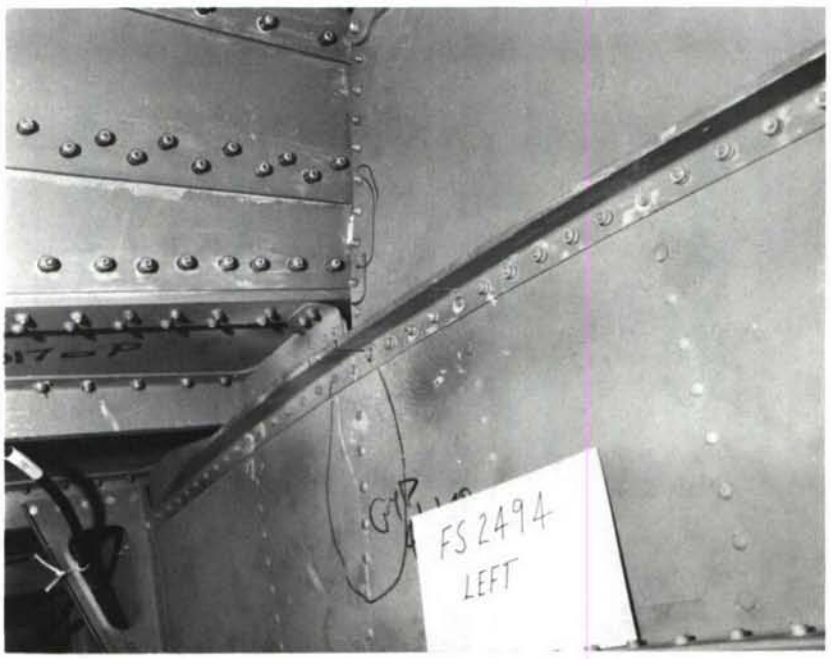

FIGURE 65. FATIGUE CRACK AT NEXT AFT FRAME STATION

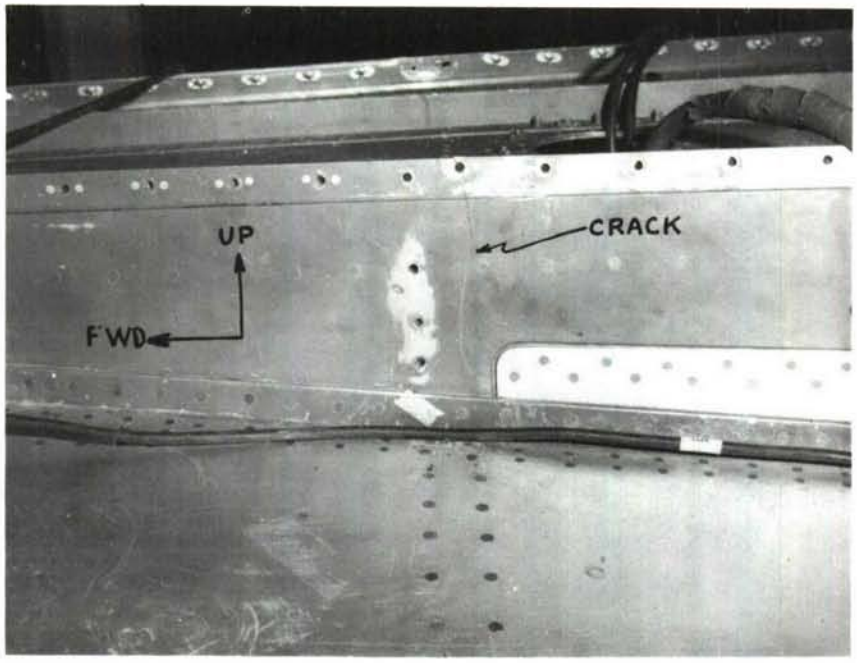

FIGURE 66. FATIGUE DAMAGE IN DORSAL LONGERON AT F.S. 2472

FIGURE 67. FATIGUE DAMAGE AT FUSELAGE FRAME STATION F.S. 2494. LOOKING AFT.

The "Visible Damage Band" is depicted as a vertical line (Fig. 56) at the time a visible fatigue crack was observed and the bandwidth is shown as a discrete portion (percentage) of the testing to the point of damage detection. The bandwidth was selected by a conservative guess and the selection of sensors as "keys" included those located in the general vicinity of the visible damage. All sensors on the fuselage, however, have a similar relationship to the fatigue damage as any other sensor not located in the immediate vicinity of the failure. The resistance change response of all sensors appear to be due to the same general loading inputs as experienced by the damaged area and the individual sensor response is a function of the discrete loading distribution and the actual strain amplification factor applied to each sensor at its particular location on the structure.

A bracket value of fatigue damage allowables in terms of sensor resistance change (ΔR) can now be established for sensors AF-6, AF-5, etc. The damage bandwidth established must consider the possibility of variations between the simulator and flight vehicles in regard to (1) strain multiplier tolerance, (2) loading spectrum, and (3) structural material and structural functions. It is anticipated that a bandwidth of sensor resistance values within $\pm$ 10% of each key sensor resistance at structural damage would be realistic.

On an expanded basis, the "key" sensors on this specimen under the applied loading condition are identified as AF-5, AF-6, AF-13, AF-15, AF-22, and AF-23. It is noteworthy that all these sensors lie in the shaded area of the structure. Although an area of high sensor resistance change has been recognized, it should be observed that this was for a specific spectrum of applied loads. It is possible that other in-service missions would provide sufficient variations in the loading spectrum to produce a different area of higher sensor resistance changes. For instance, an instrumented aircraft might be assigned to a using command where the mission service would impose a more severe buffet condition than that imposed on the laboratory specimen. Under these circumstances sensors located on the upper vertical stabilizer might well indicate the higher resistance change and hence a different area susceptible to fatigue cracks. Therefore, sensor locations on a flight vehicle should not be confined to just the shaded area shown, but should include other potentially critical areas.

5.6 SENSOR INSTALLATION RELIABILITY AND PERFORMANCE

One of the difficulties which appeared on specimen X997 as well as X996 is the deviation in actual sensor multiplier from that programmed. The true causes of these deviations have not been satisfactorily isolated; however, the following are suspected to be contributing factors.

- o The tape slitting operation of the Teflon tape supplier has produced measured tape width variations of up to ± 0.010 inch. Although this is a normal tolerance on tape width, it can produce multiplier errors in excess of ± 1% for the SAP 204DA-STE type sensor.
- o There is a tendency on the part of the technician to stretch the thin (0.002 inch) Teflon tape in removing it from the roll or to otherwise elongate the tape when pressing it into place on the structure. In any event, elongation reduces the effective tape width and decreases the programmed multiplier.
- o There is a possibility of an incomplete metal-to-metal bond to the edge of the Teflon tape, thereby producing a larger unbonded area than actually programmed.
- o Since the adhesive must sustain dimensional changes, or otherwise crack under strain, the effective unbonded length may be slightly increased by dimensional changes in the metal-to-metal bonding adhesive.
- o Although the structural surface of an aircraft will normally experience axial strains, faulty sensor installation techniques can cause an extraneous bending component to be introduced into the sensor. This may occur as a result of "warp" in the shim slotted area, or a lack of bonding pressure directly over the sensor. Initially, direct pressure on the sensor area was avoided to prevent the formation of a stress concentrator in the sensor grid as a result of pressure against the edges of the shim slot. This problem has been eliminated by stress relieving the shim to prevent warp, and allowing the viscoelastic filler to protrude slightly out of the shim slots. Bonding pressure can now be equally distributed directly over the sensor area as well as the multiplier shim ends.

A noteworthy multiplier characteristic, as demonstrated by the strain survey, is a consistency for the actual multiplier to always read higher than theoretical. Since a comparison technique is anticipated for determining the fatigue status of a similarly instrumented flight vehicle, the multiplier deviations experienced may be insignificant. If the actual multiplier obtained is either consistently higher or lower than theoretical then the variation may be taken about an average value. Generally, sensor installation on preliminary test coupons proved to have a lower than programmed multiplier while those installed on complex structure were higher. Multiplier errors can be minimized if space will permit the installation of the larger shim and sensor. For example, a dimensional error in the unbonded length of a 1/8 inch sensor would produce a proportionally larger error than the same variation in a 1/4 inch sensor.

Sensor utilization on the Aft Fuselage-Empennage was accomplished with no bond failures. The evaluation of sensor performance by the "dynamic analysis" technique discussed in Section 5.7 tends to promote user confidence since periodic checks can be made to detect any bond deterioration. The "electrical evidence" type of bond checking the fatigue sensors appears to be more practical for laboratory tests than the mechanical type checks normally conducted on conventional strain gages.

All of the sensors were moisture proofed with Baldwin-Lima-Hamilton type barrier "E" waterproofing compound, which also provided some modest mechanical protection. Although the sensor installations were subjected to humidity changes of 40 to 100%, as well as hydraulic oil splashes, electrical resistance-to-ground was never a problem. Insulation resistance measurements made periodically during the simulated 30,000 flight hour lifetime indicated no leakage-to-ground problems. During previous feasibility studies (Ref. 6) an electronic "roll around" console was developed to obtain resistance-to-ground and bond integrity information as well as sample the resistance change of each sensor. This proved to be a complex, temperamental monitoring instrument with quality control capabilities that were not needed for the existing fatigue sensor.

The techniques presently used for sensor monitoring (Section 3.9) have proven very simple and reliable. Initially it was suspected that connecting and disconnecting the monitoring instrument to the sensor at a central termination panel could produce variable contact resistance and hence an error in the sensor reading. Considerable experimentation proved any changes in contact resistance were undetectable with an SR-4 indicator (any variation was less than one micro ohm). The use of pressure contact probes to connect directly at the sensor terminals has proven unfeasible since contact resistance may vary with operator pressure.

Structural inspections and/or modifications to either the test fixture or test specimen continues to produce the most sensor casualties. Usually, these are minor, such as cable damage, and cutting of interconnecting wires, which can be repaired and the data recovered with minimum losses. It was anticipated that foot traffic or structural modifications might damage the sensor grid itself, forcing a replacement, however this did not occur. The more extensive inspections conducted at the end of each lifetime produce the greatest number of losses, since some sensors must be removed to facilitate dye checking.

One is always faced with the possibility that testing and evaluation of a new concept will reveal more problems in addition to those actually solved. Although several unknown factors existed at the start of this program, a review of sensor performance after progressing through two specimens have indicated no physical barriers to a practical sensor application on flight aircraft.

5.7 EVALUATION OF SENSOR REPLACEMENT TECHNIQUES

Experience with the C-5A Aft Fuselage - Empennage structure has shown that over one simulated lifetime of the aircraft some sensor "casualties" may be anticipated. The basic causes of these casualties are listed as follows:

- o Overranging the sensor resistance change capabilities.
- o Local structural failure, resulting in removal of structure containing the sensor.
- o Physical damage to the sensor by such means as foot traffic.

Regardless of how the sensor was damaged or why it ceased to function, it is believed the monitoring site should not be abandoned, especially if it had been producing informative data. An example of sensor overranging is illustrated by AF-13 and AF-15 requiring replacement after approximately five passes. Replacement requires that the sensor's unbonded length be confirmed by removal and inspection of the installation. Inspection revealed that the original sensor installations (AF-13 and AF-15) actually had a multiplication factor of six (as programmed); however, this produced excessive sensitivity. Therefore, a downward adjustment of the multiplier was in order. The replacement of these overranged sensors permitted the continuation of load exposure monitoring at these locations. A technique for an evaluation of data from the replaced sensors is illustrated in Figure 68. It is recognized that useful data (Fig. 57) is still being generated by the replacement sensors, however, the question of interpretation for maximum validity now becomes pertinent. The data should be interpreted and displayed in a manner that will allow a valid correlation with data obtained on flight vehicles. Two possibilities for utilizing the data from replacement sensors are illustrated in Figures 68(A) and (B). Figure (A) shows the relative slopes (ΔR) of the original sensors as compared with the replacement sensors. It appears that more meaningful information is provided, if the response curve of the replacement sensor is relocated to the zero base line as in (A), rather than just shown as a continuation of the original curve. Another possibility would be to maintain the same slope and shift the curve so that it passes through zero as shown in (B); however, the non-linearity of the sensor or changes in mission service of flight aircraft, may compromise the validity of this approach for flight vehicles. It is anticipated that any sensors replaced on in-service aircraft would be replaced as a result of physical sensor damage and would therefore be replaced with the original multiplying factor. Regardless of whether a replacement is forced by overranging or physical damage, it is believed that the data generated following the replacement can be utilized in a rational manner to assess the general fatigue exposure experienced by the structure.

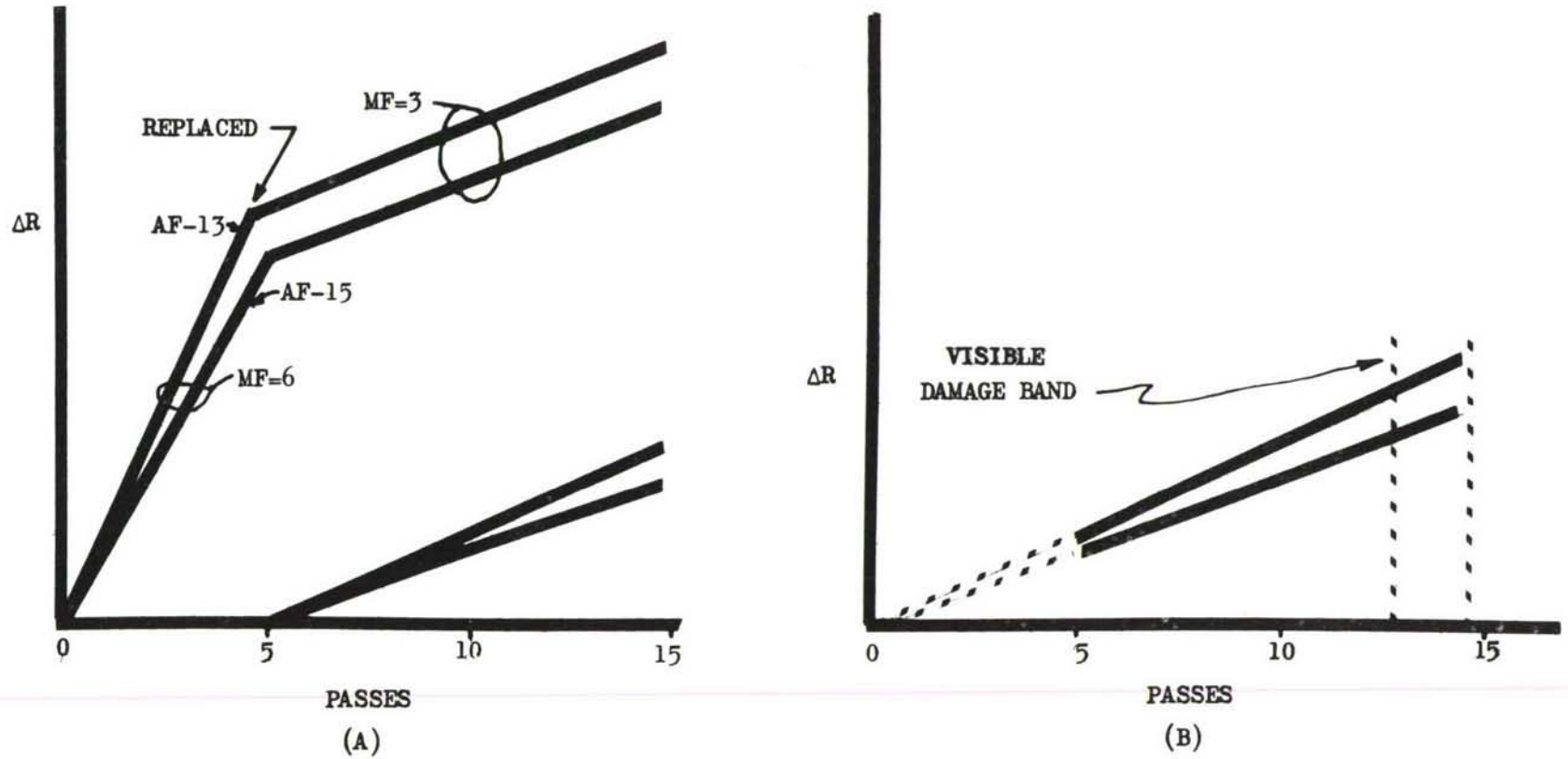

FIGURE 68. TWO POSSIBLE TECHNIQUES FOR THE EVALUATION OF SENSOR REPLACEMENTS

A valid technique for the replacement of sensors and interpretation of the resultant data appears very necessary for satisfactory utilization on service aircraft. The ever present possibility of a structural retrofit to a fatigue sensor instrumented service aircraft may also force a removal and replacement of one or more sensors. Therefore, special attention was given to the response of the test article sensors after the repair of the fatigue damage experienced during pass 14. An analysis of the sensor response curves, after structural repairs and the retrofit of a redesigned frame at F.S. 2472, indicated no pronounced variation in the rate of sensor resistance change. This behavior was attributed to the localized nature of the fatigue damage and its subsequent repair.

If the sensor installation is damaged by a cutting of wires, etc., such that the channel is only open circuited, the sensor is still registering and storing cyclic strain. There is no loss of data and replacement of the sensor is not required, since the information can be recovered simply by reconnecting the wiring.

Experience has shown that it is possible and desirable to periodically monitor the dynamic output of each sensor for peak strain excursions, while the specimen is being subjected to cyclic loads. This is possible, because of the relatively low rate of cycling (5 to 20 cpm) and the capability of the SR-4 strain indicator to repetitively indicate peak strain. The precision with which the indicator's galvanometer needle consistantly returns to a "nulled zero" position verifies not only the repeatability of the sensor, but the repeatability of specimen loading. This type of sensor dynamic analysis permits additional quality control checks throughout its utilization period on the laboratory test article. The advantage of performing these sensor quality checks are enumerated as follows:

- Verify the sensor metal-to-metal bond dynamically.
- Determine which load conditions produce cyclic strain levels in excess of sensor threshold sensitivity.
- Observe sensor response for any bond deterioration or sensitivity change by contrasting peak strains produced during initial load conditions with subsequent repeat load conditions.

The dynamic analysis of sensor outputs has proven to be an effective control tool for monitoring sensor quality during its lifetime. This technique provides information relative to any deterioration in sensor performance and provides guidance in regard to sensor replacement or modification of its sensitivity.

SECTION VI

TEST PROGRAM - WING FUSELAGE SPECIMEN (X998)

6.1 TEST SPECIMEN DEFINITION

The C-5A wing-fuselage fatigue test specimen designated Lockheed serial no. X998 is defined as a full scale production line fabricated airplane, (Fig. 68) complete except for parts and assemblies considered non-pertinent to the fatigue test. All holes, brackets, shelves, clamps, or any other items causing points of stress concentrations, or which otherwise might affect the test results,were included in the test specimen. Non-structural items such as fairings, gear doors, spoilers, ailerons, and radomes as illustrated in Figure 69, were omitted from the specimen. A number of dummy items were designed to simplify load application to the test specimen. These items include dummy engines, empennage, main gear and nose struts.

Since the aft fuselage-empennage test on X997 substantiated the structure aft of F.S. 2200 only that portion of this specimen forward of F.S. 2273 was considered test structure. Some degree of overlap between the gear, empennage, and the wing-fuselage test programs was therefore obtained.

6.2 GENERAL TEST REQUIREMENTS

The purpose of the fatigue test program on the C-5A wing fuselage specimen (X998) was to evaluate the structural integrity of the C-5A airplane by applying loads to the test specimen similar to the loads encountered during the expected life of the airplane. The loads were developed from the 15 mission profiles supplied to the Lockheed-Georgia Company by the Air Force. These profiles include loads due to manuevers, vertical gust, contour flying, landing impact, taxi, landing runout, engine runup, ground-air-ground, and kneeling loads. The test program was scheduled to maintain a 4:1 lead time over the fleet airplanes (cyclic test hours versus actual flight hours). This procedure enables the engineers to locate the areas that were susceptible to fatigue damage at the earliest possible time and then take the necessary corrective action for fleet airplanes and to make design improvements for airframes yet to be manufactured.

Since the test structure is basically wing and fuselage, and since wing loads feed into the fuselage structure, it was desirable to develop the test spectrum primarily from the analytical wing loads. Laboratory test procedures were developed that determined the grouping of the analytical loads and allocated the number of mean loads, variable loads, and cycles for each grouping. Then compatible loads were developed for the primary control surfaces, wing pylons, and the fuselage. The fuselage loads also included the effects of the gear loads, empennage loads and pressurization. The fatigue test spectrum originally developed to represent these loads is shown in TABLE VII, and constitutes one pass or 1500 cyclic test hours (the equivalent of 5% of the aircraft service life). The specimen was subjected to repeated passes of the loading spectrum which was applied in reverse order on successive passes.

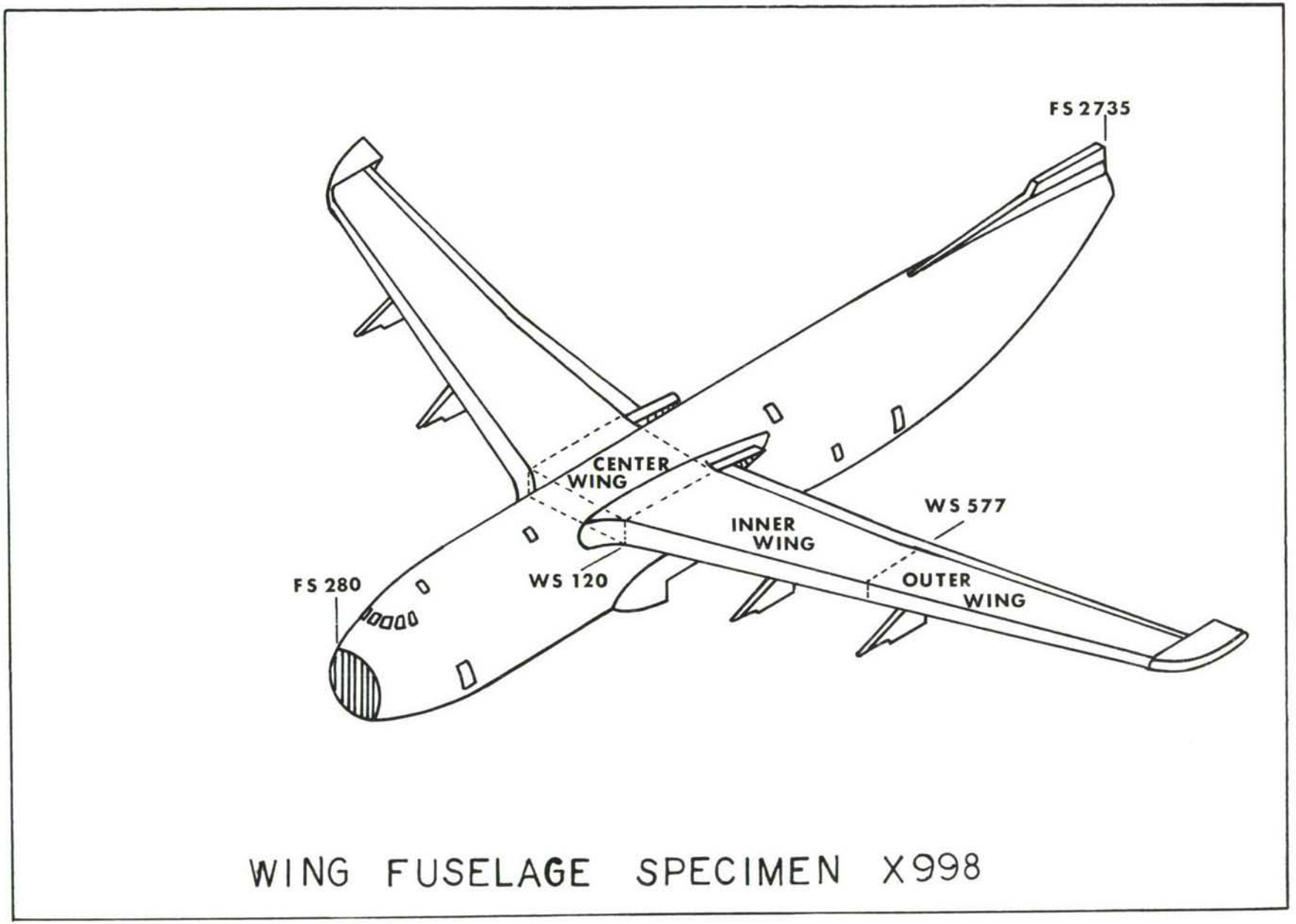

FIGURE 69. GENERAL STRUCTURAL CONFIGURATION OF THE WING FUSELAGE FATIGUE TEST SPECIMEN

TABLE VII

FATIGUE TEST LOADING SPECTRUM FOR THE WING FUSELAGE SPECIMEN

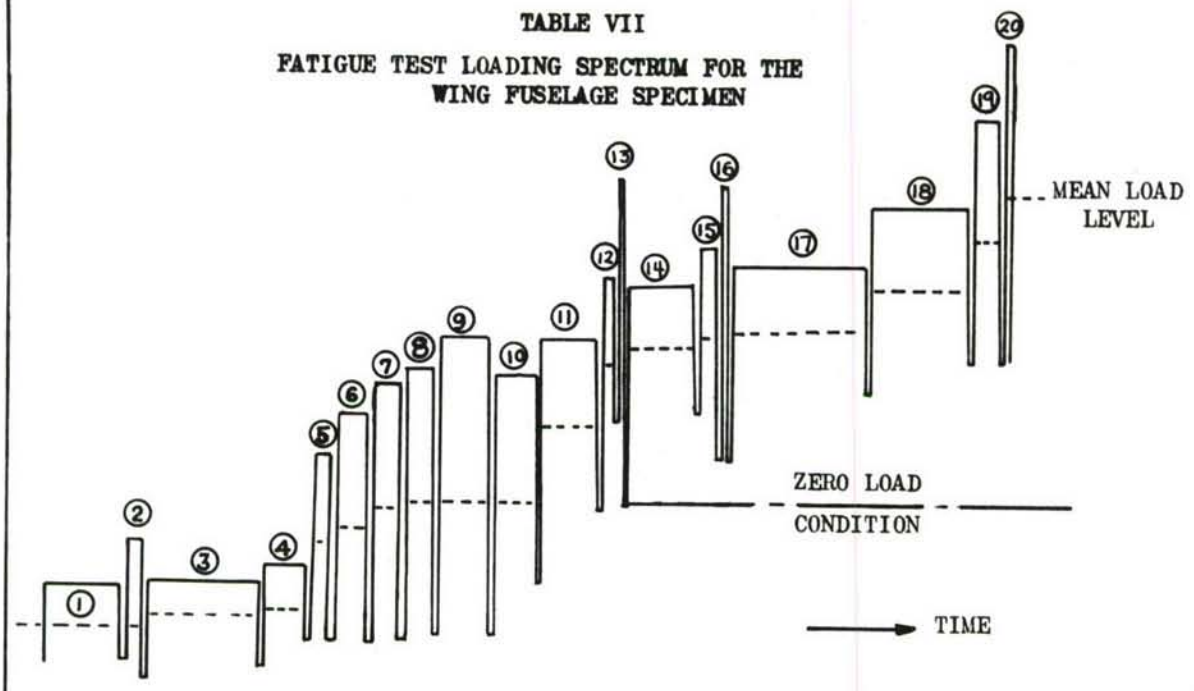

ORIGINAL SPECTRUM FOR 1500 CYCLIC TEST HOURS

SEQUENCE NUMBER	TEST GROUP	TEST CYCLES PER PASS
1	G-2B	1953.25
2	G-2A	18.75
3	G-3A	3000.0
4	G-1B	836.75
5	G-1A	13.25
6	Kneeling I	250.
7	Kneeling II	250.
8	GAG-1 A	79.225 *
9	GAG-2 W	81.050 218.325 *
10	GAG-3 A	221.4

SEQUENCE NUMBER	TEST GROUP	TEST CYCLES PER PASS
11	F-1C	1122.0
12	F-1B	13.0
13	F-1A	0.25
14	F-2C	1923.0
15	F-2B	22.0
16	F-2A	0.25
17	F-4A	7000.0
18	F-3C	3488.25
19	F-3B	11.0
20	F-3A	0.25

* Cycles with 8.3 psig hydrostatic fuselage pressurization, all other cycles without.

The basic objective of this spectrum derivation was to develop a schedule of loads which can be applied to the test article and which will produce fatigue effects on the specimen similar to those which are produced during the predicted service life of the aircraft, within a reasonable number of test loads and test cycles. The C-5A fatigue test requirements were based on a one lifetime goal of 30,000 flight hours, 12,000 landings, and 5,950 fuselage pressure cycles.

The test spectrum initially developed and applied for only the first two passes is shown in Table VII. To expedite the basic fatigue test program, subsequent passes were modified so that each load condition was repeated twice before a "change over" to the next load condition. This abbreviated procedure served to reduce the number of passes required for one lifetime from twenty to ten and double the number of cycles applied during each load condition. The revised spectrum also deleted the kneeling loads. These changes permitted the application of 3000 cyclic test hours per pass, (Fig. 70) with no detrimental effects on the evaluation of fatigue sensor data. To avoid any ambiguity in the sensor response plots, the base line of the response curves were still continued on a one pass per 1500 cyclic test hour basis.

Safety measures were incorporated to protect the specimen from inadvertant overload, local damage (falling objects), stress corrosion and corrosive environment (both air and water). Water was used for the pressure medium due to its low compressibility and to avoid major secondary damage in the event of minor damage to the pressure shell.

Safe conduct of the basic test program required the use of approximately 900 strain gages located at strategic control points for periodic or continuous monitoring. Both structural and non-structural test specimen members were inspected periodically to determine the extent and rate of fatigue damage due to the applied spectrum loads. Visual aids, including dye penetrant, magnaflux, and X-ray techniques were employed as required.

The basis for sensor allocation on specimen X998 followed the same line of reasoning employed on the two previous specimens, i.e., X996 and X997. Experience gained on the two previous specimens however, could be implemented on the wing-fuselage specimen (X998) since it was the last specimen to be instrumented. As a result of the previous practical experiences, it was possible to formulate some additional guidelines for selecting sensor locations. A survey of the advantages and disadvantages of sensor location choices on various structural components are examined as follows.

1. SPLICE FITTINGS - These are generally too "beefy" and can be prestressed as a result of over torque on the attachment fasteners. These fittings are usually designed for stiffness rather than strength so that the operating strain level will be relatively low, however, they do constitute well defined load paths. Erratic sensor readings may also be the result of joint slippage. Sensors IW31, IW32, IW39, IW40 and IW42 installed at the W.S. 120 splice are examples of sensors installed in a marginal location.

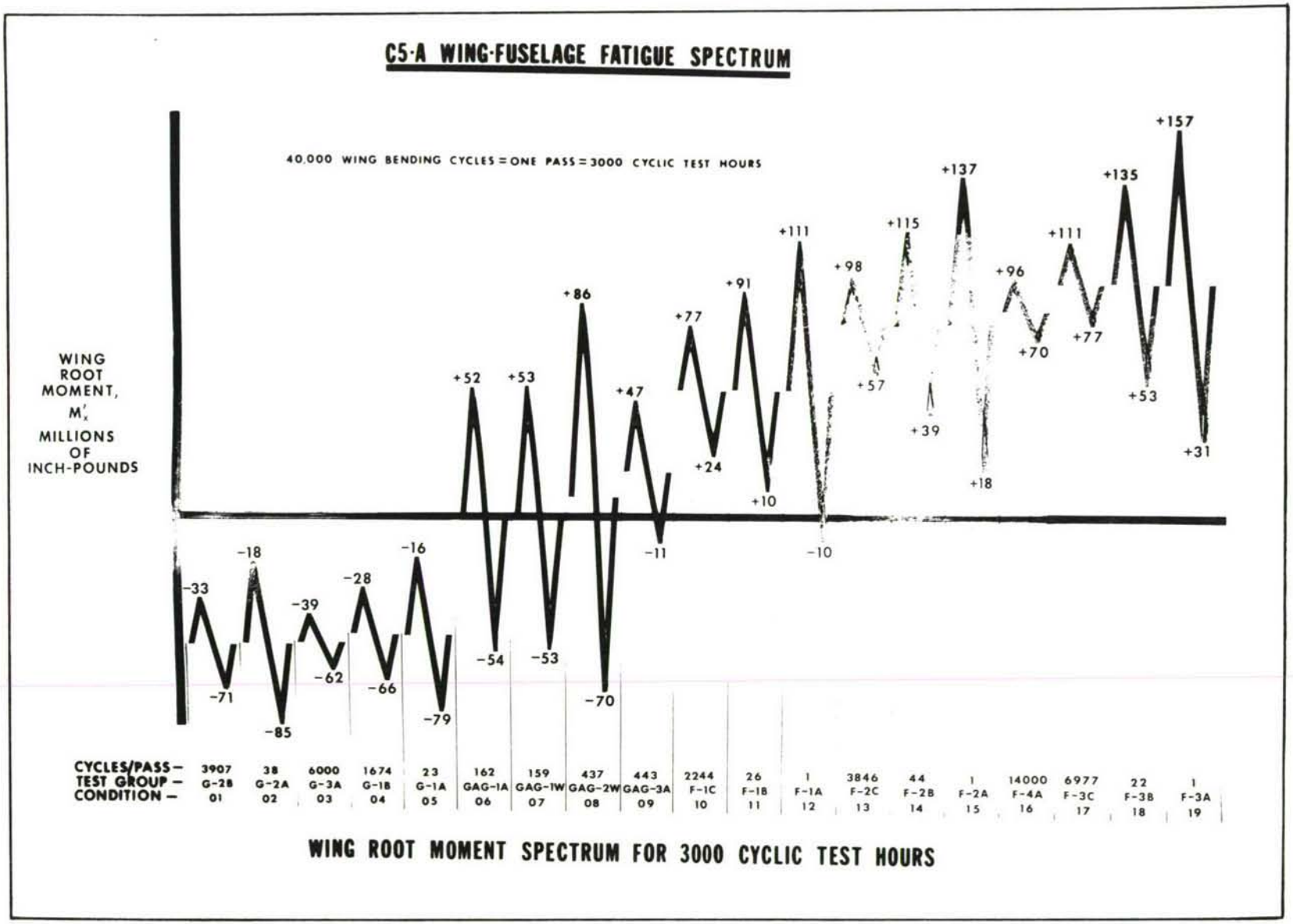

FIGURE 70. DIAGRAM ILLUSTRATING THE WING ROOT MOMENT OVER ONE SPECTRUM PASS

2. ACCESS DOORS - During a test program access doors are removed and reinstalled many times, increasing the liklihood of sensor mechanical damage. Variations in fastener replacements apparently results in variations of the sensor zero balance with each removal of the door. The strain pattern around these doors may also cause erratic behavior. Sensor OW70 is a case in point.

3. THIN WEBS - Thin webs of wing beams, etc., which may produce temporary buckles at the higher cyclic loads will produce inconsistencies of sensor response. This was revealed by component tests to be experimentally impractical and has not been pursued at all on the C-5A fatigue test specimens.

4. SPLICE JOINTS - Experimentation has shown that clean nominal areas of primary structure provides the most dependable locations. In this respect nominal areas adjacent to splice joints i.e., W.S. 120 and W.S. 577 appeared desirable and constituted the bulk of sensor locations on the wing.

5. HONEYCOMB PANELS - Installation on honeycomb panels also appear acceptable at this stage. The effects of repeated load exposure on pressure bulkheads is of interest and these are usually constructed of honeycomb panels, consequently the accurate monitoring of the effects of pressurization cycles is desirable. Sensors PB71 through PB75A are prime examples.

6. FUSELAGE PRESSURE VESSEL - Sensors may be located within the fuselage pressure shell to sense repetitive longitudinal and/or hoop strains. In this program the sensors were aligned along the longitudinal crown areas of the fuselage, primarily to respond to fuselage bending loads.

The sensor location sketches (Fig. 72 through 104) are also used in the data analysis therefore, some structural dimensions may become relevant. Information relative to structural dimensions (Fig. 72) as well as a precise definition sensor location is shown where necessary.

6.3 STRAIN SURVEY

A minimum utilization of strain gage data in support of sensor quality evaluations occurred on the final test specimen (X998). This was partly due to increased confidence in the installation capabilities of the technicians to obtain the desired sensor multiplying factor, and partly because the basic test program schedule did not permit extensive strain surveys prior to specimen cycling. One of the initial surveys, which was of particular interest, involved an upbending condition (F-3A) to evaluate the effectiveness of attachment fittings on the upper and lower rear beam caps at W.S. 120.

Although attachment fittings represent secondary structure, a strong temptation to instrument these areas exists because they constitute well defined load paths and sensor resistance change may be significantly affected by local failure. The fatigue sensors installed on W.S. 120 upper and lower rear beam attachment fittings (Figs. 80 through 84) are of some special interest, therefore, the sensitivity and performance of these sensors were checked during initial strain surveys. The load condition F-4A was applied in static increments up to a max cyclic load imposed on the mean load. The sensors were read in increments of 20%, 40%, 60%, and 100%, of the upbending loads and are plotted as shown in Figure 71. The sensors on the lower beam fitting indicated tension and those on the upper beam indicated compression as expected. The lone exception was IW 50 which indicated 100 micro strain of the wrong sign. This behavior is not too unusual considering that the sensor is on an attachment fitting which may have joint slippage. Generally sensors were located on primary structure where joint slippage is not a consideration; however, in this case an exception has been made. This sensor (IW 50) was monitored dynamically and periodically examined for a deterioration of bond; however, none was detected.

In general, sensor behavior on attachment fittings has proven difficult to interpret due to pre-load in fasteners, joint slippage, etc. however it is believed this approach should be pursued until proven unreliable. A correlation of sensor multiplier factor to adjacent strain gages on the W.S. 120 fittings has not been practical due to the fitting configuration and the location of the gages with respect to the sensor. A correlation was indicated,however, in regard to strain distribution in the fittings.

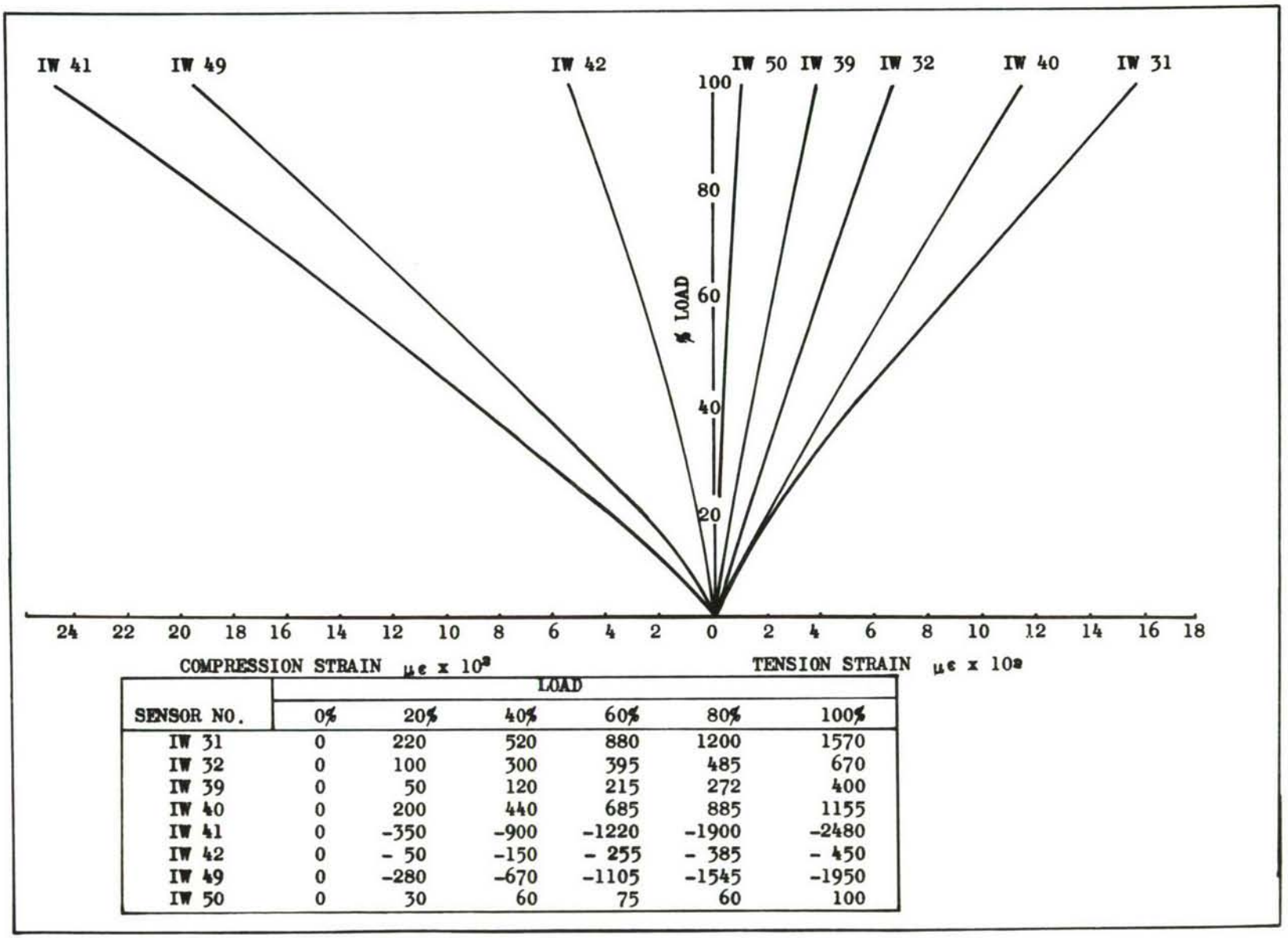

SENSOR NO.	LOAD 0%	20%	40%	60%	80%	100%
IW 31	0	220	520	880	1200	1570
IW 32	0	100	300	395	485	670
IW 39	0	50	120	215	272	400
IW 40	0	200	440	685	885	1155
IW 41	0	-350	-900	-1220	-1900	-2480
IW 42	0	- 50	-150	- 255	- 385	- 450
IW 49	0	-280	-670	-1105	-1545	-1950
IW 50	0	30	60	75	60	100

FIGURE 71. RESPONSE OF SENSORS ON THE UPPER AND LOWER REAR BEAM ATTACHMENT FITTINGS FOR THE STATIC LOAD CONDITION F-4A

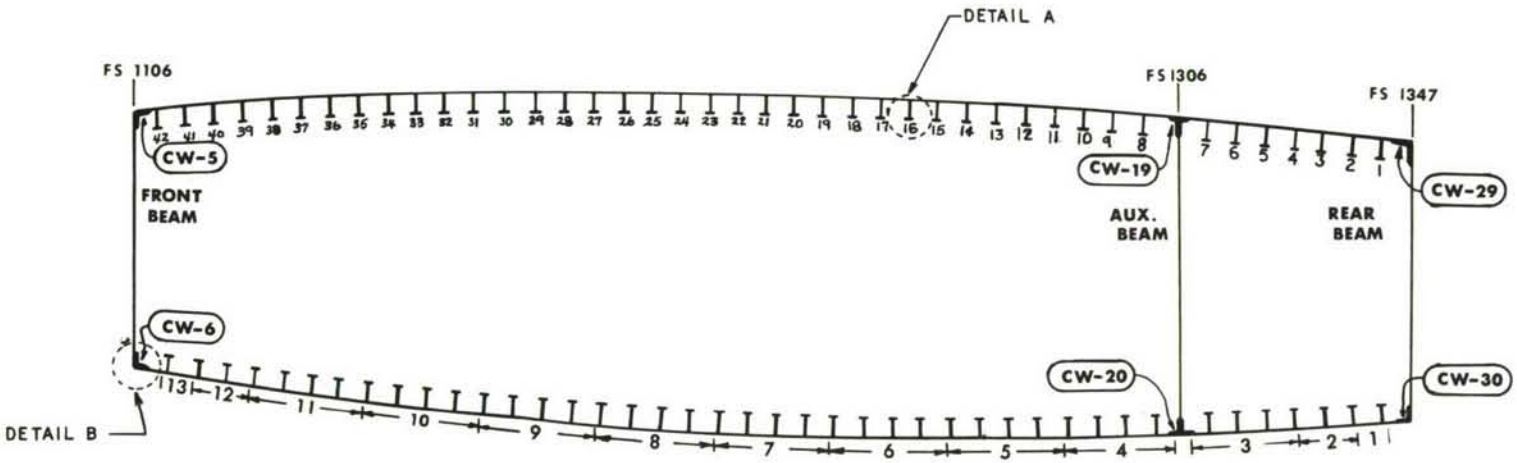

N Denotes Panel No. and Width

10 Denotes Stringer No.

UPPER SURFACE					LOWER SURFACE				
PANEL	W_F	T_W	T_{SK}	H	PANEL	W_F	T_W	T_{SK}	H
10, 11, 12, 13	2.52	.163	.226	4.47	10, 11, 12	2.52	.140	.190	4.44
7, 8, 9	2.52	.190	.240	4.47	7, 8, 9	2.52	.160	.200	4.44
4, 5, 6	2.52	.215	.265	4.47	4, 5, 6	2.52	.170	.230	4.44
1, 2, 3	2.52	.200	.255	4.47	1, 2, 3	2.52	.175	.228	4.44

ALL DIMENSIONS ARE CONSTANT IN A SPANWISE DIRECTION

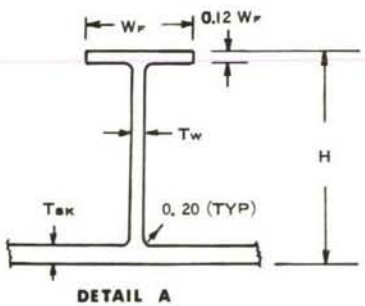

DETAIL A

CENTER WING SECTION B.L.0

FIGURE 72. CHORDWISE VIEW OF CENTER WING SHOWING GENERAL CONSTRUCTION AND SENSOR LOCATIONS

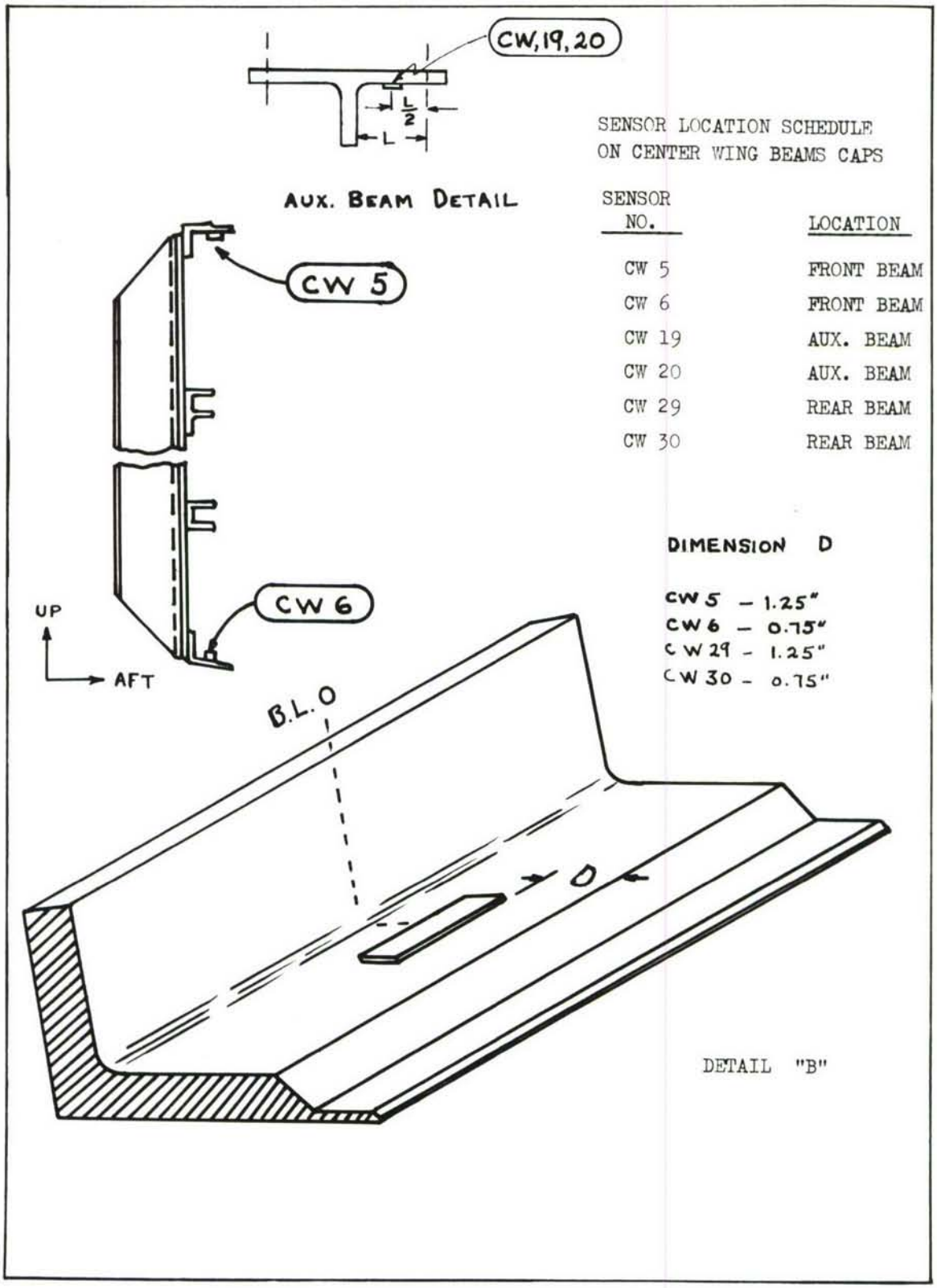

FIGURE 73. TYPICAL SENSOR INSTRUMENTATION DETAILS ON THE CENTER WING BEAM CAPS

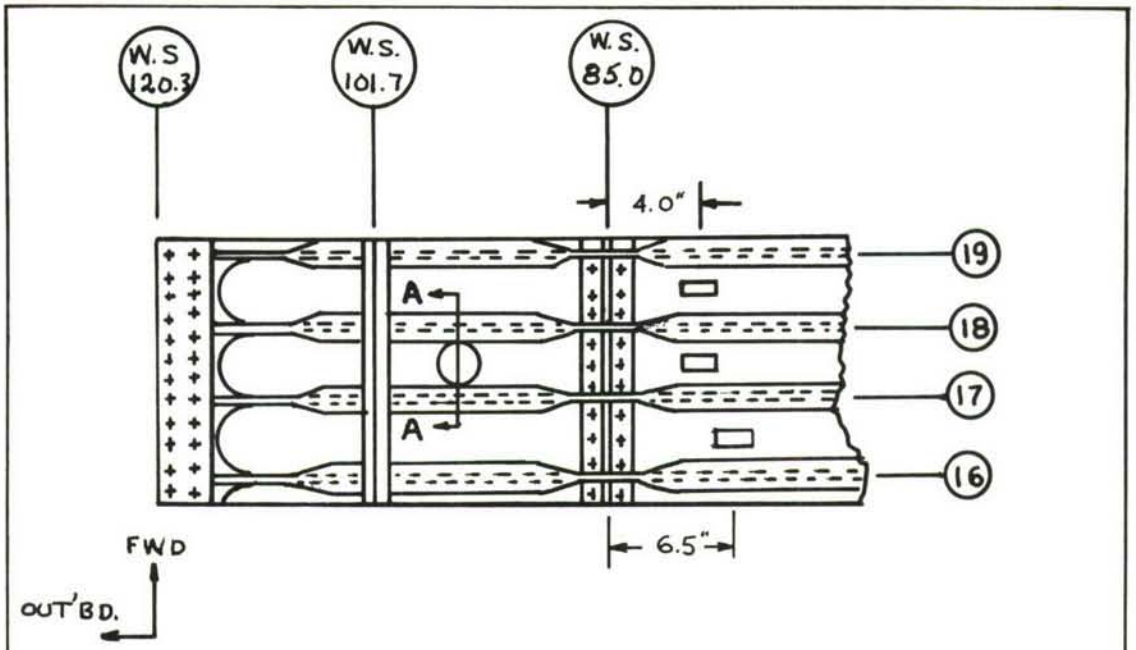

SCHEDULE

SENSOR NO.	BETWEEN STRINGERS
CW 7	18-19
CW 8	17-18
CW 9	16-17
CW 10	17-18

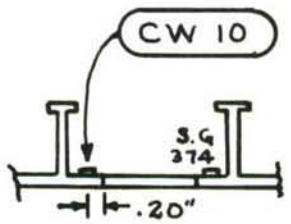

SECTION A-A

DETAIL OF FUEL LINE ACCESS HOLE

FIGURE 74. SENSOR INSTRUMENTATION ON THE LOWER SURFACE CENTER WING PANEL NO. 6

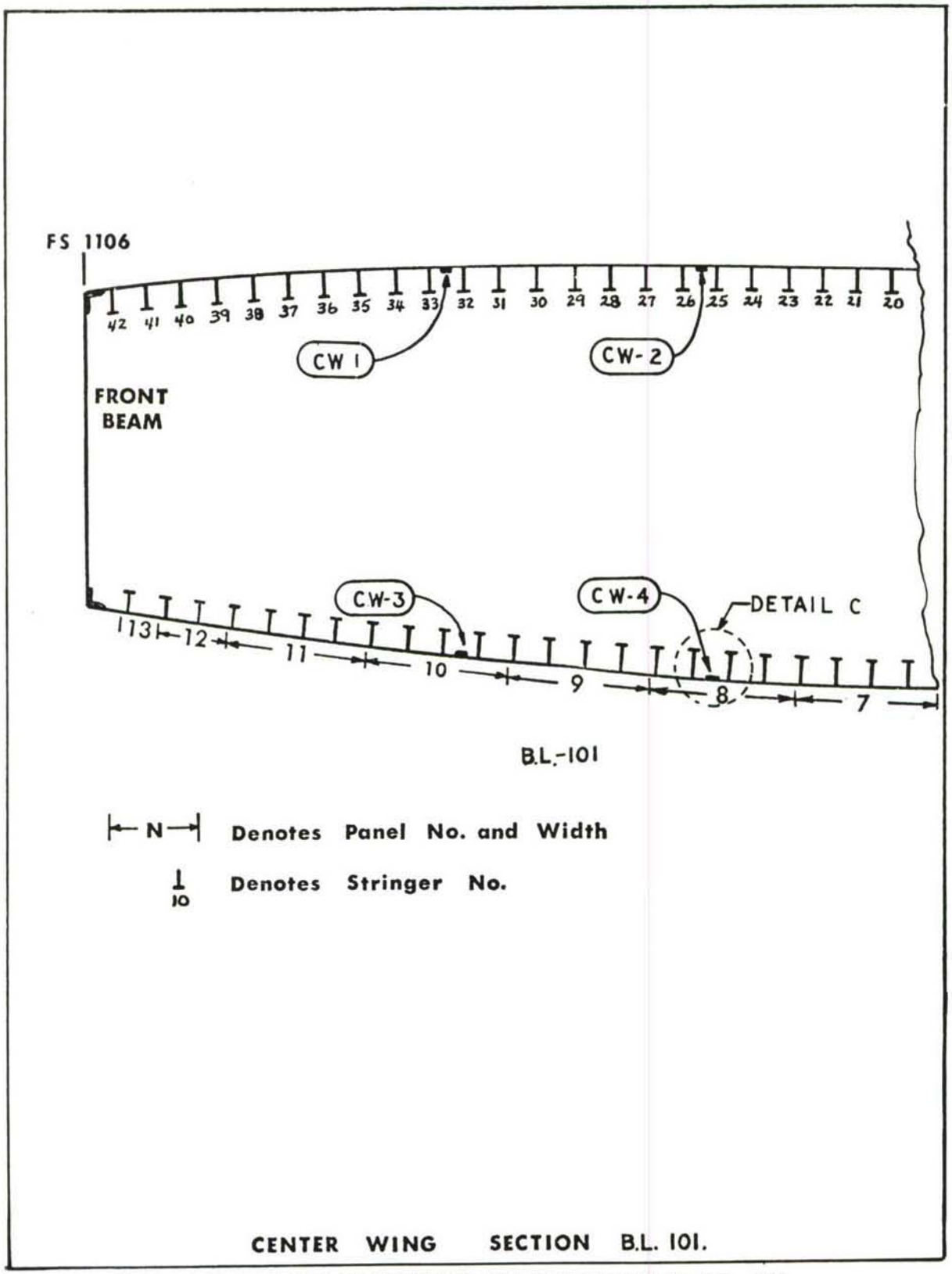

FIGURE 75. FATIGUE SENSOR LOCATIONS ON THE CENTER WING AT B.L. 101

CENTER WING DETAIL C

RISERS IN AREA OF B.L. 101 RIB
TYPICAL UPPER AND LOWER SURFACE

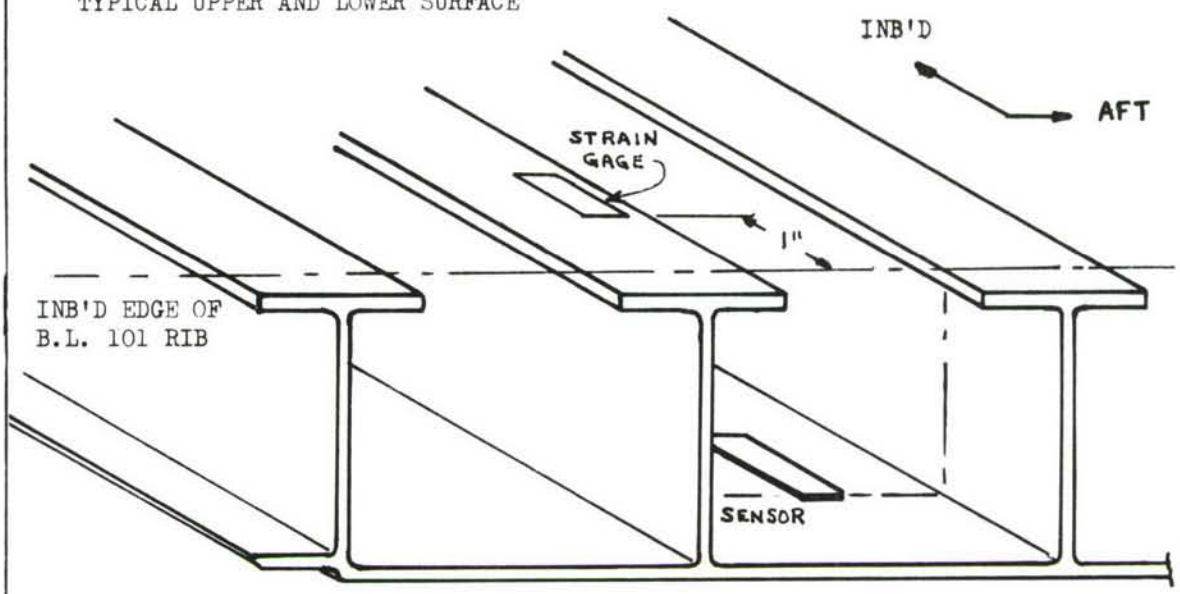

TYPICAL SENSOR INSTALLATION

SCHEDULE OF SENSORS AND STRAIN GAGES
IN THE CURVED RIB AREA - B.L. 101

SENSOR NO.	PANEL NO.	BETWEEN STRINGERS	RELATED GAGE
CW 1	10	32 - 33	322A
CW 2	8	25 - 26	321A
CW 3	10	32 - 33	327A
CW 4	8	25 - 26	326A

FIGURE 76. TYPICAL SENSOR INSTALLATIONS ON THE C-5A CENTER WING CURVED RIB AREA

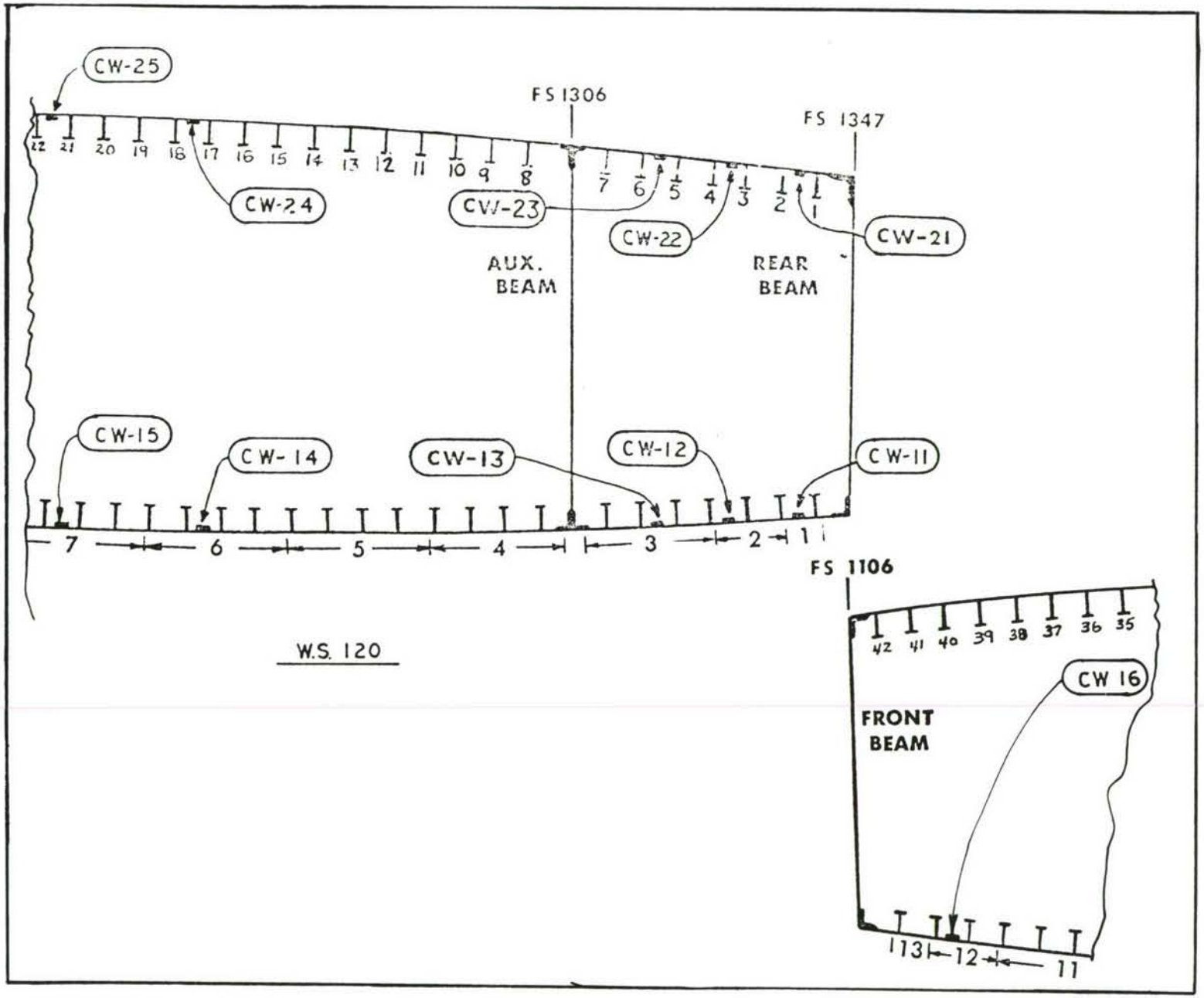

FIGURE 77. FATIGUE SENSOR LOCATIONS AT W.S. 120

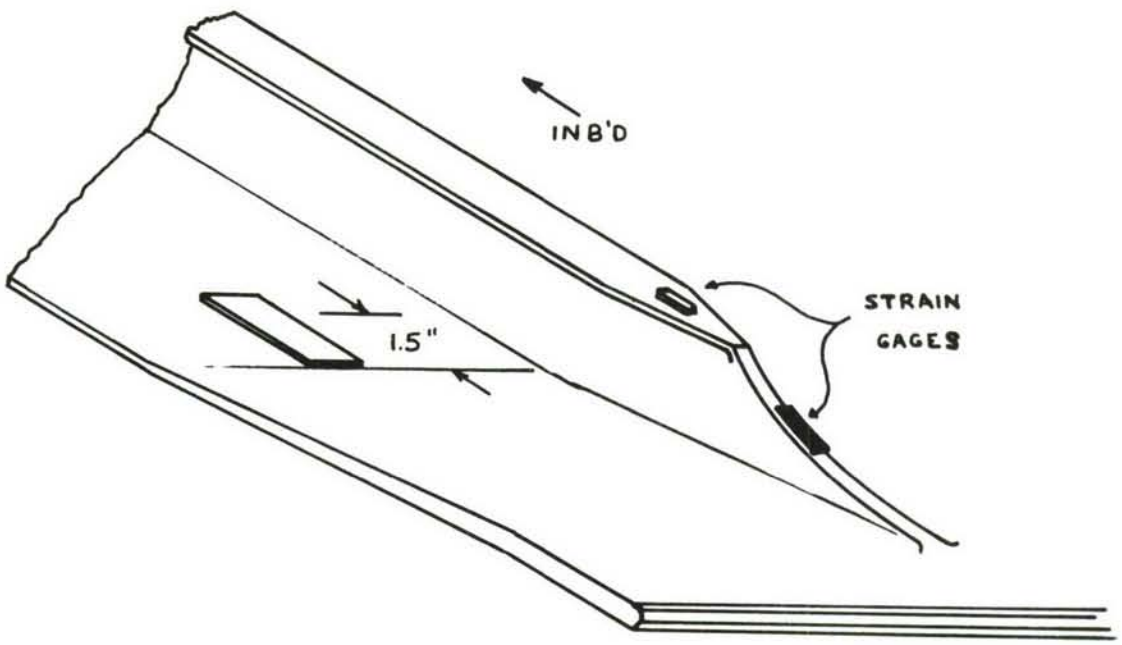

CENTER WING B.L.120 SPLICE

STRAIN GAGE AND SENSOR SCHEDULE

LOWER SURFACE				UPPER SURFACE			
SENSOR NO.	PANEL NO.	BETWEEN STRINGERS	RELATED S.G.	SENSOR NO.	PANEL NO.	BETWEEN STRINGERS	RELATED S.G.
CW 11	1	1 - 2	118A	CW 21	1	1 - 2	112A
CW 12	2	3 - 4	120A	CW 22	2	3 - 4	114A
CW 13	3	5 - 6	122A	CW 23	3	5 - 6	116A
CW 14	6	17 - 18	348A	CW 24	6	17 - 18	342A
CW 15	7	21 - 22	351A	CW 25	7	21 - 22	347A
CW 16	12	40 - 41	356A				

FIGURE 78. TYPICAL SENSOR INSTALLATION ON THE C-5A CENTER WING AT B.L. 120 SPLICE

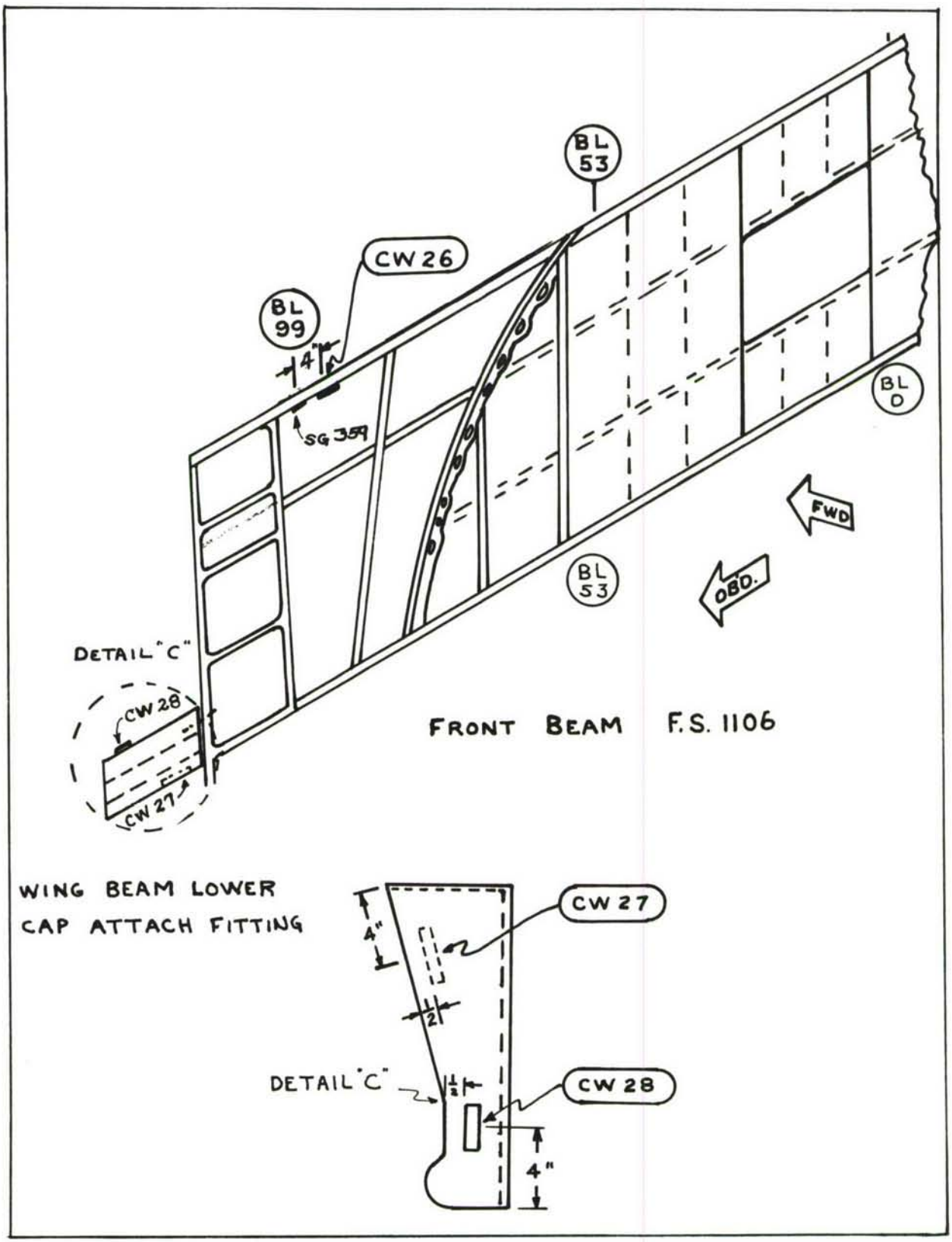

FIGURE 79. SENSOR LOCATIONS ON THE FRONT BEAM

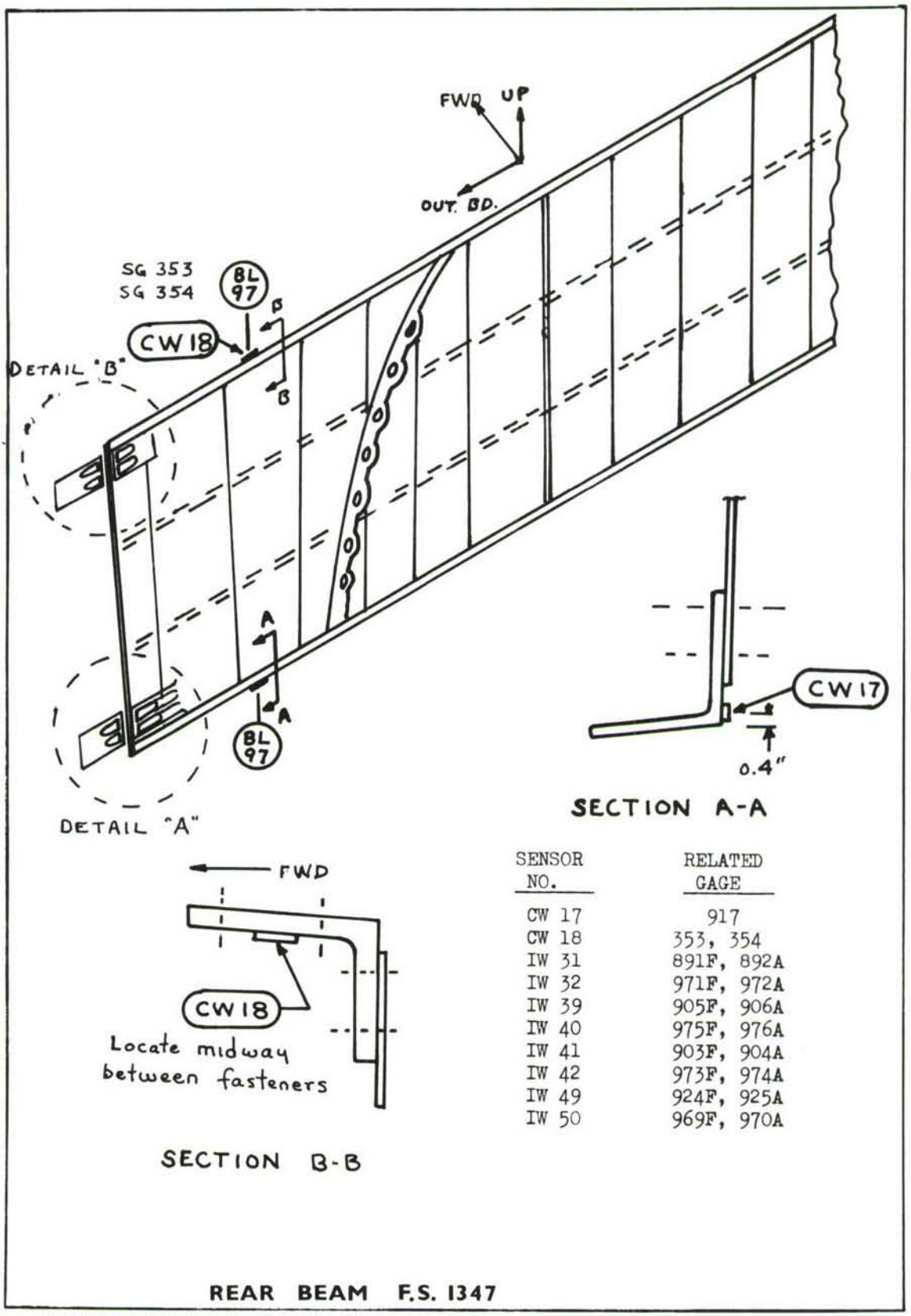

SENSOR NO.	RELATED GAGE
CW 17	917
CW 18	353, 354
IW 31	891F, 892A
IW 32	971F, 972A
IW 39	905F, 906A
IW 40	975F, 976A
IW 41	903F, 904A
IW 42	973F, 974A
IW 49	924F, 925A
IW 50	969F, 970A

FIGURE 80. SENSOR LOCATIONS ON THE CENTER WING REAR BEAM

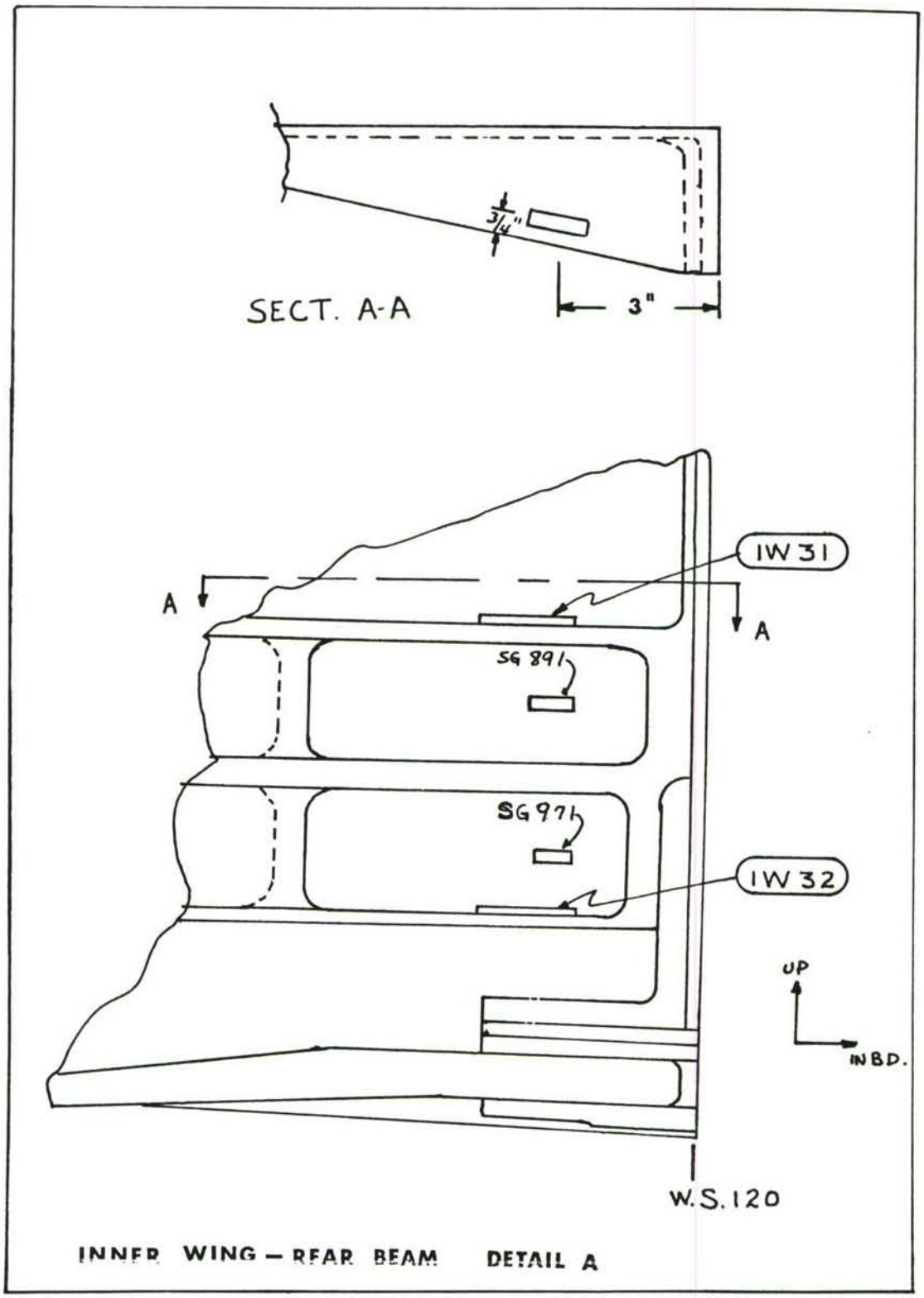

FIGURE 81. DETAIL OF STRAIN GAGE AND SENSOR LOCATIONS ON THE REAR BEAM ATTACHMENT FITTING

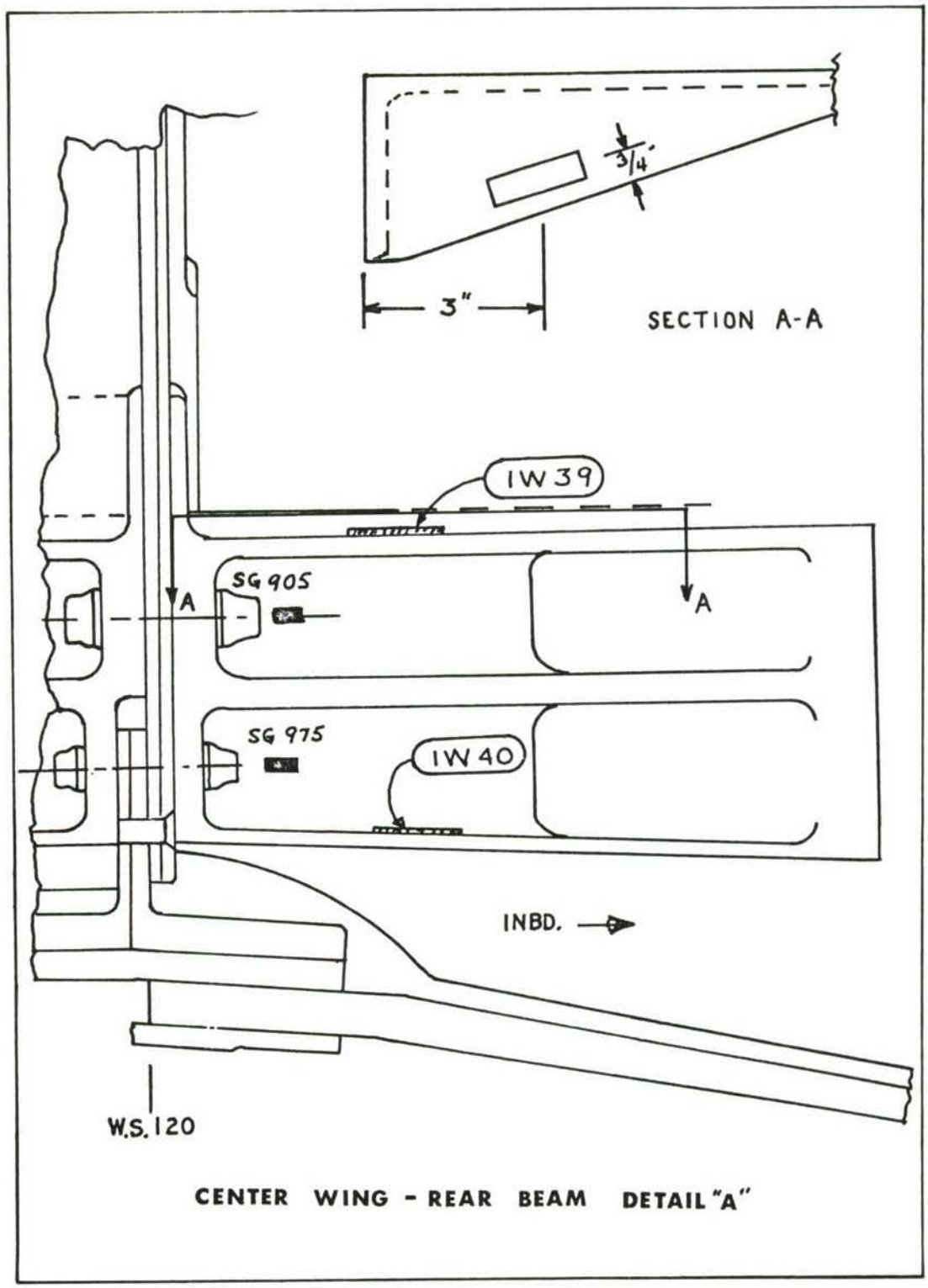

FIGURE 82. DETAIL OF STRAIN GAGE AND SENSOR LOCATIONS ON THE REAR BEAM ATTACHMENT FITTING

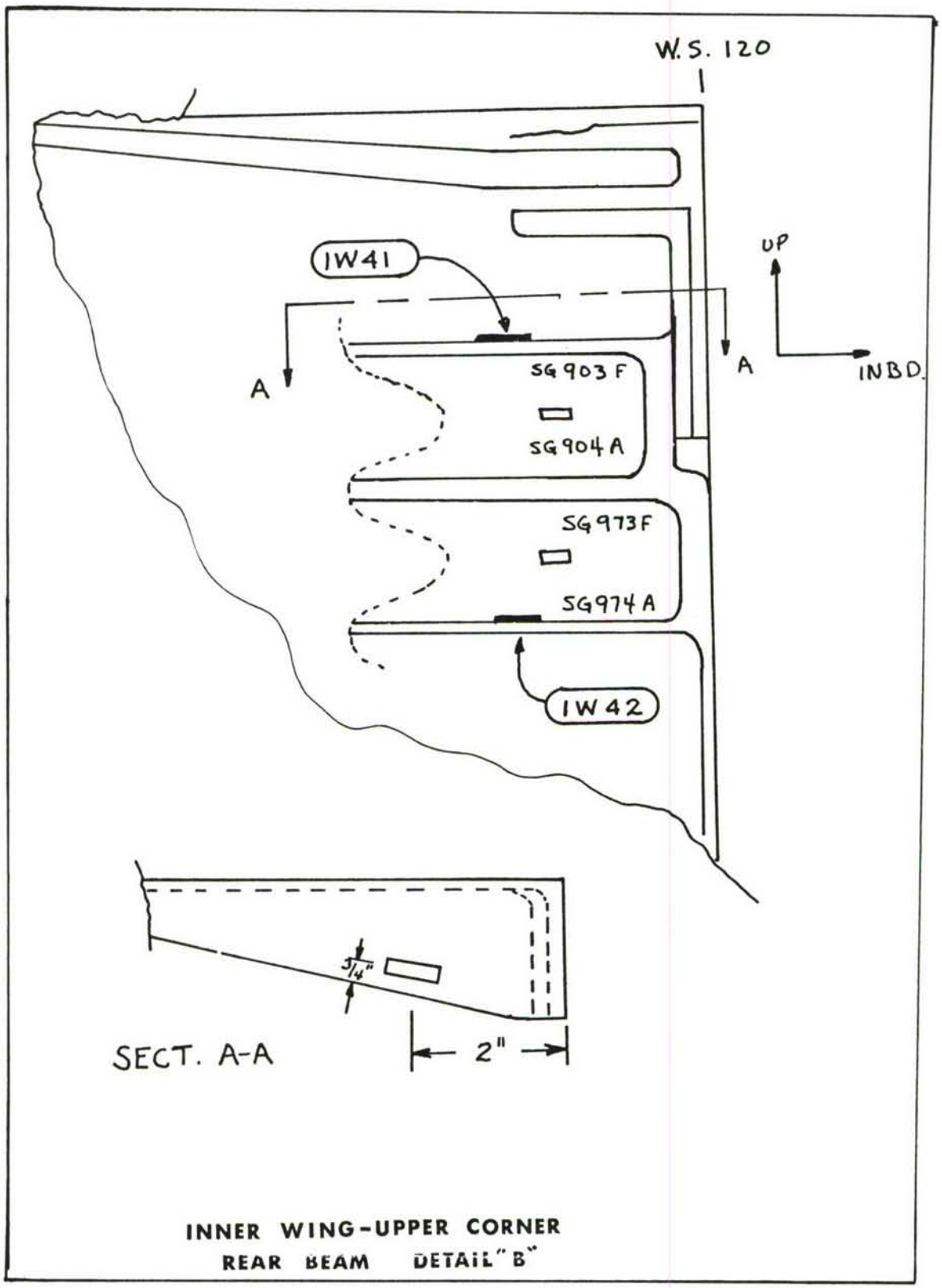

FIGURE 83. DETAIL OF STRAIN GAGE AND SENSOR LOCATIONS ON THE REAR BEAM ATTACHMENT FITTING

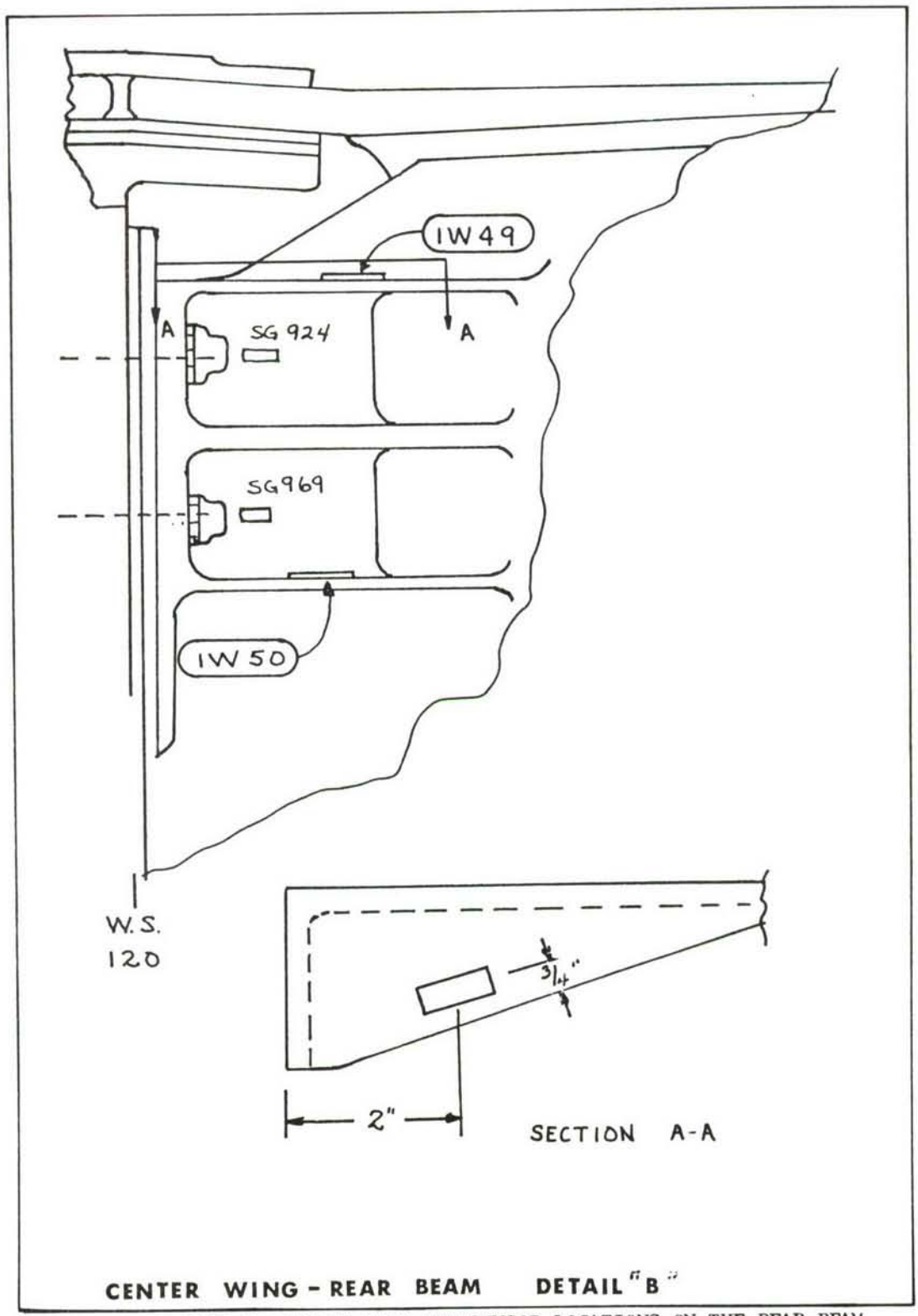

FIGURE 84. DETAIL OF STRAIN GAGE AND SENSOR LOCATIONS ON THE REAR BEAM ATTACHMENT FITTING

1. All sensors located mid bay between stringers.
2. All sensors located on inside surface in dry bay area.
3. "A" - Designates sensor added at the end of 9000 simulated flight hours.

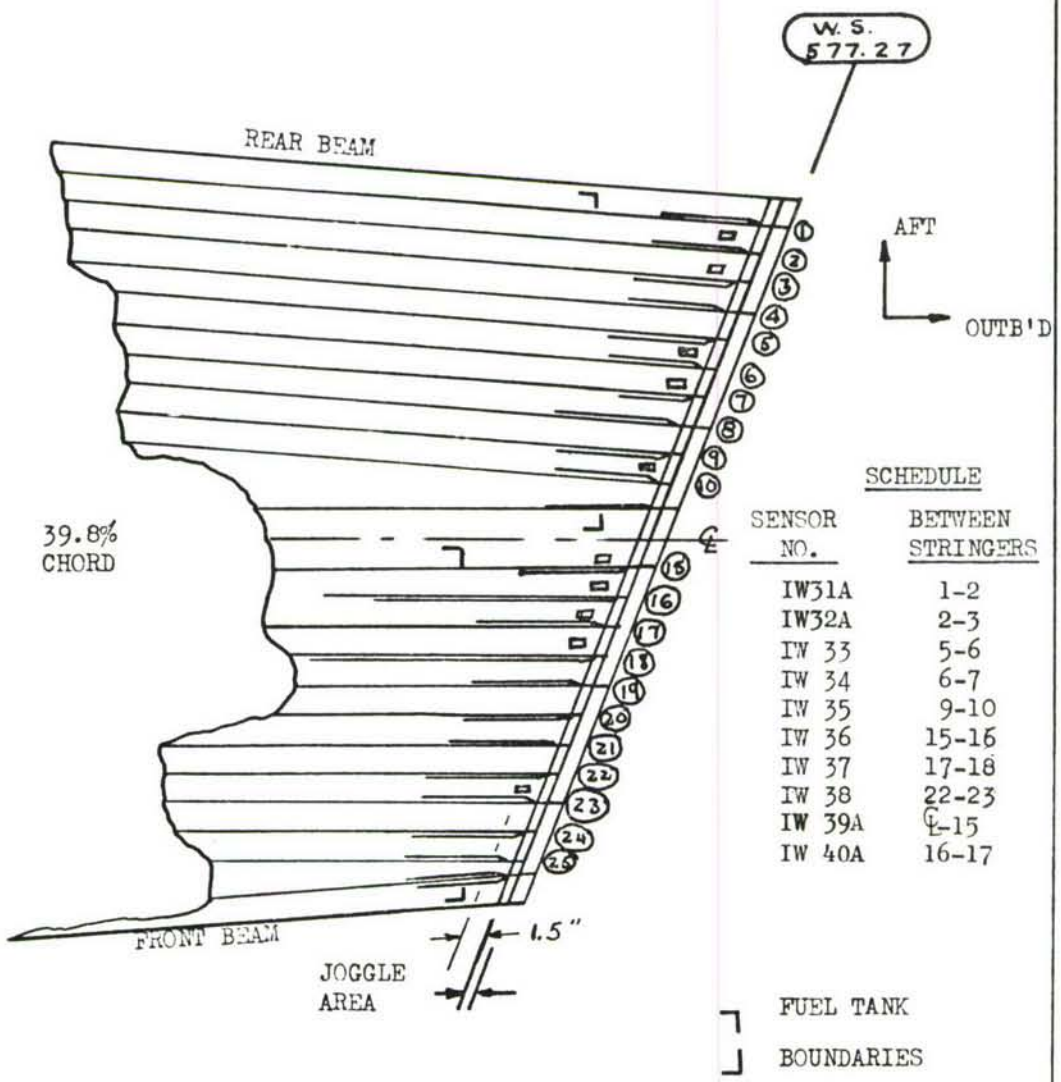

SCHEDULE

SENSOR NO.	BETWEEN STRINGERS
IW31A	1-2
IW32A	2-3
IW 33	5-6
IW 34	6-7
IW 35	9-10
IW 36	15-16
IW 37	17-18
IW 38	22-23
IW 39A	℄-15
IW 40A	16-17

FIGURE 85. C-5A LOWER SURFACE INNER WING SPLICE JOINT AT W.S. 577 SHOWING SENSOR LOCATIONS

1. All sensors located mid bay between stringers.
2. All sensors located on inside surface in dry bay area.

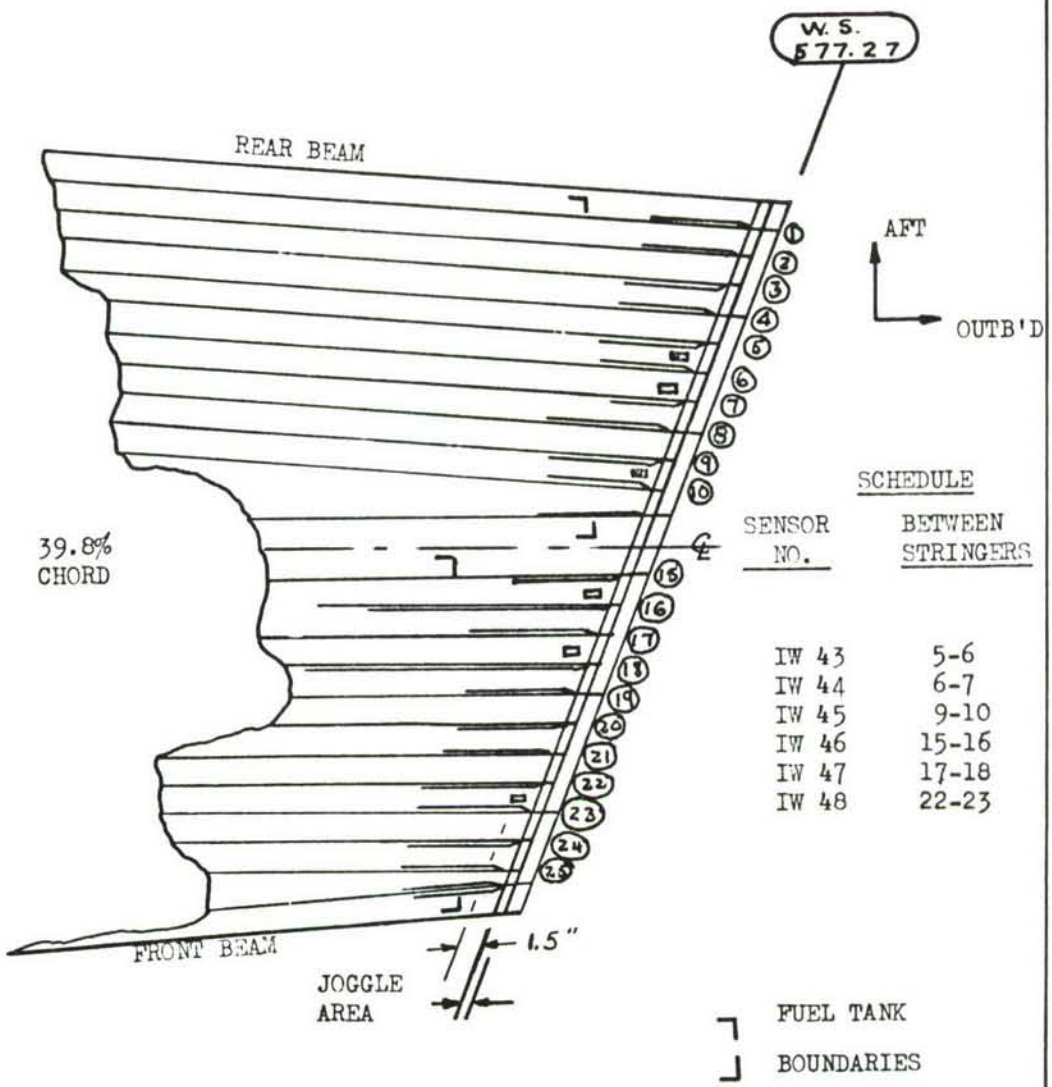

FIGURE 86. SENSOR LOCATIONS ON THE UPPER SURFACE INNER WING SPLICE JOINT AT W.S. 577

1. All sensors located mid bay between stringers.
2. All sensors located on inside surface.
3. "A" - Designates sensor added at the end of 9000 simulated flight hours.

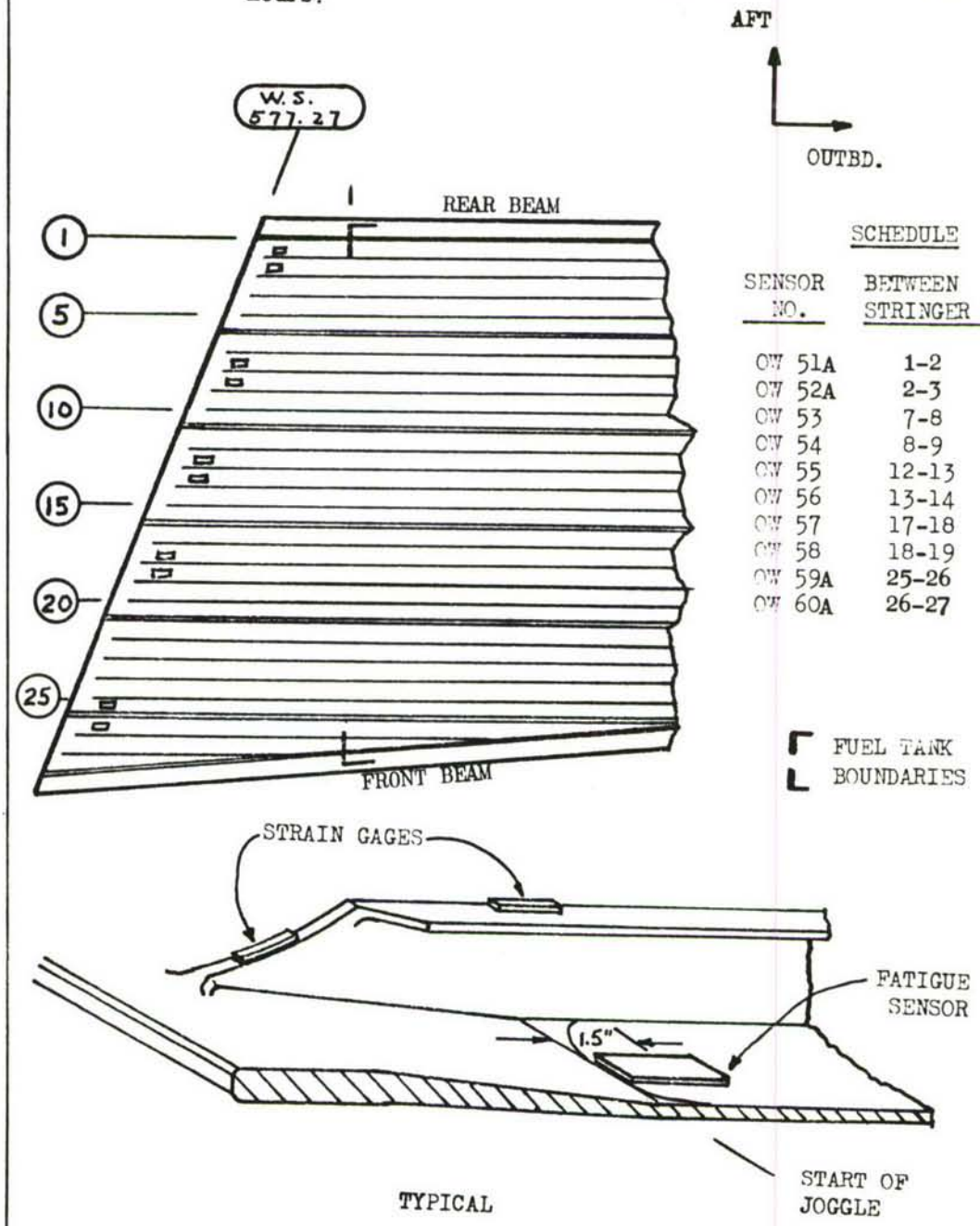

FIGURE 87. SENSOR LOCATIONS ON THE UPPER SURFACE OUTER WING AT W.S. 577

1. All sensors located mid bay between stringers.
2. All sensors located on inside surface in dry bay area.
3. "A" - Designates sensor added at the end of 9000 simulated flight hours.

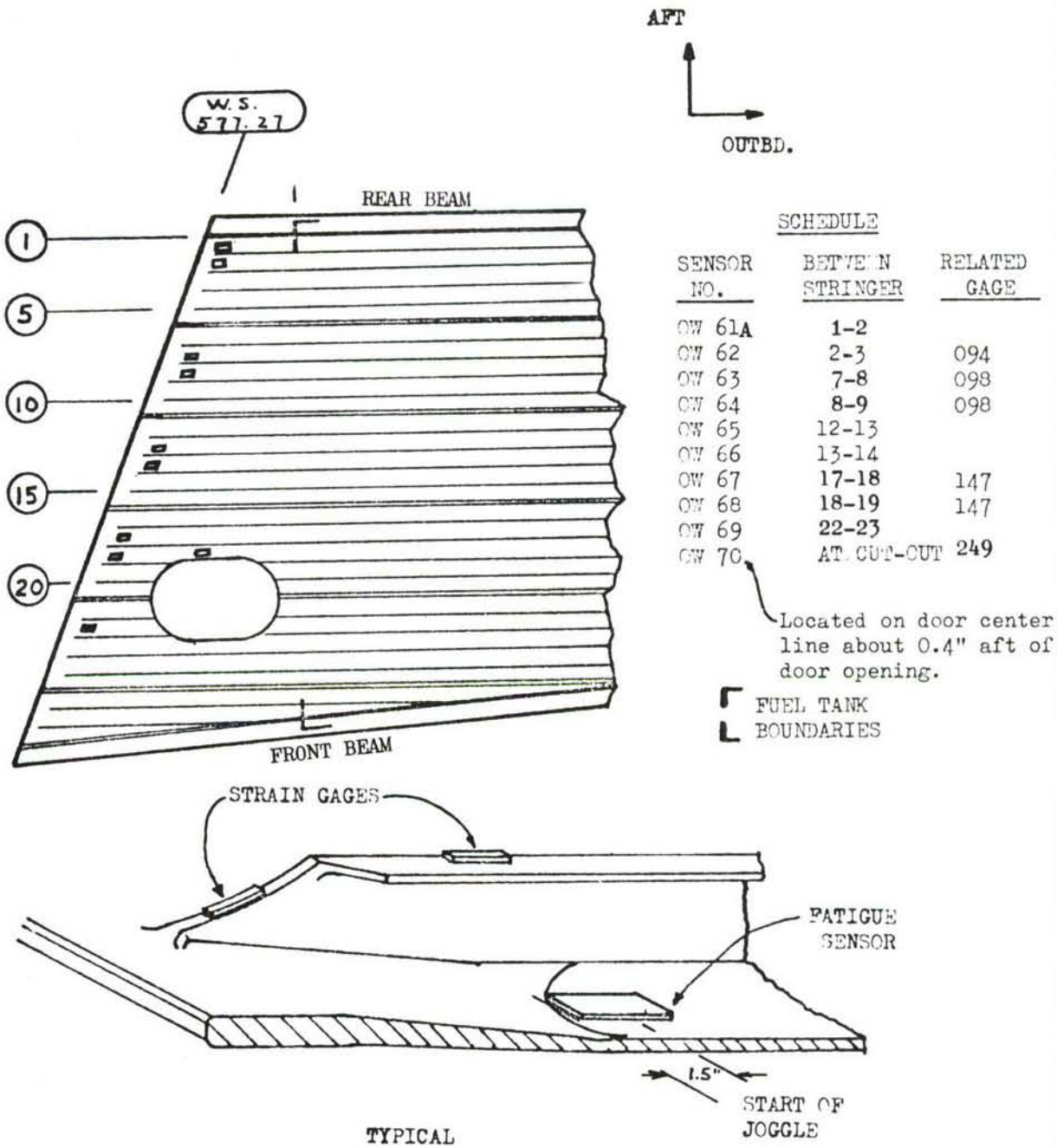

FIGURE 88. SENSOR LOCATIONS ON THE LOWER SURFACE OUTER WING AT W.S. 577

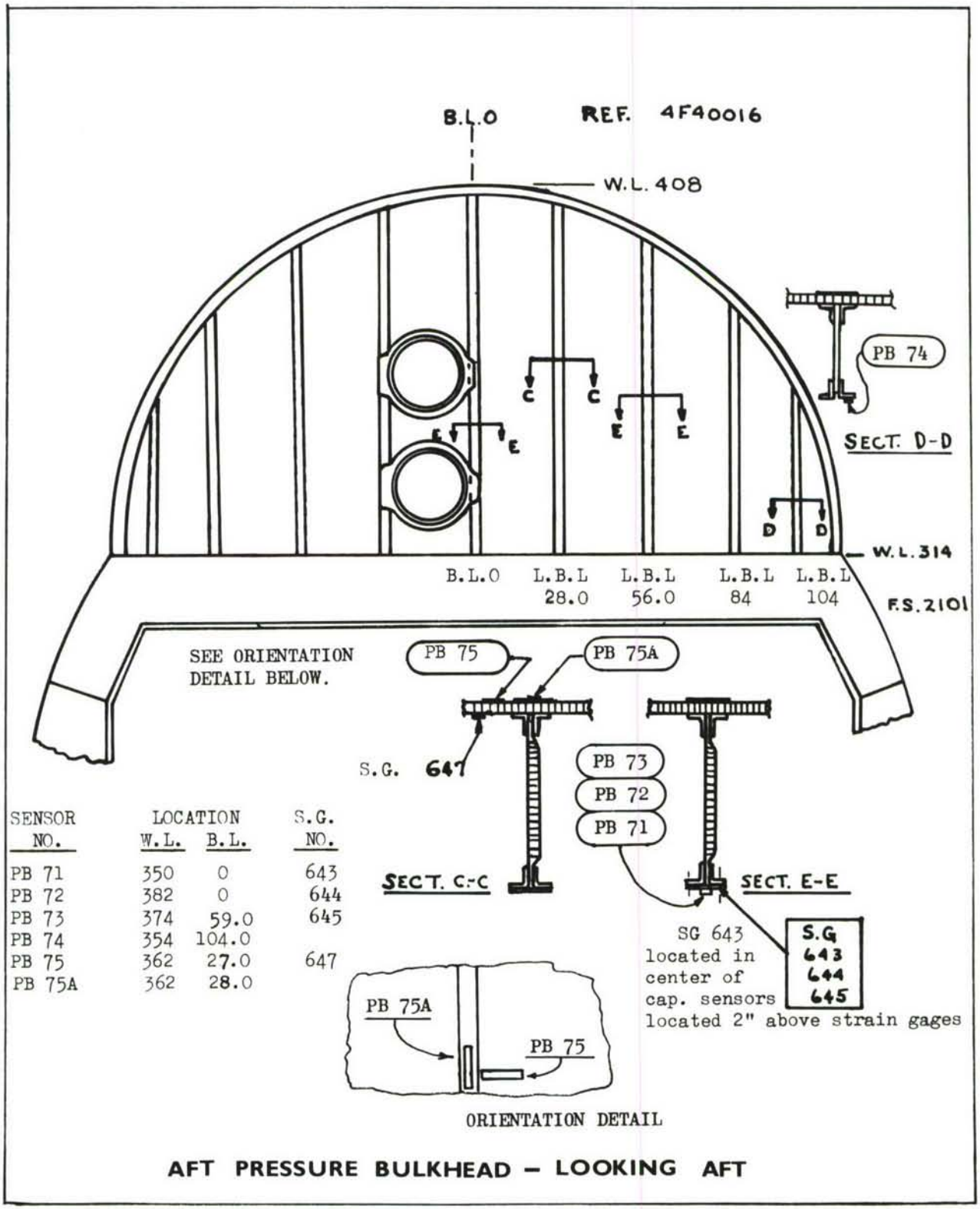

SENSOR NO.	LOCATION W.L.	LOCATION B.L.	S.G. NO.
PB 71	350	0	643
PB 72	382	0	644
PB 73	374	59.0	645
PB 74	354	104.0	
PB 75	362	27.0	647
PB 75A	362	28.0	

FIGURE 89. SENSOR LOCATIONS ON THE AFT FUSELAGE PRESSURE BULKHEAD

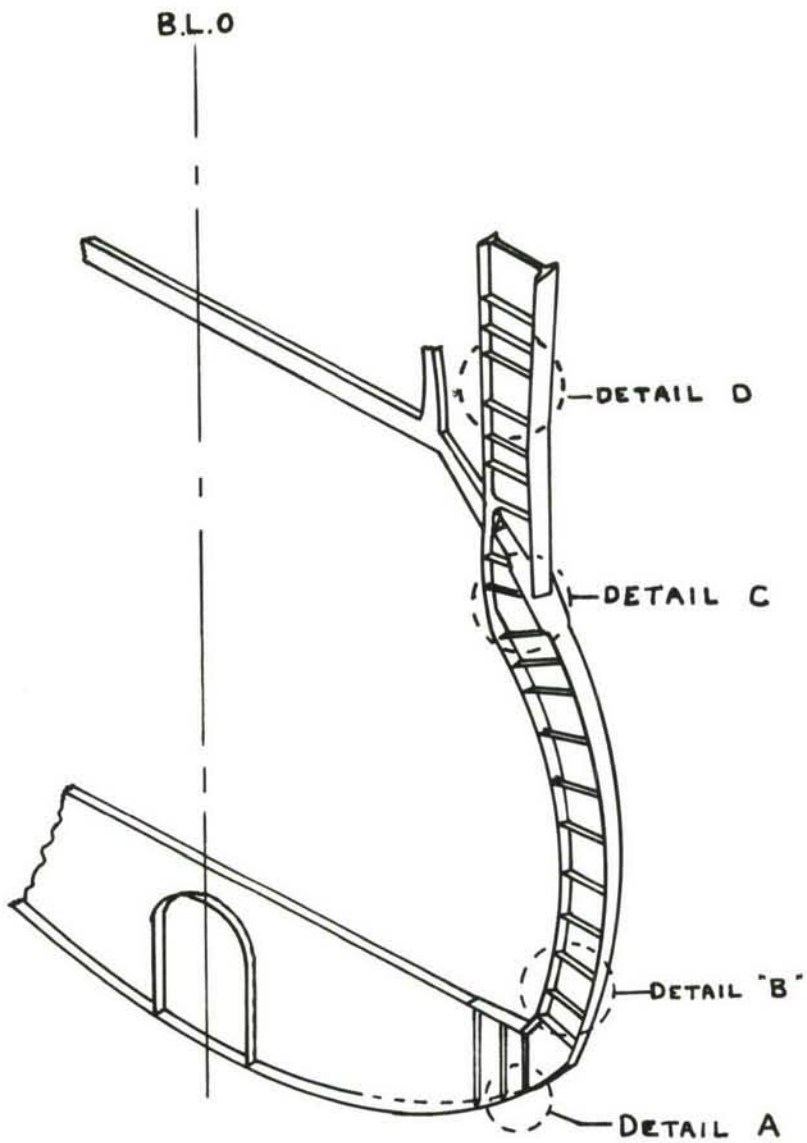

FIGURE 90. GENERAL SENSOR LOCATION AREA ON FUSELAGE MAIN FRAME F.S. 1106

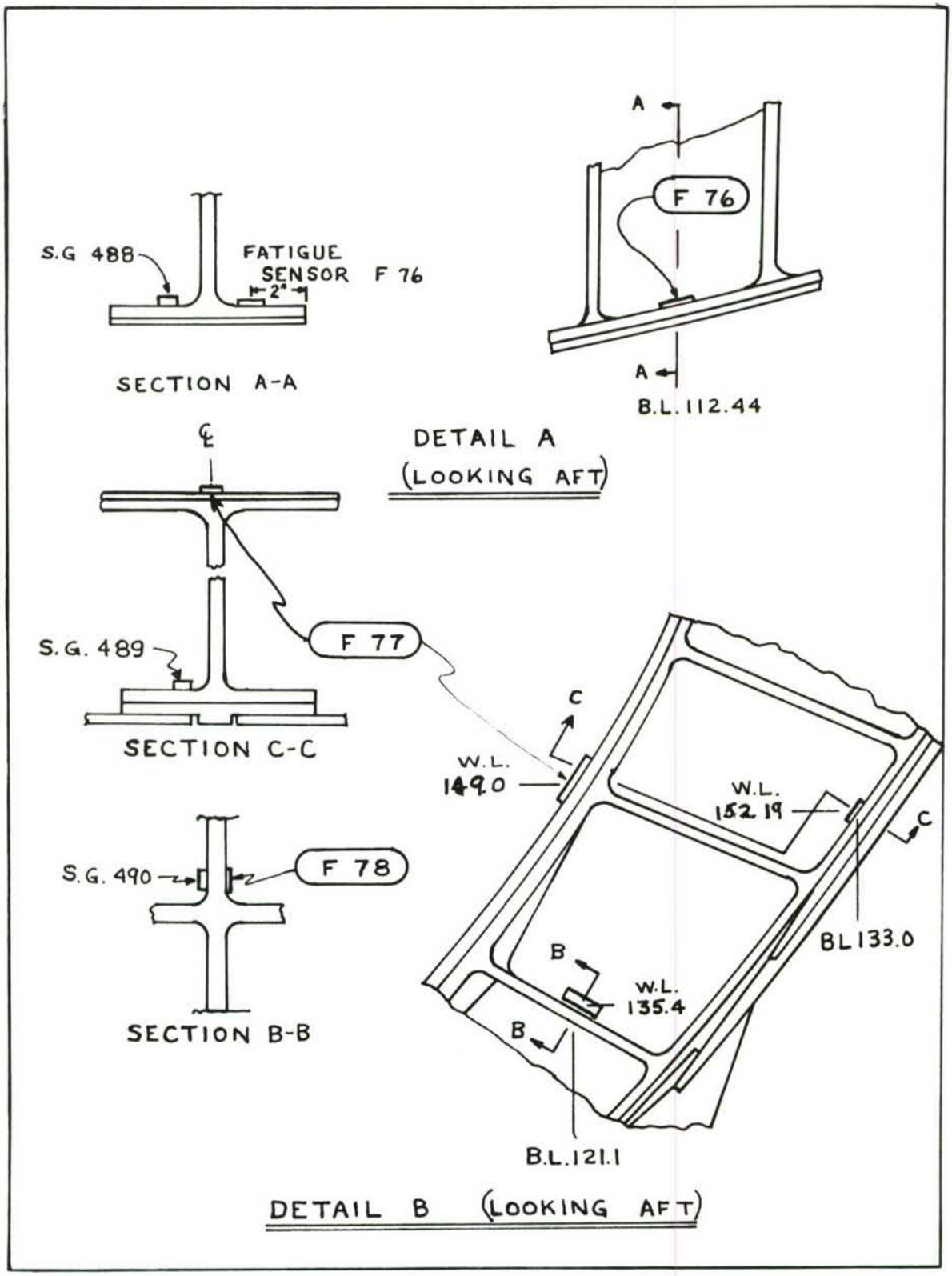

FIGURE 91. SENSOR LOCATION DETAILS ON THE FUSELAGE MAIN FRAME AT F.S. 1106

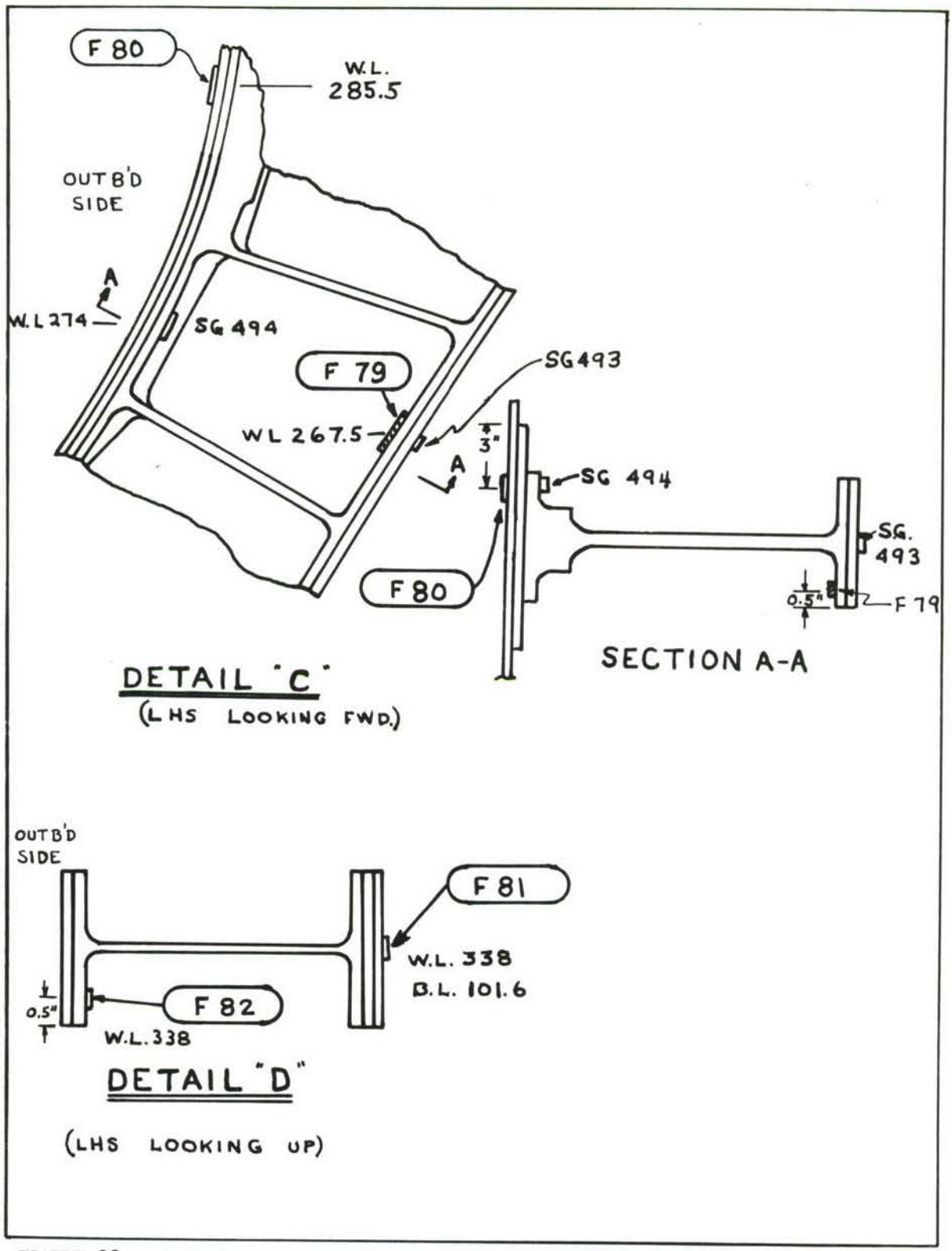

FIGURE 92. SENSOR LOCATION DETAILS ON THE FUSELAGE MAIN FRAME AT F.S. 1106

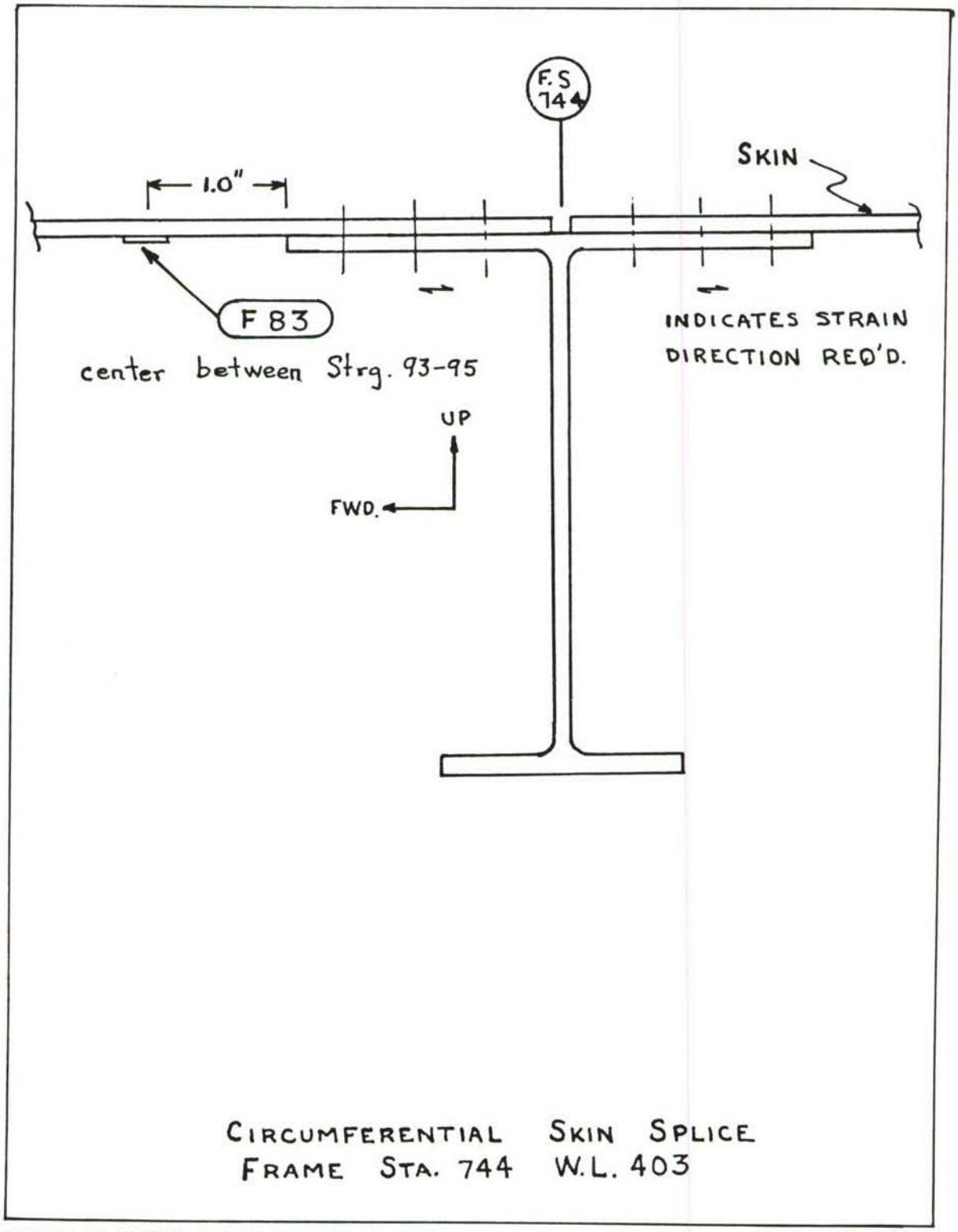

FIGURE 93. SENSOR LOCATION ALONG THE CROWN OF THE FORWARD FUSELAGE

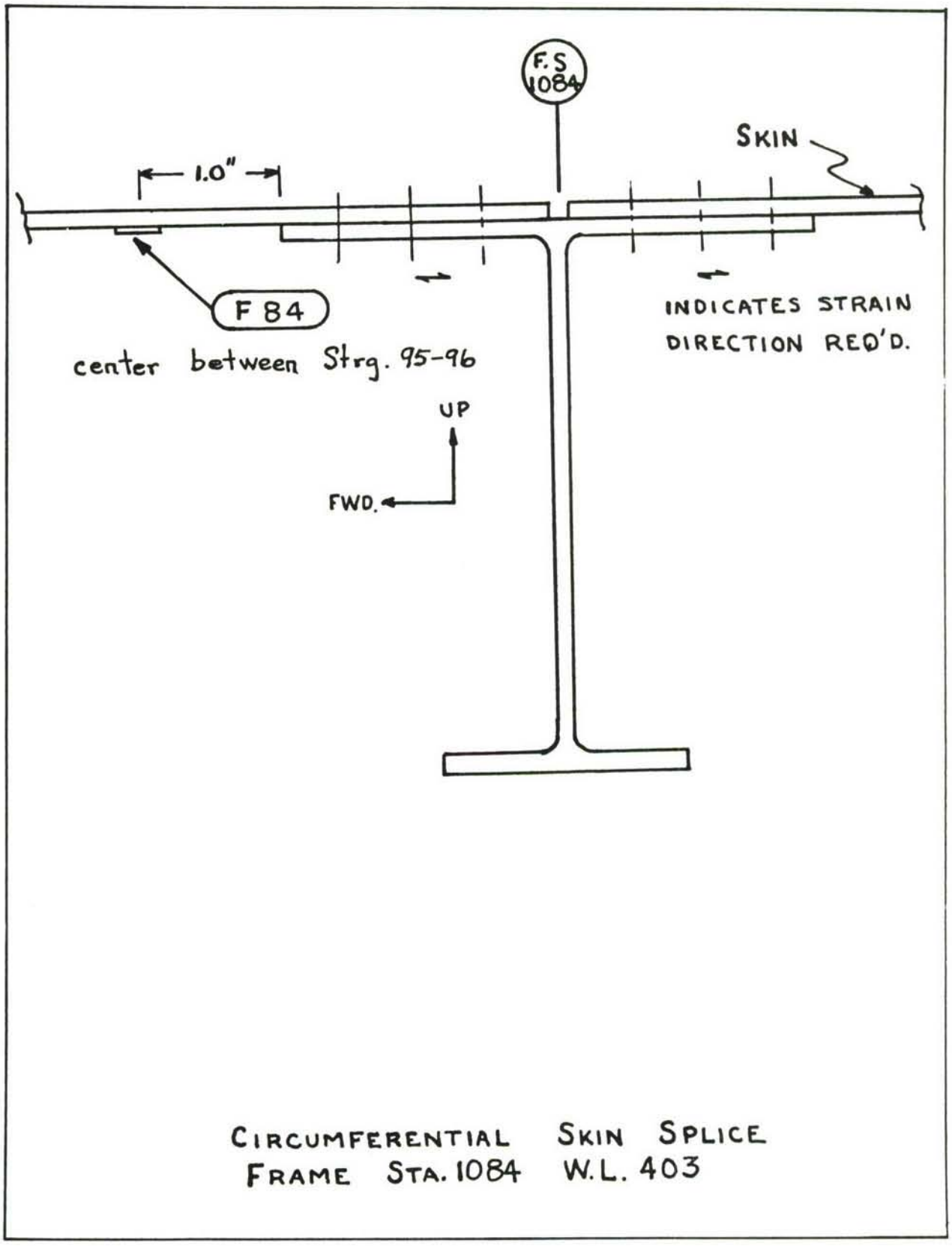

FIGURE 94. SENSOR LOCATION ALONG THE CROWN OF THE FUSELAGE IMMEDIATELY FORWARD OF THE WING

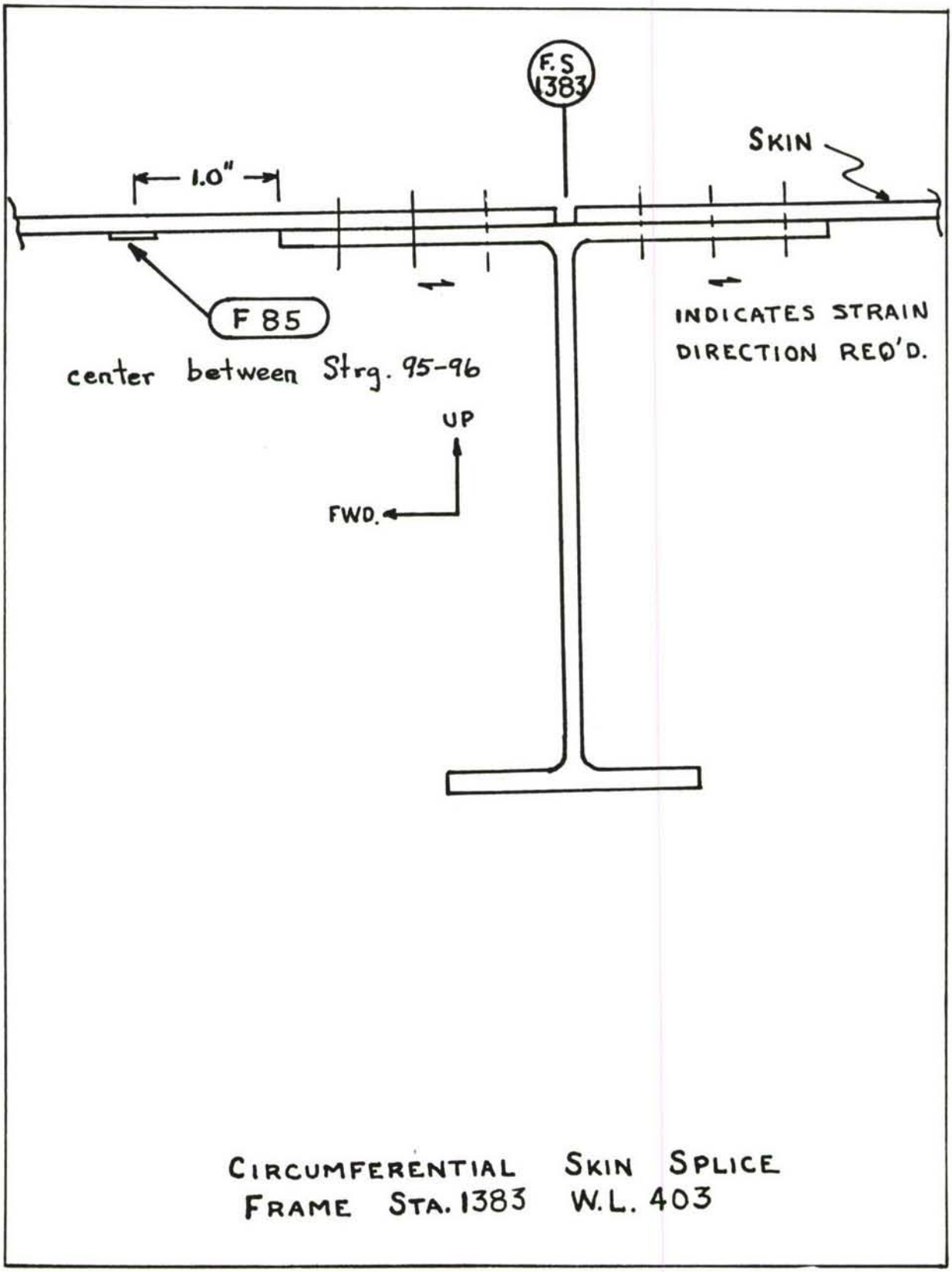

FIGURE 95. SENSOR LOCATION ALONG THE CROWN OF THE FUSELAGE IMMEDIATELY AFT OF THE WING

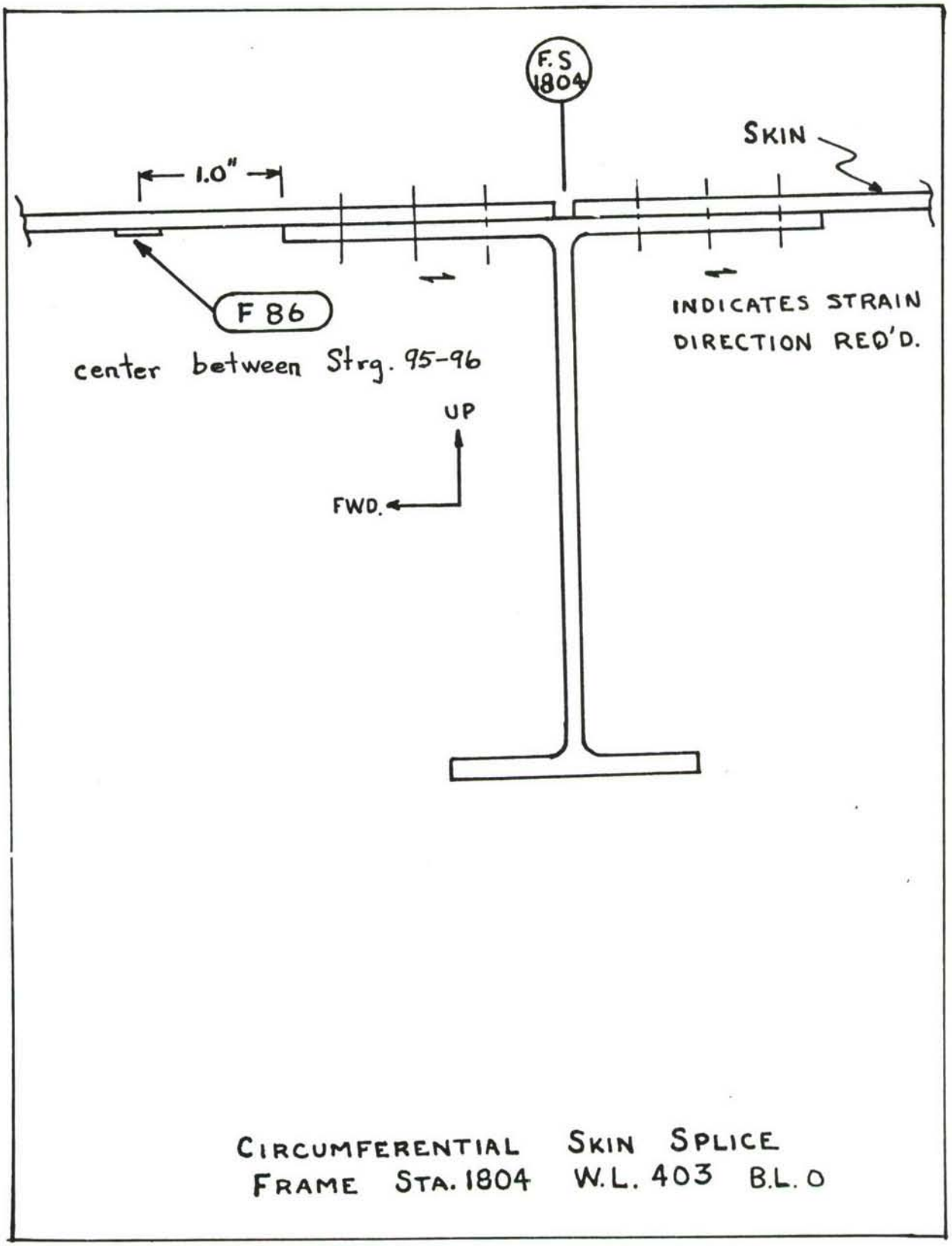

FIGURE 96. FATIGUE SENSOR LOCATION ALONG THE AFT FUSELAGE CROWN

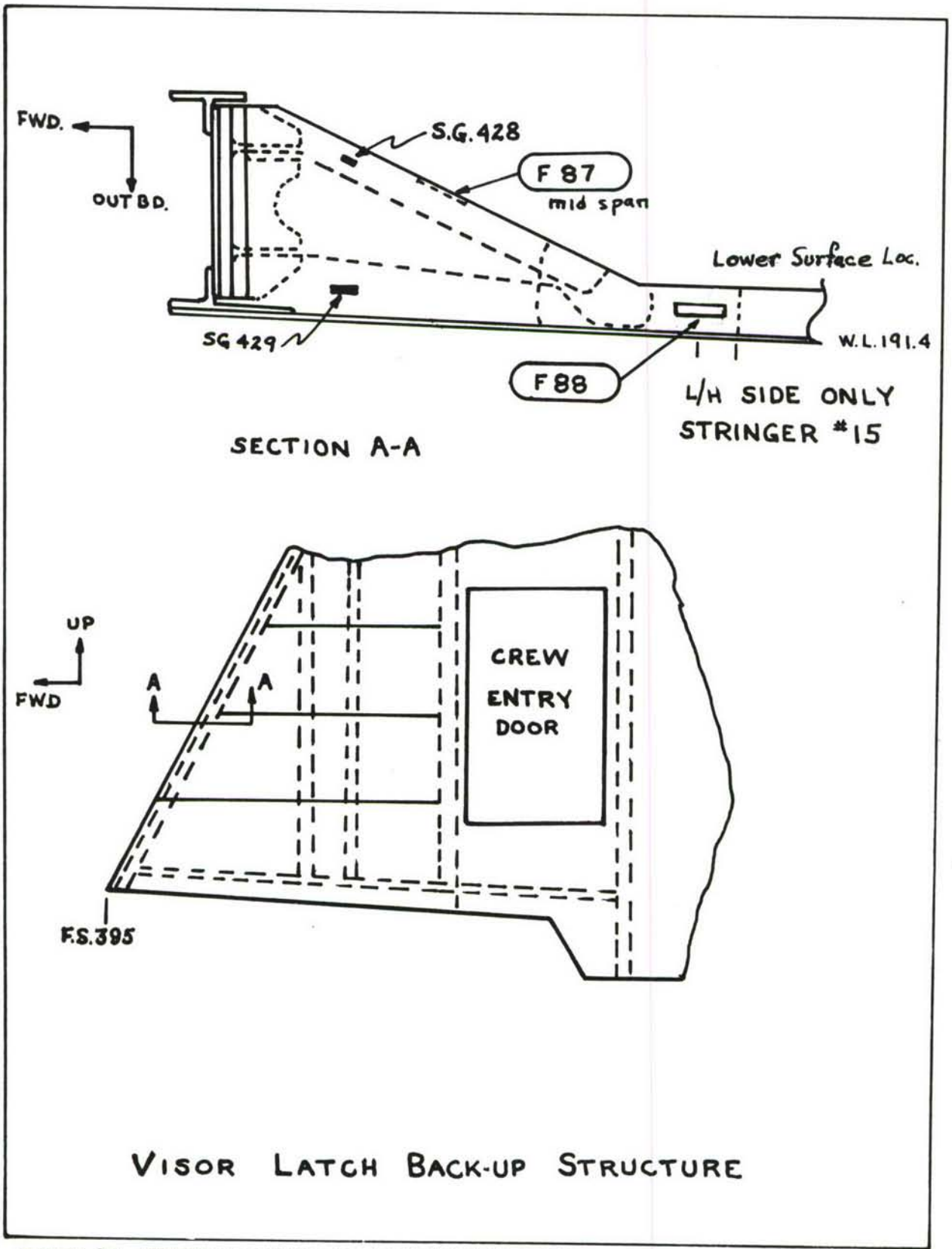

FIGURE 97. SENSOR LOCATIONS ON THE FUSELAGE VISOR BACK-UP STRUCTURE

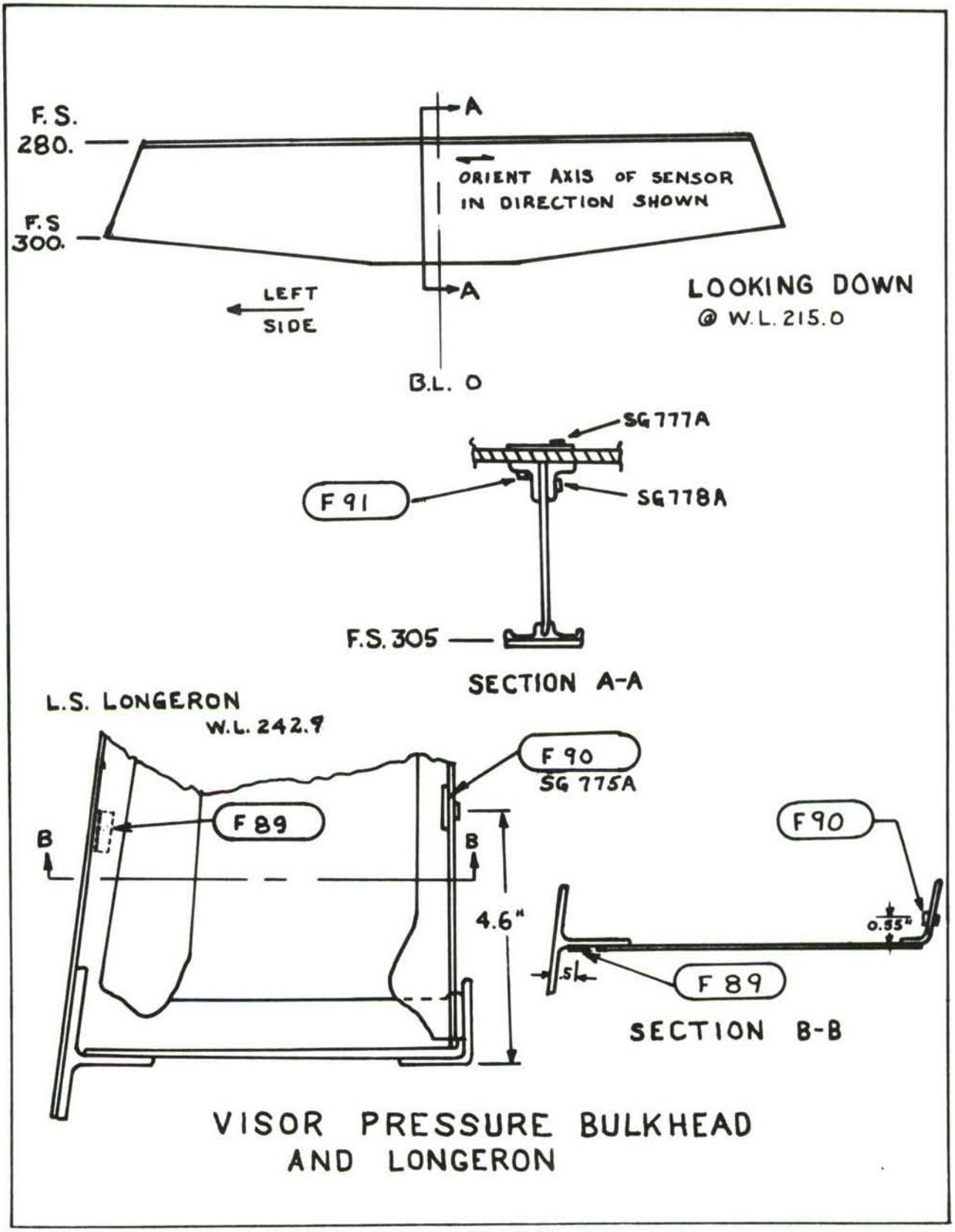

FIGURE 98. SENSOR LOCATIONS ON THE NOSE VISOR

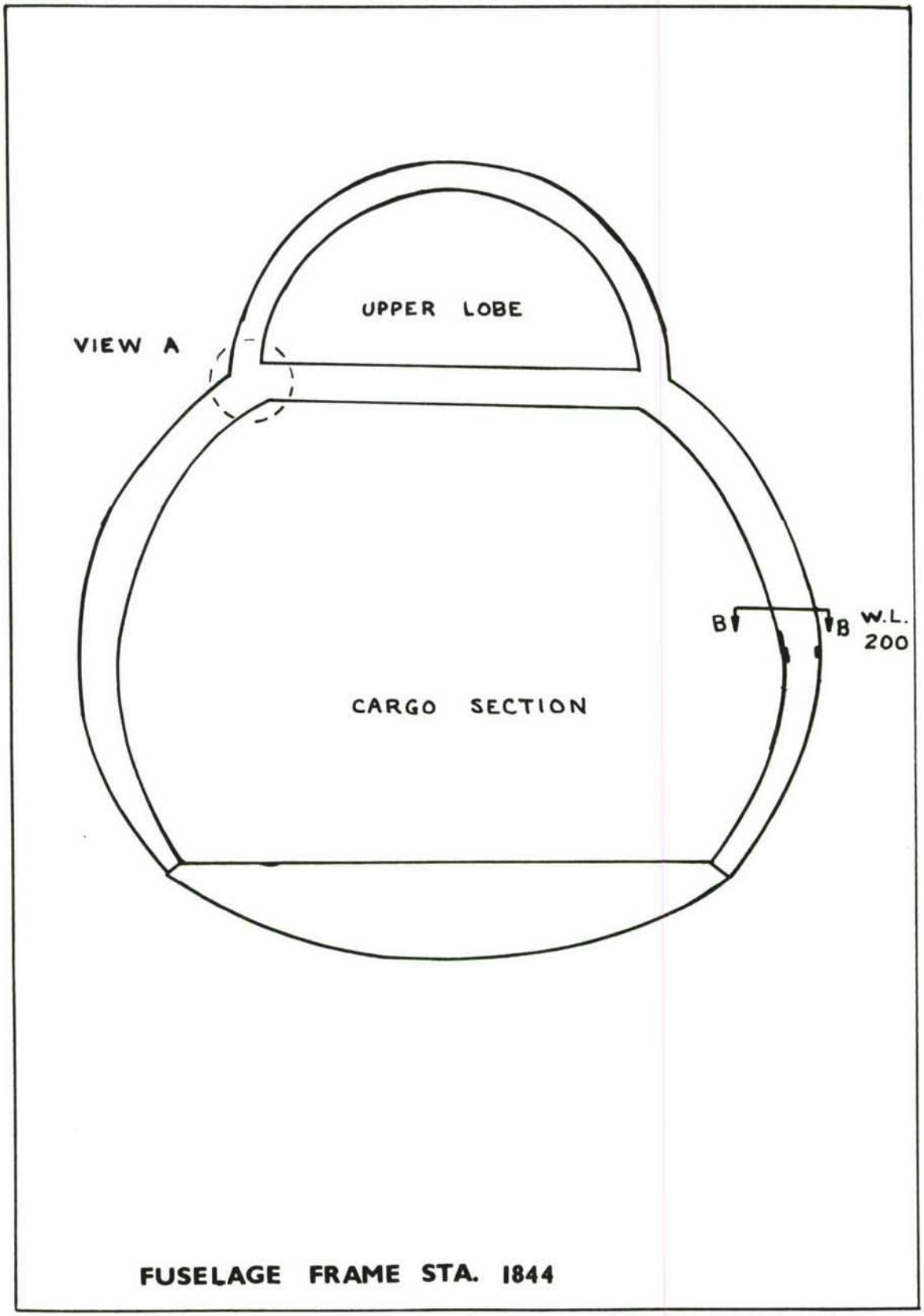

FIGURE 99. GENERAL SENSOR LOCATION AREA AT AFT FUSELAGE STATION 1844

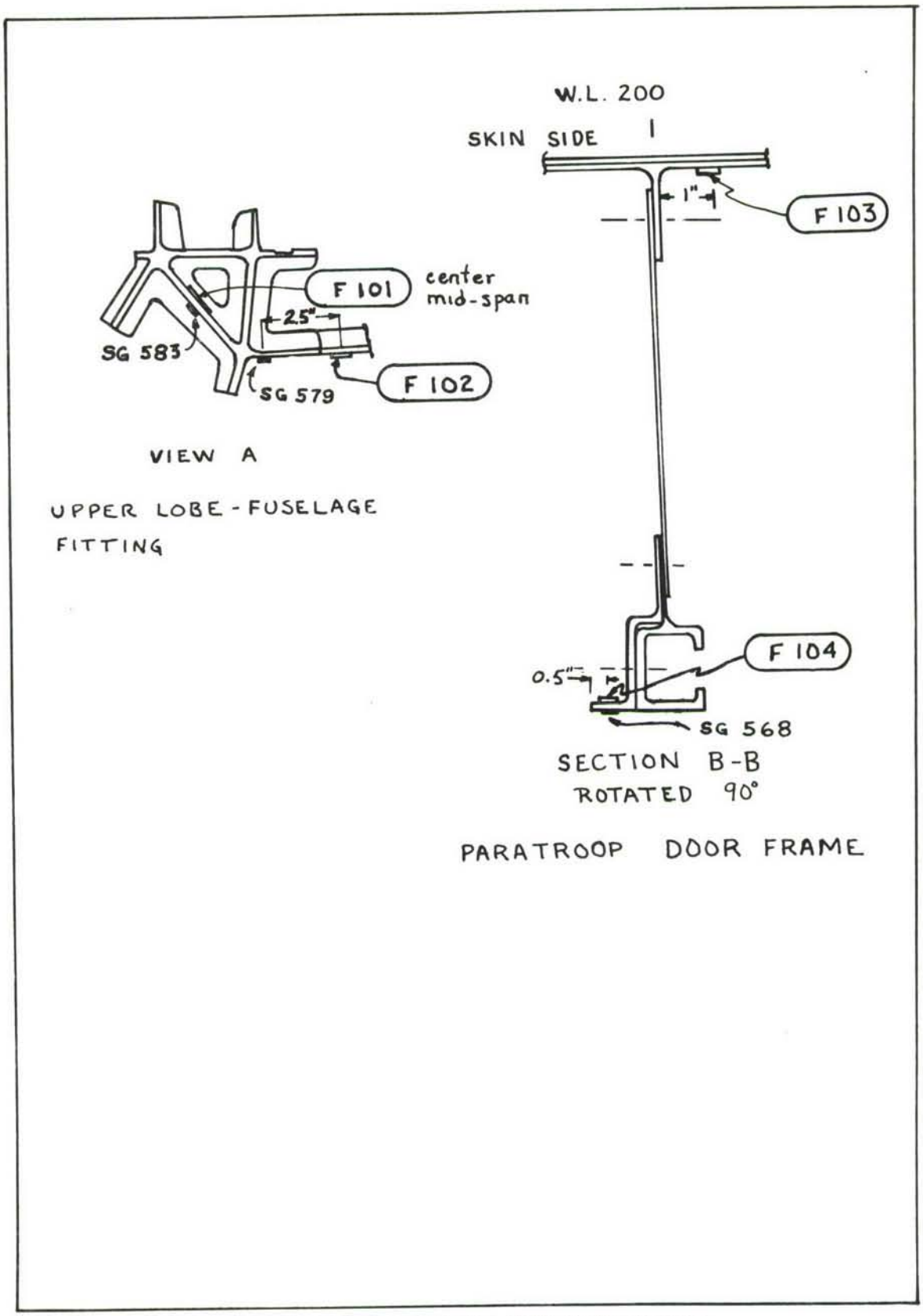

FIGURE 100. SENSOR LOCATION DETAILS AT FRAME STATION 1844

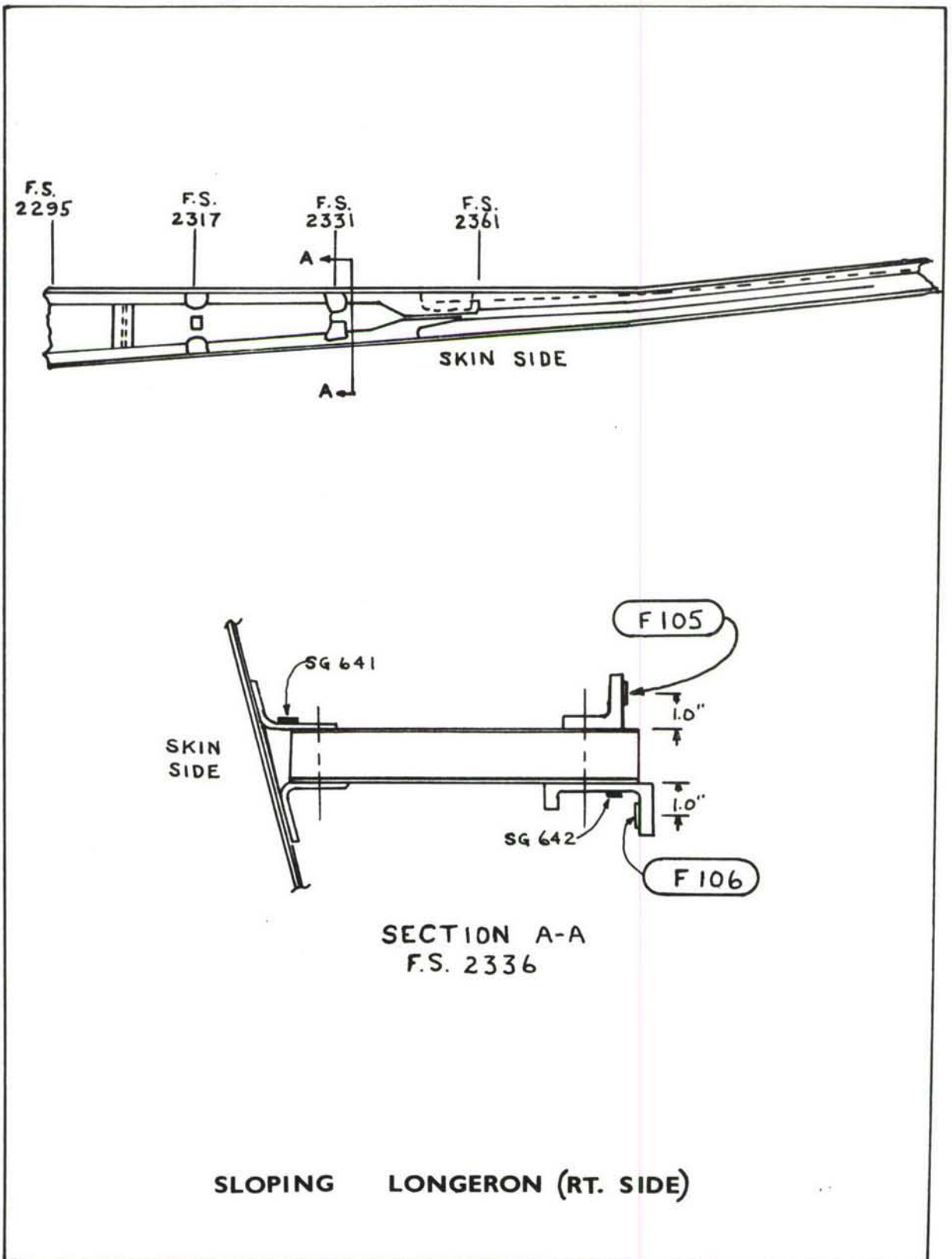

FIGURE 101. SENSOR LOCATIONS ON THE RIGHT HAND SLOPING LONGERON

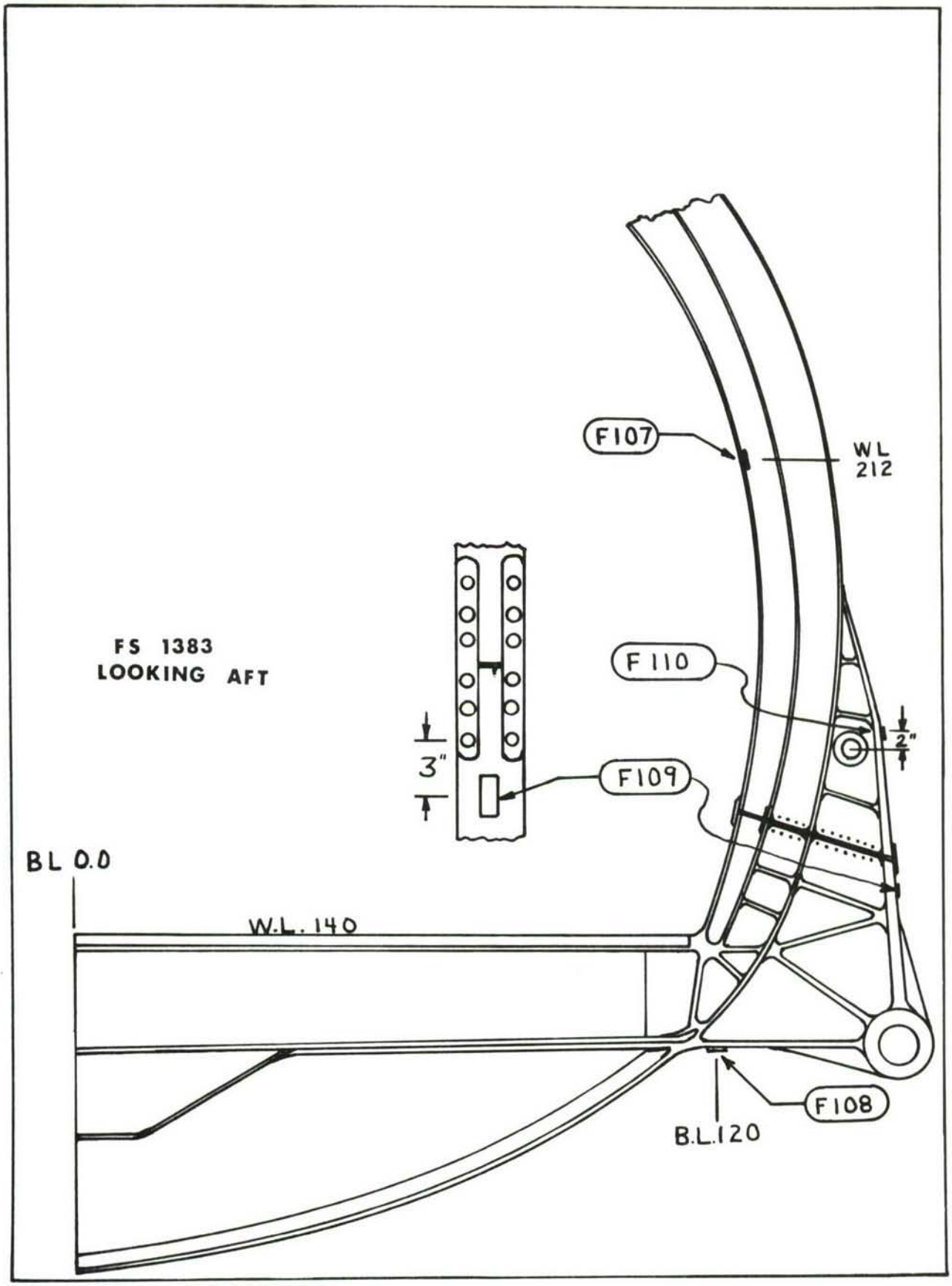

FIGURE 102. SENSOR LOCATIONS ON THE FORWARD LANDING GEAR MAIN FRAME

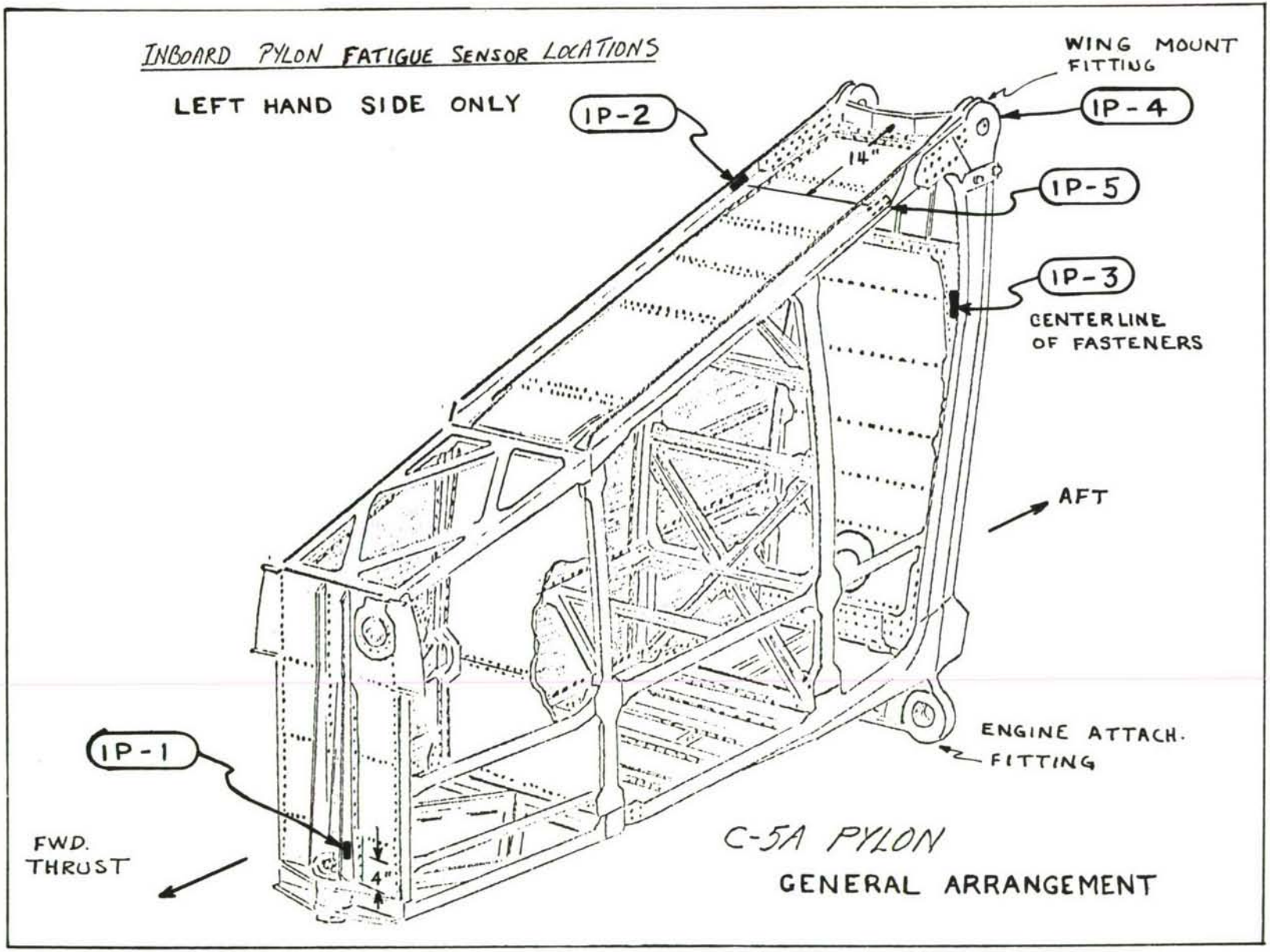

FIGURE 103. SENSOR LOCATIONS ON THE LEFT INBOARD ENGINE PYLON

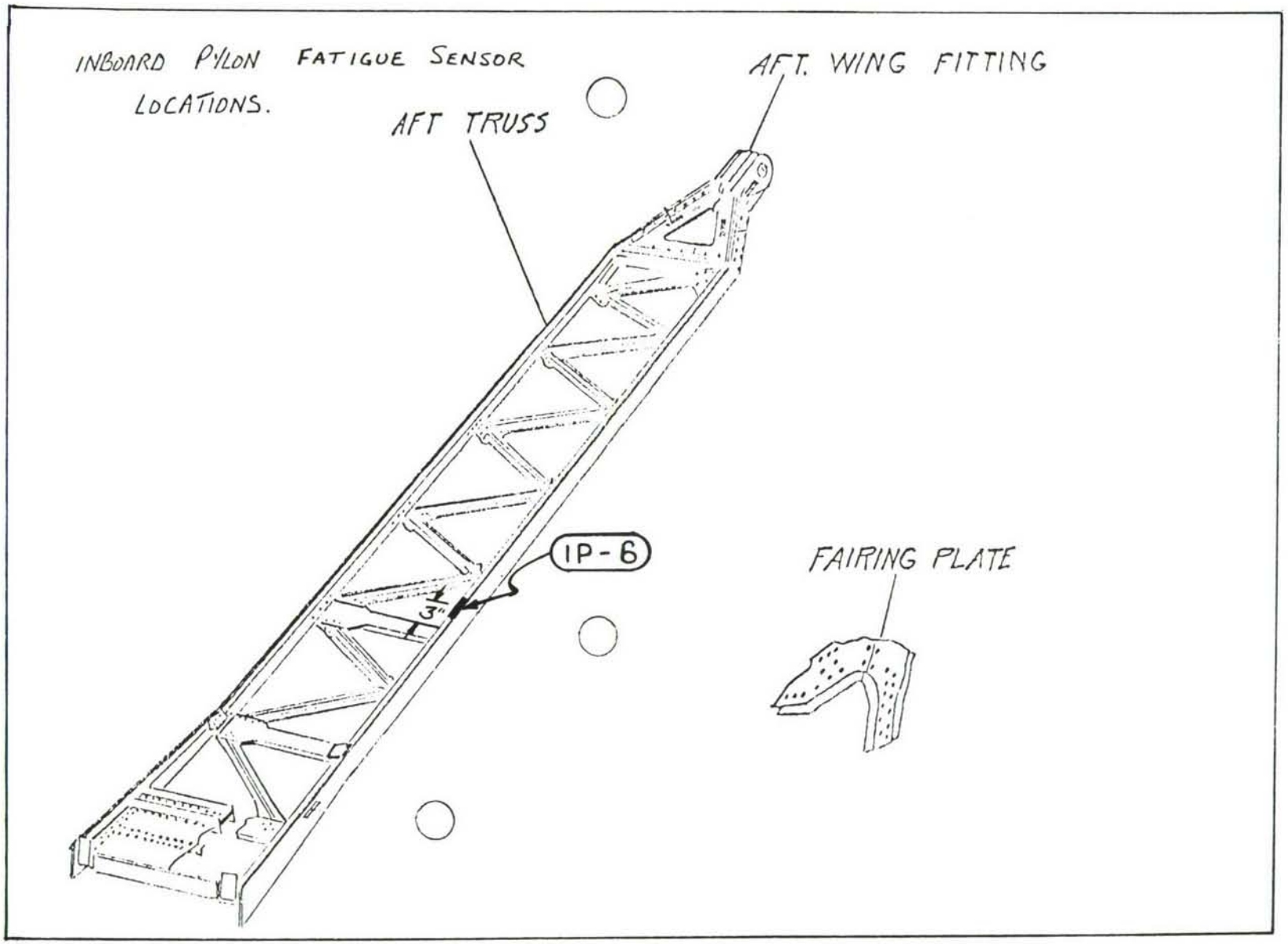

FIGURE 104. SENSOR LOCATED ON PYLON AFT TRUSS FITTING

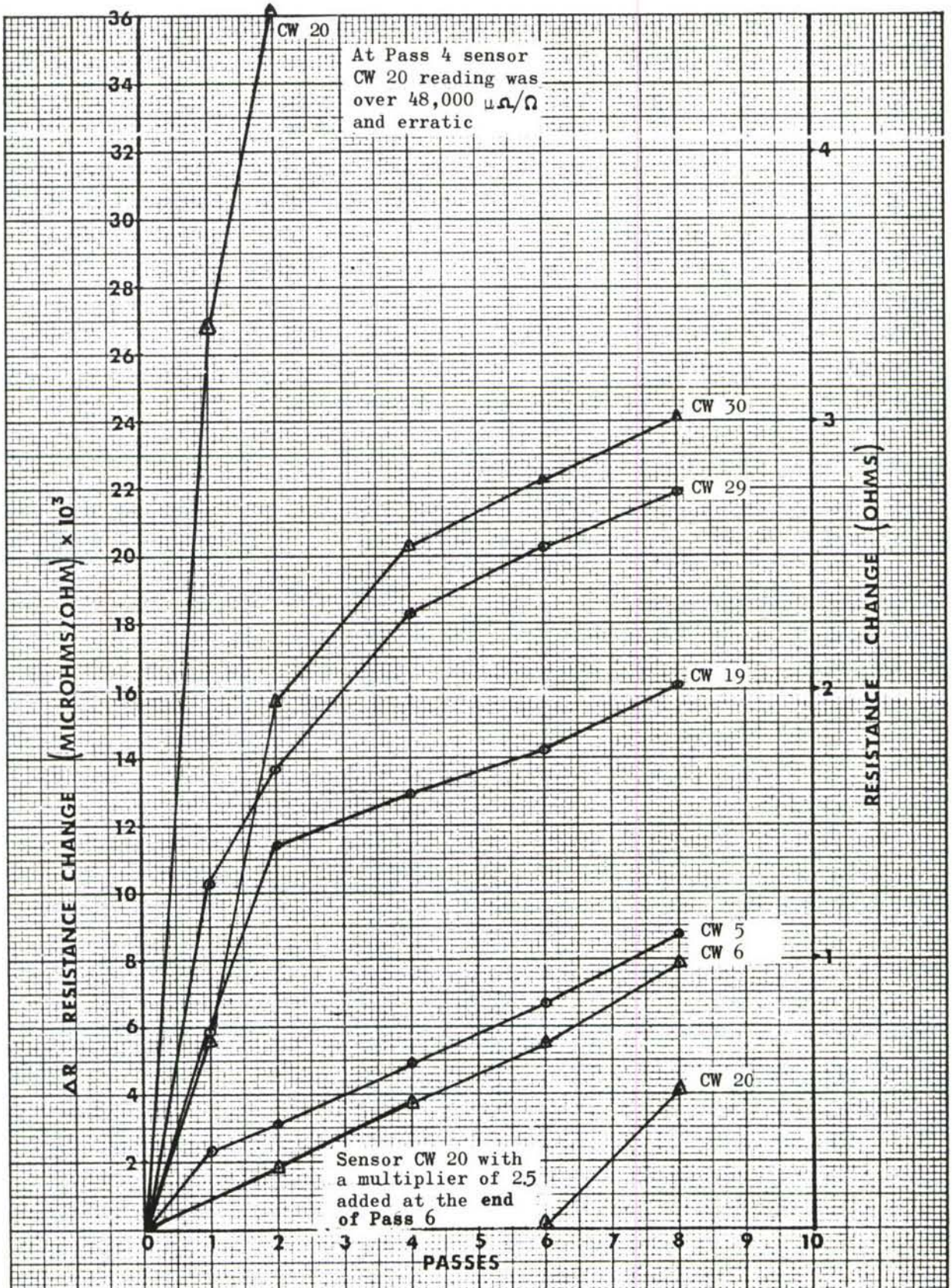

FIGURE 105. SENSOR RESPONSE ON THE CENTER WING AT B.L.0

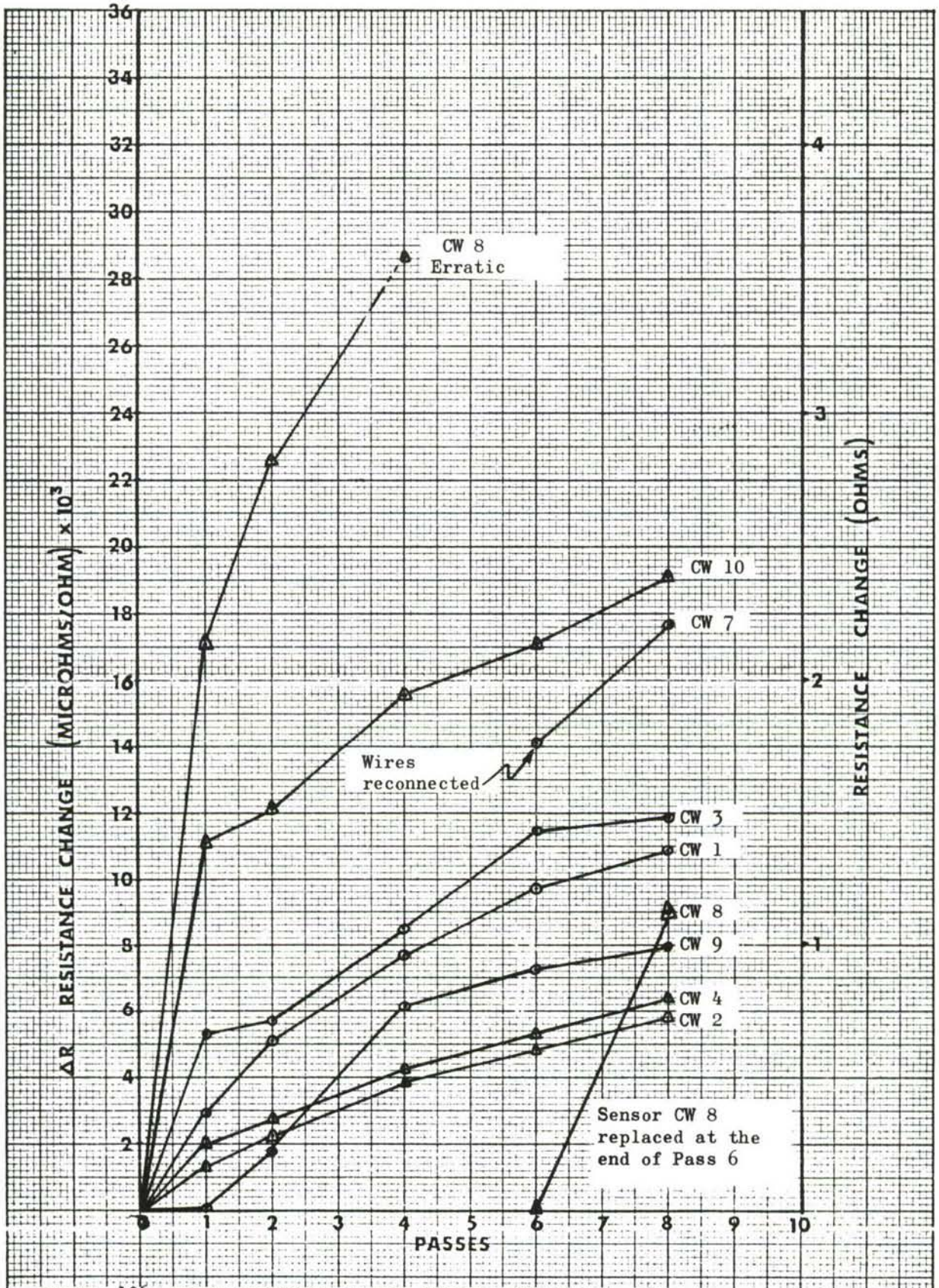

FIGURE 106. SENSOR RESPONSE ON THE CENTER WING AT B.L. 101

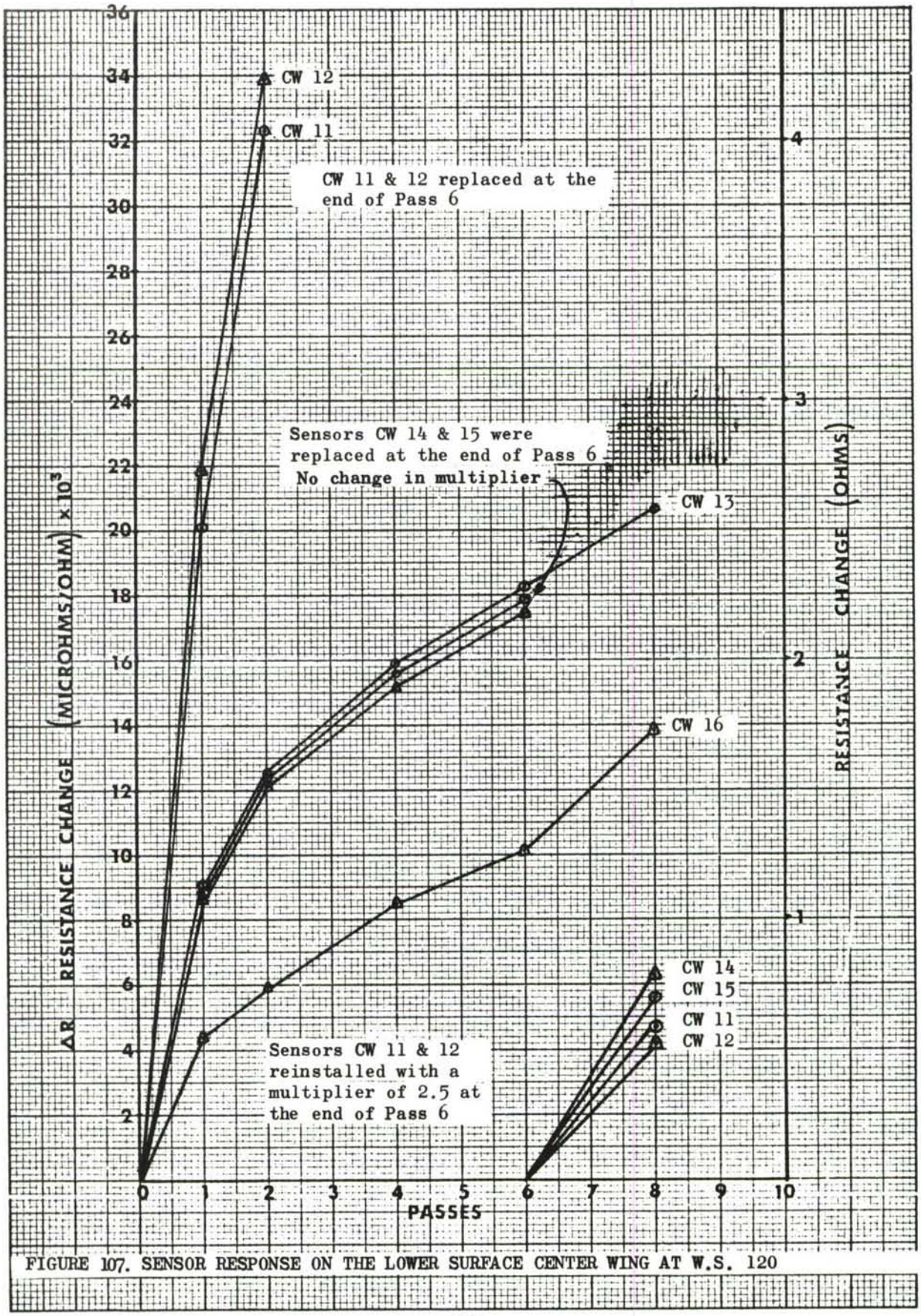

FIGURE 107. SENSOR RESPONSE ON THE LOWER SURFACE CENTER WING AT W.S. 120

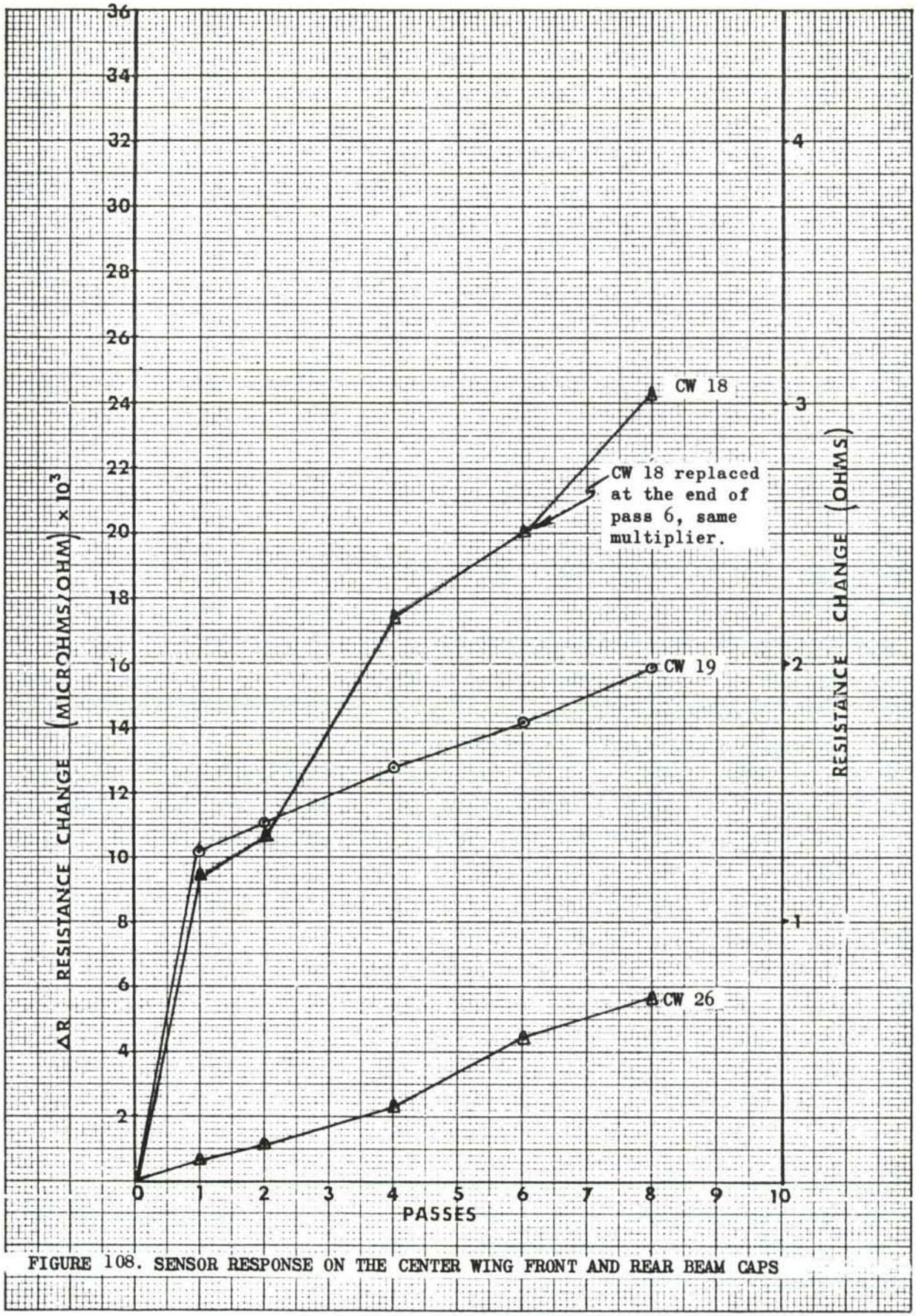

FIGURE 108. SENSOR RESPONSE ON THE CENTER WING FRONT AND REAR BEAM CAPS

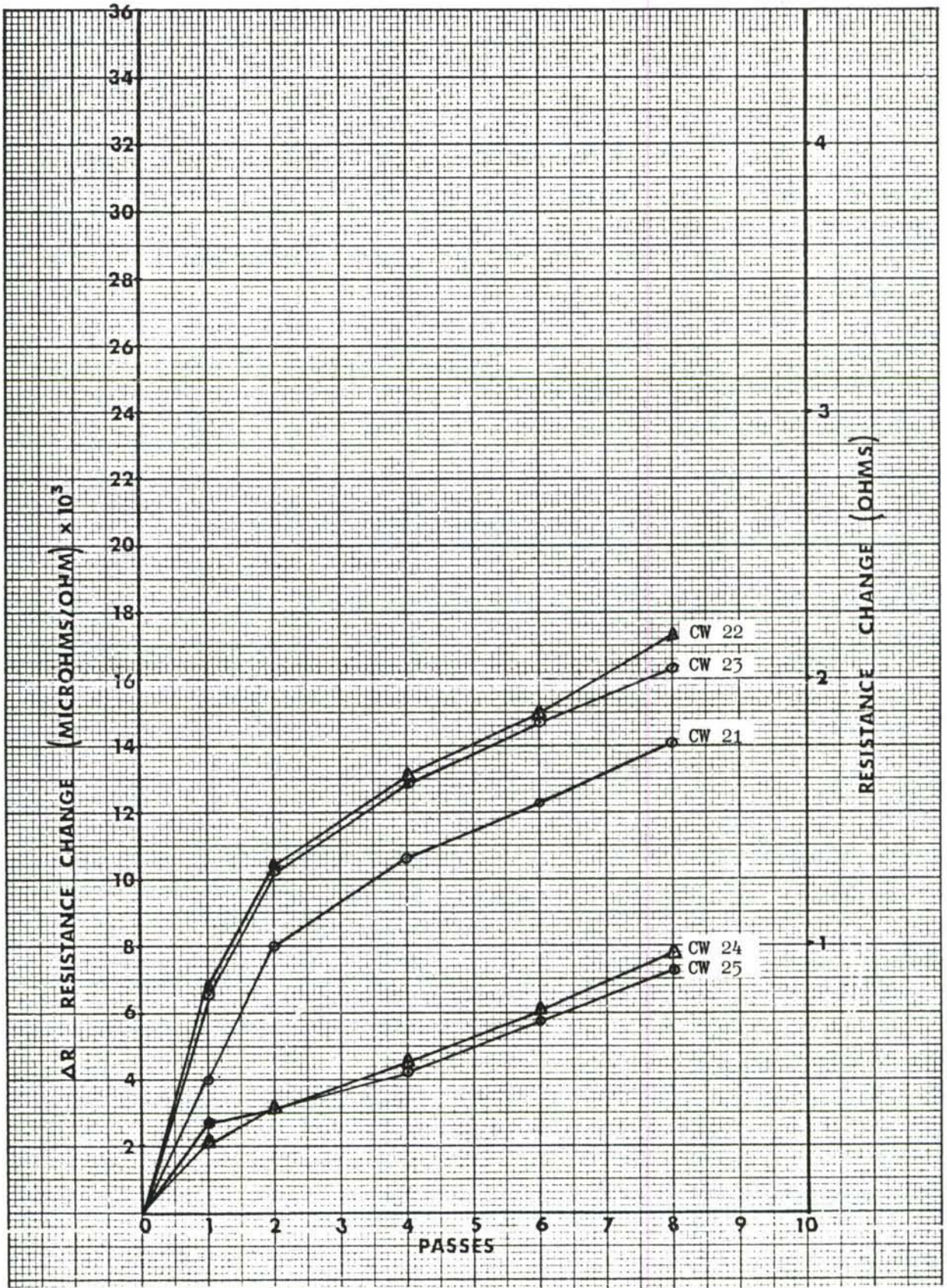

FIGURE 109. SENSOR RESPONSE ON THE UPPER SURFACE CENTER WING AT W.S. 120

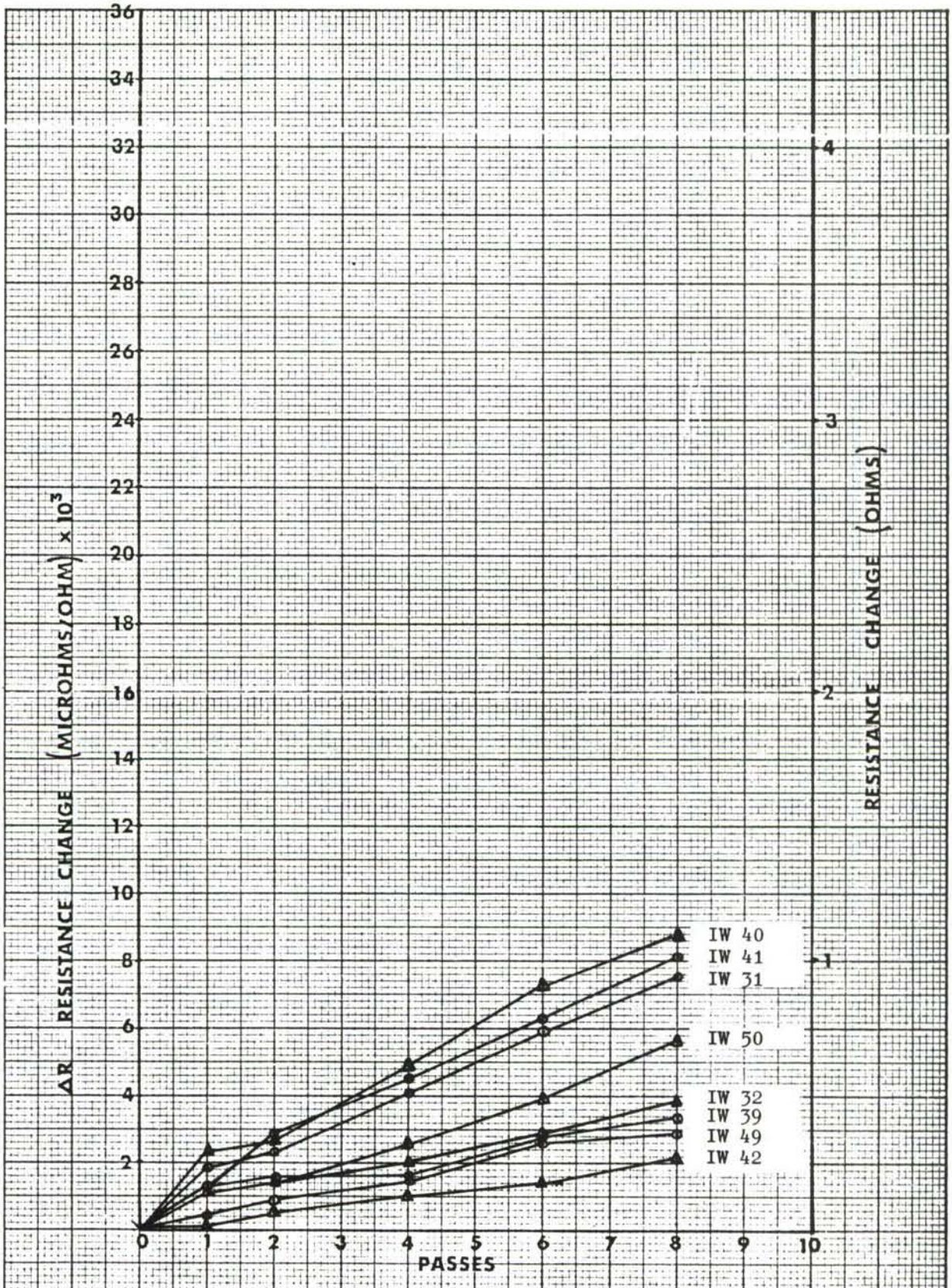

FIGURE 110. RESPONSE OF SENSORS LOCATED ON THE FRONT AND REAR BEAM ATTACHMENT FITTINGS AT W.S. 120

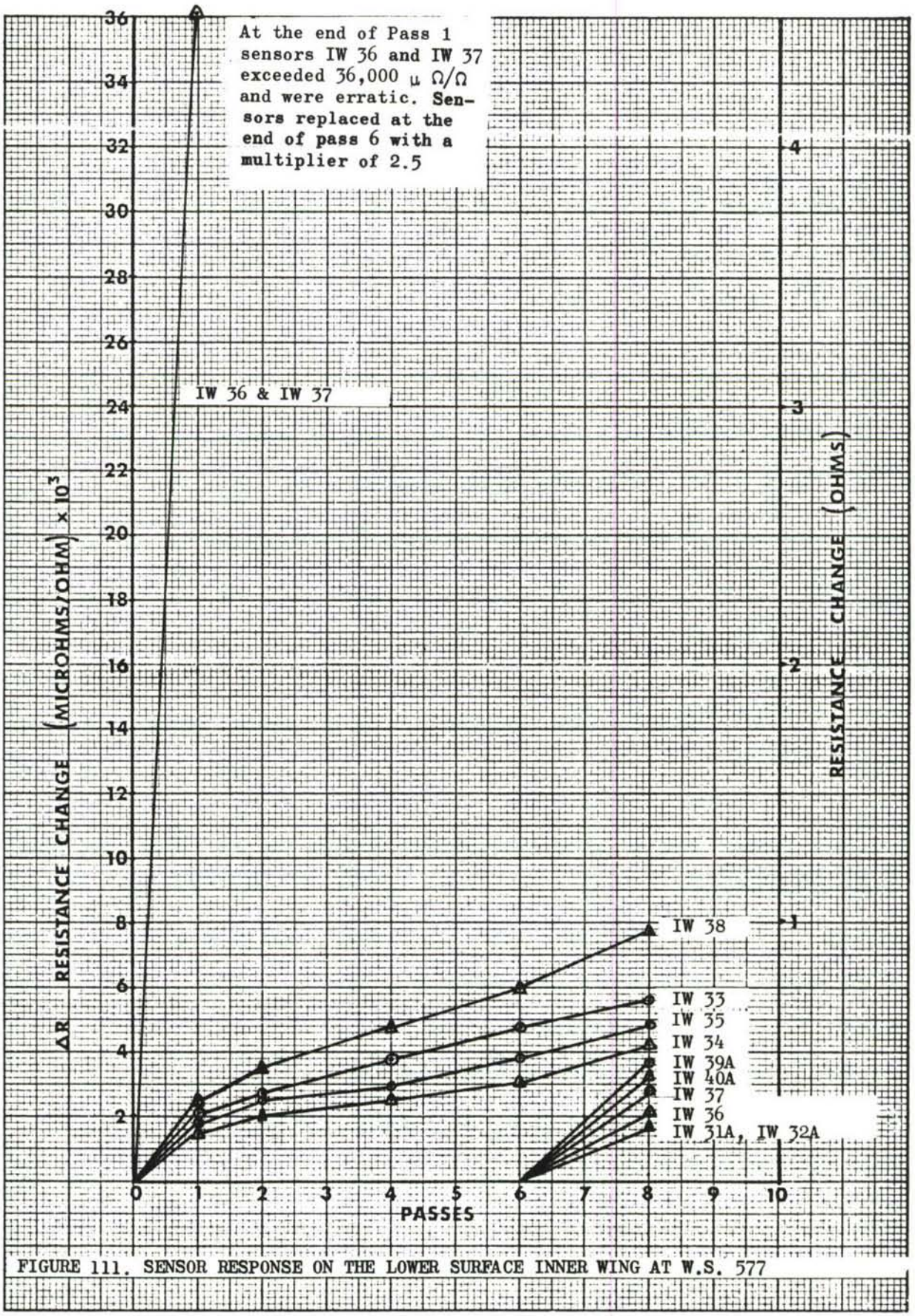

FIGURE 111. SENSOR RESPONSE ON THE LOWER SURFACE INNER WING AT W.S. 577

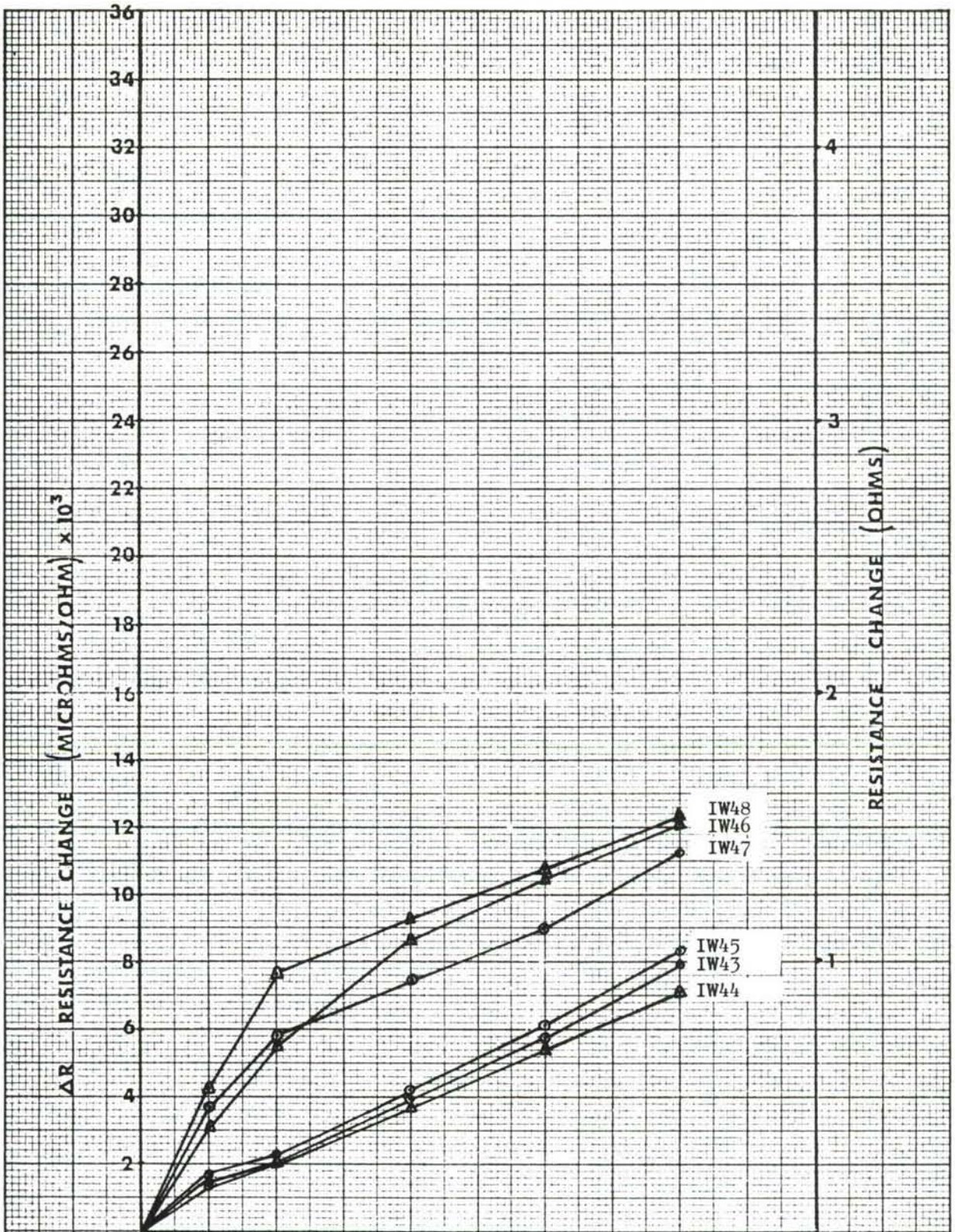

FIGURE 112. SENSOR RESPONSE ON THE UPPER SURFACE INNER WING AT W.S. 577

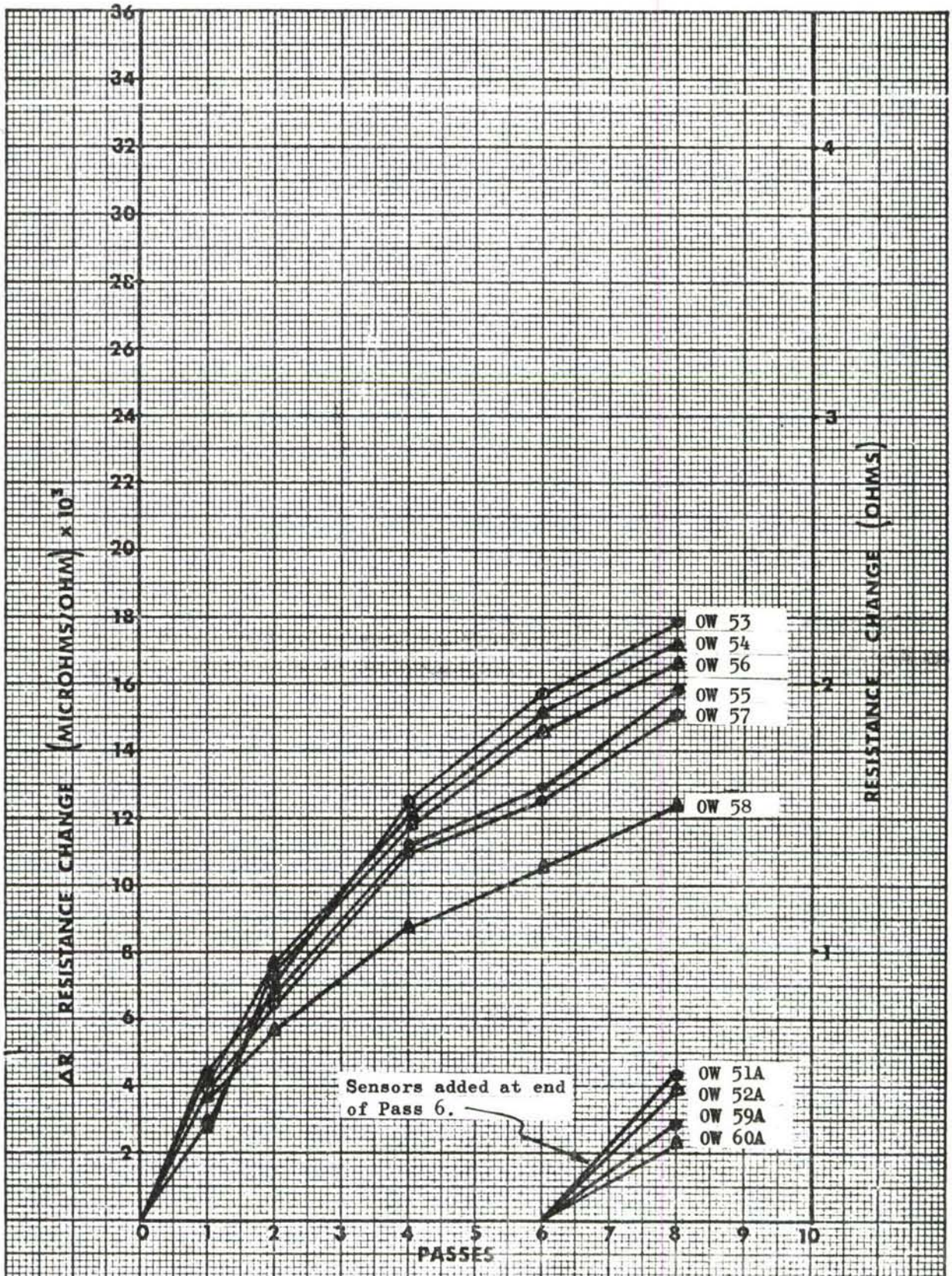

FIGURE 113. SENSOR RESPONSE ON THE UPPER SURFACE OUTER WING W.S. 577

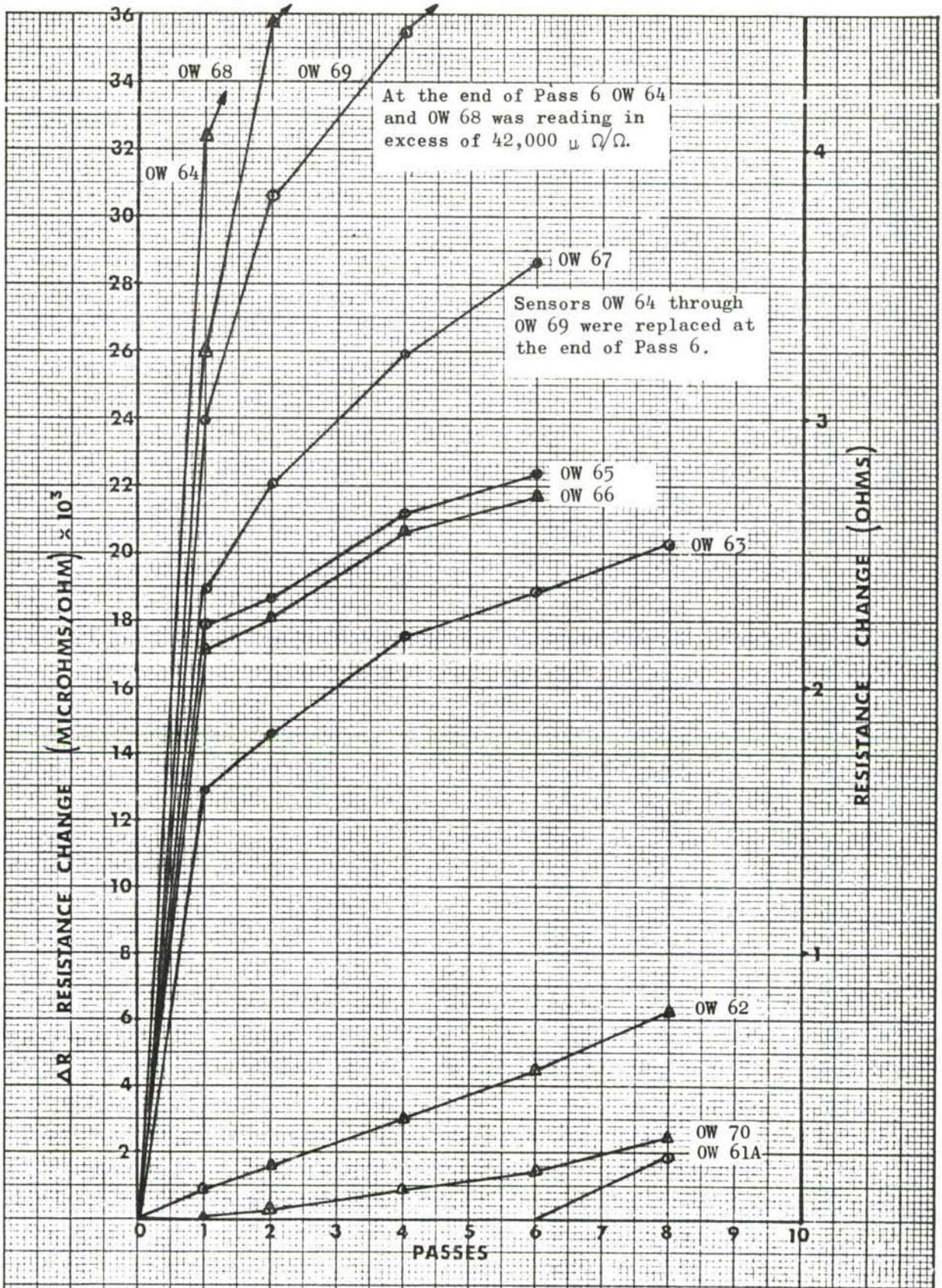

FIGURE 114.. SENSOR RESPONSE ON THE LOWER SURFACE OUTER WING AT W.S. 577

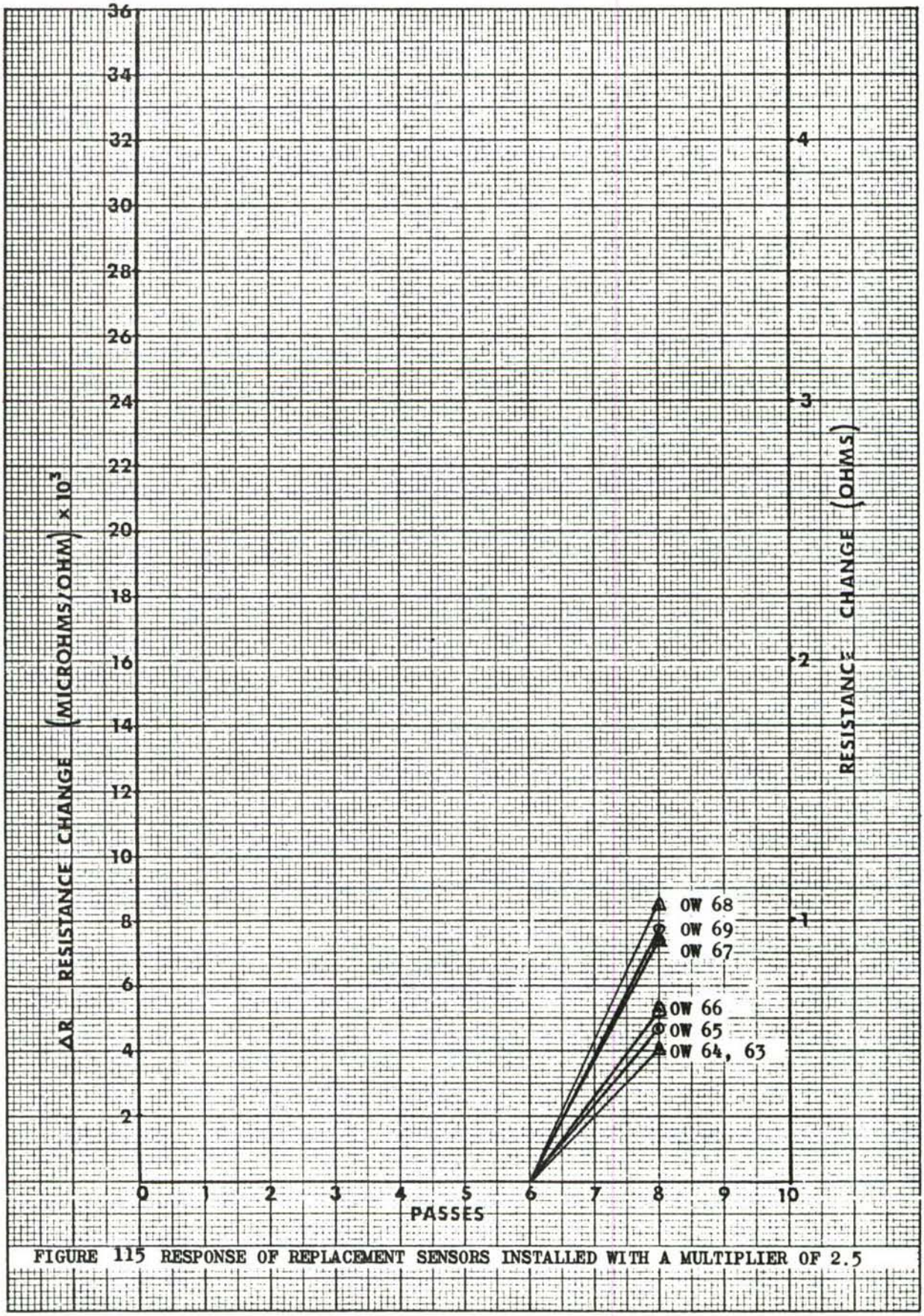

FIGURE 115 RESPONSE OF REPLACEMENT SENSORS INSTALLED WITH A MULTIPLIER OF 2.5

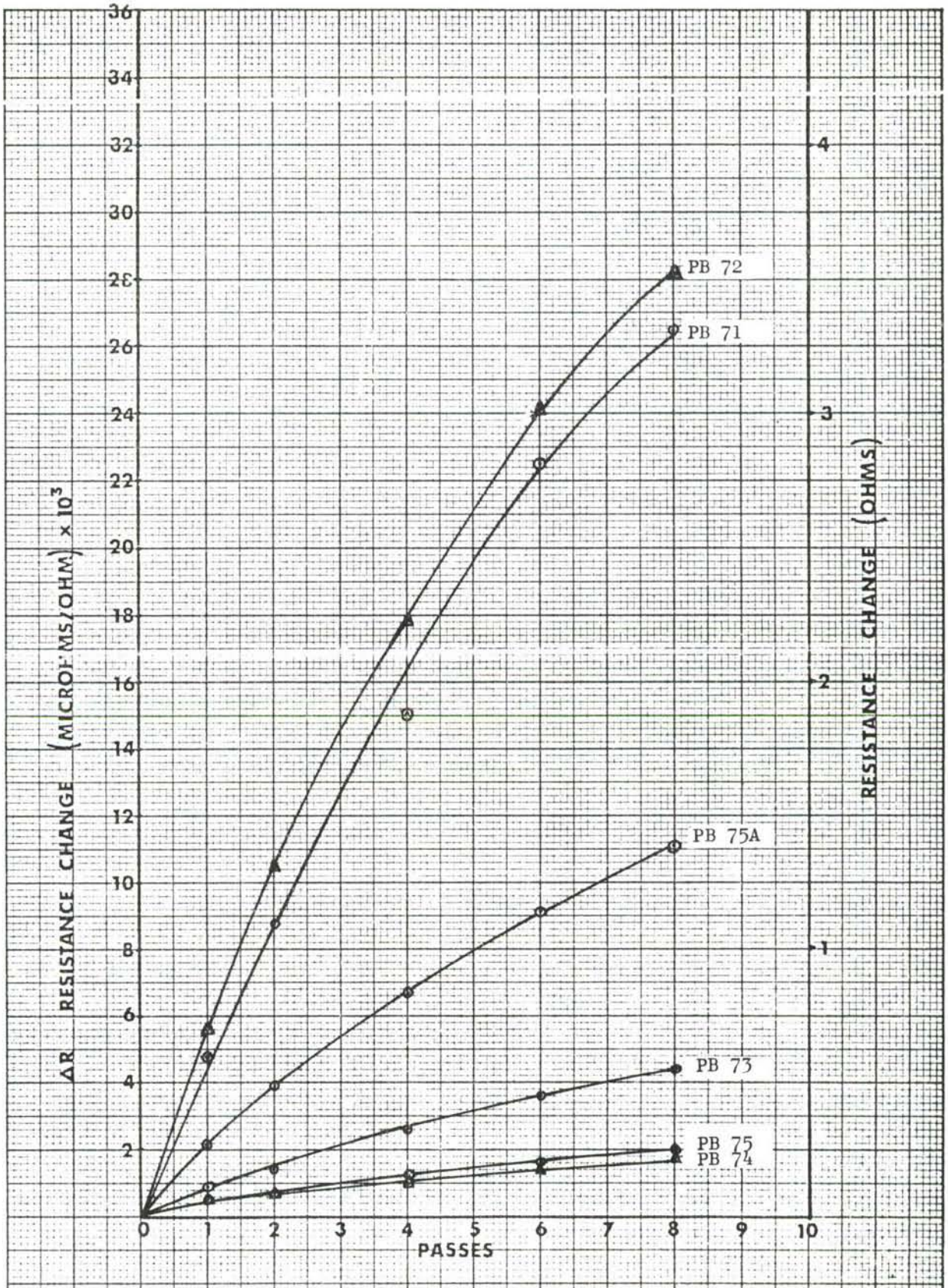

FIGURE 116. SENSOR RESPONSE ON THE AFT FUSELAGE PRESSURE BULKHEAD

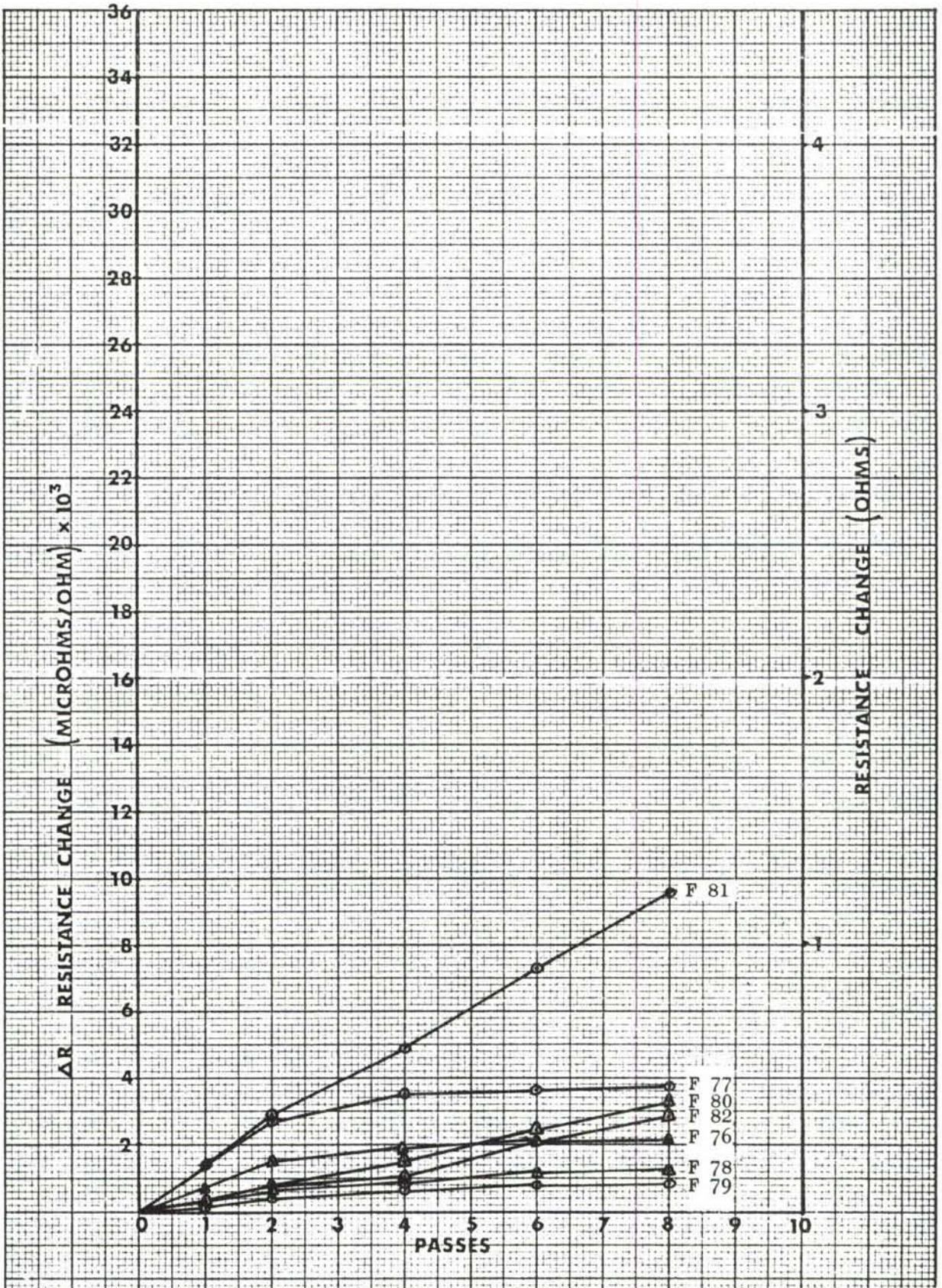

FIGURE 117. SENSOR RESPONSE ON THE FUSELAGE MAIN FRAME AT F.S. 1106

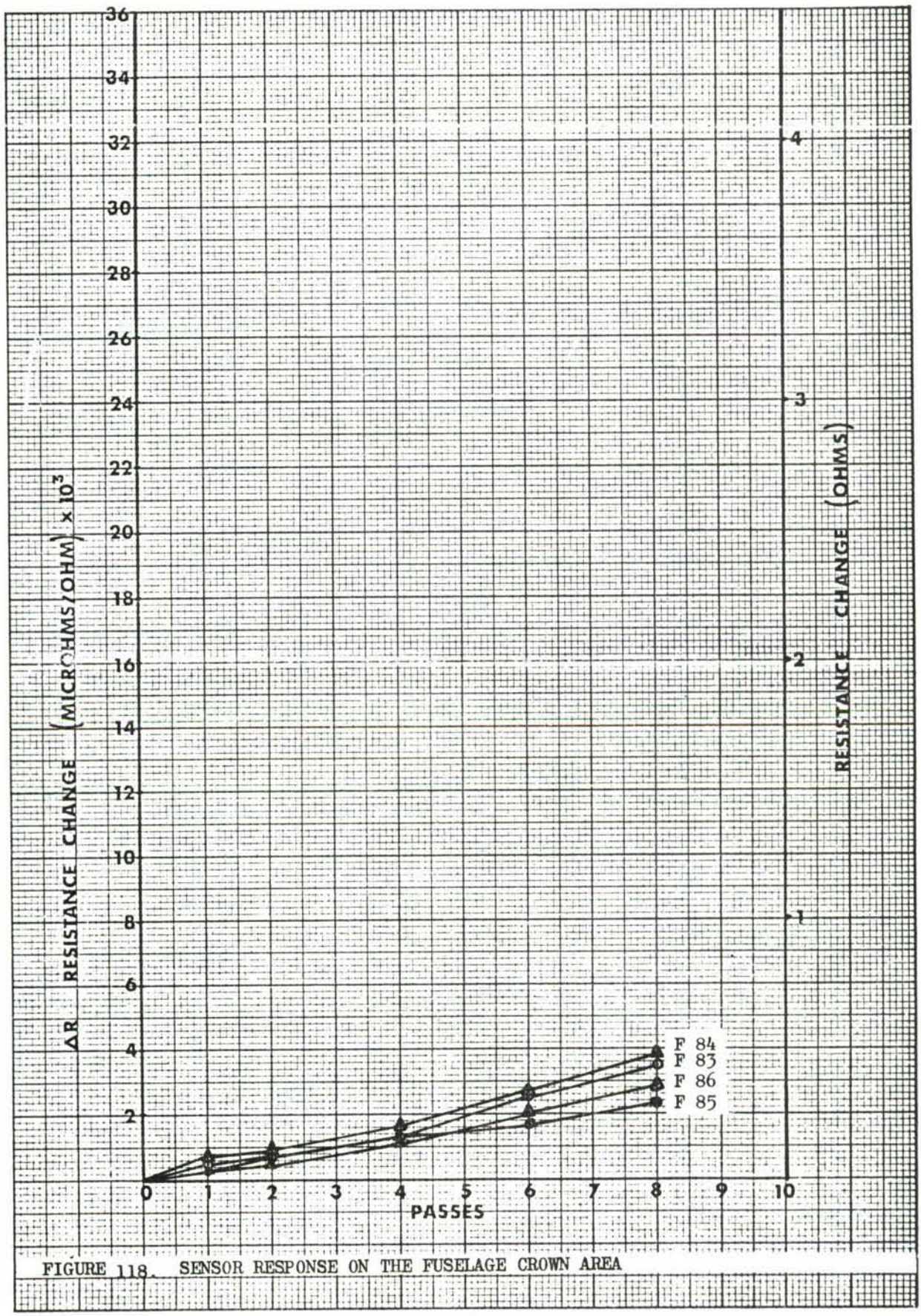

FIGURE 118. SENSOR RESPONSE ON THE FUSELAGE CROWN AREA

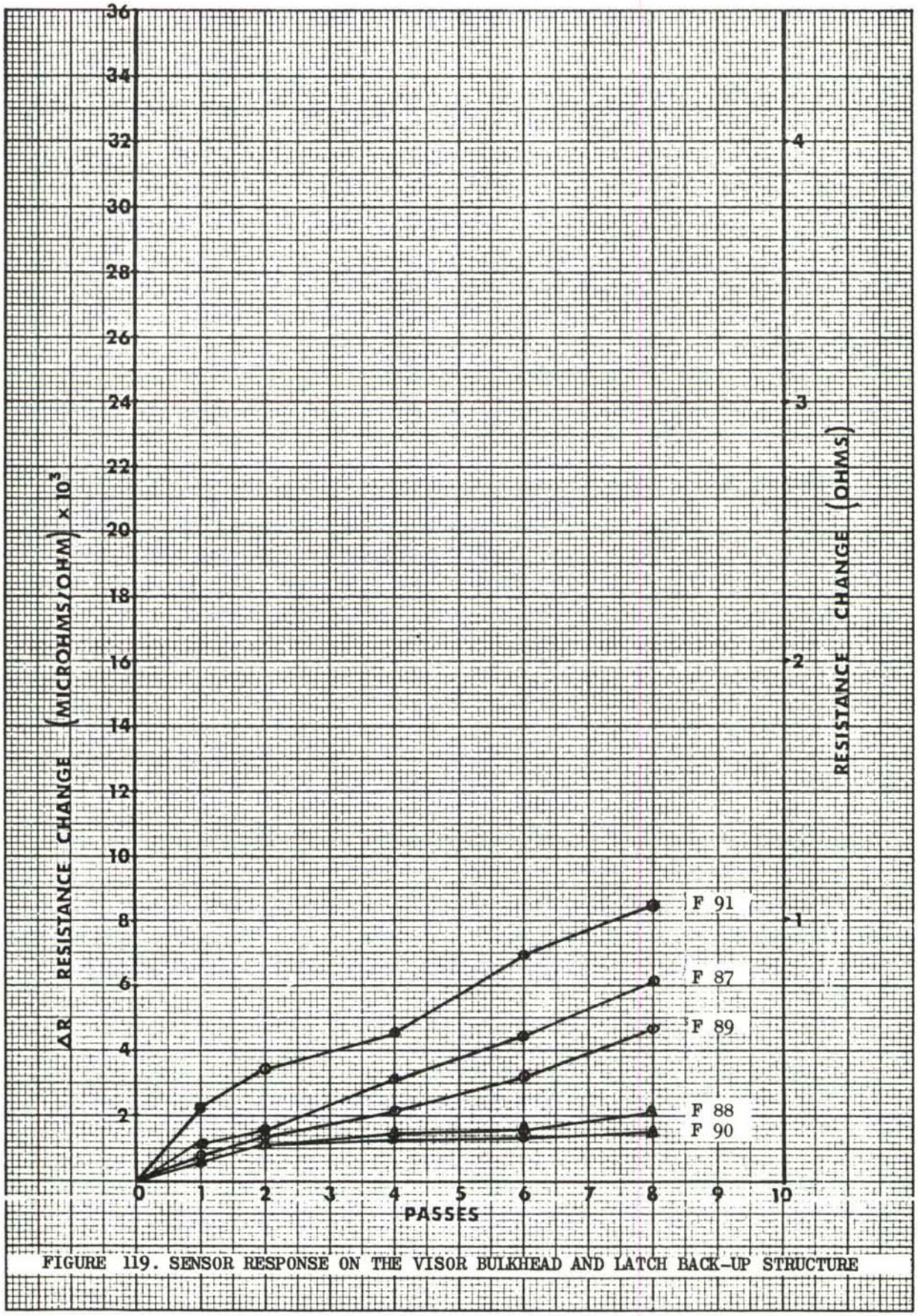

FIGURE 119. SENSOR RESPONSE ON THE VISOR BULKHEAD AND LATCH BACK-UP STRUCTURE

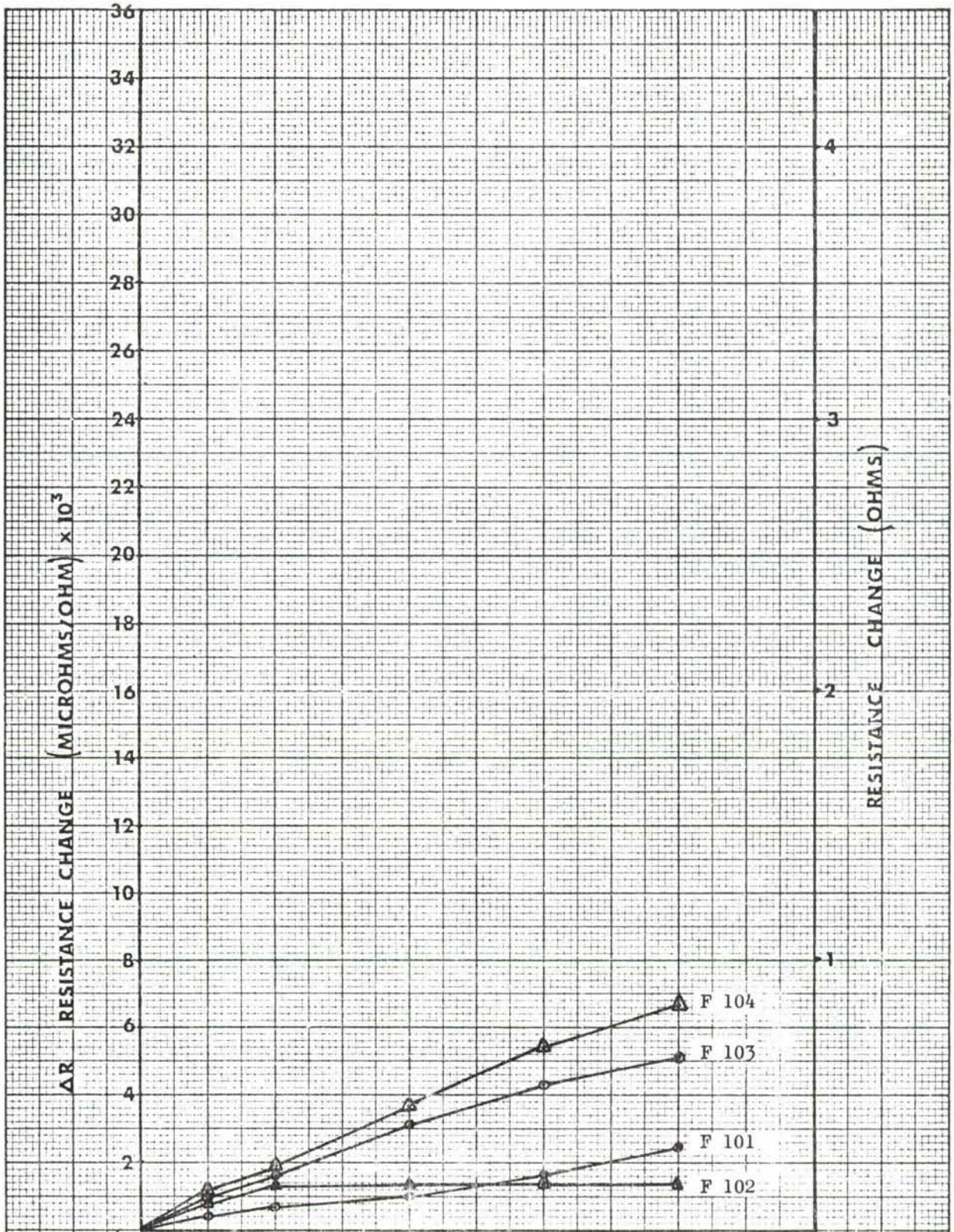

FIGURE 120. SENSOR RESPONSE AT THE AFT FUSELAGE FRAME STATION 1844

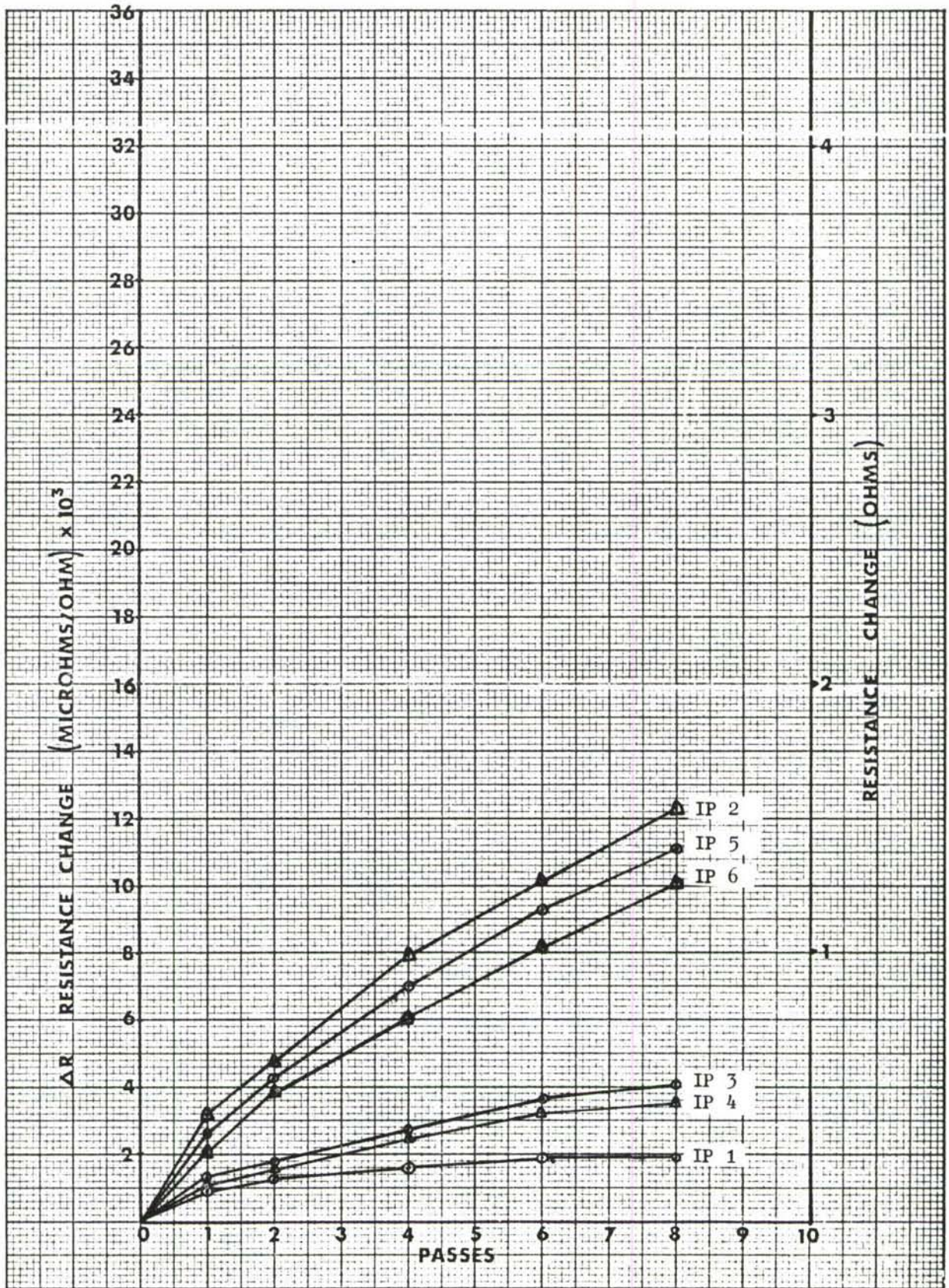

FIGURE 121. SENSOR RESPONSE ON THE LEFT INBOARD PYLON

6.4 DATA EVALUATION

Fatigue testing of the C-5A wing-fuselage specimen has provided a vehicle for continuing the evaluation of the fatigue sensor. Sensor data has been collected for an airplane loading corresponding to 12000 equivalent flight hours. The change in resistance experienced by each of the sensors in this specimen as a function of the number of passes of the test spectrum is depicted in Figures 105 through 121. Location of the sensors may be determined by referring to Figures 72 through 104.

The wing-fuselage specimen is a particularly challenging specimen for the evaluation of the fatigue sensor. A broad range of loading conditions are experienced by the major structural components such as the wing, pylons and fuselage. Under these circumstances, areas of the wing are affected by a combination of load sources, each of which contributes a particular characteristic to the service load spectrum. For example, low slope taxi spectra as well as the normally higher slope gust spectra must be considered along with the ground-air-ground transition cycle which may contribute significantly to the accumulation of fatigue damage. Load sources of particular interest in the case of the pylon include forward and reverse thrust, lateral gust and inertia loads whereas in the fuselage, load sources which combine with fuselage pressurization are of primary concern. It cannot be overemphasized that sensor locations and strain multipliers must be properly selected on the basis of measured or projected local cyclic strain-histories to achieve useful results.

A review of the detail stress analysis and derived stress spectra for pertinent areas of the structure indicated that satisfactory sensor data could be obtained using a constant strain multiplier throughout the wing-fuselage specimen. As a result, the initial sensors installed on the wing-fuselage specimen were applied on shims intended to develop a theoretical strain multiplier of 3.0. Variations in stress levels caused by load distribution effects were used in combination with the strain multiplier to achieve a broad range in the change of sensor resistance corresponding to a given period in the service life of the airplane. The single level multiplier provides a potential for a direct qualitative comparison of relative cyclic load exposure simply by observing the magnitude of the change in resistance of the various sensors. These comparisons, however, must recognize certain limitations and characteristics of the sensor such as the threshold sensitivity of the system and the sensor response to compressive loading. For best results, comparisons should be limited to areas that are susceptible to common sources of fatigue damage where the primary difference in the change in resistance of a group of sensors is caused by variations in normal cyclic stress levels. Due to these and other factors, fatigue damage cannot be assumed to be directly proportional to relative values of sensor resistance change.

TABLE VIII

SENSORS REQUIRING REPAIRS OR REPLACEMENTS

The sensors requiring repairs or replacement during the program and the corrective action taken are tabulated as follows.

CHANNEL NUMBER	ORIGINAL MULTIPLIER	TYPE OF DEFECT	FINAL MULTIPLIER	CORRECTIVE ACTION
CW 7	3	A	3	Reconnected Wires
CW 8	3	B	3	Replaced
CW 11	3	C	2.5	Replaced
CW 12	3	C	2.5	Replaced
CW 14	3	F	3	Replaced
CW 15	3	F	3	Replaced
CW 18	3	F	3	Replaced
CW 20	3	B, C	2.5	Replaced
IW 36	3	B, D	2.5	Replaced
IW 37	3	D	2.5	Replaced
OW 64	3	D	2.5	Replaced
OW 65	3	F	2.5	Replaced
OW 66	3	F	2.5	Replaced
OW 67	3	F	2.5	Replaced
OW 68	3	C	2.5	Replaced
OW 69	3	E	2.5	Replaced

The nature of the defect or discrepancy requiring corrective action is detailed in the following legend.

A - open circuit

B - erratic operation

C - overranged by the end of pass 4

D - overranged between pass 1 and 2

E - overranged by the end of pass 6, first major shutdown inspection

F - steep slope of sensor response curve indicating a high rate of resistance change and probable overranging prior to one lifetime.

TABLE IX

SENSOR ADDITIONS

Additional sensors were installed after the completion of 9000 cyclic test hours (pass 6) and during the first major shut down inspection period. It was expected that these additional sensors at W.S. 577 splice joint would better define the distribution of totalized strain in this critical area.

CHANNEL NUMBER	MULTIPLICATION FACTOR	GENERAL AREA
IW31A	3	Lower Surface Rear Beam Cap
IW32A	3	Lower Surface Rear Beam Cap
IW39A	3	Lower Surface Mid Beam Run-out
IW40A	3	Lower Surface Mid Beam Run-out
OW51A	3	Upper Surface Rear Beam Cap
OW52A	3	Upper Surface Rear Beam Cap
OW59A	3	Upper Surface Front Beam Cap
OW60A	3	Upper Surface Front Beam Cap
OW61A	3	Lower Surface Rear Beam Cap

TABLE X - SENSOR DATA AT THE END OF PASS 6

ΔR MICROHM/OHM

LOCATION (1)	CENTER WING						INNER WING		OUTER WING	
	W.S. 0		W.S. 101		W.S. 120		W.S. 577		W.S. 577	
	UPPER SURFACE	LOWER SURFACE	UPPER SURFACE	LOWER SURFACE	UPPER SURFACE	LOWER SURFACE	UPPER SURFACE	LOWER SURFACE	UPPER SURFACE	LOWER SURFACE
Rear Beam	20200	22200								
1-2					12300	(0-R)				
2-3										4400
3-4					14900	(0-R)				
5-6					14700	18300	5700	4800		18800
6-7							5400	3000		(0-R)
Aux. (2) Beam	14200	(0-R)								
7-8									15600	
8-9									15100	
9-10							6100	3800		
12-13									12900	22300
Mid (3) Beam										
13-14									14500	21600
15-16							10400	(0-R)		28600
16-17										(0-R)
17-18					6100	17400	9000	(0-R)	12500	
18-19									10500	
20-21										(0-R)
21-22					5700	17900				
22-23							10700	6000		
25-26			4800	5300						
26-27										
32-33			9700	11500						
40-41						10100				
Front Beam	6700	5500								

NOTES: (1) SPAR CAPS OR RISER NUMBER
(2) CENTER WING ONLY
(3) INNER WING ONLY
(0-R) OVERRANGED

In selecting the sensor locations on the wing, attention was given to the variation of spanwise stress across the wing chord to regulate the sensor response. The airplane stress analysis and strain gage data indicate that in the center wing and portions of the inner wing, the higher stress levels occur in the covers of the aft torque box. As the single cell outer wing is approached, the stresses tend to peak closer to where the wing thickness reaches a maximum dimension. These trends are consistent with normal wing sweep effects and beam bending theory. Table X represents a summary of data for the wing surface sensors which show general agreement with the established trends in stress distribution. Resistance values are shown for a point in time corresponding to the conclusion of six passes of the test spectrum, or the equivalent of 9000 flight hours. Selection of this time interval permits comparison of sensor data based on a common level of strain multiplier. As the test progressed beyond this point, sensors indicating a high rate of resistance change were replaced and the strain multipliers were reduced in most of these cases (Table VIII).

Observation of the data in Figures 105 through 121 show that a broad range of sensor resistance change can be experienced across the chord of the wing at various wing stations. It can be seen that adequate sensitivity can be achieved for fatigue monitoring purposes with a strain multiplier of 3.0 by properly selecting the placement of the sensors. The demonstrated sensitivity and reproducibility of the system is dependent on the achievement of the desired strain multiplying effect and the accuracy in duplicating the location of the sensors in each airplane. The influence of the latter condition can be alleviated by selecting locations relatively free of stress gradients. Based on the results of the program, as shown in Figures 105 through 121, suitable areas are available from this standpoint. For example, the lower surface data indicates that uniform conditions prevail in the area bounded by sensors CW 13, CW 14 and CW 15 and, at a higher level of resistance change, in areas bounded by CW 11 and CW 12. Either location would be suitable provided the proper level of strain multiplier is selected. In the case of the upper surface, sensors CW 22 and CW 23, and CW 24 and CW 25 indicate sufficient uniformity in sensor response to support the useful application of the sensor system. Chordwise data at other sections of the wing show similar results. The overranged condition of some of the sensors is due to higher than design stresses or strain multipliers that amplify the nominal strains beyond desired values. Previous studies on sensor response to constant amplitude fatigue loading have shown that large differences in resistance can occur with relatively small differences in load level for a given number of cycles.

Potential differences in sensor response for duplicate installations can be observed by considering the response of sensors CW 14 and CW 15 in in Figure 107. The sensors were replaced after pass six with the same type of sensor that was initially installed at these locations and the strain multiplier was maintained at a theoretical value of 3.0.

It can be observed that the change in sensor resistance for the initial pass of the spectrum experienced by the two groups of sensors differ considerably. The apparent lack of reproducibility of results in these cases is incompatible with the scatter assessments previously conducted (Section 2.3) on the basic sensor. A number of reasons may be hypothesized regarding the cause of these inconsistencies.

After initial sensor zero's were taken, the check out of the servo loading equipment required experimental load applications to the structure for the sole purpose of checking the electronic and hydraulic equipment. Also numerous reruns of the static strain surveys as well as "false starts" at cycling contributed to the application of additional loads over and above those required for the first pass. The effect of these initial check out loads upon the resistance change of the sensor were therefore "added in" with the sensor resistance change for the first pass cyclic loads. Discrepancies of this type and magnitude would not be expected on service aircraft and the proposed correlation analyses described in Section 2.4 would consider the variations present in the baseline calibration airplane.

The influence of a change in the level of the strain multiplier on the response of the sensor is aptly illustrated in Figure 105, 107, 111, 114, and 115. Whereas in these cases the theoretical strain multiplier was reduced from 3.0 to 2.5 in order to slow down the change in resistance of the sensors with repeated load exposure, the strain multiplier can be increased to obtain the opposite result. A visual examination of sensors IW36 and IW37 revealed that these sensors had been installed partly in the "joggle" area of the W.S. 577 splice joint resulting in exposure to bending strains. These sensors were over ranged very early in the program but could not be replaced until a schedule shutdown period at the end of pass six. The replacement sensors were located clear of the joggle area using a multiplier of 2.5 which produced a slope consistent with anticipated behavior (Fig. 111). A review of the sensor data taken on large fittings and in many areas of the fuselage indicate that the analytically justified suitability of a strain multiplier of 3.0 was generally inadequate for these areas of structure. Figure 118 shows the response of sensors located to reflect the combined effects of longitudinal stresses due to fuselage pressurization and fuselage bending loads. The combined effects were obviously less than anticipated. A similar condition prevailed in the case of the fuselage main frames (Fig. 117) which support the wing and main landing gear. Sensors in these areas are of particular interest since they respond to the interactive effects of the ground and flight loads concentrated in these elements of structure. A comparison of sensor response curves illustrated by Figure 117 and Figure 120 shows that improved results are obtained in the case of the frame at fuselage station 1844. The majority of the sensors on the main frame at fuselage station 1106 have reached an apparent condition of reduced sensitivity whereas sensors F 103 and F 104 at station 1844 continue to experience a change in resistance with applied cyclic loads. The use of a dynamic analysis technique to verify sensor bond integrity as discussed in Section 5.7, did not reveal any deterioration of the bond. Improved sensitivity, however, could be achieved in those areas with a higher strain multiplier.

TABLE XI

SUMMARY OF FATIGUE DAMAGE AND RELATED SENSOR INFORMATION

COMPONENT	GENERAL AREA	DAMAGE ITEM NUMBER	FIGURE NUMBER	SENSOR NUMBER	ΔR μΩ/Ω	CYCLIC TEST HOURS	CLASSIFICATION
No. 3 Pylon	Pylon Rib W.S. 481	3	122	IP2 IP5 IP6	10,170 9,210 8,050	9000	Minor
Fwd. Fuselage	Stringer at F.S. 452	63	123	F87 F91	4,420 6,970	9000	Minor
Fuselage	Stringer at F.S. 1843	64	124	F86	2,010	9000	Minor
Inner Wing	Lower Rear Beam Cap W.S. 432	225	125	IW33	5,620	12000	Minor
Inner Wing	Rear Beam Web W.S. 432	226	126	IW33	5,620	12000	Minor
Inner Wing	Front Beam Cap W.S. 444	228	127	IW38	7,710	12000	Minor

Sensors on the aft fuselage pressure bulkhead are for the purpose of correlating fatigue damage related to fuselage pressurization loads. Six fatigue sensors (multiplier of 3) were installed on the bulkhead honeycomb face sheet and the back-up beam caps in locations as shown in Figure 89. These locations were selected to give a profile of the cyclic load distribution across the bulkhead from B.L.0. It was assumed that the distribution of internal loads would be symmetrical about the center line (B.L.0.). The sensors PB 75 and PB 75A were installed on the honeycomb face sheet at right angles to each other in much the same manner as a rosette strain gage. The sensor grid axis oriented vertically (PB 75A) shows a substantially higher cumulative resistance change than its horizontally oriented companion sensor. All of the sensors except PB 75A and PB 75 are installed on the back-up beam caps which means that sensors in these locations will receive tension strains while those on the forward face sheet of the honeycomb bulkhead will see compression strains. An evaluation of sensor output versus each load condition reveals that the sensors on the aft pressure bulkhead respond primarily to load conditions GAG-1 and GAG-2, which are the only load conditions with fuselage pressurization (Table VII). The shape of the sensor response curves (Fig. 116) on the aft fuselage pressure bulkhead are characteristic of the constant amplitude type curves obtained during sensor evaluation on test coupons. In this case the constant amplitude strain cycles are not completely reversed but range from zero to a peak strain. The data of Figure 116 indicate that suitable sensor response can be measured with the selected instrumentation to perform the desired monitoring function. The variation of the bonding stress along the span of the stiffeners as a result of the pressure load may, however, require close control on sensor installation to conduct comparative analyses on fleet aircraft.

Excellent data were also collected on the engine pylon structure. Sensors IP 2, IP 5 and IP 6 are well located to respond to the principal test loads applied to the pylon. It should be observed that the stress history experienced by sensors IP 2 and IP 5 are essentially identical and that the sensor response at these points, shown in Figure 121, are in close agreement. Good repeatability of results is indicated in this case.

The results of the sensor evaluation on the wing-fuselage specimen are encouraging. Because of the nature of the program, a larger number of sensors were used than would be necessary in a practical fatigue monitoring system. The results indicate that a choise of locations can be selected from the accumulated material that would provide adequate data for correlating the occurrence of fatigue damage.

6.5 DAMAGE CORRELATION

The use of the fatigue sensor in a fatigue monitoring system is dependent on two functions: the sensor must provide an approach for determining the fatigue load exposure of a structure and there must exist a calibration which relates the occurrence of structural fatigue damage with load exposure. In this manner, fatigue damage is related to a change in resistance of specific sensors selected to monitor particular structural areas or components. Although no major failures have occurred in the fatigue test of the wing-fuselage specimen, a number of small cracks of the nuisance variety have developed in the course of this program.

These cracks have not interfered with the load carrying capacity of the structure in so far as the fatigue loads are concerned. As a result, the fatigue damage is generally not found except during shut-down periods for scheduled inspections.

On the basis of accumulated results, the sensors selected for monitoring purposes are listed below.

	FATIGUE DAMAGE LOCATION	CONTROL SENSORS
1.	All wing areas	CW 5 CW 6 CW 29 CW 30
2.	Center wing upper surface	CW 1 CW 23
3.	Center wing lower surface	CW 3 CW 13
4.	Inner wing upper surface	IW 43 IW 48
5.	Inner wing lower surface	IW 33 IW 38
6.	Outer wing upper surface	OW 55
7.	Outer wing lower surface	OW 63 OW 65
8.	Engine pylon	IP 2 IP 5 IP 6
9.	All fuselage shell areas	PB 75A PB 71
10.	Fuselage shell fwd. of wing rear spar	F 83 F 84
11.	Fuselage shell aft of wing rear spar	F 85 F 86
12.	Fuselage main frame, F.S. 1106	F 81

In all cases, fatigue damage which occurs on the wing will be referenced both to the sensors located in close proximity to the damage and to the sensors located at the centerline of the airplane on the front and rear spar caps. This will provide data on which to evaluate the feasibility of using centrally located sensors to effectively monitor major components such as the wing. The occurrence of physical damage will also be referenced to sensors located in the general vicinity of the damaged area. A similar procedure will be followed in the case of the fuselage structure; however, in this case, the common basis for monitoring the occurrence of fatigue damage in the shell structure are sensors which respond primarily to the fuselage pressure cycle. Figures 122 through 127 show typical cases of fatigue damage which were located during inspections at the conclusion of 9000 and 12000 equivalent flight hours. Table XI has been prepared to illustrate typical calibration data derived from the fatigue test program.

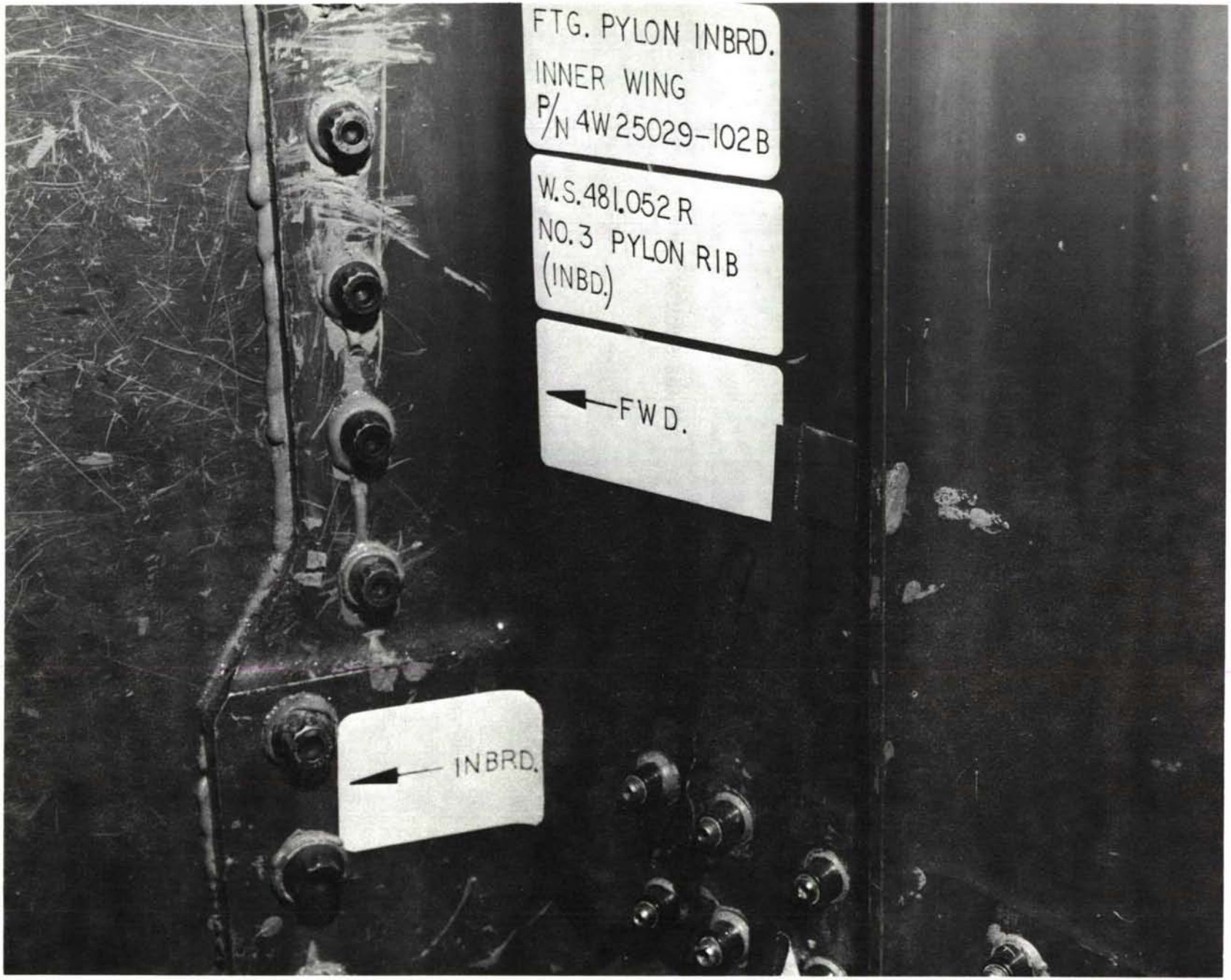

FIGURE 122. DAMAGE TO INBOARD PYLON RIB

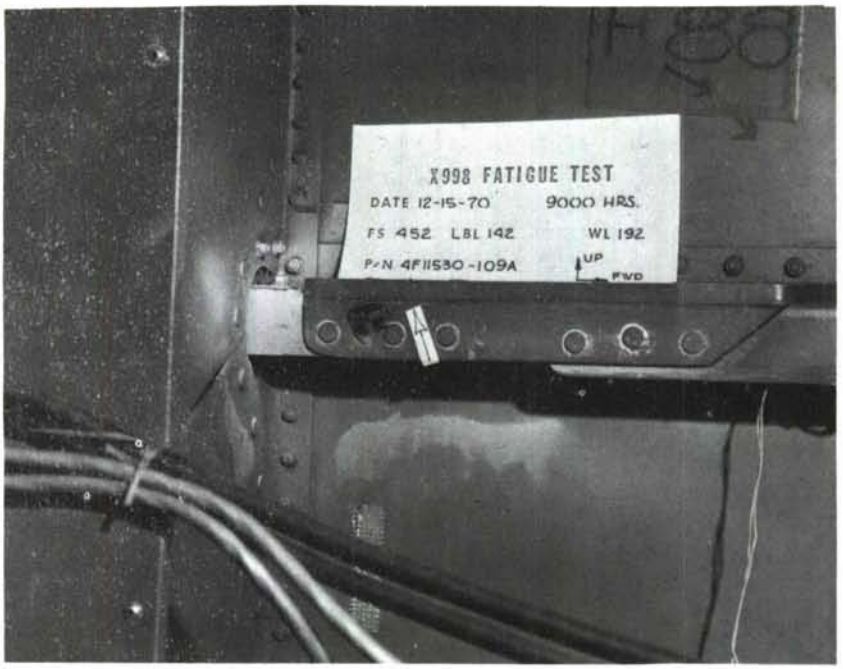

FIGURE 123. FATIGUE DAMAGE AT FUSELAGE STATION 452

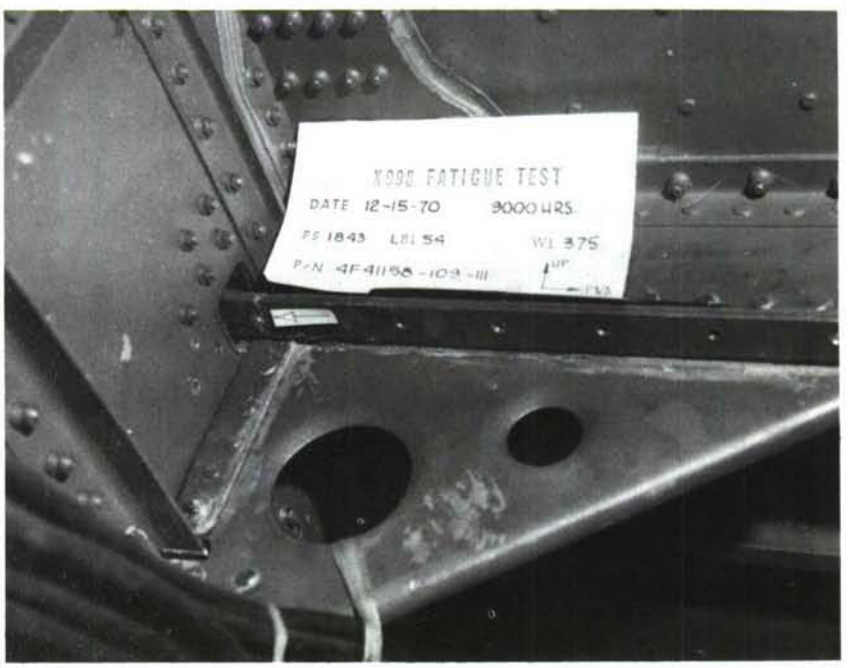

FIGURE 124. FATIGUE DAMAGE AT STRINGER 7 F.S. 1843

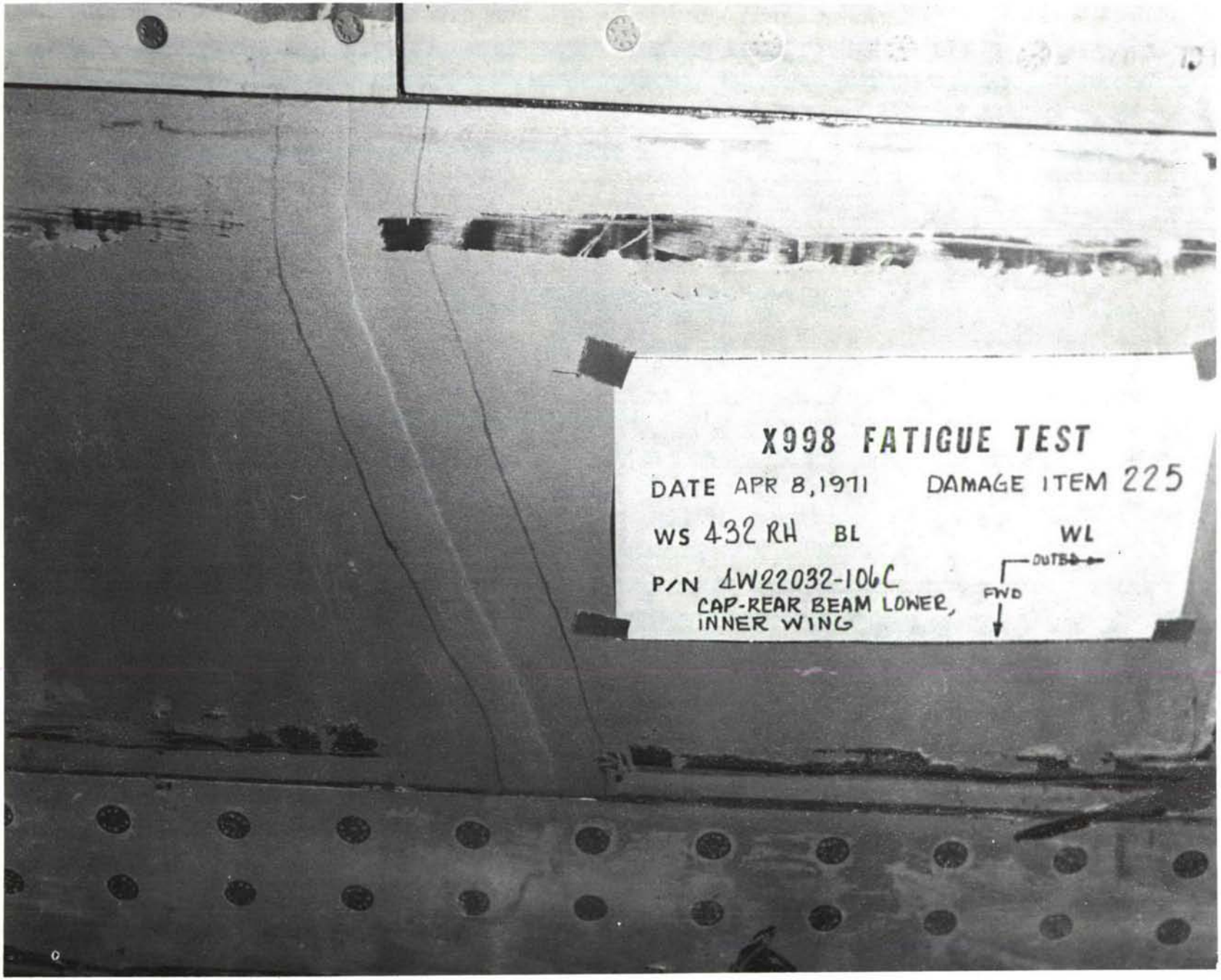

FIGURE 125. FATIGUE DAMAGE ON THE INNER WING, LOWER REAR BEAM CAP, OUTSIDE SURFACE

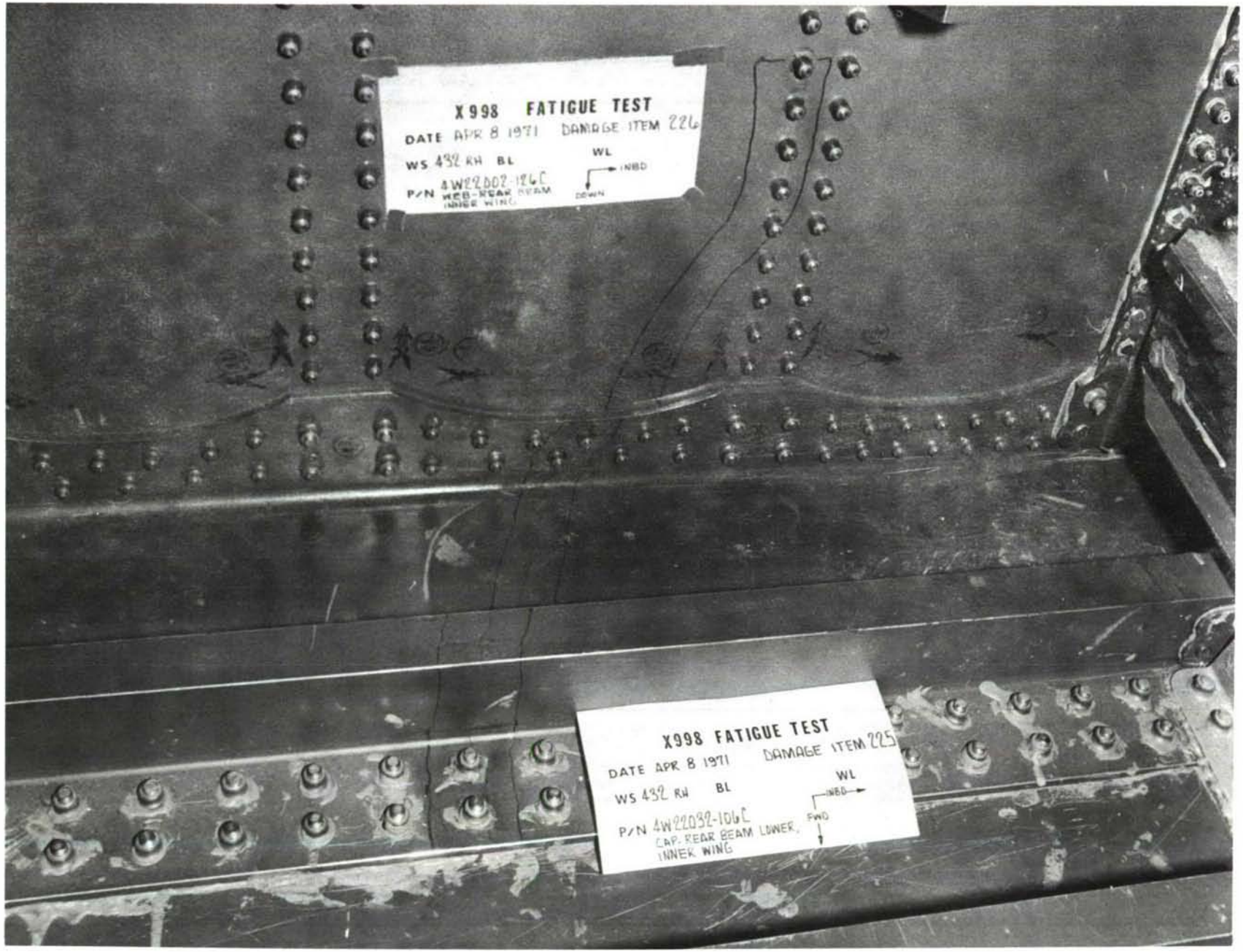

FIGURE 126. DAMAGE TO INNER WING REAR BEAM AND BEAM CAP INSIDE SURFACE

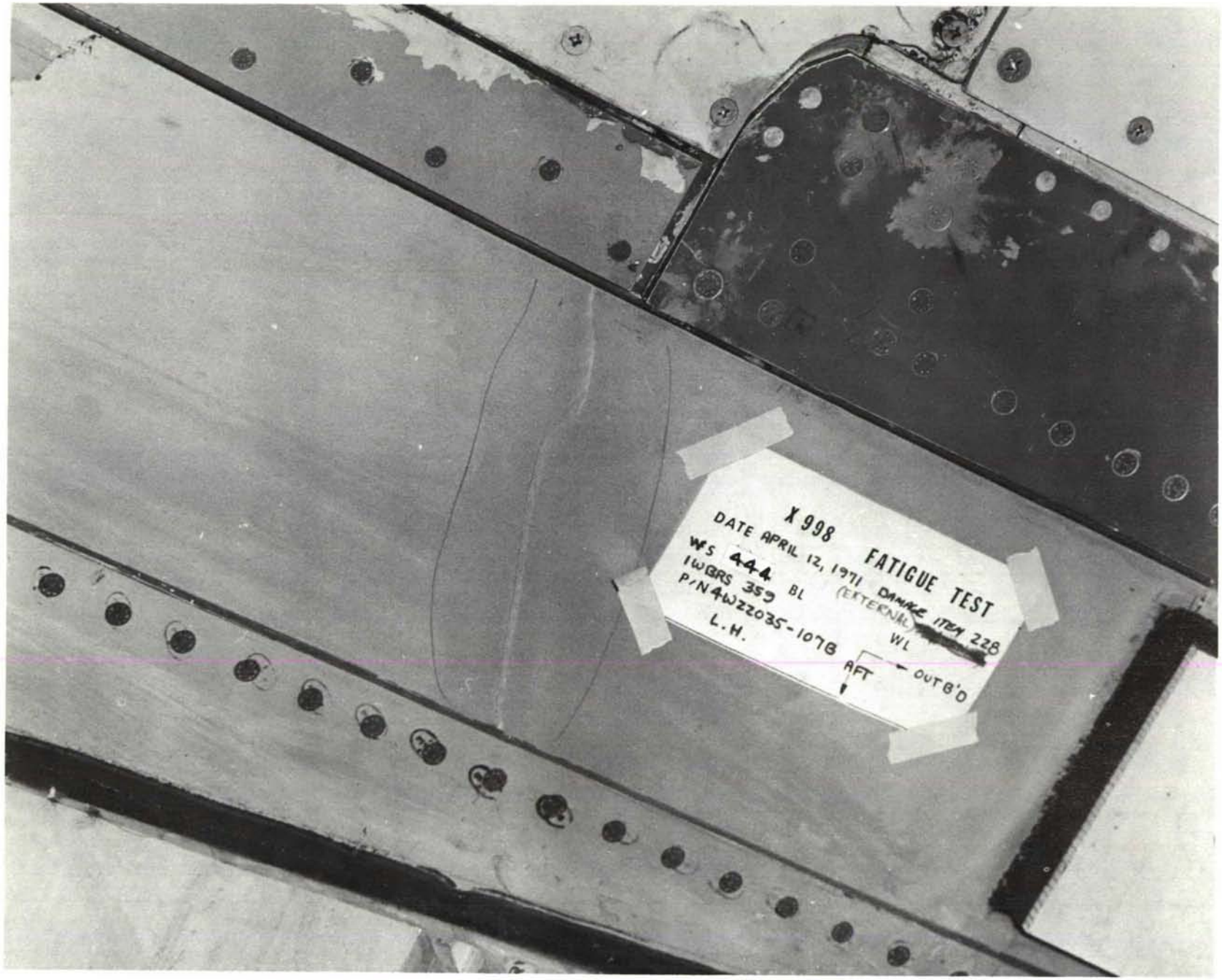

FIGURE 127. DAMAGE TO THE INNER WING FRONT BEAM CAP, OUTSIDE SURFACE

6.6 SENSOR RELIABILITY AND PERFORMANCE

The sensors installed on the wing-fuselage specimen were subjected to more adverse environmental condition than those installed on the other two test specimens. All sensors installed on this specimen were waterproofed for exposure to 8.3 psig hydrostatic pressure cycles. The sealing material used was a modified polysulphide two-part epoxy waterproofer, commercially designated Denseal No. 5 as manufactured by the Dentronics Company. The waterproofing was exposed to alternate water-pressure and ambient air temperatures over a calendar time period exceeding two years. Periodic insulation tests regarding sensor resistance-to-ground were conducted throughout the test program. All sensors exceeded a resistance-to-ground of 500 megohms with the average reading approximately 4000 megohms. The epoxy waterproofing material also provided mechanical protection against "foot traffic" or falling objects, however, sensor CW 7 did sustain lead wire damage at the start of the program. Access to this sensor could not be obtained until the end of pass 6 therefore the sensor was reconnected prior to the start of pass 7 and data are shown for only two passes.

In retrospect, sensor overranging and structural modifications produced the largest number of sensor casualties forcing a repair or replacement of the affected sensors. In any case, however, timely repairs and/or replacements were made so that very little data were lost and the use of the monitoring site was continued. In some instances sensors were replaced although they were still operating; CW 14, CW 15, and CW 18 are examples of this. In these cases it was desired to verify the unbonded length of the existing multipliers and ascertain that these sensors had the same multiplier as sensors CW 11 and CW 12 located in the same spanwise vicinity. It was determined by physical examination, that less than 15% variation in actual multiplier could exist between these sensors even though there is considerable variation in sensor resistance change values (Fig. 107). This behavior is attributed to the non-linear resistance change characteristics of the sensor as a function of cyclic strain amplitudes. A review of the strain gage data for both upbending and down bending loads on the wing indicates strain levels in the area bounded by CW 11 and CW 12 to be uniform with the strain levels in the area bounded by CW 14 and CW 15. This consideration points up the necessity of multiplier repeatability from specimen-to-specimen.

During the airplane fatigue test program, more extensive structural modification occurred on the wing fuselage than on the two previous specimens. The modified structural areas included the mid-beam of the inner wing and the addition of attachment fittings to the upper and lower rear beam caps at W.S. 120. The attachment fitting modifications were implemented on the original production structure prior to the start of cycling. Later structural modification included a beef-up of the mid-beam after the completion of 9000 cyclic test hours (pass 6). The magnitude of sensor replacements and additions believed necessary to adequately respond to these modifications are shown in Tables VIII and IX.

Progressive experimentation and evaluation of the sensor combined with the strain multiplier continues to expose some of the restrictive features of this device. These limitations can be summarized as an increase in complexity of operation and cost when compared with the use of the sensor by itself. As a trade-off, however, the user does receive improvements in apparent threshold sensitivity i.e., the resistance change characteristics of the sensor can be more closely aligned with the occurrence of structural fatigue damage.

SECTION VII

FLIGHT AIRCRAFT REQUIREMENTS

7.1 COMPARISON OF REQUIREMENTS

Previous sensor instrumentation experience and the knowledge gained from the laboratory fatigue test airplane has indicated a preferred approach for practical sensor application to service aircraft. The guidelines developed during sensor evaluation on the C-5A fatigue test airplane have been successfully incorporated into the fatigue sensor instrumentation of C-130 fleet aircraft. To date 44 service aircraft (C-130 B/E type) have been instrumented with the type SAP 202DA-C13-STK sensor in accordance with Air Force contract FO 9603-68-C-2530-P00022. Initial data evaluations have confirmed that the compensation techniques incorporated into the fleet aircraft program were desirable and necessary. The most important difference in the instrumentation of fleet aircraft compared with the laboratory fatigue test airplane involves specific sensor temperature and fuel load compensation measures and data correction techniques.

The laboratory test specimen was operated in a relatively constant temperature environment, with no variation in wing fuel load, and with a zero pay load in the cargo compartment. The test procedure was such that the test structure could always be returned to the same zero load condition. The same is not true or practical for a flight vehicle, therefore sensor corrections must be made to obtain meaningful sensor data from flying aircraft.

7.2 COMPENSATION FOR VARIATION IN FUEL LOAD

Although the permanent resistance change of the sensor is the parameter used for monitoring repeated load exposure the sensor will also measure static strains. Since the sensor resistance readings are taken under static conditions, variations in fuel loads will affect sensor readings on the wing and certain other areas of the aircraft. That is, variations in static strain will be mixed-in with the permanent resistance change of sensors located on landing gear back up structure as well as the wing and wing support structure. To avoid the requirement for a specific quantity of fuel in the wing tanks each time the sensors are sampled, electrical compensation networks were used. This technique is illustrated in Figure 128. A compensating strain gage is stacked on top of the fatigue sensor (Fig. 129) such that it will experience the same strains as the sensor regardless of any error in programmed multiplier. The sensor will produce a resistance change for both repetitive cyclic strains and static strains, however, the resistance change for repetitive strains is permanent compared to the temporary resistance change for static strains. Therefore, a compensating strain gage can be used to cancel the effects of temporary resistance changes in the sensor since it responds to instantaneous strains only. It should be noted that the sensor and the compensating strain gage must have the same nominal resistance, i.e., a 100 ohm sensor could not be matched with a 120 ohm strain gage. The compensating strain gage is placed in the adjacent arm of the half-bridge network as achematically shown in Figure 128.

7.3 TEMPERATURE COMPENSATION

Sensor temperature compensation becomes a strong consideration for aircraft structures subjected to world wide operating temperature environments. Unlike the conventional strain gage, the annealed Constantan sensor cannot be self-temperature compensated for aluminum without erasing its fatigue induced resistance change capabilities; therefore, other temperature compensation techniques should be used. One of the side benefits obtained by the compensation method used for fuel load variations is automatic temperature compensation. Since an aircraft wing, for example, is designed thermally stress free any expansion or contraction of the structure will be felt by the multiplier and amplified for both the sensor and the strain gage. Sensor resistance change as a result of apparent strain produced by structural thermal deformations is considered more significant than the resistance change produced by just the sensor TCR.

7.4 REDUCTION OF MONITORING LOCATIONS

It is also anticipated that knowledge gained from the laboratory calibration of sensors on a full-scale test specimen will permit a reduction in the number of sensors for follow-on fleet aircraft. The number of sensors initially allocated to the C-5A fatigue test specimen was considered excessive; however, this approach was believed justifiable in view of the one time pioneer nature of the effort. Adequate coverage of the same model service aircraft could be obtained with approximately 1/2 of the sensors used on a laboratory specimen. Only those sensor locations which were more informative on the calibration article would be duplicated on the service aircraft.

7.5 CORRECTION OF STRAIN AMPLIFIER ERRORS

Since an artificial structural strain is created for the sensor by means of a mechanical strain amplifier, particular emphasis must be given to techniques that will produce a consistent and reliable strain ratio. Any errors in strain multiplication factor at this stage are further compounded by the fact that the resistance change of the sensor is a logarithmic function of strain amplitudes. That is, any error in strain amplication ratio will produce sensor resistance change errors which are logarithmic in magnitude. Gross errors in strain amplication ratio should not occur except due to very poor quality controls. However, multiplication verification testing and an evaluation of technician installation capabilities to obtain a programmed multiplier has shown that some scatter must be expected. These variations must either be accepted or else data corrections must be incorporated in the assessment of structural damage. Fatigue sensor instrumentation techniques utilized during the installation of sensors on 44 C-130 flight aircraft permitted the determination of the actual multiplier obtained. Since fatigue sensor data for aircraft damage assessments are presently incorporated in a computer program, logarithmic correction coefficients for the multiplier can also be concurrently processed. The administrative mechanics and field procedures for handling sensor data from operational aircraft are presently being field proven on C-130 B/E airplanes.

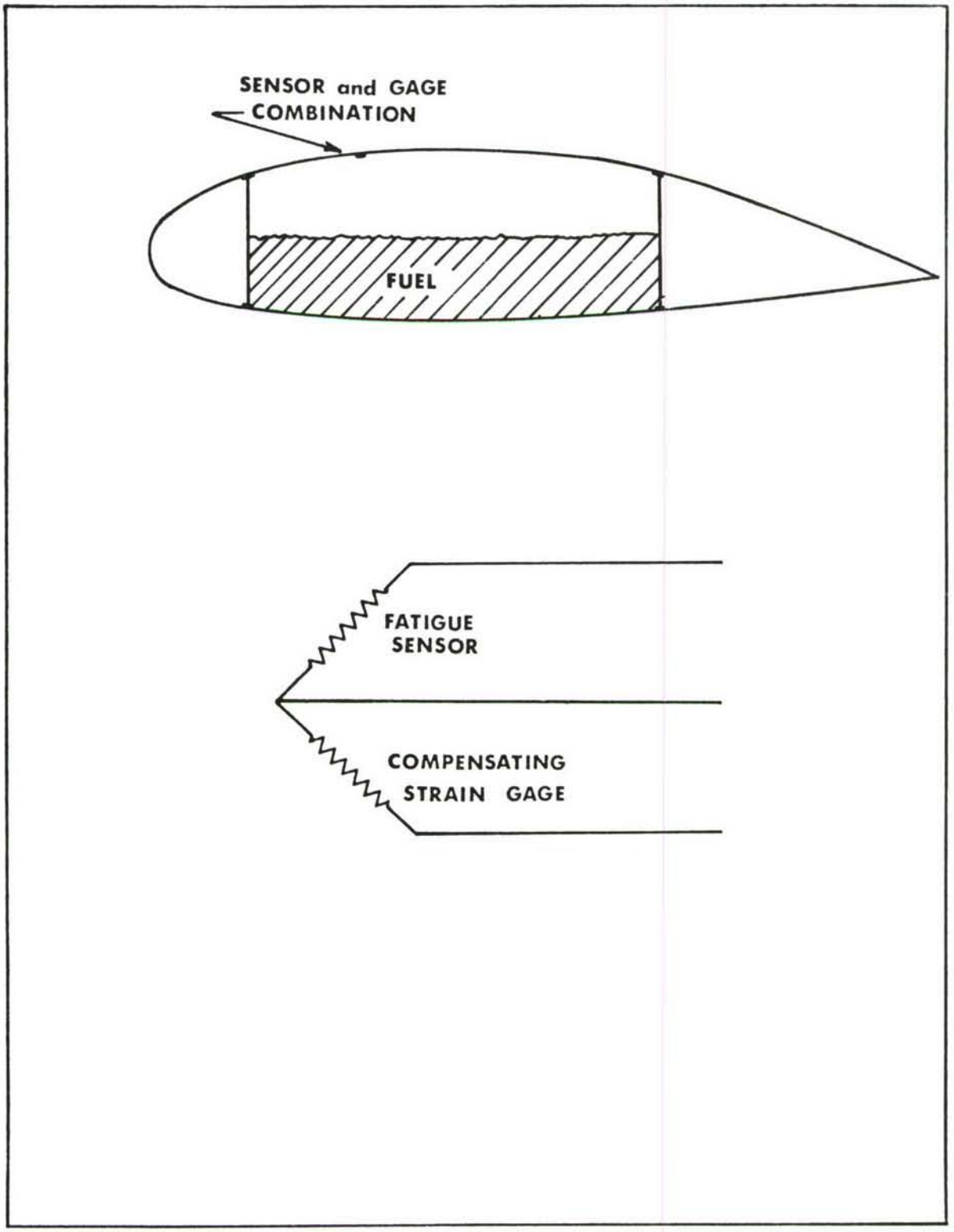

FIGURE 128. PREFERRED INSTRUMENTATION ARRANGEMENT FOR SERVICE AIRCRAFT

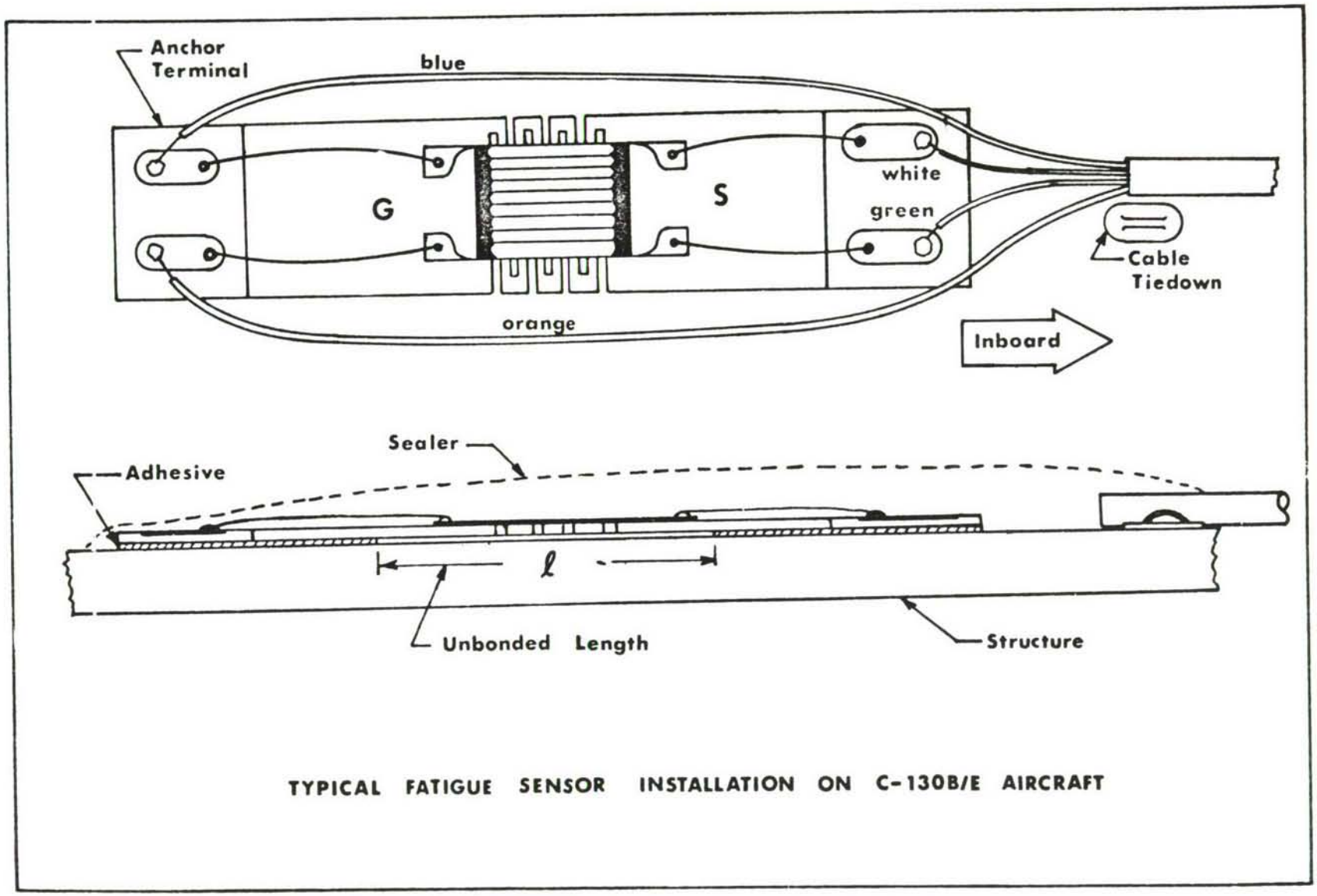

FIGURE 129. INSTALLATION SHOWING A FATIGUE SENSOR AND COMPENSATING STRAIN GAGE STACKED ON THE SAME MECHANICAL MULTIPLIER.

SECTION VIII

SUMMARY AND CONCLUSIONS

Whenever a hardware system is considered for potential application on in-service aircraft, the applicability of the system should be tested in a practical manner to permit a realistic evaluation of its functional operation, mechanical suitability, and economics of application. Such an evaluation has been performed using a system of fatigue sensing devices installed on a full-scale C-5A fatigue test airplane. The fatigue sensor installation on the three C-5A fatigue test specimens can be described as a simple and inexpensive load summing system in which each sensor responds to and stores the cumulative effects of the amplitude and number of structurally imposed cyclic loads. The operational characteristics of the sensors installed on this full-scale airframe assembly were consistent with previous results observed during the feasibility study and sensor application to the C-5A fatigue test components. Data obtained from this stage of testing and evaluation has further supported original findings that a structure's exposure to repeated load occurrences can be monitored. It has been shown (Section 5.5 and 6.5) that a functional correlation between structural fatigue damage and sensor resistance change (ΔR) can be established.

The physical attributes of the sensor have been especially encouraging and indicate its unique suitability for application to subsonic fleet aircraft structure. Mechanical as well as operational characteristics of the sensor/strain multiplier have been evaluated under conditions which simulate loads experienced during a long term (10 to 15 years) of field service. The results have shown that mechanical difficulties should not be encountered during utilization on military aircraft.

The material, installation, and maintenance costs have been modest and reasonable for the intended application. Sensor installation on the C-5A fatigue test structure has required no structural modifications and it is possible that none would be required for service aircraft.

The applicability of the sensor to subsonic aircraft structure is enumerated in greater detail as follows:

FUNCTIONAL

- o Sensor Does Not Require Continuous Electrical Energization

  The mechanically induced electrical resistance change is permanent; therefore, the sensors need only be energized when it is desired to sample the resistance change. Expensive "on board" data acquisition equipment with its attendant maintenance problems can thus be eliminated.

- o Remote Observation and Recording

  Visual inspection of inaccessible airframe areas can be difficult, therefore, "electrical evidence" type measurements are desirable and possible with the fatigue sensor.

- o Operable Under Adverse Environmental Conditions

  The sensing device is bonded to the structure and sealed against the adverse effects of changes in humidity and atmospheric pressure. Structural vibration, corrosive atmospheres or temperature variations (-65°F to 200°F) have no detrimental affects upon the sensor.

- o Stability Over Long Time Periods

  Long life aircraft may realize utilization over time periods exceeding ten years; therefore, any fatigue sensing device should maintain calibration stability over a similar time period. The present sensor has demonstrated stability over calendar time periods exceeding three years and simulated in-service load experience exceeding ten years.

ECONOMICS

- o Sensor Cost

  The sensor is relatively inexpensive (less than $25. each) compared to the value of the structure being monitored.

- o Monitoring Equipment

  Sophisticated, complex, electronic data acquisition systems are not required. An inexpensive ($500.) ground based monitoring instrument could service approximately 15 aircraft at one base.

- o Installation Ease

  The simplified sensor installation can be accomplished by technicians in field areas. Sensor attachment techniques are within the state of the art.

- o Maintenance Requirements

  The sensor is essentially maintenance free, since it has no moving parts to adjust or wear. There is no complicated or delicate circuitry required.

MECHANICAL FEATURES

- o Small in Size and Weight

  The sensor is similar to a foil strain gage, consequently it is lightweight, small in size, and does not interfere with aircraft maintenance or require payload space.

- o Non-Reinforcement of the Structure

  Sensor installations are normally made on internal surfaces to prevent any alterations of aircraft aerodynamic characteristics and to limit exposure to environmental or mechanical damage. Its installation requirements will not interfere with aircraft maintenance or operating characteristics.

- o Mechanical Endurance

  Laboratory evaluations have shown a sensor/shim mechanical endurance of over one million cycles at typical in-service strain levels.

The above itemized compatible features of the sensor for practical application to aircraft structures have contributed significantly to the successful test results and overall program accomplishments. The recognized program accomplishments are enumerated as follows:

- o Improved techniques for adjusting the apparent sensor sensitivity to the envelope of structural cyclic strain ranges.
- o Identified the structural area of the aircraft producing the higher sensor resistance change and the "key" sensors for this area.
- o Generated sufficient handbook type information to permit a judicious application of sensors to a C-5A flight vehicle.
- o Developed a satisfactory technique for the replacement of sensors with a minimum loss of valid information.
- o Verified a simple and practical approach for data acquisition.
- o Confirmed the suitability of a bonded sensing device for simulated long term load exposure (one simulated lifetime) on a complex aircraft structure.
- o Instituted sensor documentation procedures for this program which will provide sufficient information to permit duplicate sensor installations on C-5A flight vehicles.
- o Provided maintenance and trend information with which to establish procedures for the efficient management of this supporting function.

The accomplishments obtained during this program must be partially attributed to the investigations and basic sensor developments which have evolved over a five year period (Refs. 6, 7, and 16). The total activity has proceeded through progressive engineering steps, each one advancing fatigue sensor technology closer to a practical application. The initial feasibility study (Ref. 6) permitted a better understanding of annealed Constantan material behavior characteristics and its capabilities as a fatigue sensor over a wide range of fatigue environments. The natural progression to sensor installations on more complex aircraft structure (Refs. 6 and 7) allowed the accumulation of experience in both the cause and cure of difficulties encountered during more advanced evaluations. It must be recalled that even at this more advanced stage of evaluation that the C-5A structure is being used to evaluate the capabilities of the sensor rather than using the sensor to evaluate the fatigue status of the C-5A structure. Anticipated follow-on sensor installation on flying aircraft would, however, be used to evaluate the fatigue status of the flight vehicle.

Information from this program and previous evaluations indicate that a typical application of the system to obtain a maximum return and utilization of the invested effort might be implemented as follows:

(1) Calibrate a system of sensing devices on a laboratory fatigue test airplane that would establish an aircraft's structural fatigue damage allowables in terms of sensor resistance change.

(2) Install sensing devices on operational airplanes to determine relative fatigue damage occurring on fleet aircraft and thus allow airplane rotation with respect to missions for the purpose of normalizing fatigue damage.

(3) Utilize system on fleet aircraft to indicate a rate of accrual of damaging service loads which in turn will indicate when and/or where structural repairs may be needed.

The above applications would provide data to effectively schedule aircraft inspections, repairs, component replacements, and structural modifications with a minimum loss of "combat readiness" to the using commands. This activity would also assist in the programming of missions on various aircraft for maximum utilization of fleet life or phase-out and replacement of aircraft.

The results of this effort have reinforced original concepts that a structure's degree of repeated load exposure can be monitored by a simple reliable system of fatigue sensors such as employed in this program. It becomes increasingly evident that the user who possesses a thorough understanding of sensor limitations and application criteria will be the user who makes the most effective use of its capabilities. There appears to be no quick or absolute solution to either the choice of a sensor or an application technique universally suitable for all structures. The results of this program indicate that the original approach was a valid one and should not be changed even if it were possible to repeat the program. It is concluded that the program objectives (Sec. 3.1) and the overall goal of obtaining fatigue sensor utilization on flight vehicles has been brought another step closer to realization by the results obtained during this effort.

REFERENCES

1. **Kossar, J. M., A Feasibility Study on the Development of a Pre-Crack Fatigue Damage Indicator, Republic Aviation Corp., ASD-TR-61-719, Aeronautical Systems Division, Wright-Patterson Air Force Base, Ohio April 1962**

2. **Air Force Structural Integrity Program: Airplane Requirements ASD-TR-66-57, Aeronautical Systems Division, Wright-Patterson Air Force Base, Ohio, February 1968**

3. Aircraft Structural Integrity Program (ASIP), AFR-80-13, Department of the Air Force, Washington, D. C., June 1969.

4. King, Troy T., "Some Developments in the Air Force Aircraft Structural Integrity Program (ASIP)", Paper presented at the Air Force Conference on Fatigue and Fracture of Aircraft Structures and Materials, Miami Beach, Florida, December 1969.

5. Freudenthal, A. M., "Fatigue Mechanisms, Fatigue Performance and Structural Integrity", Paper presented at the Air Force Conference on Fatigue and Fracture of Aircraft Structures and Materials, Miami Beach, Florida, December 1969.

6. Horne, R. S., A Feasibility Study for the Development of a Fatigue Damage Indicator, Lockheed-Georgia Company, AFFDL-TR-66-113, Air Force Flight Dynamics Laboratory, Wright-Patterson Air Force Base, Ohio, January 1967.

7. Horne, R. S., "Development of a Semiautomatic Fatigue - Evaluation System for Transport Aircraft," Lockheed-Georgia Company, Paper Presented at SESA, Ottawa, Ontario, Can., May 1967.

8. Van Bueren, "Electrical Resistance and Plastic Deformation of Metals," Z Metallk 46, No. 4, Pages 272 to 281 (1955).

9. D. K. Crampton, G. T. Stacy, H. L. Burghoff, "Effect of Cold Work Upon the Electrical Resistance of Copper Alloys", Transaction AIME Vol. 143, Pages 228 to 245, Pub. 1941.

10. Feltman, P., Brunel College of Advanced Technology, London W.3 "The Electrical Resistivity of Metals Due to Plastic Deformation", Metallurgia, August 1964.

11. Stanley, J. K., Electrical and Magnetic Properties of Metals, American Society for Metals, Metal Park, Ohio, Pages 68 - 70.

12. Menden, George T., Electrical Resistance of Metals, Plenum Press, New York, 1965.

13. Micro-Measurements, - S/N - Fatigue Life Gage, Applications Manual 2nd Edition, April 1969.

14. Harting, D. R., "Remote Sensing of Random Fatigue Damage with S/N Fatigue Life Gage," The Boeing Company, Paper presented at SESA, Philadelphia, Pa., May 1969.

15. Thomas, E.D.R., "Development of a Strain Multiplier for Fatigue-Sensor Applications," Hawker Siddeley Aviation England, Paper published in the Experimental Mechanics Journal, August 1970.

16. Horne, R. S., Improvement of a Structural Fatigue Sensor, Lockheed-Georgia Company, AFFDL-TR-70-141, Air Force Flight Dynamics Laboratory, Wright-Patterson Air Force Base, Ohio, April 1971.

17. Miner, M. A. Douglas Aircraft Company, Cumulative Damage in Fatigue, Journal of Applied Mechanics September 1945.

18. Calibration System Requirements, MIL-C-45662A, dated 9 February 1962.

19. Muchnick, S. A. Franklin Institute Laboratories, Adhesive Bonding of Metals. Paper presented at ASME, June 1955

APPENDIX I

FATIGUE SENSOR INSTALLATION PROCEDURES

GENERAL

This procedure covers the installation, wiring, checkout and record keeping that is necessary for the fatigue sensor instrumentation of the C-5A laboratory fatigue specimens. Since the installation techniques of the unamplified sensor were previously covered (Ref. 6) this procedure will detail only the metal-to-metal bonding of the shim multiplier. Although many of the techniques applicable to a quality strain gage installation are also necessary for a quality fatigue sensor installation, additional care must be taken during certain critical steps. The fact that the sensor is mounted on an aluminum multiplying shim requires that a metal-to-metal bond be effected, which in turn requires a departure from standard strain gaging procedures. The handling of the unsupported multiplying shim is also critical in that an out of tolerance sensor may result from any flexing of the shim prior to bonding to the structure.

SENSOR LOCATION

The precise sensor locations are established by sketches or drawings and no deviations are permitted without engineering approval. The specified location is marked within 1/16 of an inch in both axis with a non-graphite type pencil or a fiber tip pen. Ball point pens are not permitted. The location lines will be long enough so that sanding the gage area will not entirely remove the lines. A china marking pencil may be used to identify the location in a manner suitable for photographing.

CLEANING AND SURFACE PREPARATION

The specimen surface preparation requires that an area about twice that of the shim be thoroughly cleaned. Basically the area to be cleaned should be large enough to accommodate the sensor shim and waterproofing. After removal of paint and grease by sanding and solvents (MEK) the surface is then scrubbed with Alconox and Scoth Brite. The surface is now rinsed with distilled water, etched with a mixture of chromic sulphuric acid and barium sulphate powder for ten minutes (puddling technique) rinsed and air dried. After drying, the surface is primed with EC 2320 and then recleaned with MEK just prior to bonding the shim. The primer contains a corrosion inhibitor and also retards the formation of aluminum oxides.

After one or more bonding areas have been prepared, the sensors are carefully removed from the package and visually checked for damage. A resistance check using an ohmmeter is conducted to determine if the sensor is open or shorted. At this time the gage or sensor type can be noted in the record sheet. Before cleaning the shim the cardboard support is carefully removed from the shim, without flexing the shim. Cellophane tape placed across the top of the shim lengthwise will facilitate handling of the shim. The cleaning operation is simplified somewhat by the fact that the mounting shim has been pre-cleaned and primed by the supplier. After the EC 2320 blue primer is recleaned by a swab saturated with MEK, the shim is ready for bonding.

BONDING

The cellophane carrier tape is used to accurately align the sensor and to position the sensor while applying the adhesive and Teflon spacer. The epoxy adhesive (Denex 6) is obtained from stock and mixed according to the manufacturer's specifications. The Teflon spacer is centered on the structure and the shim-mounted sensor is positioned in place. The tape with the sensor adhering to it is now accurately positioned on the mounting area and the tape pressed down to hold the sensor in position. Avoid excessive pressure and rubbing of the sensor area as this will induce cold working in the foil resulting in an out of tolerance sensor. Now cover the sensor and shim strip, first with a small piece of thin teflon followed by a 1/16 inch thick piece of silicone gum rubber or neoprene. Hold it in place with a small strip of cellophane tape. On top of this sandwich, place a contoured metal pad approximately the shape of the surface contour. Apply a pressure to this plate with a squeeze clamp, negator spring, or other weight equal to five to ten pounds per square inch. C-clamps are not permitted since their use tends to twist the sensor. Proceed now with the recommended curing cycle for the epoxy, which is three hours at 185°F. After curing, if the installation is correct, the tape will peel off cleanly leaving the sensor on the surface. Check the sensor with an ohmmeter at this stage to see if the sensor grid has been opened or otherwise damaged. Mechanically check the shim metal-to-metal bond by applying a slight separating force at each corner of the shim with a pen knife or other sharp object. Do not disturb the slotted portion of the shim.

LEAD ATTACHMENT

The sensor solder dots may be cleaned by rubbing with a Q-tip which has been moistened with MEK. A rubber pencil eraser or fiberglass brush may also be used to remove oxides, and epoxy flash over. After this has been done, the end of the interconnecting wire must be tinned. This is done by first putting a small spot of Kester Number 44 flux on the solder dots and wire ends. A quick touch of a pencil type soldering iron using 1/8" tip and Kester Number 44 solder will tin the tip of the wire. Preferably use a 0.015 to 0.020 inch diameter wire solder. Without additional solder, the interconnecting wire should be touched with the iron to make the joint. Avoid overheating the solder dot. The cable should be mechanically anchored to the test member about 1/2 to 3/4 inch away from the shim strip to avoid undue strain on any solder joints. One end of the 34 gage enamel insulated jumper wire is soldered to the sensor tab and the other end to the anchor terminal as shown in Figure 129. The cable leads may now be soldered directly to the anchor terminals. Wash solder joints with a neutralizer to prevent corrosive action from fluxes. Plastic tape or Q-3 sealer may be used as a temporary hold-down for the interconnecting wire. The bonded resistance of the sensor should be recorded to the nearest 0.1 ohm any time after the interconnecting wires are soldered to the sensor. The pressure check is to be performed by connecting a strain indicator to the sensor leads and applying enough pressure to the structure to obtain a needle deflection. A drift or non-return to zero condition will be considered as a poor bond.

LEAD ATTACHMENT

It is important that sensor cables and leads be properly secured so that no mechanical damage may occur to the sensor from cable displacements.

Plastic identification sleeves are to be secured to both ends of the extension cable. If the installation had not been previously photographed this may be done prior to waterproofing.

INSTALLATION CHECKOUT

Prior to waterproofing, preliminary quality assurance checks are to be conducted. These checks are to be made at the cable termination end after soldering to the panel mounted connector. A strain indicator balance check made from the connector end should be within $\pm$ 5000 micro-inches/inch of mid-scale on the indicator. Cold solder joints or a stretched sensor can throw an installation out of the acceptable range.

The required final resistance-to-ground check is made at the connector end using a Weston Model 799 megohmeter. A reading of at least 1000 meg ohms at the cable termination end is required. The leakage resistance may be improved by the use of heat lamps, taking care not to exceed a surface temperature of 200°F. If these checks indicate a good installation the sensor is ready for sealing.

WATERPROOFING

The BLH barrier "E" waterproofing used for sealing requires no mixing and no cure time. The aluminum bonding surface is recleaned with MEK and the sheet form sealer cut to size. A small patch of the sealer with the neoprene carrier removed is placed under the leads at the point where the leads will exit from the sealed area. The waterproofing compound is pressed down over the sensor and around the wiring, taking care to work carefully around the edges. A red and white plastic "INSTRUMENTATION" label is to be stuck to the waterproofing patch in the most conspicuous place. The installation is then liberally covered with a polyurethane coating over the neoprene carrier, extending over the cable and on to the structure. A final resistance-to-ground check can now be made.

FUEL PROOFING

For installations exposed to jet fuels (JP-4) a modified polysulphide epoxy (Denseal 5) is mixed and applied according to manufacturer's instructions. Apply the compound over the sensing device, leadwires, and cable end taking care to work it in around the cable end. A second coat of the fuel proofing compound may be required on overhead or vertical surfaces to assure that the patch is built up to a 1/4 inch thickness. The fuel proofing patch should extend at least 1/4 inch beyond all sides of the sensor/amplifier assembly and the cable end. After the compound has cured, an INSTRUMENTATION label is placed on the patch and the area is liberally coated with the polyurethane varnish.

LIST OF MATERIALS

CLEANING MATERIALS

Cotton balls, Kim Wipes (Kimberly Clark)
Q-tips (Johnson Company)
Abrasive cloth - 240, 400, 180 grit aluminum oxide abrasive
Alconox, Methyl Ethyl Ketone (MEK)
Scotch Brite (3M Company)
Fiberglass Brush (Baldwin Cat. No. 201614)
Chromic Sulphuric Acid (LAC 0120)
EC 2320 primer (3M Company)
Barium Sulphate Powder
Distilled water

BONDING AND INSTALLATION MATERIALS

Denex 6 adhesive (Dentronics Inc.)
Teflon tape, 1/2", 5/8", 3/4" width type HM 225 (CHR Company)
Cellophane tape, 1" wide
Electrical plastic tape
Paper masking tape
Heat lamps, heat pad
Pressure pads, clamps, metal shims

WIRING MATERIAL AND EQUIPMENT

Kester 44 solder, liquid flux, neutralizer
28 gage, stranded, plastic insulated wire
Irvalite plastic sleeves
Green armament tape, cable calmp, tie cord
Fit caps, heat shrinkable
Soldering Iron, 25 watt or less
#34 Soldereze Enamel Wire

QUALITY ASSURANCE MATERIAL AND EQUIPMENT

Dual Range Therm-o-meter - Simpson Model 389-3L

Weston megger - Model 799

Multimeter - Simpson Model 260

Wheatstone bridge - L & N Model K

SR-4 Strain Indicator - Baldwin "N" Type

WATERPROOFING MATERIALS

BLH barrier "E"

Polyurethane sealer - Magna Laminar X-500 2 part - coating resin component and hardener

Denseal 5

Instrumentation labels

APPENDIX II

MISCELLANEOUS CALCULATIONS

Adhesive Shear Strength Requirements

The shear strength requirements of the metal-to-metal bonding adhesive may be approximated in view of its anticipated operating environment and desired accuracies of the sensing device. Some possibilities are examined as follows.

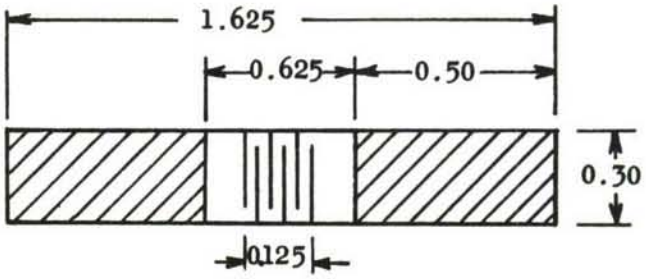

STRAIN AMPLIFIER SHIM
FOR THE TYPE SAP202DA-E SENSING DEVICE

Assume that equal areas on both ends of the strain amplifier shim shown above are mechanically bonded to the specimen structure. The forcing function then becomes the structure and all displacement of the shim occurs across its slotted area. The total unbonded length of the shim is defined by the width of the thin Teflon tape used as a spacer e.g., 5/8 inch wide tape as illustrated above. The significant parameters may be determined as follows.

$A = W \times \ell$

$A = 0.30 \times 0.50$

$A = 0.15$ sq. in.

Where:

A = Bonded area of one end of the shim (sq. in.)

W = Width of shim (in.)

ℓ = Bonded length of one end of the shim (in.)

Assuming an apparent strain($\frac{\Delta L}{L}$) of 6000 μ in./in. then:

$$Ss = \frac{F_{max}}{A}$$

$$Ss = \frac{3.25 \text{ lbs.}}{0.15 \text{ sq. in.}}$$

$Ss = 21.66$ psi

Where:

L = Length of slotted area (in.)

ΔL = Change in length (in.)

F_{max} = Maximum end force imposed on shim (3.25 lb) Fig. 8

Ss = Shear stress (psi)

This shear stress value appears well within the capabilities of commercially available epoxy adhesive, however, if one requires no breakdown of the mechanical bond within 0.01 inch of the bonded edge the requirements become more severe. Assume that the initial unbonded length of the shim must be held within 0.01 inches for the fatigue life of the device, the shear stress requirement now becomes:

$$Ss = \frac{F_{max}}{A} \qquad A = W \times \ell$$

$$Ss = \frac{3.25 \text{ lb.}}{0.003 \text{ in.}} \qquad A = 0.30 \times 0.01$$

$$A = 0.003 \text{ sq. in.}$$

$$Ss = 1080 \text{ psi}$$

Therefore, high quality adhesives and bonding techniques are required to assure that bond breakdowns do not occur adjacent to the edge of the Teflon tape spacer. Calculations for the transfer of load across a bonded joint and the stress distribution therein can become an extensive exercise (Ref. 19). The important point to consider, however, is that while the end load on the shim is quite small (Fig. 8), the uniformally distributed load on the shim's bonded area can be relatively large.

Attenuation of Compressive Strains

The use of an elastic filler in the strain amplifier slots has permitted the de-emphasis of compressive strains upon the resistance change of the sensor compared to that produced by tension strains. That is, the filler can be designed to expand freely in the tension direction while contraction of the slots will be resisted so that the slotted area deformation in the compressive direction is minimized. The schedule of testing did not permit extensive evaluations of this characteristic, however, experimental evaluations indicated that the filler selected produced an attenuation of approximately 30%. This was verified by means of static strain surveys of the sensor response on simple test coupons. A typical output is illustrated below.

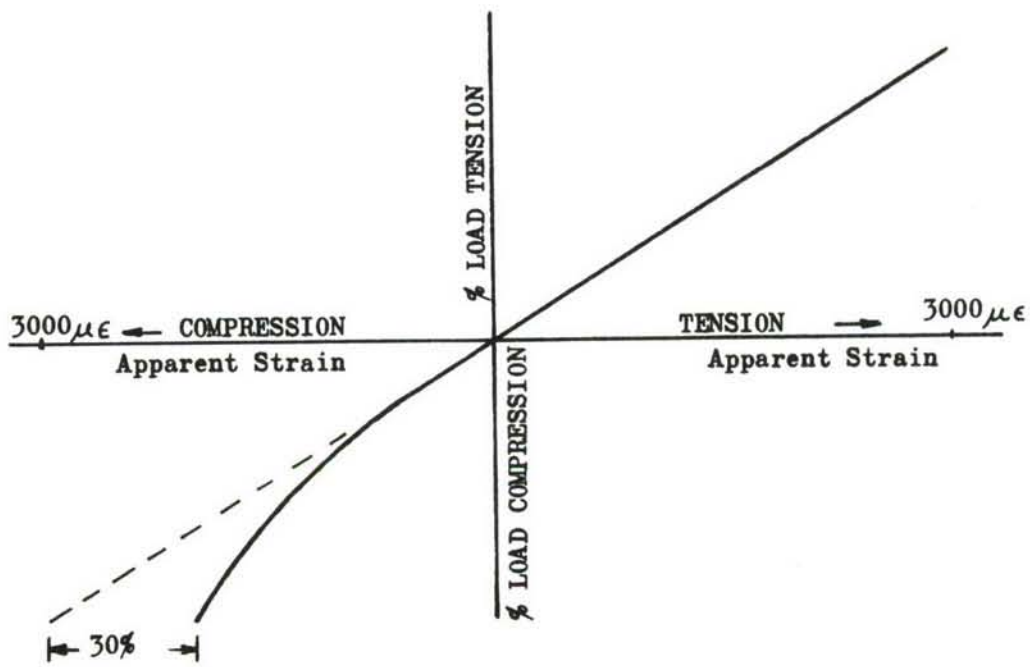

Probably all filler materials having an elastic nature would exhibit the above characteristic behavior to some degree. The material selected, however, appeared reasonable for the intended application. One must also consider that a 30% decrease in strain amplitude will produce a significantly larger percentage decrease in sensor resistance change for repetitive strain cycles. The exact percentage resistance change is of minimal interest due to the comparative nature of the application. The end result of this technique is to minimize the influence of compressive load cycles upon sensor resistance change and to bring the sensor response more in line with the structural fatigue damage actually incurred.

UNCLASSIFIED

Security Classification

DOCUMENT CONTROL DATA - R & D

(Security classification of title, body of abstract and indexing annotation must be entered when the overall report is classified)

1. ORIGINATING ACTIVITY *(Corporate author)*
LOCKHEED-GEORGIA COMPANY
86 S. COBB DRIVE
MARIETTA, GEORGIA 30060

2a. REPORT SECURITY CLASSIFICATION
UNCLASSIFIED

2b. GROUP

3. REPORT TITLE
ANNEALED FOIL FATIGUE SENSOR DEVELOPMENT

4. DESCRIPTIVE NOTES *(Type of report and inclusive dates)*
FINAL REPORT - DECEMBER 1967 to MAY 1971

5. AUTHOR(S) *(First name, middle initial, last name)*
ROBERT S. HORNE and OSCAR L. FREYRE

6. REPORT DATE	7a. TOTAL NO. OF PAGES	7b. NO. OF REFS
	240	18

8a. CONTRACT OR GRANT NO.	9a. ORIGINATOR'S REPORT NUMBER(S)
F33615-68-C-1221	ER 11411
b. PROJECT NO. 3170	
c. Task No. 317007	9b. OTHER REPORT NO(S) *(Any other numbers that may be assigned this report)*
d.	AFFDL-TR-71-127

10. DISTRIBUTION STATEMENT Approved for public release; distribution unlimited.

11. SUPPLEMENTARY NOTES	12. SPONSORING MILITARY ACTIVITY
	AIR FORCE FLIGHT DYNAMICS LABORATORY WRIGHT-PATTERSON AFB, OHIO 45433

13. ABSTRACT

The development testing of the C-5A full-scale fatigue specimens presented a timely opportunity to continue the development of a system of fatigue sensing devices. The fatigue sensor selected for use was previously evaluated during an Air Force funded feasibility study and has been adapted to meet the application requirements on full-scale C-5A structure. This document constitutes the final report regarding this effort and applies specifically to an evaluation of the sensor on the C-5A laboratory fatigue test specimens. The techniques of sensor installation, location, data acquisition methods, and analysis of sensor response are herein evaluated in view of potential utilization on fleet aircraft. A review of the test results indicates that a structure's relative exposure to repeated load occurrences can be monitored, and the cumulative strain history can be registered and stored by a simple foil sensor.

DD FORM 1 NOV 65 1473

UNCLASSIFIED

Security Classification

14. KEY WORDS	LINK A		LINK B		LINK C	
	ROLE	WT	ROLE	WT	ROLE	WT
(1) Instrumentation: Fatigue						
(2) Fatigue Damage Indicator						
(3) Fatigue Measurement						
(4) Aircraft Structural Fatigue						
(5) Structural Testing						

☆U.S.Government Printing Office: 1972 — 759-084/487